

AL/EQ-TP-1997-0017

**UNITED STATES AIR FORCE
ARMSTRONG LABORATORY**



**Field and Laboratory Studies of Pulsed
Pumping For Cleanup of Contaminated
Aquifers**

**Douglas M. McKay, R. D. Wilson, M. J. Brown, William P. Ball,
Donald P. Durfee, Gushou Zia, and Chongxuan Liu**

**Department of Earth Sciences
University of Waterloo
Waterloo, Ontario, N2L 3G1, Canada**

**Department of Geography and Chemical Engineering
The Johns Hopkins University
313 Ames Hall, Baltimore Maryland, 21218**

July 1997

19971215 061

Approved for public release; distribution is unlimited.

**Enviroics Directorate
Environmental Risk
Management Division
139 Barnes Drive, Suite 2
Tyndall Air Force Base FL
32403-5323**

NOTICES

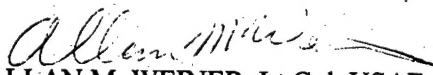
This report was prepared as an account of work sponsored by an agency of the United States Government. Neither the United States Government nor any agency thereof, nor any employees make any warranty, expressed or implied, or assume any legal liability or responsibility for the accuracy, completeness, or usefulness or any privately owned rights. Reference herein to any specific commercial process, or service by trade name, trademark, manufacturer, or otherwise does not necessarily constitute or imply its endorsement, recommendation, or favoring by the United States Government or any agency, contractor, or subcontractor thereof. The views and opinions of the authors expressed herein do not necessarily state or reflect those of the United States Government or any agency, contractor, or subcontractor thereof.

When Government drawings, specifications, or other data are used for any purpose other than in connection with a definitely Government-related procurement, the United States Government incurs no responsibility or any obligations, whatsoever. The fact that the Government may have formulated or in any way supplies the said drawings, specifications, or other data, is not to be regarded by implication, or otherwise in any manner construed, as licensing the holder or any person or corporation; or as conveying any rights or permission to manufacture, use or sell any patented invention that may in any way be related thereto.

This technical report has been reviewed by the Public Affairs Office (PA) and is releasable to the National Technical Information Service, where it will be available to the general public, including foreign nationals.

This report has been reviewed and is approved for publication.


ALISON THOMAS
Project Manager


ALLAN M. WEINER, Lt Col, USAF
Chief, Environmental Risk Management
Division

REPORT DOCUMENTATION PAGE			Form Approved OMB No. 0704-0188	
Public reporting burden for this collection of information is estimated to average 1 hour per response, including the time for reviewing instructions, searching existing data sources, gathering and maintaining the data needed, and completing and reviewing the collection of information. Send comments regarding this burden estimate or any other aspect of this collection of information, including suggestions for reducing this burden, to Washington Headquarters Services, Directorate for Information Operations and Reports, 1215 Jefferson Davis Highway, Suite 1204, Arlington, VA 22202-4302, and to the Office of Management and Budget, Paperwork Reduction Project (0704-0188), Washington, DC 20503.				
1. AGENCY USE ONLY (Leave blank)		2. REPORT DATE July 28, 1997		3. REPORT TYPE AND DATES COVERED April 1993 - March 1997
4. TITLE AND SUBTITLE Field and Laboratory Studies of Pulsed Pumping for Cleanup of Contaminated Aquifers			5. FUNDING NUMBERS Contract No. F08635-C-0032	
6. AUTHOR(S) Douglas M. Mackay ¹ , R. D. Wilson ¹ , M. J. Brown ¹ , William P. Ball ² , Donald P. Durfee ² , Guoshou Xia ² and Chongxuan Liu ²				
7. PERFORMING ORGANIZATION NAMES(S) AND ADDRESS(ES) ¹ Department of Earth Sciences, University of Waterloo, Waterloo, Ontario N2L 3G1, Canada ² Department of Geography and Environmental Engineering, The Johns Hopkins University, 313 Ames Hall, Baltimore, Maryland, 21218, USA			8. PERFORMING ORGANIZATION REPORT NUMBER NA	
9. SPONSORING/MONITORING AGENCY NAME(S) AND ADDRESS(ES) Armstrong Laboratory Environics Directorate (AL/EQ), Suite 2, 139 Barnes Drive, Tyndall Air Force Base, Florida 32403-5319.			10. SPONSORING/MONITORING AGENCY REPORT NUMBER AL/EQ-TR-1997-0017	
11. SUPPLEMENTARY NOTES AL/EQM Project manager was Alison Thomas, DSN 523-6303 or (904) 283-6303.				
12a. DISTRIBUTION/AVAILABILITY STATEMENT Approved for public release. Distribution unlimited.			12b. DISTRIBUTION CODE	
13. ABSTRACT (Maximum 200 words) A field-scale investigation of pump-and-treat remediation was conducted at Dover AFB, DE, in sheet-pile test cells isolating two adjacent segments of a long-extant groundwater plume. For a given volume of extracted water, the fractional removal of contaminant mass was higher for the pulse pumped cell (PPC) than the continuously pumped cell (CPC) for all contaminants whose maximum aquifer concentrations were at or very near the aquifer/aquitard interface. Overall, the results of this work indicate that contaminant transport and subsurface remediation are influenced not only by (1) spatial variability of the transport medium (aquifer), but also by (2) spatial variability in the pre-remediation contaminant distribution, and (3) spatial variability of the sorption properties of the impacted low permeability media (aquitards, clay lenses, etc.). The results of this work have been and will continue to be extrapolated from Dover-specific conditions to a variety of hydrogeologic situations via modeling to emphasize the effects of aquitard and "initial" contamination heterogeneity on long-term remediation by any method constrained by diffusion of contaminants from low permeability media.				
14. SUBJECT TERMS groundwater, remediation, pump-and-treat, pulsed pumping, field experimentation, field demonstration, volatile organic chemicals, tetrachloroethene, trichloroethene, chlorinated solvents, solute transport, sorption, diffusion, mass transfer, aquitard, sheet-piling, automated sampling, Dover AFB, Columbia Aquifer			15. NUMBER OF PAGES 207	
			16. PRICE CODE	
17. SECURITY CLASSIFICATION OF REPORT Unclassified	18. SECURITY CLASSIFICATION OF REPORT Unclassified	19. SECURITY CLASSIFICATION OF REPORT Unclassified	20. LIMITATION OF ABSTRACT Unlimited	

NSN 7540-01-280-5500

(The reverse of this page is blank)

Standard Form 298 (Rev. 2-89)
Prescribed by ANSI Std. Z39-18
298-102

[DTC QUALITY INSPECTED 3]

PREFACE

This report was prepared by the University of Waterloo, Department of Earth Sciences, Waterloo, Ontario, N2L 3G1, and the Johns Hopkins University, Department of Geography and Environmental Engineering, 313 Ames Hall, Baltimore, Maryland 21218, under U.S. Air Force Contract No. F08635-93-C-0032, for the Armstrong Laboratory Environics Directorate (AL/EQ), Suite 2, 139 Barnes Drive, Tyndall Air Force Base, Florida 32403-5323.

The report describes field and laboratory investigations of groundwater remediation by the pump and treat approach, comparing pulsed-pumping versus continuous pumping at a site with long-extant VOC contamination. The scientific goal was to identify the most significant sources of mass transfer rate limitation and to develop appropriate conceptual and computational models to describe and predict the resulting effects on aquifer decontamination. The overall practical goal was to use conceptual and computational models to identify under what site conditions and for what goals, if any, the pulsed-pumping approach might find advantageous application.

This work was performed from April 1993 through March 1997. The period through May 1996 was under Strategic Environmental Research and Development Program (SERDP) funding, whereas the necessary follow on work through March 1997 was funded by other sources available to Professors Mackay and Ball. The AL/EQ project officer was Dr. Mark Smith through May 1996 and Ms. Alison Thomas thereafter.

The authors wish to acknowledge the generous technical and other support provided by Dr. Milt Beck, Major Jim Mills, Tom Dunsmore, Bob Wikso, and Mick Mikula of the Environmental Flight of Civil Engineering (436 ST/CEV), Dover Air Force Base, DE. We also wish to thank Secretary Tolou, Mike Apgar, Bruce Patrick and others at the Delaware Department of Natural Resources, for their support and encouragement throughout this work. We are indebted to Robert Ingleton, Paul Johnson, Chris Flowers, Sam Vales and Dave Thomas (University of Waterloo technical staff) for installation of pumping and monitoring wells, installation of the test cells, pulling of soil core, and general technical assistance in setup of the site. In addition to his student co-authors, Professor Ball would like to acknowledge the important contributions to this project from a post-doctoral associate (Dr. Zhenhua Jiang), other graduate students (Dirk Young, Linnea Eng, Rick Johnston), and other graduate students (Joshua Bixby, Andy Roberts, Vikki Williams, Bill Cowan) at Johns Hopkins University, as well as Ms. Lisa Park (soil subsampling). Professor Terry Higgins, Wesley College, Dover, DE, kindly assisted us in arranging with some of his students to work as part-time local operators of our field experiments and also allowed occasional use of his laboratory facilities. The following current or former students of Wesley College were critical to the field work in providing on-site equipment maintenance, operations logging, sampling, analysis and countless other tasks: Dave Wolanski, Melissa Wong and Brian Hurd. Dr Mark Noll, Charlie Carter and others at Applied Research Associated, Dover AFB, provided invaluable support and assistance at many stages of the project. We thank Ms. Marge Kennedy and Dr. Owen Bricker of the U.S. Geological Survey (Reston, VA) for providing anion/cation/metal analyses of numerous aqueous samples. Dave Pergrin and others of EA Engineers provided advice on the groundwater treatment system and other experimental design issues, and packing media for the project air stripper was donated by Jaeger Products (Houston TX).

(The reverse of this page is blank)

EXECUTIVE SUMMARY

A field-scale investigation of pump-and-treat remediation has been conducted at Dover AFB, DE. Sheet-pile test cells were used to isolate two adjacent segments (3.5 m x 10 m) of a long-extant groundwater plume containing chlorinated solvents and their degradation by-products (PCE, TCE, TCA, *cis*-1,2-DCE, vinyl chloride) as well as aromatic organic contaminants (benzene, xylene, naphthalene, 2-methyl-naphthalene). One cell was subjected to continuous flushing and the other to intermittent (pulsed) flushing for over 200 days (pumped volumes corresponding to roughly 7 and 5 pore volumes, respectively). Monitoring of groundwater in the extraction wells and multilevel samplers allowed estimates of extracted contaminant mass and variations in contaminant distribution and elution within the cells. High-resolution core sampling (1 to 3 m horizontal spacing, 0.02- to 0.1-m vertical spacing) allowed characterization of the initial and postpumping distributions of PCE and TCE contamination. Samples of the cored material were used to characterize transport properties of the various geologic materials.

Comparison of the efficiencies of the pulse pumped cell (PPC) and the continuously pumped cell (CPC) requires careful consideration of the differences in initial conditions between the two cells. Although the cells were separated laterally by only 1.5 m and were located roughly along the centerline of the PCE and TCE plumes, our work has shown that there were important differences in contaminant distribution within them prior to initiation of the pumping experiments. Thus it was necessary to make comparisons between the cells on some normalized basis, for example mass removal as a fraction of total initially present in the cell. For a given volume of extracted water (>1 to 2 pore volumes), the fractional removal of contaminant mass was higher for the PPC than the CPC for the majority of contaminants (whose maximum aquifer concentrations were at or very near the aquifer/aquitard interface). This and other evidence suggests that the pulsed approach is slightly more efficient at mass removal for contaminants with significant reservoirs of mass in the aquitard. Given the depth of the aquitard contamination and the estimated rates of diffusion in this material, greater benefits would be expected if the duration of pump off periods could be extended beyond those studied here. On the other hand, practical pulsed-pumping approaches would not be able to reach the ideal "off" conditions we obtained (zero flow). Unless the pump-off period could be longer *and* the area influenced by "flushing" made large relative to the area re-contaminated during natural gradient flow (two potentially conflicting objectives), a large-scale pulsed-pumping approach in the Dover AFB aquifer is likely to have minimal advantage over a continuously pumped approach. Nevertheless, the knowledge gained over the course of this project has important and broader application.

Overall, the results of this work indicate that contaminant transport and subsurface remediation at this site are influenced not only by (1) spatial variability of the transport medium (aquifer), but also by (2) spatial variability in the preremediation contaminant distribution, and (3) spatial variability of the aquitard sorption properties. Our field data present a clear picture of diffusion-controlled aquitard contamination, in which persisting sorbed chemicals in the aquitard serve as a long-term source of contaminant to the otherwise relatively easily flushed aquifer. Rates of contaminant release from the aquitard are strongly dependent on both (2) and (3) above. In addition to providing valuable field evidence regarding rates of aquifer decontamination under pumped conditions, the field tests, laboratory investigations, and modeling studies conducted in this project have provided new insights into the nature of contaminant transport to and from low-permeability zones. The results of this work have been and will continue to be extrapolated from Dover-specific conditions to a variety of hydrogeologic situations via modeling to emphasize the effects of heterogeneity of permeability and "initial" contamination on long-term remediation by any method constrained by diffusion of contaminants from low permeability media.

TABLE OF CONTENTS

1. INTRODUCTION:	1
1.1. OBJECTIVES	1
1.2. BACKGROUND	2
1.3. OVERVIEW OF PROJECT APPROACH	5
1.4. REFERENCES	7
2. METHODOLOGY	12
2.1. GENERAL SITE CHARACTERISTICS	12
2.2. SITE DESIGN	17
2.3. PRELIMINARY CORING AND WATER SAMPLING	19
2.4. SHEET PILE DESIGN, INSTALLATION AND TESTING	21
2.5. SITE INSTRUMENTATION	24
2.6. REFERENCES	35
3. FIELD EXPERIMENTAL PROCEDURES	37
3.1. PUMPING SCHEDULE	37
3.2. TRACER TEST SCHEDULE	37
3.3. SAMPLING SCHEDULE	40
4. SITE CHARACTERIZATION RESULTS	43
4.1. GEOLOGY	44
4.2. INORGANIC WATER QUALITY	45
4.3. HYDRAULIC CONDUCTIVITY ESTIMATES	52
4.4. TRACER TEST RESULTS	56
4.5. SOLIDS CHARACTERIZATION STUDIES	66
4.6. REFERENCES	92
5. INITIAL AND FINAL SITE CHARACTERIZATION	96
5.1. SOIL VOC MEASUREMENTS	96
5.2. AQUEOUS-PHASE VOC ANALYSES	105
5.3. REFERENCES	117
6. MASS BALANCE CALCULATIONS	119
6.1. TETRACHLOROETHENE (PCE)	119
6.2. TRICHLOROETHENE (TCE)	123

6.3. OTHER VOCs: CIS-DCE, TCA, VC AND DCM	127
6.4. SUMMARY	129
6.5. REFERENCES	133
7. SUMMARY AND CONCLUSIONS	134
7.1. BACKGROUND.....	134
7.2. OBJECTIVES	135
7.3. APPROACH	135
7.4. RESULTS	136
7.5. CONCLUSIONS.....	137
APPENDIX A. FENCE DIAGRAMS OF CORE LOGS	139
APPENDIX B. PRE-PUMPING INORGANIC WATER QUALITY DATA.....	148
APPENDIX C. POST-PUMPING INORGANIC WATER QUALITY DATA	161
APPENDIX D. CATION EXCHANGE CAPACITY	163
APPENDIX E. SORPTION ISOTHERM STUDIES	171
APPENDIX F. SNAPSHOT VOC MEASUREMENTS -- METHODS AND ADDITIONAL SOIL CORE RESULTS	177
APPENDIX G. ELUTION DATA	186
APPENDIX H. ESTIMATION OF PRE-PUMPING AND POST-PUMPING CONTAMINANT MASS AND MASS BALANCE CALCULATIONS.....	191

LIST OF FIGURES

Figure 1	Location of the experimental site on the Dover Air Force Base, Delaware.	12
Figure 2	Layout of the facilities at the experimental site.	18
Figure 3	Locations of core collection and well installation.	20
Figure 4	Detail of the sealable joint in the Waterloo Barrier™ sheet pile.	21
Figure 5	Schematic illustration of the installation of the sheet pile....	22
Figure 6	Schematic of the extraction-injection system used in each cell.	27
Figure 7	Schematic of the Automated Sampling and Analytical Platform....	28
Figure 8	Locations of points monitored automatically for VOCs.	32
Figure 9	Timeline for major events in field experimental work.	38
Figure 10	Hydraulic conductivity results (Hvorslev well recovery test).	54
Figure 11	Injection well history for between-cell tracer test.	57
Figure 12	Sampling point history for between-cell tracer test.	59
Figure 13	Injection well history for SF ₆ tracer in CPC-IW-2	61
Figure 14	Sample point histories for SF ₆ tracer test in CPC.	62
Figure 15	Stratified layer simulations of SF ₆ response at CP-EW-2.	65
Figure 16	CXTFIT model simulations of SF ₆ response at CP-EW-2.	66
Figure 17	PCE sorption isotherms with gray sand from core B3, with linear (top) and Freundlich (bottom) interpretation.	85
Figure 18	PCE sorption isotherms with gravelly orange sand from core B3, with linear (top) and Freundlich (bottom) interpretation	86
Figure 19	PCE sorption isotherms with OCSL from core B3, with linear (top) and Freundlich (bottom) interpretation	87
Figure 20	PCE sorption isotherms with OCSL aquitard material from test cells, with linear (top) and Freundlich (bottom) interpretation	88
Figure 21	PCE sorption isotherms with PPC-11 aquitard materials, with linear (top) and Freundlich (bottom) interpretation	89
Figure 22	TCE sorption isotherms with aquitard materials, with linear (top) and Freundlich (bottom) interpretation	90
Figure 23	1,2,4-Trichlorobenzene sorption isotherms with PPC-11 OCSL material, with linear (top) and Freundlich (bottom) interpretation	91
Figure 24	Locations of final coring	97

Figure 25	Initial and final PCE concentrations in CPC and PPC (core data)	99
Figure 26	Comparison of initial and final TCE and PCE results in cores with high density sampling: initial (PPC-11) verses final (PPC-12)	100
Figure 27	Initial and final TCE concentrations in CPC and PPC (core data)	103
Figure 28	Initial and final PCE concentrations in CPC and PPC (multilevel data)	108
Figure 29	Initial and final TCE concentrations in CPC and PPC (multilevel data)	109
Figure 30	Initial and final <i>cis</i> -DCE concentrations in CPC and PPC (multilevel data)	110
Figure 31	Initial and final TCA concentrations in CPC and PPC (multilevel data)	111
Figure 32	Initial and final VC concentrations in CPC and PPC (multilevel data)	112
Figure 33	Initial and final DCM concentrations in CPC and PPC (multilevel data)	113
Figure 34	Percent cumulative removal of PCE, TCE, <i>cis</i> -DCE and TCA (normalized by total extracted mass)	122
Figure 35	Percent cumulative removal of PCE, TCE, <i>cis</i> -DCE and TCA (normalized by initial multilevel mass estimate)	126
Figure A-1	Locations of geological cross sections	140
Figure A-2	Lithologic legend	141
Figure A-3	Geological cross section (CPC1 – CPC-1')	142
Figure A-4	Geological cross section (CPC-2 – CPC-2')	143
Figure A-5	Geological cross section (PPC-1 – PPC-1')	144
Figure A-6	Geological cross section (PPC-2 – PPC-2')	145
Figure A-7	Geological cross section (Transverse-1 – Transverse-1')	146
Figure A-8	Geological cross section (Transverse-2 – Transverse-2')	147
Figure B-1	Prepumping depth profiles for the continuously pumped cell for (a) dissolved oxygen (DO) by probe, (b) DO by Chemetrics test, (c) Eh, and (d) Fe(II).	149
Figure B-1 (continued)	Prepumping depth profiles for the continuously pumped cell for (e) pH (field), (f) pH (Lab), (g) conductivity, and (h) Ca ⁺⁺ .	150
Figure B-1 (continued)	Prepumping depth profiles for the continuously pumped cell for (i) Mg ⁺⁺ , (j) Na ⁺ , (k) K ⁺ , and (l) Fe (total).	151

Figure B-1 (continued)	Prepumping depth profiles for the continuously pumped cell for (m) Al, (n) Mn, (o) Cl ⁻ , and (p) Br ⁻ .	152
Figure B-1 (continued)	Prepumping depth profiles for the continuously pumped cell for (q) NO ₃ ⁻ , (r) SO ₄ ⁻ , (s) HCO ₃ ⁻ , (t) NPOC.	153
Figure B-1 (continued)	Prepumping depth profiles for the continuously pumped cell for (u) SiO ₂ .	154
Figure B-2.	Prepumping depth profiles for the pulse-pumped cell for (a) dissolved oxygen (DO) by probe, (b) DO by Chemetrics test, (c) Eh, and (d) Fe(II).	155
Figure B-2 (continued)	Prepumping depth profiles for the pulse-pumped cell for (e) pH (field), (f) pH (lab), (g) conductivity, and (h) Ca ⁺⁺ .	156
Figure B-2 (continued)	Prepumping depth profiles for the pulse-pumped cell for (i) Mg ⁺⁺ , (j) Na ⁺ , (k) K ⁺ , and (l) Fe (total).	157
Figure B-2 (continued)	Prepumping depth profiles for the pulse-pumped cell for (m) Al, (n) Mn, (o) Cl ⁻ , and (p) Br ⁻ .	158
Figure B-2 (continued)	Prepumping depth profiles for the pulse-pumped cell for (q) NO ₃ ⁻ , (r) SO ₄ ⁻ , (s) HCO ₃ ⁻ , (t) NPOC.	159
Figure B-2 (continued)	Prepumping depth profiles for the pulse-pumped cell for (u) SiO ₂ .	160
Figure C-1.	Postpumping depth profiles: (a) dissolved oxygen (DO) by probe in the CPC, (b) Fe(II) in the CPC, and (c) DO (by probe) in the PPC.	162
Figure F-1	Results of Prepumping and Postpumping Concentrations of TCE (top) and PCE (bottom) in Selected Downgradient CPC Soil Cores.	181
Figure F-2	Results of prepumping and postpumping concentrations of TCE (top) and PCE (bottom) in selected mid-cell CPC soil cores.	182
Figure F-3	Results of prepumping and postpumping concentrations of TCE (top) and PCE (bottom) in selected downgradient PPC soil cores.	183
Figure F-4	Results of prepumping and postpumping concentrations of TCE (top) and PCE (bottom) in selected mid-cell PPC soil cores.	184
Figure G-1	Selected elution curves for the combined effluent of the CPC extraction wells (CP-EXT).	188
Figure G-2	Selected elution curves for the combined effluent of the PPC extraction wells (PP-EXT).	188
Figure G-3	Selected elution curves for the sampling point CP-ML-8-1	189
Figure G-4	Selected elution curves for the sampling point PP-ML-8-1	189
Figure G-5	Selected elution curves for the sampling point CP-ML-8-2	190
Figure G-6	Selected elution curves for the sampling point PP-ML-8-2	190

Figure H-1	Surface contour map of OSCL and DGSL layers	204
Figure H-2	Cumulative mass removal of PCE and TCE vs. volume of water pumped	205
Figure H-3	Cumulative mass removal of <i>cis</i> -DCE, TCA, VC, and DCM vs. volume of water pumped	206

LIST OF TABLES

Table 1	Summary of piezometer installation and core acquisition depth intervals.	25
Table 2	Volume of sample loops on ASAP at Dover AFB.	30
Table 3	Method detection limits for various analytes.	34
Table 4	Results of test of carryover during automated analysis of VOCs.	35
Table 5	Timing of major events during field experiments.	39
Table 6	Overview of core logging results for DAFB test cells.	46
Table 7	Inorganic water quality sampling -- snapshot sampling events	47
Table 8	Average concentrations and mean injection times for between-cell tracer test.	58
Table 9	Parameter estimates for model-simulated SF ₆ transport at multilevel monitoring points.	64
Table 10	CXTFIT parameters for simulating CPC transport to CP-EW-2 as a single-layered porous medium.	65
Table 11	Amalgamated samples of subsurface aquifer solids at DAFB, DE.	68
Table 12	Mineralogical analysis by optical microscopy.	71
Table 13	Characteristics of DAFB aquifer and aquitard samples.	74
Table 14	Particle size distribution of amalgamated samples	77
Table 15	Simplified particle size distributions of four major strata.	78
Table 16	Organic carbon content of DAFB solids.	81
Table 17	Selected PCE and TCE sorption data with DAFB solids.	83
Table 18	Initial aqueous concentrations of chlorinated VOCs (µg/L)	106
Table 19	Initial aqueous concentrations of aromatic VOCs (µg/L)	107
Table 20	Final aqueous concentrations of chlorinated VOCs (µg/L)	114
Table 21	Final aqueous concentrations of aromatic VOCs (µg/L)	115
Table 22	Comparison of initial and final aqueous concentrations of chlorinated VOCs (µg/L)	116
Table 23	Comparison of initial and final aqueous concentrations of aromatic VOCs (µg/L)	117
Table 24	PCE mass (grams) in aquifer and aquitard of test cells	120
Table 25	Extracted and calculated mass removal of each compound	120
Table 26	TCE mass (grams) in aquifer and aquitard of test cells	124
Table 27	Initial, final and calculated % removed of all six VOCs	128

Table D-1	CEC results for subsurface samples from Dover AFB, DE	165
Table D-2	Summary of individual CEC results for subsurface samples from Dover AFB, DE	166
Table E-1.	Summary of K_d experiments with PCE --- rate experiments	172
Table E-2	Summary of K_d experiments with PCE --- single concentration	173
Table E-3	Summary of K_d experiments with PCE --- full isotherms	174
Table E-4	Summary of K_d experiments with TCE	175
Table E-5	Summary of complete sorption isotherm data	176
Table H-1	Densities, moisture contents and porosities used in mass estimation	194
Table H-2	K_{ow} , K_{om} , K_d and R used in mass estimation from aqueous concentrations	196
Table H-3	Mass estimates for TCE and PCE: core and multilevel snapshots	200
Table H-4	Mass estimates for all six VOCs: multilevel snapshots	200
Table H-5	Mass of TCE in aquitard layers by two methods	201
Table H-6	Average concentrations of TCE in aquitard layers	201
Table H-7	Mass of PCE in aquitard layers by two methods	202
Table H-8	Average concentrations of PCE in aquitard layers	202
Table H-9	Total mass of six VOCs extracted by pumping	203

1. INTRODUCTION

The most commonly applied technique for cleanup of aquifers contaminated by organic chemicals is the "pump-and-treat" approach, in which a network of extraction wells is used to withdraw the contaminated groundwater for above-ground treatment (Mercer et al., 1990; NRC, 1994). Typical experience with this technique has been that aqueous concentrations of contaminant decrease over time, with removal rates becoming low, even while contaminant concentrations in the subsurface remain above cleanup goals (Mackay and Cherry, 1989; Olsen and Kavanaugh, 1993; Travis and Doty, 1990). This effect is usually attributed to slow mass transfer of contaminants into the flowing aqueous phase, due to some combination of slow dissolution of non-aqueous-phase liquids, slow diffusion from less permeable strata of the media, and slow desorption of sorbed contaminants from aquifer solids (NRC, 1994). Theoretical considerations suggest that there may be important advantages to periodically ceasing or slowing groundwater extraction to allow time for these slow rate processes to attain or approach equilibrium (Harvey et al., 1994; Jiang and Ball, 1994; Keely et al., 1987; Murdock et al., 1989; Sullivan, 1996), although field data to confirm this effect are currently lacking. Although intermittent pumping schemes (hereafter referred to as "pulsed pumping") are not expected to decrease the overall time for aquifer remediation, the mass of contaminant removed per unit volume of extracted water is expected to be higher than in the continuously pumped case. Resulting advantages are thought to include decreased pumping cost, lower volumes of water for above-ground treatment, and less total groundwater extraction, a feature of potentially special importance in more arid areas.

1.1. OBJECTIVES

The primary objective of this project is to determine whether there are discernible advantages of a pulsed-pumping strategy compared to continuous pumping at a "real-world" site where contamination of the groundwater and subsurface solids by volatile organic contaminants (VOCs) has been long extant. As described in more detail later, the approach taken was to conduct side-by-side controlled experiments in two isolated portions of a contaminated sand/gravel aquifer, subjecting the isolated portions of the aquifer to either continuous or pulsed

pumping, and thoroughly characterizing each with respect to the subsurface contaminant distribution both before and after the pumping. The underlying scientific goal is to identify the most significant sources of mass transfer rate limitation at the field site and to develop appropriate conceptual and computational models to describe and predict the resulting effects on aquifer decontamination. Finally, the overall practical goal is to use conceptual and computational models to identify under what site conditions and for what goals, if any, the pulsed-pumping approach might find advantageous application.

1.2. BACKGROUND

Numerous authors have discussed the role of mass transfer limitations in slowing groundwater cleanup (Mackay and Cherry, 1989; Mutch et al., 1993; NRC, 1994; Wilson, 1992). It is generally agreed that the following are the three major mass transfer limitations for saturated zones contaminated with VOCs: 1) slow dissolution of non-aqueous-phase liquids (NAPLs) into the groundwater, 2) diffusive transfer of contaminant mass from low-permeability zones (originally contaminated by diffusion of contaminants from source plumes in the more permeable strata), and 3) desorption of contaminant mass from aquifer media. Because dissolution of subsurface NAPL may in some cases take decades or centuries, it is now recognized that full remediation of subsurface source zones containing NAPL is practically infeasible by pump-and-treat techniques (NRC, 1994). When the subsurface source is isolated or insignificant, pump-and-treat can be used to effectively remediate the plume (i.e. the dissolved and sorbed phase contaminants) to meet typical regulatory criteria (Bartow and Davenport, 1995); however, even in these situations, mass transfer limitations are still likely to limit the overall rate of the remediation process, and may still be critical factors determining the success or failure of the effort (Mackay and Cherry, 1989; NRC, 1994). Such limitations become increasingly severe over the course of the remediation, since mass transfer fluxes are proportional to concentration driving forces which decline over the course of remediation.

Laboratory soil column and batch studies have demonstrated that mass transfer limitations to the rates of sorption and desorption of organic chemicals can be sufficiently severe to affect solute transport under the rapid flow conditions encountered (or induced) during remediation of

contaminated sites by groundwater extraction or injection (Ball and Roberts, 1991a; Ball and Roberts, 1991c; Grathwohl and Reinhard, 1993; Harmon and Roberts, 1994; Miller and Pedit, 1992; Oliver, 1985; Pavlostathis and Mathavan, 1992; Pignatello and Xing, 1996; Rabideau and Miller, 1994; Young and Ball, 1994). In fact, in some cases particle-scale mass transfer can be slower than conventionally conducted laboratory column experiments will detect (Ball and Roberts, 1991b; Ball and Roberts, 1991c). Although in such cases the long-term distribution coefficients (K_d) are not elucidated by conventional (short-term) batch or column experiments, they are likely to be relevant to field-scale contaminant transport and remediation (Ball and Roberts, 1991c; Miller and Pedit, 1992). In addition, there is an increasing body of evidence to suggest that so-called sorption hysteresis is simply an effect in which desorption is initiated before sorptive equilibrium has been reached (Miller and Pedit, 1992). Under such situations (where sorption is not at equilibrium when desorption is initiated), desorptive mass fluxes will be reduced (relative to an equilibrium starting point) owing to the lower driving force for diffusion, as well as by the on-going sorption into the regions not previously saturated with contaminant.

The above-described phenomena also apply at the larger scales of diffusion encountered in field-scale remediation. That is, the particle-scale rate effects noted above are likely to be overshadowed by still more significant mass transfer limitations occurring at the scale of impermeable geologic formations or inclusions (Jiang and Ball, 1994; Mutch et al., 1993; Rabideau and Miller, 1994; Wilson, 1992). For example, computer simulations of long-term, field-scale solute transport at the Borden site (Ball et al., 1990; Goltz and Roberts, 1986; Goltz and Roberts, 1988) have implied mass transfer limitations (presumably related to field heterogeneity) that are roughly 50 times slower than those implied by the batch experiments. In other field studies where conditions were sufficiently controlled to allow investigation of mass transfer effects (e.g., Bahr, 1989; Harrison and Barker, 1987; Roberts et al., 1991; Wood et al., 1990), sorption nonequilibrium has also been implicated, and there are numerous instances of slow remediation (and apparent groundwater nonequilibrium) at operating remediation sites.

In field situations, contaminants have typically been in contact with the aquifer solids for years or even decades. This long exposure time allows contaminants (initially in more permeable strata) to diffuse or be slowly convected into lower permeability zones, which sufficiently

contaminates these zones so that they then serve as long-term contamination sources during remediation. As with the particle-scale effects, however, the duration of contamination may not have been sufficient for equilibrium to have been achieved. Also in accordance with the particle-scale discussion, such a situation may lead to very slow mass fluxes during desorption (cleanup) and remediation times substantially longer than the duration of initial contamination. On the other hand, in some field situations, the less permeable zones may be sufficiently conductive that contaminants will be flushed at rates faster than the diffusion to more permeable zones. In these cases, remediation may still be slow, but will be controlled by the spatial variability of the hydraulic conductivity. This was the case in a field test in which TCE and TCA were flushed from within an existing contaminant plume in a sand aquifer at the Rocky Mountain Arsenal [Mackay et al., 1988; Thorbjarnarson and Mackay, 1997]. Irrespective of the nature of the controlling mechanism, the slow mass transfer from less conductive (or impermeable) zones will be exacerbated if there is relatively higher sorptive partitioning (higher K_d); this has yet to be shown in field results but is an expected outcome, owing to retardation of both the diffusion and convection processes (Valocchi, 1988; Valocchi, 1989).

Within the above context, the concept behind pulsed pumping is to cease the intensive pump-and-treat process periodically in order to allow the slow mass transfer from less accessible zones to "catch up" with the more rapid removal from permeable zones. In particular, pump off (or reduced pump rate) cycles represent periods during which slow processes of diffusion may act to decrease contaminant mass in less permeable zones, while replenishing mobile phase concentrations. Although continuous pumping actually removes contamination faster (by providing continuously low concentrations in the mobile phase), pulsed pumping may serve to significantly reduce costs and conserve groundwater resources in many situations. Pumping costs will be lower than during the intensive "full pump" periods and, perhaps more important, significant treatment costs and groundwater wastage can be avoided. Groundwater wastage can be an especially important consideration in arid regions where the water extracted from contaminated aquifers may not in all cases be accepted for reinjection even after extensive treatment, thus depleting important groundwater resources during their remediation. In such cases, it may be argued that minimization of pumped volume is a very important goal for groundwater remediation efforts [Smith and Mackay, 1991].

Pulsed groundwater pumping has been previously promoted in the context of aquifer remediation (Keely et al., 1987) and the process has been recognized as an "available technology" (Murdock et al., 1989). The advantages of pulsed or cyclic pumping have also been recognized by practitioners attempting to remediate aquifers by "soil venting" or vapor phase extraction. However, to our knowledge, there have been no applications of pulsed pumping at remediation sites that have been sufficiently controlled to conclusively demonstrate the advantages of pulsing. In particular, no field information is available regarding the potential benefits of the strategy for VOC removal from unconsolidated sandy aquifers, despite the fact that a large fraction of the contamination plumes nationwide are of this type and are most commonly remediated by pump-and-treat methods (Mackay and Cherry, 1989).

1.3. OVERVIEW OF PROJECT APPROACH

The project was initiated by collaboration between the University of Waterloo, Johns Hopkins University and the Armstrong Laboratory (Tyndall Air Force Base, FL) to find an Air Force site suitable for this research. We sought a well-studied, mildly heterogeneous, moderately sorbing sand/gravel aquifer impacted for at least a decade with chlorinated VOCs at concentrations several orders of magnitude above typical practical quantification levels. Furthermore, we sought a site where the water table was within 20 feet of ground surface (to allow sampling by pumps at surface) and where a competent clayey aquitard was within 50 feet of ground surface (to form the bottom of the isolated portions of the aquifer, as described below). Finally, we sought a site with available power and other utilities, ease of access, security, and other amenities necessary for the research.

After reviewing a number of alternative sites at varying levels of detail, Dover Air Force Base, DE, was chosen as the most ideal location. The group then worked with staff at Dover Air Force Base (hereafter referred to as DAFB) to identify a specific site on base with as nearly optimal characteristics as possible. The site finally selected at DAFB met most of the criteria, as described in subsequent sections.

The next step was to confirm by preliminary monitoring efforts (coring and water sampling) that the properties of the selected site were as anticipated from the data available from prior area-

wide investigations (i.e., early draft copies of Dames & Moore, 1994). Although the aquifer solids at the DAFB site turned out to be more weakly sorbing than desired, its many other advantages and the fact that no better alternatives had been identified sealed the decision to proceed.

The site was prepared for the experiments by installing side-by-side sheet piling boxes, driven from surface through the aquifer into the underlying aquitard. Each box (or "cell") was extensively cored and instrumented with various types of wells. (This activity, initially scheduled for November, 1993, occurred in the period between Sept. 12 and Sept. 27, 1994, owing to administrative delays beyond our control.) During cell instrumentation, soil core were taken at many of the locations of subsequent well installation, as detailed subsequently. Analyses of both the core solids and initial (multilevel) water samples were conducted to estimate the three-dimensional distribution and total amount of contaminant mass within each cell prior to the experiments. A tracer test was conducted between the cells to evaluate the heterogeneity of groundwater flow in the aquifer and to provide preliminary data important for planning the sampling schedule for the contaminant elution tests within the cells.

The experiments were conducted in each cell in the same manner: groundwater was taken from three fully screened extraction wells at one end of the cell, treated to remove VOCs, spiked with a tracer for appropriate periods of time, and reinjected into three fully screened injection wells at the other end of the cell. Monitoring of VOCs in the extracted and injected water, as well as various points within the cells, was conducted using an on-site sampling and analytical system. In one cell water (the continuously pumped cell, or CPC), the extraction and injection were continuous for a full 5.3-month duration, leading to a continuous flush of the subsurface by the injected contaminant-free. Conditions within the CPC were meant to simulate continuous pump-and-treat remediation, during which uncontaminated groundwater (i.e., groundwater exterior to the plume) is pulled through the contaminated zone, flushing contaminants toward the extraction well(s). In the other cell (the pulse-pumped cell, or PPC), injection and extraction occurred for roughly 3 to 4 week periods at a rate similar to that in the CPC, between which the pumping was stopped for a similar duration. The pumps-on/pumps-off cycles were repeated several times in order to simulate a pulsed pump-and-treat effort. (Here we note that, during the

non-pumping periods, the conditions within the PPC were more ideally stagnant than normally possible, because of its isolation from the rest of the aquifer. Total duration of PPC operations was longer than that of the CPC, in order that final volumes of water pumped might approach similar values. During the implementation of the field tests, laboratory studies of the aquifer solids were continued and modeling efforts refined to build a body of knowledge to apply to eventual interpretation of the field results.

After the field experiments were complete, a final round of coring and water sampling was conducted in each cell to allow estimation of the amount of contaminant mass remaining in the subsurface after remediation. The water and solid sampling before and after the tests thus provided two important means of estimating the mass of contaminants removed from each cell. The data on VOCs in the extracted water from each cell provided a third estimate for comparison. These estimates, the method by which they were obtained, and the conclusions and implications to be drawn from them are the primary subjects of this report.

In addition to the overall mass estimates noted above, data from some of the individually analyzed soil cores and sampling locations were obtained. Although not a primary focus of the project, these results are also reported herein, since they have provided some critically important information relevant to our overall conclusions.

1.4. REFERENCES

- Bahr, J.M., 1989. Analysis of Nonequilibrium Desorption of Volatile Organics during Field Test of Aquifer Decontamination. *Journal of Contaminant Hydrology*, 4(3): 205 - 222.
- Ball, W.P., Goltz, M.N. and Roberts, P.V., 1990. Sorption Rate Studies with Halogenated Organic Chemicals and Sandy Aquifer Material - Implications for Solute Transport and Groundwater Remediation, *National Conference on Environmental Engineering*. American Society of Civil Engineers, Washington, D.C.
- Ball, W.P. and Roberts, P.V., 1991a. "Diffusive Rate Limitations in the Sorption of Organic Chemicals." In: R.A. Baker (Editor), *Organic Substances and Sediments in Water: Processes and Analytical*. Lewis Publishers, Chelsea, MI, pp. 273-310.

- Ball, W.P. and Roberts, P.V., 1991b. Long-Term Sorption of Halogenated Organic Chemicals -- Part 1. Equilibrium. *Environmental Science and Technology*, 25(7): 1223 - 1237.
- Ball, W.P. and Roberts, P.V., 1991c. Long-Term Sorption of Halogenated Organic Chemicals -- Part 2. Intraparticle Diffusion. *Environmental Science and Technology*, 25(7): 1237 - 1249.
- Bartow, G. and Davenport, C., 1995. Pump-and-Treat Accomplishments: A Review of the Effectiveness of Ground Water Remediation in Santa Clara Valley, California. *Ground Water Monitoring and Remediation*, XV(2): 140-146.
- Dames & Moore, 1994. *Area 6 Remedial Investigation; Dover Air Force Base, Dover, Delaware*. Report prepared for U.S. Dept. of the Air Force, Dover Air Force Base, 436 SG/CEV, Dover, DE, Dames & Moore, Inc., Bethesda, MD.
- Goltz, M.N. and Roberts, P.V., 1986. Interpreting Organic Solute Transport Data from a Field Experiment Using Physical Nonequilibrium Models. *Journal of Contaminant Hydrology*, 1(1): 77 - 93.
- Goltz, M.N. and Roberts, P.V., 1988. Simulations of Physical Solute Transport Models: Application to a Large-Scale Field Experiment. *Journal of Contaminant Hydrology*, 3(1): 37 - 63.
- Grathwohl, P. and Reinhard, M., 1993. Desorption of Trichloroethylene in Aquifer Material: Rate Limitation at the Grain Scale. *Environmental Science and Technology*, 27(12): 2360-2366.
- Harmon, T., C. and Roberts, P.V., 1994. Comparison of Intraparticle Sorption and Desorption Rates for a Halogenated Alkene in a Sandy Aquifer Material. *Environmental Science and Technology*, 28(9): 1650-1660.
- Harrison, E.M. and Barker, J.F., 1987. Sorption and Enhanced Biodegradation of Trace Organics in a Groundwater Reclamation Scheme -- Gloucester Site, Ottawa, Canada. *Journal of Contaminant Hydrology*, 1(4): 349 - 373.

- Harvey, C.F., Haggerty, R. and Gorelick, S.M., 1994. Aquifer remediation: A method for estimating mass transfer rate coefficients and an evaluation of pulsed pumping. *Water Resources Research*, 30: 1979 - 1991.
- Jiang, Z. and Ball, W.P., 1994. "Computer Simulation of Pulsed Pumping for Remediation Under Mass Transfer Limited Conditions," *Critical Issues in Water and Wastewater Treatment: Proceedings, 1994 National Conference on Environmental Engineering*. Environmental Engineering Division, ASCE, N.Y., N.Y., pp. 352-359.
- Keely, J.F., Palmer, C.D., Johnson, R.L., Piwoni, M.D. and Enfield, C.D., 1987. "Optimizing Recovery of Contaminant Residuals by Pulsed Operation of Hydraulically Dependent Remediations."
- Mackay, D.M. and Cherry, J.A., 1989. Groundwater Contamination: Pump-and-Treat Remediation. *Environmental Science and Technology*, 23: 630 - 636.
- Mercer, J.W., Skipp, D.C. and Giffin, D., 1990. *Basics of Pump-and-Treat Ground-Water Remediation Technology*. EPA 600/8-90/003, EPA, Ada, OK.
- Miller, C.T. and Pedit, J.J., 1992. Use of a Reactive Surface-Diffusion Model to Describe Apparent Sorption-Desorption Hysteresis and Abiotic Degradation of Lindane in a Subsurface Material. *Environmental Science and Technology*, 26(7): 1417-1427.
- Murdock, L., Patterson, B., Losonsky, G. and Harrar, W., 1989. *Technologies of Delivery or Recovery for the Remediation of Hazardous Waste Sites*. EPA 600/2-89/066, Environmental Protection Agency, Risk Reduction Engineering Laboratory, Cincinnati.
- Mutch, R.D., Jr., Scott, J.I. and Wilson, D.J., 1993. Cleanup of Fractured Rock Aquifers: Implications of Matrix Diffusion. *Environmental Monitoring and Assessment*, 24: 45-70.
- NRC, 1994. *Alternatives for Groundwater Cleanup*. National Academy Press, Washington, DC, 315 pp.
- Oliver, B.G., 1985. Desorption of Chlorinated Hydrocarbons from Spiked and Anthropogenically Contaminated Sediments. *Chemosphere*, 15(8): 1087 - 1106.

- Olsen, R.L. and Kavanaugh, M.C., 1993. Can Groundwater Restoration Be Achieved? *Water Environment and Technology*, 5(3): 42 - 47.
- Pavlostathis, S.G. and Mathavan, G.N., 1992. Desorption Kinetics of Selected Volatile Organic Compounds from Field Contaminated Soils. *Environmental Science and Technology*, 26(3): 532 - 538.
- Pignatello, J.J. and Xing, B., 1996. Mechanisms of Slow Sorption of Organic Chemicals to Natural Particles. *Environmental Science and Technology*, 30(1): 1-11.
- Rabideau, A.J. and Miller, C.T., 1994. Two-dimensional modeling of aquifer remediation influenced by sorption nonequilibrium and hydraulic conductivity heterogeneity. *Water Resources Research*, 30(5): 1457 - 1470.
- Roberts, P.V., Hopkins, G.D., Mackay, D.M. and Semprini, L., 1991. A Field Evaluation of In-Situ Biodegradation of Chlorinated Ethenes: Part 1, Methodology and Field Site Characterization. *Ground Water*, 28(4): 591 - 604.
- Sullivan, R.A., 1996. Pump and Treat and Wait. *Civil Engineering*: 8A-12A.
- Thorbjarnarson, K. W., and D. M. Mackay, 1997. A Field Test of Tracer Transport and Organic Elution in a Stratified Aquifer at the Rocky Mountain Arsenal, *Contaminant Hydrology*, 24(3-4): 287 - 312.
- Travis, C.C. and Doty, C.B., 1990. Can Contaminated Aquifers at Superfund Sites be Remediated? *Environmental Science and Technology*, 24(10): 1464 - 1466.
- Valocchi, A.J., 1988. Theoretical Analysis of Deviations from Local Equilibrium During Sorbing Solute Transport Through Idealized Stratified Aquifers. *Journal of Contaminant Hydrology*, 2(3): 191 - 207.
- Valocchi, A.J., 1989. Spatial Moment Analysis of the Transport of Kinetically Adsorbing Solutes Through Stratified Aquifers. *Water Resources Research*, 25(2): 273 - 279.
- Wilson, J.L., 1992. "Removal of Aqueous Phase Dissolved Contamination: Non-Chemically Enhanced Pump and Treat." In: C.H. Ward (Editor), *Subsurface Restoration Conference Proceedings*. Rice University, Houston.

- Wood, W.W., Kraemer, T.F. and Hearn, J.P., 1990. Intragranular Diffusion: An Important Mechanism Influencing Solute Transport in Clastic Aquifers? *Science*, 247: 1569 - 1572.
- Young, D.F. and Ball, W.P., 1994. A Priori Simulation of Tetrachloroethene Transport Through Aquifer Material Using an Intraparticle Diffusion Model. *Environmental Progress*, 13: 9 - 20.

2. METHODOLOGY

2.1. GENERAL SITE CHARACTERISTICS

The selected experimental site is located at DAFB, east of U.S. Route 113 (**Figure 1**). Specifically, the site is in a grass-covered field near Building #459, roughly 50 meters east of Arnold Drive and 25 meters south of 9th Street. Topography is flat and there are no surface water bodies in the near vicinity. The experimental site overlies a plume of ground water contamination in an unconfined coastal plain aquifer referred to as the Columbia Aquifer (Dames & Moore, 1994). As described below, the contaminant plume originates from upgradient releases, the nearest of which is believed to lie roughly 450 meters upgradient, and with contamination having started on the order of 30 years ago. Thus the site was far enough from the source(s) so that NAPL phase was unlikely to be present in the saturated zone but near enough so that the aquifer media had likely been exposed to VOC contamination for a decade or more.

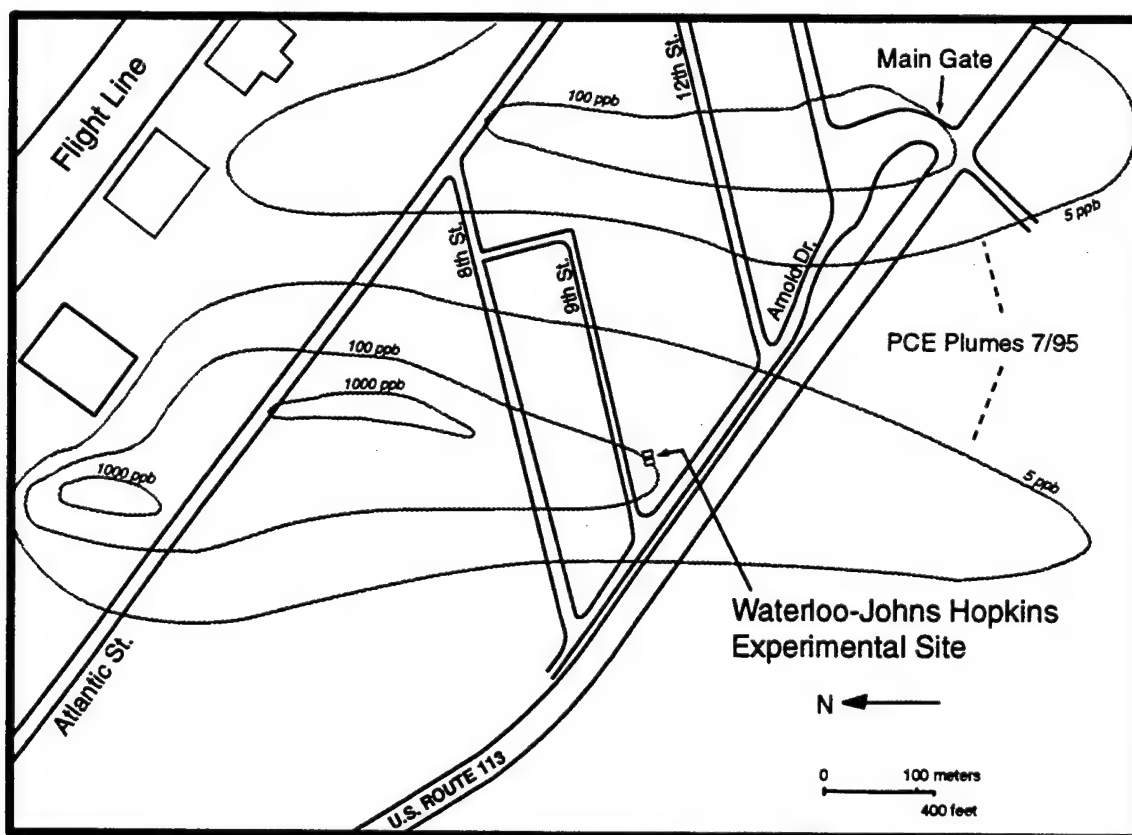


Figure 1. Location of the Experimental Site on the Dover Air Force Base, Delaware.

Hydrogeologic conditions in the vicinity have been described previously in HAZWRAP (1990, 1991), Dames & Moore (1990, 1991, 1994), and EA Engineers (1992). The surficial aquifer below the study area consists predominantly of poorly sorted fine to coarse grained sand containing localized lenses of silt, clay, and gravel. In general, the subsurface material comprises fine to medium sand in the upper 6.1 meters (20 feet) below ground surface (bgs) (intermixed with some noncontiguous gravel and clay layers, as noted subsequently), with a clearly defined region of a more uniform gray-white medium sand from roughly 6.1 to 9.1 meters (20 to 30 feet) bgs and a second clearly defined region of orange to rust-colored coarse sand and gravel from roughly 9.1 to 14.3 meters (30 to 47 feet) bgs. This sandy formation has commonly been referred to as the Columbia Formation in prior studies (Dames & Moore, 1994), but the site is now believed to include either the Scotts Corners Formation or Lynch Heights formation (above roughly 9.1 meters bgs), overlying Columbia Formation material (Ramsey, 1993 and personal communication, K.W. Ramsey, 1996). As described elsewhere (Ramsey, 1993; Ramsey and Xchenck, 1990), the Scotts Corners and Lynch Heights formations are believed to be of Late Pleistocene age, and both are interpreted as depositional environments associated with an ancestral location of the Delaware Bay (Lynch Heights) and its associated estuaries, beaches, and/or marshes (Scotts Corners). The Scotts Corners Formation has been interpreted to be more recent than the Lynch Heights formation, although both are interpreted to have resulted from a cycle of sea-level rise and fall subsequent to that which created the underlying Columbia Formation. The Columbia formation is believed to be of Early Pleistocene age.

The groundwater table near the study site is located on the order of 3.7 meters (12 feet) above mean sea level, at approximately 4.6 to 4.9 meters (15 to 16 feet) below ground surface (bgs). Groundwater flow direction in the Columbia Aquifer is generally to the south at the site, with previously measured hydraulic conductivity in the range of 0.017 to 0.052 cm/sec (pump tests) and 0.0021 cm/sec to 0.0044 cm/sec (slug tests), with the former believed to more accurately reflect aquifer characteristics owing to the larger volume affected by such tests (Dames & Moore, 1994). A hydraulic gradient in the range of 0.0008 to 0.0019 has been estimated, with groundwater velocity (assuming an "average" hydraulic conductivity of 0.035 cm/sec and a porosity of 0.3) estimated to fall in the range of 0.08 to 0.19 m/day and groundwater flow generally to the south-southeast in the area of our site (Dames & Moore, 1994). There is some

seasonal variation in groundwater elevations and flow directions. Hydraulic heads in the shallow (upper 8 feet) and deep (bottom 10 feet) of the unconfined Columbia Aquifer were often observed to be identical, with vertical hydraulic gradients estimated to average only 6×10^{-4} [Dames & Moore, 1994].

The Columbia aquifer overlies a low-permeability material tentatively identified as the Upper Confining Unit of the Calvert Formation, which serves as a confining layer (aquitard) separating the overlying Columbia Aquifer and the underlying Frederica aquifer [Dames & Moore, 1994]. A sharp aquifer/aquitard interface was found to be ubiquitously present at depths between 14.0 and 14.6 meters below ground surface (bgs) in all cores that have been taken to date from the research site (27 cores over a roughly 150 square meter area). A study over a larger region around our site [Dames & Moore, 1994] has shown that the aquitard thickness is typically between 4.3 m and 6.7 m in this region and the hydraulic conductivity (K) of the aquitard material has been estimated to range between 2×10^{-8} and 3×10^{-7} cm/sec, based on laboratory measurements [Dames & Moore, 1994]. To our knowledge, hydraulic gradients in and across the aquitard have not been measured. In this context, others have shown that diffusion is likely to dominate solute transport when vertical velocities are less than 0.2 cm/year [Johnson et al., 1989]. Assuming the given estimates of aquitard permeability, a downward hydraulic gradient of roughly 0.02 to 0.3 would be required to yield such a vertical velocity in the aquitard at this site.

An overview of the contaminant plume in the Columbia Aquifer, within which the experiments described herein were conducted, is provided by Dames & Moore (1994). The apparent source of much if not all of the chlorinated solvent contamination is located about 450 meters north (upgradient) of the experimental site, at a site referred to as WP-21 and previously identified as T-1 (Dames & Moore, 1994)). Site WP-21 consisted of a series of industrial waste basins, oil water separators, and settling basins. The industrial waste basins accepted wastes from an engine overhaul shop and other base facilities between 1963 and 1981. The accepting basins were closed in 1986. The soils around the area were excavated in 1986 and the area backfilled and capped at that time. Groundwater in the area has been under monitoring supervision since (Dames & Moore, 1994). More recently, subsurface pure-phase trichloroethene (TCE) contamination has been found at a nearby location, located roughly 110

meters northeast (550 meters from our test site), along the northeast edge of Building 719. This source is believed to be associated with a broken underground storage tank drainage line in this area (personal communication, Mr. Charles C. Mikula, Chief Restoration Element, DAFB).

Also, in an area between 200 and 300 meters north-northeast of our site is the site of a fuel oil tank farm and a 1980 diesel fuel tank spill, identified as OT54 and SS36, respectively (formerly FOTF and SP-2) (Dames & Moore, 1994). Dames & Moore (1994) note that 1991 investigations at this location (HAZWRAP 1991) found evidence of a wide range of polyaromatic hydrocarbons in soil samples at this location (total PAH on the order of 10^2 to 10^5 ug/kg), as well as lower concentrations (4 to 30 ug/kg) of acetone, methylene chloride, and 1,1,1-TCA, and that ethylene glycol (deicing agent) storage and subsurface release also occurred at the site. More recent groundwater investigations suggest that remaining effects on groundwater include only dimethyl-phthalate and naphthalene, with chlorinated organic contamination of the site groundwater attributed to upgradient sources near WP-21.

Dames & Moore (1994) also describe monitoring data from "shallow" well screens installed close to the water table and "deep" well screens located at the base of the Columbia Aquifer. Groundwater contamination close to and downgradient of site WP-21 consists predominantly of a variety of chlorinated aliphatic compounds. The most concentrated and widespread of these pollutants are trichloroethylene (TCE), tetrachloroethylene (PCE), and 1,2-dichloroethylene (1,2-DCE). The monitoring data are consistent with the occurrence of biological reductive dechlorination processes within the plume, a matter under investigation by the Remedial Technology Development Forum (RTDF) due to its potential importance for intrinsic bioremediation of the chlorinated aliphatic compounds in the groundwater.

Monitoring data from September 1989 (HAZWRAP, 1990) showed that, close to Site WP-21, contaminants were detected in both the shallow and deep wells. It is likely that some of the VOC mass entered the subsurface as dense non-aqueous phase liquids (DNAPLs) at this location, with at least some of the contaminants penetrating downwards through the vadose and saturated zones and subsequently dissolving into the groundwater. With this scenario of DNAPL contamination throughout the saturated groundwater zone, the contamination plume at this location is likely to span (or at least to have spanned) the entire saturated thickness of the

Columbia Aquifer. However, the majority of the downgradient contaminant plume is located near the base of the Columbia Aquifer, perhaps due to a combination of factors including 1) the most permeable units in the Columbia Aquifer are coarse sand and gravel strata which occur predominantly in the lower 3 meters (10 feet) of the aquifer and which may have served as a preferred path for contaminant migration downgradient; 2) most of the DNAPL mass from site WP-21 may have migrated down to the upper surface of the Kirkwood Formation, thus leading to a stronger source at depth than in shallower strata; and 3) microbial bioremediation in the upper aquifer regions was more successful, possibly related to fluxes of other contaminants from the OT54 site. (For example, the lighter than water (or highly soluble) non-chlorinated contaminants at the OT54 site may have preferentially contaminated the upper portion of the saturated aquifer and subsequently served as critically needed carbon sources and/or electron acceptors for the microbial degradation process in this zone.)

Irrespective of cause, samples from well locations further downgradient of site WP-21 show chlorinated contaminants to be virtually absent from shallow wells but still present in the groundwater at deeper screened intervals. An example is well nest MW-236 located about 360 meters south (downgradient) of Site WP-21 and about 150 meters north-northeast of our experimental site. At MW-236, samples from a "deep" well screened from about 10.7 to 13.7 meters (35 to 45 feet) bgs contained 350 ppb TCE, 74 ppb PCE, and 6300 ppb 1,2-DCE. Samples from a "shallow" well screened from approximately 3.0 to 6.1 meters (10 to 20 feet) bgs at the MW 236 location indicated no detectable TCE, PCE, or 1,2-DCE. Detailed monitoring of our experimental site, discussed later, confirm that the plume is confined to the lower portion of the Columbia Aquifer.

A working hypothesis of this project has been that biotransformation of contaminants over the 9-month duration of the field experiments may be of negligible concern within our test cells, especially once oxygen has been re-introduced into the subsurface via the pump-and-treat scheme. A corollary of this hypothesis is that most of the less-chlorinated "biotransformation products" that we initially see at our location (e.g. *cis*-DCE, VC) are the result of upgradient natural dehalogenation processes, particularly since upgradient locations have historically had a better supply of the more soluble and biodegradable organic contaminants that typically serve as

carbon sources and electron donors for such anaerobic biological processes. As discussed later in this report, initial conditions at our location were only mildly reducing, and therefore perhaps not ideal for reductive dehalogenation. On the other hand, as discussed later, there is also clear evidence that reductive dehalogenation has occurred in the deeper levels of the aquifer, at least upgradient. In addition to the VOC intermediate reaction products (*cis*-DCE and VC), the concentrations of chloride (a reaction product of dehalogenation) were also found to be markedly higher in the deeper regions of the aquifer. All told, the data are consistent with a growing consensus that intrinsic dehalogenation of PCE and TCE has occurred at these depths at DAFB, DE (Ellis et al., 1996; Klecka et al., 1996). Unanswered questions are whether such reactions might be occurring at our test site location and, if so, the rates at which they may have proceeded. As noted in later sections of the report, we believe that, over the course of the field experimental work, any such rates would decline, probably precipitously, since dissolved oxygen was successfully introduced into the groundwater at most (but not all) sampling locations within the portions of the subsurface investigated in our experiments.

2.2. SITE DESIGN

2.2.1. Site Layout

Figure 2 presents an overview of the layout of facilities at the experimental site, with the two sheet piling cells as the major feature. Note also that the downgradient end of the elongated area between the cells was closed off with a few extra sheet piles to enhance the overall utility of the test site. In particular, this closed channel forms a prototype funnel-and-gate system (Starr and Cherry, 1994), closed at one end but open to the existing groundwater plume at the other. In this case, the upgradient cell walls form the “funnel” and the area between the cells can be thought of as a “gate” through which contaminated groundwater is made to pass (e.g., by pumping an extraction well installed at the downgradient end of the channel). This design was included in order that performance testing of semi-passive in situ treatment methods or other technologies installed at the upgradient end of the gate might be conducted at some future time, with minimal additional setup cost. For the purposes of our current project, the arrangement also permitted more well-controlled flow conditions for preliminary tracer experiments within the channel, as

further described subsequently. During the experimental work, the ground surface area above this channel was dedicated to return flow lines from the extraction wells, and associated equipment. A table was set up in a portion of this area to hold equipment for monitoring injected flow rate and spiking the injection water for each cell with tracers.

A mobile office trailer, 8.5 meters (28 feet) by 2.4 meters (8 feet), was used to house the analytical equipment and other equipment and supplies. This trailer was parked near the north (injection) end of the two sheet pile cells. At the south (extraction) end of the cells, groundwater treatment systems and the main electrical supply for extraction pumps and other equipment were located. The test cells, trailer, and treatment systems were sheltered by a weatherproof building constructed of tubular aluminum frame and a vinyl-coated canvas cover, which was manufactured and installed by Rubb, Inc. (Sanford, Maine). This shelter is 15.2 meters (50 feet) long, 10.7 meters (35 feet) wide, and 6.1 meters (20 feet) high at its peak.

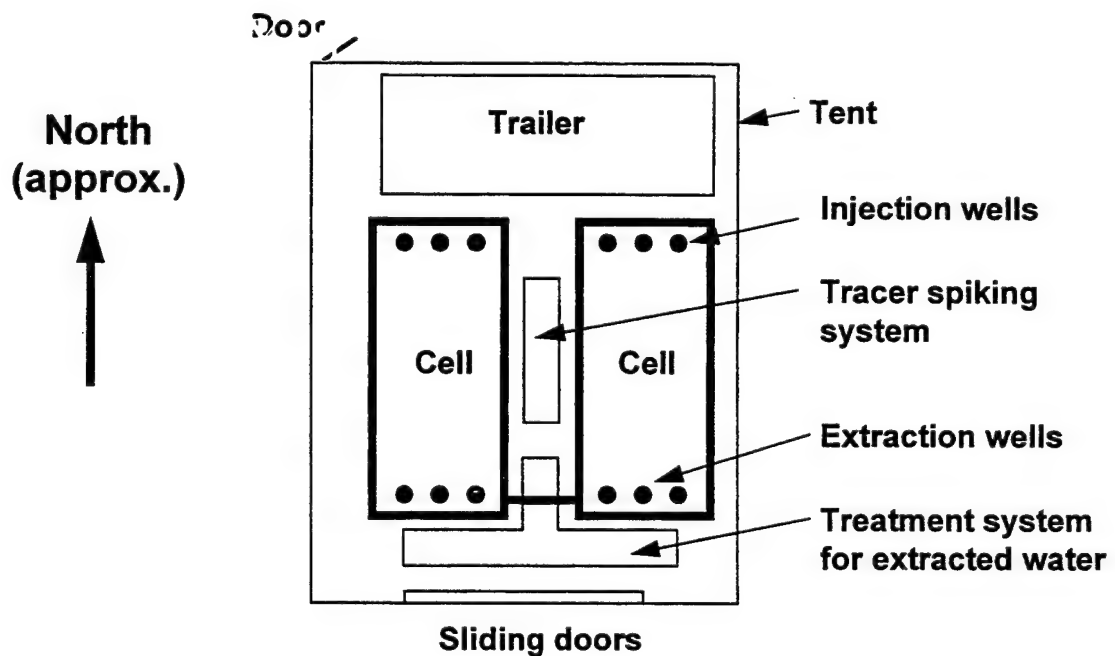


Figure 2. Layout of the Facilities at the Experimental Site. Schematic is not to scale. Sheet piling is depicted as bold lines. Solid dots denote locations of injection and extraction wells.

2.3. PRELIMINARY CORING AND WATER SAMPLING

As part of the initial site characterization efforts in 1993 and 1994, cores were collected at 6 locations on the perimeter of the site, designated B1 to B6 on **Figure 3**. Two of these core holes (B1 and B5) were instrumented with multilevel piezometers to be used for groundwater sampling. The multilevel piezometer design consists of a 1.3 cm (1/2 inch) PVC pipe as a central stalk for support, with 3.2 mm (1/8 inch) stainless steel (SS) tubes extending to different sampling depths strapped to the PVC stalk with SS cable ties. A small piece of SS mesh is soldered to the end of each sampling tube to reduce the incidence of tubes becoming clogged with fine sediments during sampling.

The piezometers were installed using vibratory hammer equipment powered by an air compressor to drive a hollow 5.1-cm (2-inch) steel casing into the subsurface. When the desired depth was reached, the assembled piezometer was lowered into place and held down, forcing a disposable aluminum knockout tip out of the bottom of the casing as the casing is extracted with an electric winch. Once the casing was fully extracted, aquifer material below the water table collapsed back into the open hole against the piezometer, holding it firmly in place.

The preliminary coring and monitoring (conducted in ML-1 and ML-5) confirmed that (1) the aquitard was within the desired depth from ground surface at all four corners of the area within which the sheet pile cells were to be installed (i.e. no more than about 15.6 meters from ground surface, a depth we anticipated that sheet pile could be installed without difficulty); (2) VOC contamination was present in the aquifer at concentrations suitable for the intended experiments; and (3) VOC concentrations and stratigraphy were relatively uniform in the horizontal direction. These findings suggested that the site was appropriate for the experiments in that it appeared likely that two side-by-side sheet pile cells could be constructed which would have an effectively impermeable bottom (the aquitard) and contain portions of the contaminated subsurface which were as similar as practically feasible. Another important function of this preliminary monitoring effort was the initial shakedown of the hot methanol extraction method for determining the total concentration of selected VOCs in the core samples. In this regard, cores B5 and B6 were analyzed in the same manner as the final adapted protocol (Ball et al., 1997), whereas cores B1 to B4 were analyzed with a preliminary method, yielding useful

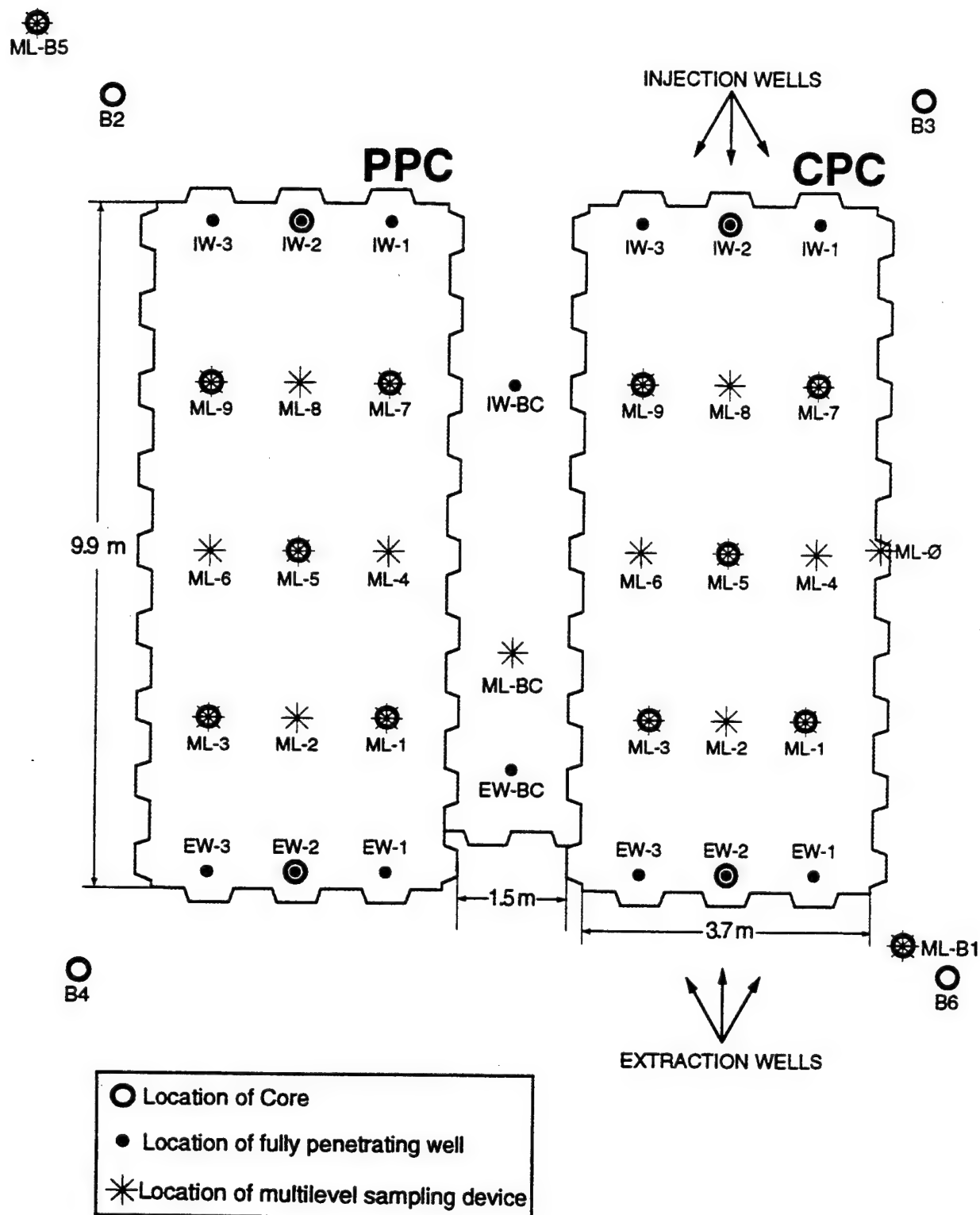


Figure 3. Locations of Core Collection and Well Installation.

information, but of less precision than subsequent data. Aside from the soil VOC results from B5 and B6, the preliminary coring and monitoring data are not further described in this report.

2.4. SHEET PILE DESIGN, INSTALLATION AND TESTING

Two adjacent blocks of the contaminated subsurface were isolated in practically identical sheet piling boxes, referred to (previously and hereafter) as sheet piling "cells". These cells were constructed from 15.9 m (51 foot) long Waterloo Barrier™ WZ75 steel sheet piling (7.5 mm thick) manufactured by Canadian Metal Rolling Mills of Cambridge, Ontario. A detailed description of similar applications of sealable joint sheet piling is given by Starr et. al. (1992). As illustrated in **Figure 3**, each sheet piling cell was approximately 9.9 meters (32 feet) long and 3.7 meters (12 feet) wide. **Figure 4** illustrates the configuration of the WZ75 sheet piling joints. As schematically depicted in **Figure 5**, the sheet piling walls protrude about 0.3 meters (1 foot) above ground surface (ags) and extend to approximately 15.6 meters (50 feet) bgs. Thus, the piling walls are keyed roughly 0.6 to 1.2 meters (46 to 48 feet) bgs, as mentioned earlier.

The sheet piling cells were installed by a construction crew using a crane-mounted vibratory

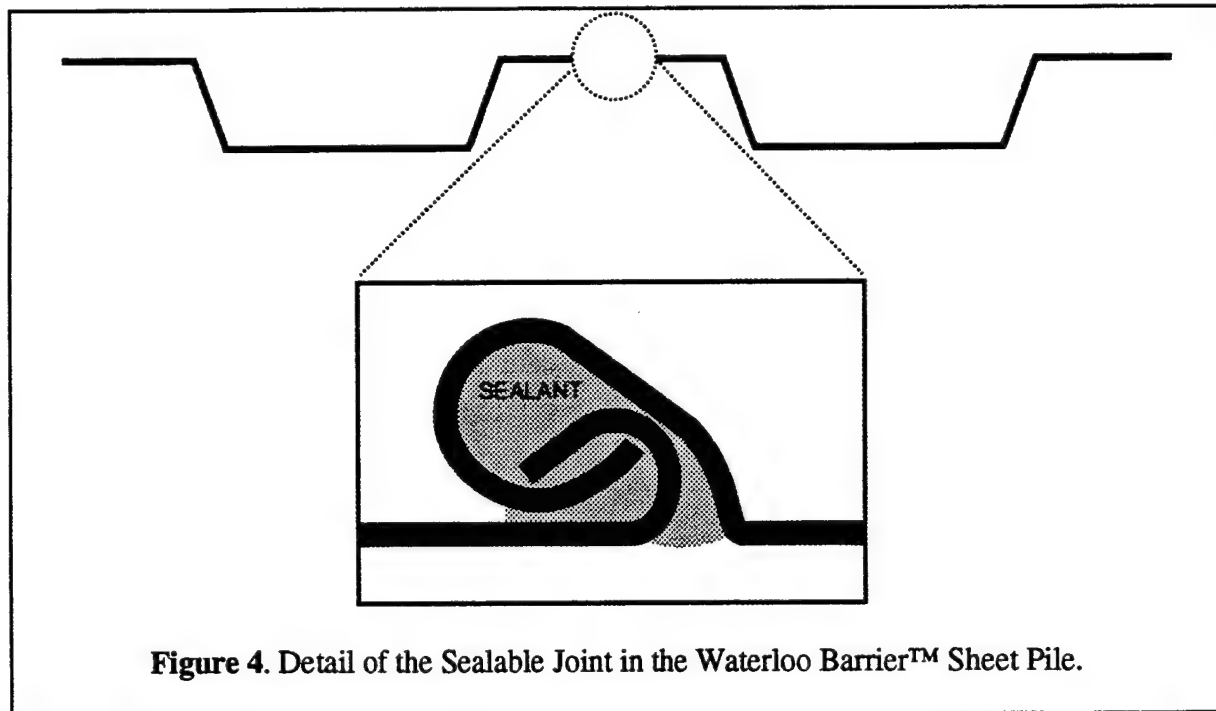


Figure 4. Detail of the Sealable Joint in the Waterloo Barrier™ Sheet Pile.

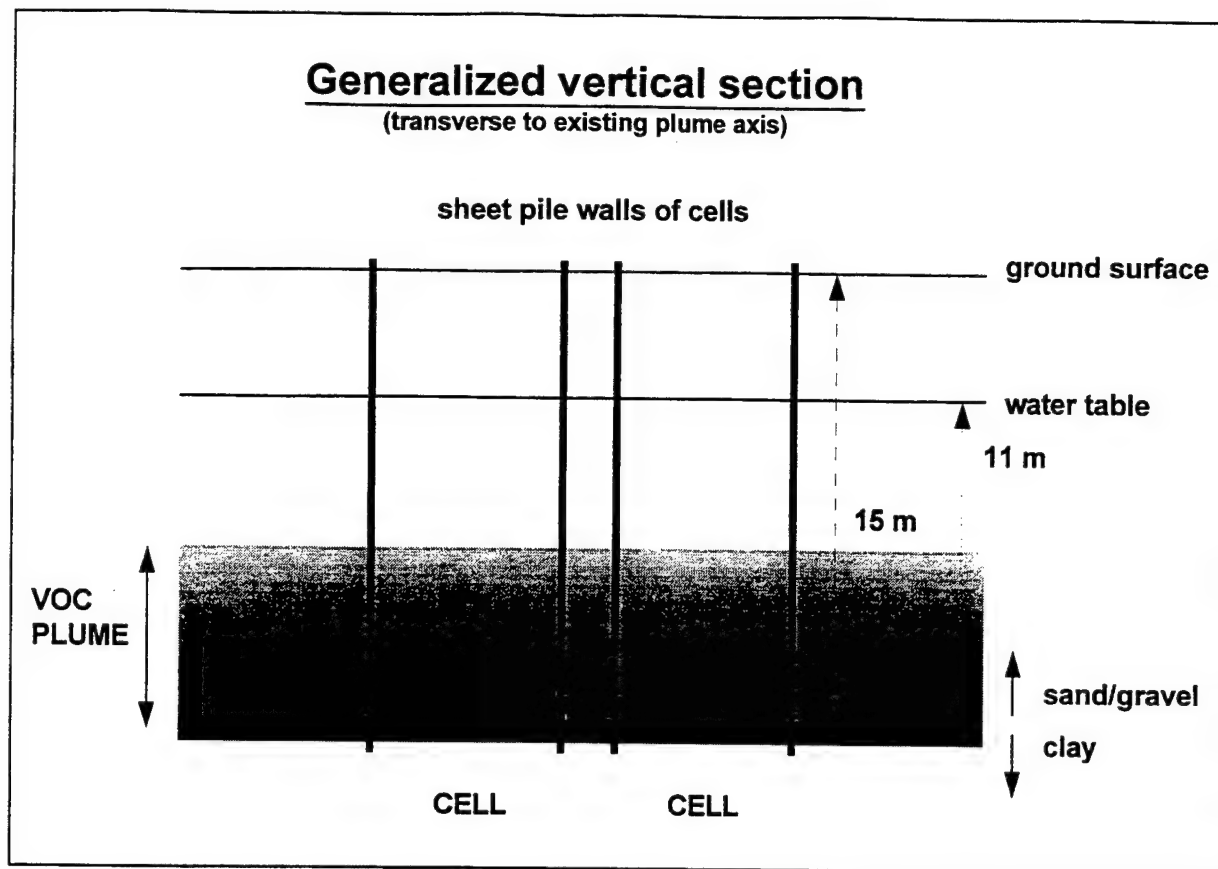


Figure 5. Schematic Illustration of the Installation of the Sheet Pile through the Sand/Gravel Aquifer Containing the VOC Plume and into the Underlying Aquitard. Dimensions and descriptions are approximate, and the figure is not to scale.

hammer to drive the sheet piling vertically down to the aquitard. Once the boxes were installed, sediment in the modified Waterloo Barrier™ joints was washed out with tapwater under high pressure, and a bentonite slurry was injected under pressure to seal each joint in the manner depicted in **Figure 4**.

Bulk permeability of the two sheet piling cells was tested soon after installation to confirm that they were properly installed and sealed, producing essentially impermeable enclosures. The injection water used to clean the joints just prior to sealing produced an elevated water table within the test cells relative to the surrounding aquifer. Hydraulic heads were monitored periodically following cell installation, using standpipe piezometers and screened wells located inside and between the two cells. In general, the water table in each test cell dropped slowly with time, due to leakage driven by the strong outward hydraulic gradients. The outward leakage rates

were estimated by a simple application of Darcy's Law:

$$K = Q / IA \quad (1)$$

In this equation, K is bulk hydraulic conductivity of the walls in a given test cell (L/T), Q is the measured leakage flux (L³/T), I corresponds to the hydraulic gradient imposed across the walls (L/L), and A is the saturated cross-sectional area available for leakage through the cell walls (L²). The leakage flux was estimated for each cell by measuring the head drop over a certain period of time, and considering the aquifer porosity and cell dimensions to determine the leakage volume per unit time. The difference between head inside and outside of the cells was used to calculate the gradient across the wall thickness (7.5 mm). Four sets of head measurements collected during a 20-hour test suggested that bulk hydraulic conductivities of the two test cells were 1.5×10^{-8} cm/sec and 1.3×10^{-8} cm/sec for the PPC and CPC, respectively. The calculations reported above are based on an assumption that all of the observed outward leakage occurred via the cell walls, neglecting the possibility of leakage through the clay aquitard. To the extent that leakage also occurred through the aquitard, then the actual bulk hydraulic conductivity of the cell walls will be lower than these estimates. However, we believe the aquitard contribution to have been minor, based on the following arguments:

1. We recognize that flow around the sheet pile wall bottoms (located between 0.6 meters and 1.2 meters below the sandy region interface) will dominate over vertical flow through the (roughly 5 meters thick) aquitard, but that both flows are possible;
2. If we assume that there is negligible gradient between the unconfined and confined aquifers (see subsequent estimates of contaminant penetration into the aquitard (Ball *et al.*, 1997)), the pressure force for flow around the sheet pile bottoms and through the aquitard is the same as that for the sheet pile walls;
3. Assuming the previously noted measured values for the hydraulic conductivity of the aquitard material (3×10^{-8} cm/sec), straight forward flow-net calculations can be used to demonstrate that aquitard flow is likely to have been only a small portion of the total loss.

Thus, our estimates of conductivity for the piling walls are believed to be reasonably accurate.

2.5. SITE INSTRUMENTATION

The zone of aquifer contained within the two sheet piling cells, and to a lesser extent the area between and around the cells, have been heavily instrumented in an attempt to control and characterise contaminant behaviour during the pumping tests. In-ground installations include multilevel piezometers, fully screened pumping and injection wells, and standpipe piezometers. Above-ground equipment such as dedicated extraction pumps, a treatment system, flowmeters, filters, a reinjection manifold, and sampling equipment were also necessary.

2.5.1. *Initial Coring and Well Installation*

After the completion of the sheet piling cells, 20 multilevel piezometers were installed within or between the cells at the site in conjunction with additional coring events. **Figure 3** depicts the locations of the coring conducted at this time and also the location of the multilevel devices. The coring method, multilevel design and installation techniques are similar to that previously described in section 2.3. Multilevel piezometers were installed at 10 cored locations in the test cells, 9 non-cored locations in the cells, and 1 noncored location between the cells. The 19 piezometers installed within the test cells each include 8 sampling depths, with ports located at the vertical positions listed in **Table 1**. Note that the depth of the deepest point varied because we attempted to locate this sampling port close to the aquifer-aquitard interface, based on the best available core information at the time of construction. The bases of the 1.3 cm (1/2 inch) PVC stalks on most of the piezometers extended from 0.3 to 0.8 meters (1 to 2.5) feet into the clay aquitard. The multilevel piezometer located between the cells (ML-BC) has 10 sampling ports located at depths indicated in **Table 1**.

2.5.2. *Extraction and Injection System*

As illustrated in **Figure 3**, three injection wells and three extraction wells were installed at opposite ends of each cell. The 5.1-cm (2-inch) PVC wells were installed with 10.2-cm (4-inch) ID hollow stem augers driven by a Canterra drill rig. No sandpack was used for the injection or extraction wells, which were developed by surging and cyclic pumping. Dedicated positive displacement pumps (Model RP1A, Protec, Inc., Tulsa, Oklahoma) were installed in each of the extraction wells, anchored to steel casings set in concrete. Sampling positions (SS valves) in the

TABLE 1. SUMMARY OF PIEZOMETER INSTALLATION AND CORE ACQUISITION DEPTH INTERVALS.

Location name		Top of clay in core (feet bgs)			Stalk elevation above ground (feet ags)	Length of PVC stalk (feet)	Depth of stalk base (feet bgs)	Sampling tube depths* (feet bgs)									
Piezometer	Core only	Measured in split core	Corrected for core compression	With add'l correction to datum used for MLs				level 1	level 2	level 3	level 4	level 5	level 6	level 7	level 8	level 9	level 10
	PPC-10	46.83	46.25	NA													
PP-ML-1		47.25	47.19	47.36	1.17	50	48.83	47.33	42.83	37.83	32.83	29.83	24.83	19.83	16.83		
PP-ML-2		NA	46.58	46.53	1.30	50	48.70	47.20	42.70	37.70	32.70	29.70	24.70	19.70	16.70		
PP-ML-3		47.00	45.96	45.86	1.10	50	48.90	45.90	42.90	37.90	32.90	29.90	24.90	19.90	16.90		
PP-ML-4		NA	46.72	46.68	1.54	50	48.46	46.46	42.46	37.46	32.46	29.46	24.46	19.46	16.46		
PP-ML-5		46.33	46.28	46.24	1.54	50	48.46	46.46	42.46	37.46	32.46	29.46	24.46	19.46	16.46		
PP-ML-6		NA	45.73	45.66	1.58	50	48.43	46.43	42.43	37.43	32.43	29.43	24.43	19.43	16.43		
PP-ML-7		46.25	46.25	46.13	1.13	50	48.88	45.63	42.88	37.88	32.88	29.88	24.88	19.88	16.88		
PP-ML-8		NA	46.38	46.47	0.91	46.75	45.84	45.59	43.09	38.09	33.09	30.09	25.09	20.09	17.09		
PP-ML-9		46.83	46.50	46.45	1.05	50	48.95	45.70	42.95	37.95	32.95	29.95	24.95	19.95	16.95		
	PPC-11	46.17	45.93	NA													
	CPC-10	48.33	48.29	NA													
CP-ML-1		47.92	47.82	47.87	0.95	50	49.05	47.55	43.05	38.05	33.05	30.05	25.05	20.05	17.05		
CP-ML-2		NA	47.66	47.64	1.02	48.83	47.81	47.48	42.98	37.98	32.98	29.98	24.98	19.98	16.98		
CP-ML-3		47.75	47.50	47.69	0.81	50	49.19	47.69	43.19	38.19	33.19	30.19	25.19	20.19	17.19		
CP-ML-4		NA	47.43	47.71	0.73	48.83	48.11	47.78	43.28	38.28	33.28	30.28	25.28	20.28	17.28		
CP-ML-5		47.83	47.97	48.03	0.94	50	49.06	47.56	43.06	38.06	33.06	30.06	25.06	20.06	17.06		
CP-ML-6		NA	47.27	47.50	0.78	48	47.23	46.73	43.23	38.23	33.23	30.23	25.23	20.23	17.23		
CP-ML-7		47.00	47.03	47.28	0.75	50	49.25	45.75	43.25	38.25	33.25	30.25	25.25	20.25	17.25		
CP-ML-8		NA	47.03	47.06	0.97	47.66	46.69	46.36	43.03	38.03	33.03	30.03	25.03	20.03	17.03		
CP-ML-9		46.25	47.03	47.42	0.61	50	49.39	46.39	43.39	38.39	33.39	30.39	25.39	20.39	17.39		
CP-ML-12		NA		NA	0.95	48.83	47.88	47.55	43.05	38.05	33.05	30.05	25.05	20.05	17.05		
	CPC-11	46.25	45.70	NA													
ML-BC		NA		NA	1.41	48.69	47.28	46.28	43.28	40.28	37.28	34.28	31.28	28.28	24.28	20.28	17.28

*All depths are reported relative to a datum defined as the ground surface at PP-LK-2, located near the center of the PPC. This datum is 1.110 feet below a benchmark engraved in the northeastern corner of the CPC.

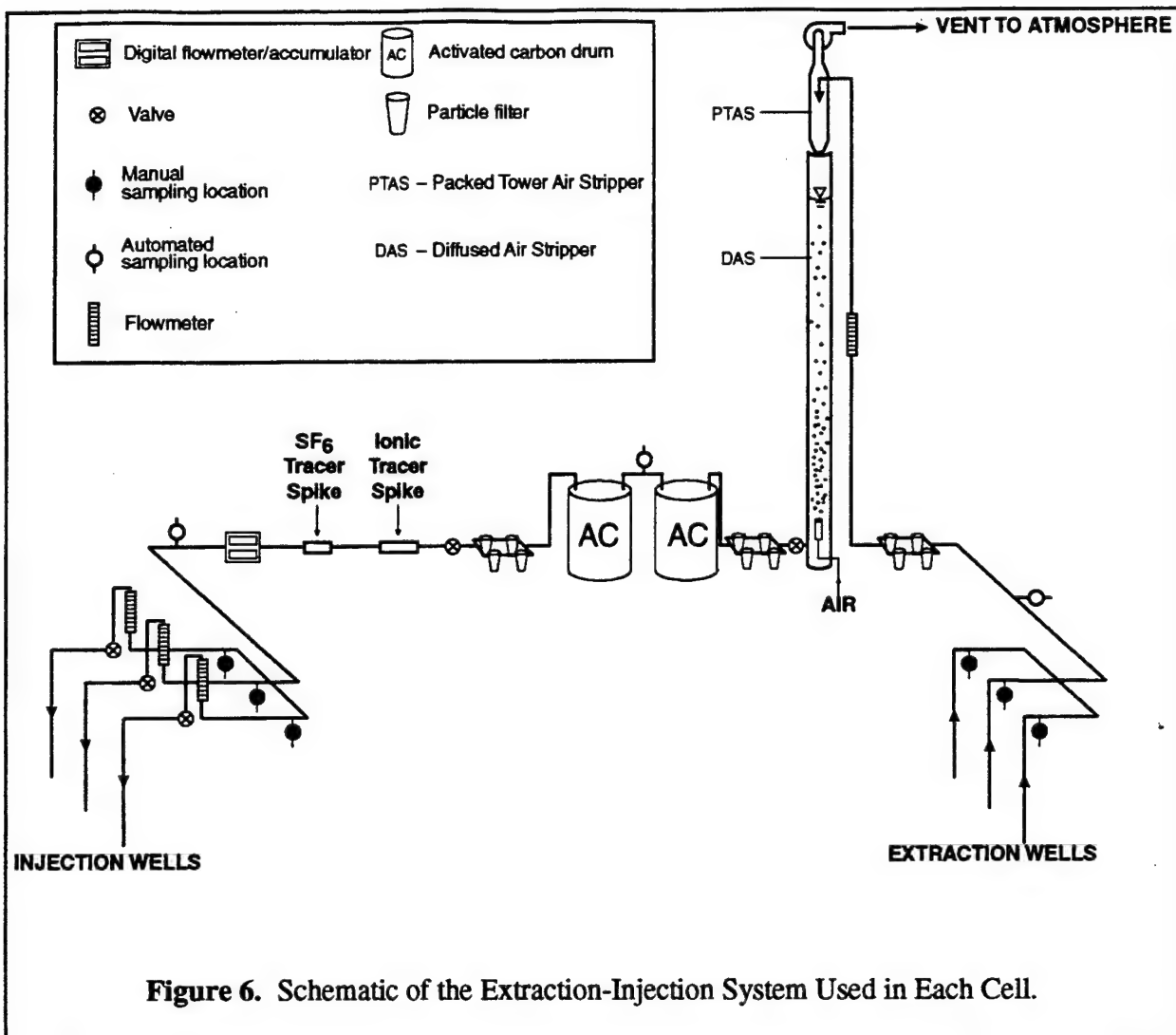
effluent line from each extraction pump allowed manual sampling. A manifold of 1.3 cm (1/2 inch) PVC pipe connected the effluent lines from all three extraction wells in each cell to produce a composite effluent line outfitted with a SS sampling position for automated sampling and analysis of VOCs (discussed below).

Figure 6 presents a schematic of the system used in each cell to collect and treat the extracted water, monitor its flow, reinject it into the cell, spiked periodically with tracer(s). Downstream of the composite sampling position the composite effluent from each cell was directed by flexible PVC hose to a flowmeter, followed by a series of two filters, and then to the top of a packed tower air stripper whose function it was to remove as much as possible of the VOCs. The air effluent from the air stripper was vented outside the tent. The water effluent from the air stripper was allowed to fall by gravity into a 3.0 meters (10 feet) tall, 10.2 cm (4 inch) ID clear PVC column (with a 0.6 meters opaque PVC extension on the bottom to vertically position the column) serving as a diffused air stripper and head reservoir. The effluent from the PVC column was directed by flexible PVC hose to a series of two 208 liter (55 gallon) activated carbon drums (Fluid Technologies, Baltimore, Maryland) for final polishing of the water to achieve negligible VOC concentrations. Flow through the carbon drums was maintained by keeping the liquid level in the PVC column about 3 meters (10 feet) above ground surface.

Effluent from the carbon tanks was directed by flexible PVC hose to a series of two filters (to remove any fines, including activated carbon particles). Effluent from the filter series was conveyed by 1.3 cm (1/2 inch) PVC through a tracer injection tee (for introduction of bromide spiking solution fed from a mixed reservoir by a peristaltic pump), through the sending unit of an electronic flowmeter, through a device for spiking the water flow with SF₆ tracer, and through a sampling position (SS fitting) connected to the automated sampling and analytical system. After that, the water was directed to an injection manifold constructed largely of 1.3 cm (1/2 inch) PVC) and outfitted with a SS manual sampling valve for the influent to each of the injection wells and also a flowmeter to allow the total flow to be split into equal portions for each well.

2.5.3. Automated Sampling and Analytical System

For VOC monitoring, we installed a system capable of automated sampling and analysis of 76 total points, 64 of which were multilevel points within the cells and the rest were various



points along the treatment trains for each cell to confirm their proper operation. The system, called an Automated Sampling and Analytical Platform (ASAP), is manufactured by Analytic and Remedial Technology, Inc. (ART, Milpitas, CA). The ASAP was installed in a room of the trailer which could be temperature-controlled via heaters or air conditioners.

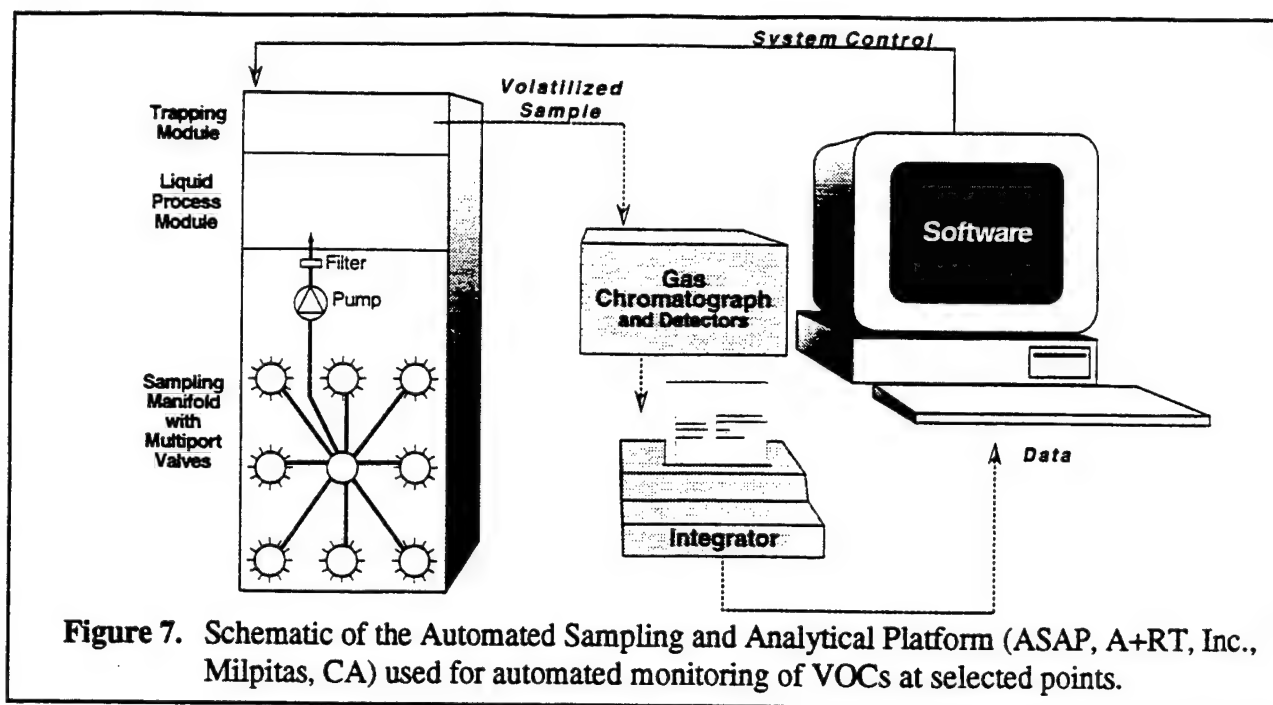


Figure 7. Schematic of the Automated Sampling and Analytical Platform (ASAP, A+RT, Inc., Milpitas, CA) used for automated monitoring of VOCs at selected points.

2.5.3.1. General operation of the ASAP

The ASAP is schematically illustrated in **Figure 7**. Its operation and database generation are controlled by a personal computer (PC) running proprietary AR⁺T software. The following is a brief discussion of the general operation of the ASAP.

Water samples were collected automatically by the ASAP by pumping them via 3.2 mm (1/8-inch) O.D. stainless steel tubing directly from the multilevel sampling device or sampling position along the treatment trains to a central manifold on the ASAP unit. The sampling manifold is composed of electronically-activated, stainless steel, multiport valves with connecting stainless steel tubing of 3.2 mm (1/8-inch) O.D. Because the depth to groundwater was too great to allow the ASAP to direct the sample through the manifold before encountering the pump (too much head loss for reliable pumping and sample delivery), we modified the system such that the sample was drawn from the 1/8-inch O.D. tubing directly through a peristaltic pump outfitted with a short section of viton tubing.

The sample was thus under positive pressure when it exited the viton tubing and entered the stainless steel ASAP manifold. By appropriate switching of the multiport valves (an automatic process), the sample was then directed through a stainless steel filter (to trap fines) and delivered by 1.6-mm (1/16-inch) O.D. stainless steel tubing to the sample selection valve on the "liquid process module" of the ASAP.

The filter was periodically blown out with purified helium and/or replaced if there was evidence of its becoming clogged enough to affect sample flow rate; this was found necessary on occasion in the early stages of the experiments but was found to be less of an issue as time went on.

The liquid process module's sample selection valve was an electronically activated stainless steel eight-port valve with fittings for 1.6-mm (1/16-inch) O.D. stainless steel tubing. This valve served to select the source of water for analysis from four alternatives:

1. One port for an "on-line sample" of water from the ASAP manifold (automatically collected as just described, directed to proper location by multiport switching valves).
2. One of five ports for an "off-line sample" which was generally a manually collected sample contained in a standard 40-mL VOA vial (e.g. samples collected from multilevel points or treatment train sampling locations not connected to the ASAP manifold for automated sampling). The sample was prepared for analysis by placing the vial in a rack below the liquid process module and inserting through the VOA's septum both a sample line (1.6-mm stainless steel tubing from one of the ports on the sample selection valve, whose other end was sharpened and configured to avoid plugging during insertion through the septum) and a vent to atmosphere (syringe needle). The sample line was inserted to near the bottom of the vial (but well above any sediment, if present) whereas the vent was inserted to just below the septum. The function of the vent was to allow air to be drawn in (avoiding creation of a vacuum) as the sample was pumped out of the VOA vial through the sample selection valve.
3. A calibration standard, which was contained within a special glass syringe with stainless steel plunger (mounted on the side of the ASAP system). The calibration syringe was connected via 1.6-mm O.D. stainless steel tubing to a port on the sample

selection valve of the liquid process module.

4. A blank, which was VOC-free water provided by a special system described below.

Water drawn through the sample selection valve was directed to the sample loop valve, a stainless steel, electronically activated valve which allowed a specific, reproducible volume of the sample to be collected in one of potentially six loops, numbered 2 through 7 (no sample loop was installed in position 1 of the multiport loop selection valve). For various reasons, we did not use loops 2 or 7 in the DAFB field work; the volumes of Loops 3-6 are listed in **Table 2**.

TABLE 2. VOLUME OF SAMPLE LOOPS ON ASAP AT DOVER AFB.

LOOP NUMBER	LOOP VOLUME (ML)
3	0.50
4	1.0
5	2.1
6	4.1

After the loop was flushed several times (determined automatically by the ASAP), the loop was switched out of sample collection mode and into sample delivery mode, in which the sample was pushed out of the loop by a flow of VOC-free water to an ASAP module which, in essence, is a purge and trap concentrator. Thus the sample was run through a stripping cell and the analytes purged by a flow of purified helium to a standard trap held at ambient temperature. After purging, the trap was isolated, heated to an elevated temperature, and then connected via a heated transfer line to the column of a HP 5890E gas chromatograph. In this manner, the concentrated analytes were injected onto the column. The GC was equipped with a 5240 PID/ELCD tandem detector (Oceanography International, College Station, TX) whose signals were processed by a two-channel integrator (Chromjet, Thermal Separation Products, San Jose, CA). The integrator produced a hard copy of the chromatograms and integration results and also sent an electronic report of results to the PC for entry into the database.

In principle, this system should have been capable of 24-hour per day operation, 365 days a year (less time for maintenance, setup of off-line samples and calibration standards, etc.).

However, a number of problems occurred and some recurred to reduce the sample processing efficiency of the system; these problems included power outages, unidentified electronic disturbances experienced by all electronic equipment at the site, apparent bugs in the A*RT software, apparent bugs in the Chromjet software, and operator error. Fortunately, as described during the discussion of results, these problems, although extremely annoying in the moment and subsequently during data reduction, did not prevent the system from collecting a more than sufficient set of reliable data. Reliable data were identified by direct examination of the hard copy of the chromatograms, confirmation of satisfactory periodic calibration runs, correction of integration errors, if any, for both the calibration runs and the sample analyses, and correction, if necessary, of the results stored in the database.

2.5.3.2. Sampling strategy

An initial snapshot sampling was conducted in each cell by manual collection of samples from all multilevel points. The samples were analyzed using the ASAP in off-line mode. A final snapshot was also conducted after pumping was ceased, with samples again manually collected. The samples were analyzed using the ASAP in off-line mode, starting first with the deepest samples and proceeding to shallower depths until analytes were no longer detected.

During the pumping portion of the field work, three points along the treatment train in each cell were automatically monitored at a high frequency: after the effluents from the three extraction wells were combined (to determine the total mass of analytes extracted over time), between the two activated carbon drums (to confirm proper operation of the air strippers and first activated carbon drum and give early warning if treatment efficiency were to degrade over time), and before the treated (and periodically tracer-spiked) water was subdivided to the three injection wells (to confirm that analyte concentrations were very low or below detection limit in the injected water). Occasional samples were manually taken from the individual effluent lines from the three extraction wells.

Automatic monitoring also was conducted at a variable frequency at various points on four of the multilevel devices in each cell, as indicated in **Figure 8**: PP-ML-4, PP-ML-5, PP-ML-6 and PP-ML-8 in the PPC, and CP-ML-4, CP-ML-5, CP-ML-6 and CP-ML-8 in the CPC. This

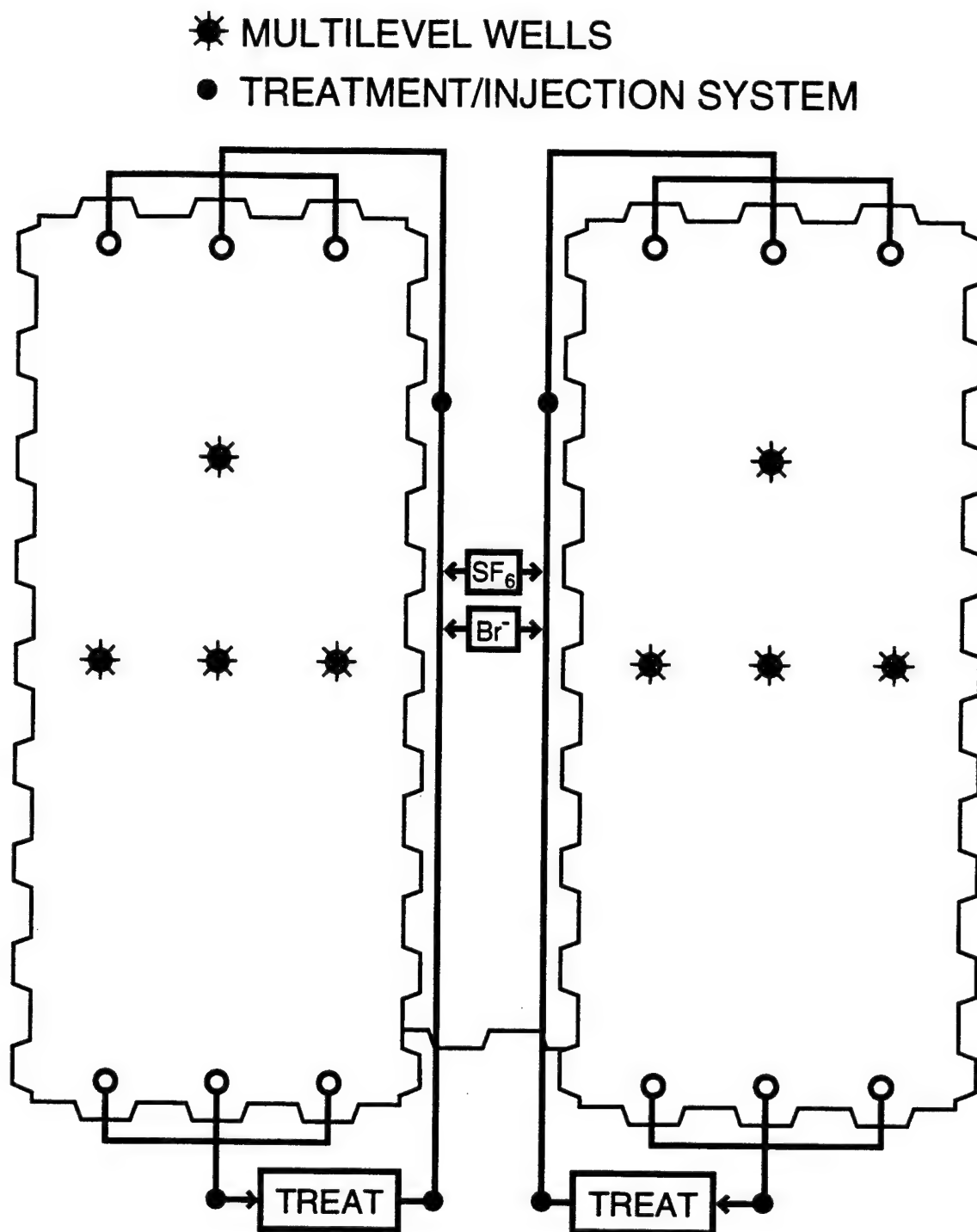


Figure 8. Location of Points Monitored Automatically for VOCs. (Frequency of monitoring varied among the points and over time, as discussed in text.)

monitoring was generally limited to those levels at which significant analyte concentrations had been detected in the snapshot sampling, although occasional samples were taken at the next shallowest points to confirm that no analytes were present at detectable concentrations. The frequency of monitoring was variable over the course of the pumping period in each cell, planned to allow reasonable resolution of the elution curves by accounting for the distance of the points from the injection wells and the expected horizontal flow rate in the sampled stratum (estimated from the initial between-cell tracer test).

2.5.3.3. Target analytes and method detection limits

Based on initial monitoring efforts, the desire to monitor analytes with a range of properties (hydrophobicity, aerobic/anaerobic degradation potential), and the capabilities of the ASAP analytical components, we selected a set of target analytes for the field analyses. The target analytes are listed in bold in **Table 3**. Also listed in **Table 3** are a number of other analytes detected at relatively lower concentrations in the groundwater at the site. Finally, **Table 3** lists the practical MDLs for our field and analytical conditions. These were estimated for Loop 6, the largest loop used in this study, by careful examination of chromatograms collected over the course of the field experiments, noting when peaks were present but not identified by the system.

In August 1995, we conducted a simple test to determine the carryover under the worst conditions, i.e. a sample with negligible concentrations of the analytes run immediately after a sample with among the highest encountered concentrations of the contaminants. **Table 4** presents the results of this test, listing only the analytes with significant detected concentrations for each detector. Note that the ELCD was relied upon in this work for quantification of all chlorinated alkanes, and the PID was relied upon for the aromatics. As evident in **Table 4**, carryover of all analytes was either not detectable or insignificant, even though for this test we used loop 7 for the low concentration sample; during the experiments, loop six, which has a higher detection limit, was used for such samples. Nevertheless, as an extra margin of safety, we attempted, throughout the experiment, to avoid running low concentration samples immediately after high concentration samples.

TABLE 3. METHOD DETECTION LIMITS FOR VARIOUS ANALYTES

Analyte (target analytes in bold)	Abbreviation	Estimated MDL (Loop 6) at Dover field site (ug/L)
vinyl chloride	VC	5
dichloromethane	DCM	NE
cis-1,2-dichloroethylene	c-1,2-DCE	0.1
1,1,1-trichloroethane	TCA	0.05
trichloroethylene	TCE	0.05
tetrachloroethylene	PCE	0.01
benzene	B	NE
toluene	T	NE
ethylbenzene	E	NE
o,m-xylene	X	NE
p-xylene	X	NE
naphthalene	naph	NE
2-methylnaphthalene	2-methnaph	NE
NE: Practical MDL not yet estimated for these compounds. For the purposes of this report, we focused only on the analytes of major concern.		

The ASAP was calibrated by periodic analyses of a standard solution containing known concentrations of the analytes highlighted in **Table 3**. More frequent “continuing calibration checks” were conducted by analyzing the standard solution to confirm that the reported concentrations differed from the known concentration by less than 10%. When a greater difference was noted for any of the target analytes (except for vinyl chloride for which wide variability is common and was also found here), another analysis of the standard solution would be run and the system allowed to recalibrate on its results.

TABLE 4. RESULTS OF TEST OF CARRYOVER DURING AUTOMATED ANALYSIS OF VOCS.

Detector	Analyte	Concentration at Sampling Point (ug/L)		Fractional carryover [CP-ML-6-8]/[CP-ML-6-1]
		CP-ML-6-1 (using loop 4)	CP-ML-6-8 (using loop 7)	
ELCD				
	vinyl chloride	1070	ND	0
	DCM	215	ND	0
	c-1,2-DCE	1930	1.7	0.0009
	TCA	708	ND	0
	TCE	795	0.7	0.0009
	PCE	172	0.09	0.0005
PID				
	2-methylnaphthalene	37	ND	0

2.6. REFERENCES

- Ball, W.P., Xia, G., Durfee, D.P., Wilson, R., Brown, M. and Mackay, D.M., 1997. Hot-Methanol Extraction for the Analysis of Volatile Organic Chemicals in Subsurface Samples from Dover AFB, DE. *Groundwater Monitoring and Remediation*, 17(1): 104-121.
- Dames & Moore, 1994. *Area 6 Remedial Investigation; Dover Air Force Base, Dover, Delaware*. Report prepared for U.S. Dept. of the Air Force, Dover Air Force Base, 436 SG/CEV, Dover, DE, Dames & Moore, Inc., Bethesda, MD.
- Ellis, D.A., Lutz, E.J., Klecka, G.M., Pardieck, D.L., Salvo, J.J., Heitkamp, M.A., Gannon, D.J. et al., 1996. "Remediation Technology Development Forum Intrinsic Remediation Project at Dover Air Force Base, Delaware," *Symposium on Natural Attenuation of Chlorinated Organics in Ground Water*, EPA/540/R-96/509. U.S. EPA Office of Research and Development, Washington, D.C., Dallas, TX, pp. 93-97.

- Johnson, R.L., Cherry, J.A. and Pankow, J.F., 1989. Diffusive Contaminant Transport in Natural Clay: A Field Example and Implications for Clay-Lined Waste Disposal Sites. *Environmental Science and Technology*, 23(3): 340-349.
- Klecka, G.M., Wilson, J.T., Lutz, E.J., Klier, N., West, R., Davis, J., Weaver, J. et al., 1996. Intrinsic Remediation of Chlorinated Solvents in Groundwater, *Conference on Intrinsic Bioremediation, March 18-19, 1996*, London, England.
- Ramsey, K.W., 1993. *Geologic Map of the Mifflord and Mispillion River Quadrangles*. Geologic Map Series No. 8, Delaware Geological Survey, Newark, DE.
- Ramsey, K.W. and Xchenck, W.S., 1990. *Geologic Map of Southern Delaware*. Delaware Geological Survey Open File Report No. 32, scale 1:100,000, Delaware Geological Survey, Newark, DE.
- Starr, R.C., Cherry, J.A. and Vales, E.S., 1992. A New Type of Steel Sheet Piling with Sealed Joints for Groundwater Pollution Control, *45th Canadian Geotechnical Conference*, Toronto, Ontario.

3. FIELD EXPERIMENTAL PROCEDURES

3.1. PUMPING SCHEDULE

3.1.1. *Continuously Pumped Cell (CPC)*

The three extraction pumps were started on October 1, 1995 at approximately 2:00 pm, and were allowed to run continuously until final shutdown on March 5, 1996 at 8:45 am. At various times during the experiment the pumps were shut off for brief periods for maintenance, unscheduled repairs, or pump failures due to mechanical problems. None of these shutdowns exceeded two days in duration, and most were on the order of 3-4 hours. Exact records of breakdown occurrences were not kept, but failures occurred roughly once per month.

3.1.2. *Pulse-Pumped Cell (PPC)*

The extraction pumps were started October 1, 1995 at approximately 2:00 pm. Initially, we intended for the pump-on cycles to be on the order of 28 days and the pump-off cycles approximately 21 days for the duration of the experiment. However, actual on and off periods, illustrated in **Figure 9** and detailed in **Table 5** varied due to logistic and other constraints. There were 5 major on/off cycles in total, but the final cycle was interrupted by power and pump failures on two occasions, for a total interruption during that cycle of 7 days.

3.2. TRACER TEST SCHEDULE

3.2.1. *Between-Cells Test*

Prior to the experiments within the cells, two tracer tests were conducted in the space between the two cells. The first, involving the injection of two tracers (SF_6 and bromide) was from April 19 to May 11, 1995. The second, involving the injection of two tracers (SF_6 and bromide) was from August 6-8, 1995. Samples were collected twice daily from three positions at different depths within the injection well for the duration of each injection period. Sampling of the extraction well and multilevel continued roughly daily until August 31, 1995. These tests were conducted to (1) experiment with various plumbing configurations, (2) test equipment, (3)

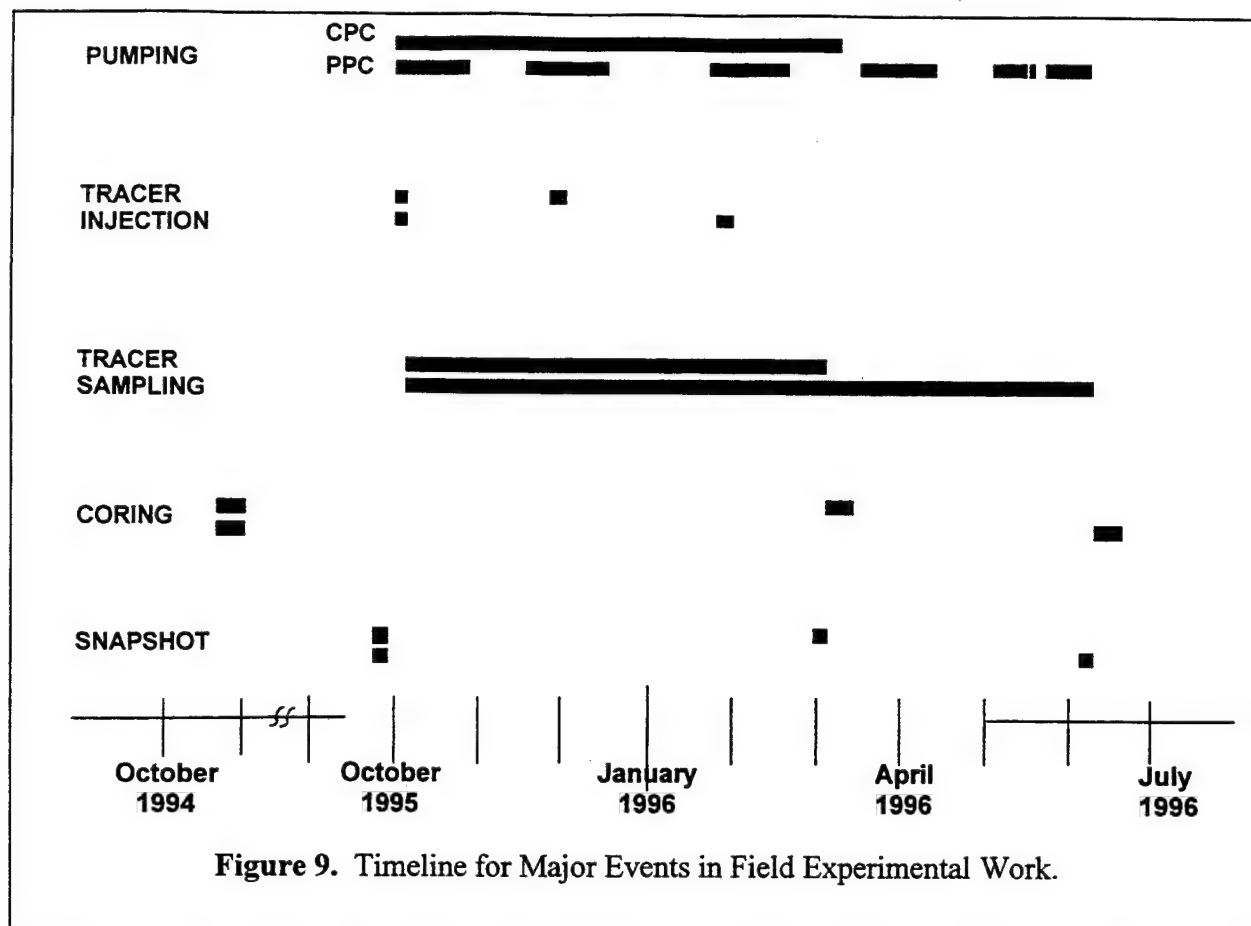


Figure 9. Timeline for Major Events in Field Experimental Work.

calibrate flow meters, (4) test the treatment and injection system, and (5) evaluate the performance of the SF_6 spiking system, (6) compare the behavior of the two tracers (to determine if SF_6 could reliably be used as a conservative tracer in our in-cell experiments), and (7) provide information to determine the appropriate sampling schedule for the in-cell test for the various multilevel positions.

3.2.2. In Cell Test: SF_6 /Bromide

SF_6 and bromide injection in the CPC and PPC began when the pumps were started on October 1, 1995, and continued until October 7, 1995. SF_6 is very volatile and it was therefore expected to be stripped completely by the treatment system and not reinjected, whereas bromide was expected to be recirculated. Since recirculation confounds the interpretation of the tracer breakthrough within the cell, SF_6 was the preferred tracer for use in the in-cell tests. However, for insurance in the event of difficulties with SF_6 , bromide was also included.

TABLE 5. TIMING OF MAJOR EVENTS DURING FIELD EXPERIMENTS

Event	Action	Pulsed Pumping Cell	Continuous Pumping Cell
Pumping of Cell	ON	October 1, 1995, 2:00 pm	October 1, 1995, 2:00 pm
	OFF	October 28, 1995, 9:10 pm	March 5, 1996, 8:45 am
	ON	November 17, 1995, 4:35 pm	
	OFF	December 15, 1995, 3:40 pm	
	ON	January 23, 1996, 3:00 pm	
	OFF	February 21, 1996, 3:25 pm	
	ON	March 14, 1996, 12:20 pm	
	OFF	April 11, 1996, 10:20 am	
	ON	May 2, 1996, 12:35 pm	
	OFF-PF*	May 14, 1996, 11:30 pm	
	ON	May 15, 1996, 9:30 am	
	OFF-PF*	May 16, 1996, 10:00 am	
	ON	May 22, 1996, 12:30 pm	
	OFF	June 5, 1996, 12:50 pm	
Br/SF ₆ Tracer Test	Inject Start	October 1, 1995, 2:00 pm	October 1, 1995, 2:00 pm
	Inject Stop	October 7, 1995, 4:50 pm	October 7, 1995, 4:50 pm
Cl ⁻ /SF ₆ Tracer Test	Inject Start	January 23, 1996, 4:10 pm	November 29, 1995, 9:15 am
	Inject Stop	January 29, 1996, 10:50 am	December 5, 1995, 12:20 pm
Snapshot Sampling	Initial	September 25-27, 1995	September 25-27, 1995
	Final	June 1-4, 1996	March 2-4, 1996
Soil Coring	Initial	October 19-27, 1994	October 19-27, 1994
	Final	June 5-8, 1996	March 5-8, 1996
* OFF-PF denotes cessation of pumping due to power failure.			

3.2.3. In Cell Test: SF₆/Chloride

A second tracer test was conducted to further characterize some parameters not sufficiently resolved by the first tracer test. Due to the presence of recirculated bromide in both cells, chloride was used as the ionic (backup) tracer in this second test. Injection of SF₆ and chloride in the CPC started November 29, 1995 at 9:15 am and was stopped December 5, 1995 at 12:20 pm. Injection in the PPC started January 23, 1996 at 4:10 pm and stopped January 29, 1996 at 10:50 am. The second tracer test in the PPC was delayed in time to occur at extracted pore volumes similar to that of the second tracer test in the CPC.

3.3. SAMPLING SCHEDULE

3.3.1. Soil coring and Snapshot Sampling

3.3.1.1. Initial (Prepumping)

Initial coring of both cells was conducted October 19-27, 1994, concurrent with multilevel and injection/extraction well installation. Core segments were removed from the borehole and immediately split open, subsampled, and logged. Logging in real time was needed to allow appropriate design of the multilevel samplers, which were constructed as coring was in progress. When a core hole was completed, the multilevel that was being built based on the lithologic information from the core was installed in the open core hole. A total of seven continuous cores from 15-50 feet was collected in each cell.

A snapshot of water samples was collected from the multilevel positions September 25-27, 1995, to establish the distribution of the analytes immediately before starting the extraction pumps.

3.3.1.2. Final (Postpumping)

Final coring was conducted over the three days following the shutdown of extraction pumps in each cell. Cores were collected as close as possible to the centroid formed by the initial core locations (multilevel positions). The CPC was cored March 5-8, 1996 and the PPC was cored June 5-7, 1996. A total of 4 cores from 35-50 feet were collected from each cell. A less

extensive vertical interval was cored in these final coring efforts since pore water sampling from the multilevels suggested that all of the remaining mass was located in the bottom 5 feet of the aquifer and upper few feet of the underlying aquitard.

A final snapshot of water samples was collected over the 3 days leading up to final pump shutdown in each cell. In the CPC this occurred March 2-4, 1996; in the PPC this occurred from June 1-4, 1996.

3.3.2. Temporal Sampling

3.3.2.1. Routine (ASAP) Sampling

Sample locations accessed by the automated sampling and analytical platform (ASAP) are controlled by a programmed sample order list defined by the user. This list, which the ASAP cycles through repeatedly, is adjusted periodically so that the desired sample frequency is achieved for the sample locations of interest at any given time. Each complete sampling and analysis event performed by the ASAP took approximately 1.5 hours to complete, so roughly 18 samples were collected and analyzed per day. The combined effluent from the 3 extraction wells in each cell and the bottom 4 multilevel positions from CP-ML-5 and PP-ML-5 (the center position in the center row of multilevels in each cell) were deemed to be the highest priority, and were sampled at least once per day. The other multilevel positions and treatment system monitoring positions (stripping tower, between carbon drums, injection line) were sampled approximately every 3 days. Only the bottom four positions of all the multilevels were sampled temporally by the ASAP. This allowed the sample order to be completed, and thus repeated, every 3 days.

Periodic adjustment of the sample order list was made by the operators on the basis of the compiled analytical data. Thus, since contaminants were eluted from various positions within the cell at different times, the sampling frequency for the various points could be adjusted to allow resolution of the elution curves.

3.3.2.2. Tracer Test Sampling

Samples were collected roughly every 12 hours for the duration of tracer injection from three

positions in the center injection well: 4.9, 7.6, and 10.7 m (16, 25, and 35 feet) from the top of casing. Injection well samples were collected periodically thereafter to characterize any recirculation of either tracer through the treatment system. Daily samples were collected from the bottom 7 levels of CP-ML-5 and PP-ML-5, and also from the combined effluent of the 3 extraction wells for the first month of each test. As warranted based on compiled results, sampling of various points was reduced in frequency or stopped as tracer elution proceeded.

4. SITE CHARACTERIZATION RESULTS

Geologic bore logs and other subsurface characterization efforts at Dover AFB, DE, have been previously conducted and are described elsewhere (Dames & Moore, 1994 and references therein). As part of this project, we sought a more detailed characterization of the subsurface environment in the confined area of this project, with particular emphasis on those properties affecting solute transport. Characterization efforts included all of the following elements:

1. visual logging of soil cores taken from the site (at locations indicated in **Figure 3**);
2. snapshot sampling of the groundwater chemistry (anions, cations, selected trace metals) both before and after the pilot remediation effort;
3. in-situ slug tests and laboratory permeametry experiments for the purposes of characterizing hydraulic conductivity;
4. in-situ tracer experiments for the purposes of characterizing subsurface flow characteristics (velocity and dispersivity estimates); and
5. laboratory characterization of the subsurface solids obtained from the soil cores. The latter types of study were conducted in order to better understand the following characteristics of the different geologic strata: mineralogical composition, in-situ porosity and bulk density, particle-size distribution, cation exchange capacity, organic carbon content, and contaminant sorption properties. In the latter regard, sorption rate studies and isotherm studies were conducted for the two principle organic contaminants being investigated -- PCE and TCE.

The core samples used to characterize subsurface geology and to obtain samples for the solids characterization work have been more fully explained elsewhere (Ball et al., 1997b; Starr and Ingleton, 1992). Solids collection and subhandling are more fully described in Section 4.5 (Solids Characterization Studies). Aqueous sampling of the multilevel samplers is more fully described in Section 4.2 (inorganic parameters) and in Appendix F, section A.2 (VOCs).

Each of the five areas of investigation noted above are described in separate subsections. Characterization results with respect to volatile organic chemical (VOC) contamination at the site

(including data taken before, during, and after the pump-and-treat operations) are discussed subsequently in Chapter 5.

4.1. GEOLOGY

As noted in prior work (Dames & Moore, 1994) and confirmed by our own core logs, the shallow unconfined aquifer in the study area consists predominantly of poorly sorted fine to coarse-grained sand containing a few localized lenses of silt, clay, and gravel, but dominated by medium to coarse sand in the interval between 6.1 meters (20 feet) and 14.2 meters (47 feet). In general, the subsurface material comprises fine to medium sand in the upper 6.1 meters (20 feet) bgs (intermixed with some non-contiguous gravel and clay layers, as noted subsequently), with a clearly defined region of a more uniform gray-white medium sand from roughly 6.1 meters to 9.1 meters (20 to 30 feet) bgs and a second clearly defined region of orange to rust-colored coarse sand and gravel from roughly 9.1 meters to roughly 14.2 meters (30 to 47 feet) bgs. This bottom region clearly coarsens downward in many of the cores, with gravelly sands located in the bottom 1 to 1.5 meters (3 to 5 feet) at many locations. At the bottom of this sandy region is a sharp interface with a fine-grained unit, tentatively identified as the Upper Confining Unit of the Calvert Formation, and more fully described subsequently.

The sandy formation described above has been referred to as the Columbia Formation in prior studies (Dames & Moore, 1994), but the site is now believed to include either the Scotts Corners Formation or Lynch Heights formation (above roughly 30 feet bgs), overlying Columbia Formation material (Ramsey, 1993 and personal communication, K.W. Ramsey, 1996). As described elsewhere (Ramsey, 1993; Ramsey and Xchenck, 1990), the Scotts Corners and Lynch Heights formations are believed to be of Late Pleistocene age, and both are interpreted as depositional environments associated with an ancestral location of the Delaware Bay (Lynch Heights) and its associated estuaries, beaches, and/or marshes (Scotts Corners). The Scotts Corners Formation has been interpreted to be more recent than the Lynch Heights formation, although both are interpreted to have resulted from a cycle of sea-level rise and fall subsequent to that which created the underlying Columbia Formation. The Columbia formation is believed to be of Early Pleistocene age.

The sandy formation described above is underlain by a low-permeability aquitard that has been identified as the Upper Confining Unit of the Calvert Formation by previous investigations (Dames & Moore, 1994, p. 3-43). This unit is considered to be a confining layer that separates the Columbia Aquifer from the underlying Frederica Aquifer, and its thickness has been estimated at between 4.3 meters and 6.7 meters in the area around the experimental site (Dames & Moore, 1994). Our own examination of nineteen soil core taken from the site (Figure 2-3) has found this confining unit to be consistently present in our experimental area, with its top surface located at depths between 14.1 meters and 14.6 meters (46.2 and 48.0 feet) bgs. The hydraulic conductivity (K) of the aquitard material has been previously estimated to range between 2×10^{-8} and 3×10^{-8} cm/sec, based on laboratory measurements (Dames & Moore, 1994).

Although individual core logs are not presented in this report, generalized logs (from the fourteen core locations within the confines of the test cells) have been used to construct longitudinal and transverse fence diagrams for the site. These are presented in Ball *et al.* (1997). A general summary of the core log results (Ball *et al.*, 1997b) is presented on the following page as **Table 6**.

4.2. INORGANIC WATER QUALITY

Samples were taken for the analysis of inorganic water quality on 4 separate occasions between September, 1993, and June, 1996. In addition to preliminary sampling in the vicinity of the cells, 3-day to 1-week events characterized by the sampling of multiple in-cell monitoring points were conducted at several points in time. These latter sampling events have been designated "snapshot sampling events" and were conducted with regard to both inorganic water quality and VOC contamination. VOC contamination data are presented subsequently (Chapters 5 and 6). This section reports inorganic water quality data only.

The four snapshot sampling events for inorganic water quality are as outlined in **Table 7**. Sampling and analytical methods for the various analytes will be described subsequently.

TABLE 6. OVERVIEW OF CORE LOGGING RESULTS FOR DAFB TEST CELLS.*

Segment I.D.	Depth (bgs)		Overview of Observed Stratigraphy	Other Notes and Comments
	m	ft		
1	3.1 ↓ 4.6	10 ↓ 15	<i>Gray or orange clay</i> layer (5 to 40 cm thick) in upper half of all cores examined. Poorly defined layering of <i>silty sand</i> , <i>sandy gravel</i> , and medium <i>gray sand</i> .	Coring only at 6 locations: B1, B2, B3, CPC-1, CPC-3, CPC-5.
2	4.6 ↓ 6.1	15 ↓ 20	Intermixed layers of <i>fine sand</i> , <i>coarse sand</i> , and <i>gravel of mixed coloration</i> ; 0.3 to 0.6 m <i>gravelly-sand or gravel</i> layer observed or suspected in upper to middle range of all cores except CPC-1.	Incomplete collection in all cores except CPC-1, CPC-3, and B2. <i>Light gray clay</i> layer (5 cm thick) at 5.3 m in CPC-1 and CPC-3.
3	6.1 ↓ 7.6	20 ↓ 25	Sharp transition (at 5.6 to 7.0 m bgs) from above <i>gravel and orange sand</i> to more uniform <i>gray-green sand</i> of fine to medium texture. (Transition zone occurs in segment 2 for B1, CPC-5, CPC-7, CPC-9 and PPC-1.)	In 11 cores, 0.3 to 0.9 m of relatively uniform medium <i>orange sand</i> overlays a sharp transition to <i>gray-green sand</i> .
4	7.6 ↓ 9.1	25 ↓ 30	<i>Gray-green sand</i> of fine to medium texture; transition (at between 8.8 and 9.6 m bgs) to orange sand of varying texture and poor uniformity. (Transition occurs in segment 5 for B1, B2, PPC-5, PPC-7, PPC-11.) B1 was an exception, w/ full length occupied by gray/white sand w/ orange-stained lenses.	Transition from <i>gray-green sand</i> to <i>orange sand</i> occurred at segment end (9.1 m) for 6 cores. In 12 of 17 cores, <i>pebbles or gravel</i> were observed in the 15 to 25 cm transition.
5	9.1 ↓ 10.7	30 ↓ 35	Rust-colored <i>orange sand</i> of varying texture (typ. medium to coarse) and poor uniformity. In B1, B2, PPC-5, PPC-7, PPC-11 transition to orange sand occurred in upper 0.6 m.	In one core (CPC-10), a 10 cm layer of <i>orange clay</i> was observed at 9.6 m bgs.
6	10.7 ↓ 12.2	35 ↓ 40	Rust-colored <i>orange sand</i> of varying texture (typ. medium to coarse). Generally few fines, coarsening downward.	Some poorly defined layers of <i>pale green sand</i> in upper 0.5 m of PPC-10.
7	12.2 ↓ 13.7	40 ↓ 45	Rust-colored <i>orange sand</i> of medium to coarse texture and varying uniformity; darker rust color observed in deeper sections of some cores; <i>pebbles</i> throughout.	Upper half of most cores had few fines. Lower sections had moderate to abundant <i>fines</i> .
8	13.7 ↓ 15.2	45 ↓ 50	Rust-colored <i>orange sand</i> as above, with sharp transition to cohesive <i>orange silty clay loam (OSCL)**</i> at 13.9 to 14.7 m bgs. Most core had 2nd sharp transition to cohesive <i>dark gray silt loam (DGSL)</i> . In two cores, transition back to <i>OSCL</i> was observed.	Abundant <i>pebbles</i> at sand-OSCL interface. <i>OSCL</i> layer ranged from 0.3 to 0.8 m thick. <i>DGSL</i> was 0.2 to 0.3 m thick where observable (two cores).

* Core locations in Figure 2-3 except B4, B5, and B6 (no formal logging at the latter 3 locations.)

** The OSCL comprised a cohesive matrix, dominated by orange material but mottled by very thin (< 1 mm) light gray clay strata and veins.

TABLE 7. INORGANIC WATER QUALITY SAMPLING -- SNAPSHOT SAMPLING EVENTS

Sampling Dates	Purpose	Sampling Location(s)	ML Points Sampled	Parameters Evaluated ^a
9/18/93	Pre-test characterization	ML-1	8 depths (16 to 48 ft bgs)	D.O.; Eh; pH; Fe(II), HS ⁻ cations ^b , anions ^c , other ^d
8/15/95	Initial water quality in test cells	CPC (3 MLs) PPC (2 MLs)	8 depths (16 to 48 ft bgs)	D.O.; Eh; pH; Fe(II), HS ⁻ cations ^b , anions ^c , other ^d
3/19/96	Final water quality in CPC test cell	CPC (5 MLs)	6 depths (30 to 48 ft bgs)	D.O., Fe(II)
3/25/96	Late-cycle water quality in PPC test cell	PPC (3 MLs)	7 depths (20 to 48 ft bgs)	D.O.

^a D.O.= dissolved oxygen; Eh = reduction/oxidation potential; Fe(II) = ferrous iron (total suspended and dissolved)

^b Cations: Ca⁺⁺, Mg⁺⁺, K⁺, Na⁺, NH₄⁺

^c Anions: SO₄⁼, Br⁻, Cl⁻, F⁻, HCO₃⁻, HPO₄⁻, NO₂⁻, NO₃⁻

^d Other: Al, Fe(total), Mn(total), SiO₂, and non-purgeable dissolved organic carbon (NPOC)

With regard to the information in **Table 7**, note that personnel, time and budget constraints regrettably prevented the analysis of the full suite of analytes at project end. Also note that the initial water quality testing in the test cells (8/15/95) occurred roughly 10 months after cell installation, soil coring, and first installation of multilevel piezometers (10/25/94). There was no groundwater pumping during this interval. Finally, water quality data external to the cells at various points in time (and at numerous screened-well locations throughout DAFB, DE) are available from other sources (Ellis et al., 1996).

4.2.1. Sampling

Aqueous samples were drawn to the surface under vacuum by means of a peristaltic pump. For the purposes of the inorganic sampling described here, the pumped groundwater flowed from the stainless steel multilevel sampling tubes through some combination of the following items, in the order cited: (1) in-line flow-through cells equipped with micro-electrodes for pH, Eh, and/or dissolved oxygen measurement ; (2) headspace-free in-line plastic vials, equipped with two-hole teflon stoppers and teflon inflow and outflow lines; (3) the peristaltic sample pump (fitted with

viton tubing); and (4) pump effluent tubing, sometimes directed to the bottom outlet of a small plastic sampling funnel, for purposes of evacuated ampoule sampling, as described subsequently (CHEMetrics technique). Effluent was otherwise disposed external to the sample cells.

Subsequent to the stainless steel multilevel tubing, sample tubing was either thick-walled tygon or thick-walled polyethylene, with short pieces of viton for connections.

4.2.1.1. Sampling and analysis in the field

Using methods similar to those described by Walton-Day et al. (Walton-Day et al., 1990), the analytes pH, Eh, DO, Fe(II), and HS⁻ were measured in the field by two methods: flow-through electrodes (pH, Eh, and D.O.) or CHEMetrics ampoule sampling (D.O., Fe(II) and HS⁻). For the preliminary (1993) testing, standard laboratory electrodes and a fabricated closed flow-through cell were used. For subsequent analyses, a lower volume flow-through system was used, obtained from Microelectrodes Inc. (Bedford, NH). This system consists of a sequence of 1/8-inch polysulfone-plastic tee-shaped flow-through cells (Model 8-730 [D.O.]; Models 8-702 [reference electrode], 8-705 [pH], and/or 8-800 [Eh], Microelectrodes, Inc., Bedford, NH), each of which was equipped with a single microelectrode screwed into the neck (or barrel) of each tee. The flow-through system was connected to the well head with approximately 2 feet of tubing. Groundwater samples were pulled through the tubing and tees with a peristaltic pump from each multilevel point sampled. Three sequential readings were obtained and the results averaged for each multilevel point sampled. Typically, D.O. (which required its own meter and no reference electrode) was measured in a separate pumping operation from the other two parameters. The D.O. probe was zeroed in an oxygen-free chamber in the laboratory and was calibrated immediately prior to use using water equilibrated with atmospheric air. Eh readings are based on a platinum electrode with Ag/AgCl reference electrode, and all reported results are corrected to reflect a standard hydrogen electrode potential (Nordstrom, 1977).

For the field analysis of D.O., Fe(II), and HS⁻, CHEMetrics sampling equipment and supplies (CHEMetrics, Inc, Calverton, VA) were made available to the project by DuPont Environmental (Wilmington, DE) through Mr. Ed Lutz. Analysis by this method involves the use of a photometer and three types of ampoules filled with different color-forming reagents. The reagents used for the measurements of DO, Fe(II), and HS⁻ are Indio-carmine, 1,10-

phenanthroline, and N,N-dimethyl-p-phenylenediamine (methylene-blue), respectively (CHEMetrics, Inc.). For the results obtained on this project, the CHEMetric ampoules (which are fabricated under vacuum to automatically aspirate sample upon opening) were snapped open while submerged beneath up-flowing groundwater sample at the bottom of a small plastic funnel. After the reagent in each ampoule had reacted completely with the corresponding analyte in the sample, a reading was made on the photometer in comparison with a blank sample, and results converted to units of concentration using tables provided (CHEMetrics, Inc.).

4.2.1.2. Sampling and analysis for off-site laboratory work

Samples of all analytes except those described above were shipped to the laboratory of Dr. Owen Bricker at the USGS facilities in Reston, VA. For these analyses, all samples were filtered through an 0.2 μm polycarbonate membrane filter (Nucleopore PC, Costar Scientific Corp., Cambridge, MA), then separated into two parts: 60 mL of sample was filtered directly into a 60-mL polyethylene bottle and then acidified to $\text{pH} < 2.0$ with 1 mL of concentrated HNO_3 for cation measurement and the other 60 mL of the sample was filtered directly into a 60 mL polyethylene bottle for anion measurement. Both anion and cation samples were kept in an iced-cooler ($< 4^\circ\text{C}$) during shipping to the laboratory.

The laboratory-based analyses were graciously performed in the USGS laboratory in Reston, VA, by Ms. Marge Kennedy, using methods published elsewhere (Karen et al., 1996). Dissolved concentrations of F^- , Cl^- , Br^- , NO_2^- , NO_3^- , $\text{SO}_4^{=}$, NH_4^+ were determined using a Dionex 2110i Ion Chromatograph (Karen et al., 1996). Dissolved concentrations of Na^+ , K^+ , Ca^{++} , Mg^{++} , total Al, total Fe, and total Mn were determined by Direct Current Plasma Atomic Emission Spectrophotometer (DCP-A) (Karen et al., 1996).

4.2.2. Pretest Characterization Results

Results of the 1993 pretest characterization have been presented previously (First Progress Report, Table B-1) and are not repeated here. Results are substantially similar to the 1995 pre-pumping results in most respects, but with the important difference that chloride concentrations in the deep aquifer were roughly half as high, presumably because the chloride groundwater plume had not yet fully progressed to the test site by the 1993 sampling date.

4.2.3. Prepumping Results

For the August, 1995, prepumping snapshot, samples for off-site analysis were taken from multiple sampling depths at 5 well locations, with 3 well locations in the continuously pumped cell (CPC) and 2 well locations in the pulse-pumped cell (PPC). The sampled well locations were CPC-0, CPC-1, CPC-7, PPC-3, and PPC-9. All 8 depth levels were sampled at each location, except that no sample was taken from PPC-3-8 (most shallow) or PPC-9-6 (third most shallow) since no flow could be obtained at these locations.

During this prepumping snapshot, field measurements (pH, Eh, DO, Fe(II), and HS⁻) were made at nine different locations, including multiple sampling depths from five well locations in the CPC and four well locations in the PPC. Sampled well locations were: CPC-0, CPC-1, CPC-3, CPC-7, CPC-9, PPC-1, PPC-3, PPC-7, and PPC-9.

Results of all completed analyses for the pre-pumping inorganic water quality data are shown in the figures of Appendix B. The plotted results include 21 graphs of CPC results (Figure B-1, a through u) and 21 graphs of PPC results (Figure B-2, a through u).

Appendix B results offer some insight into the potential for biologically mediated transformation of halogenated organic contaminants to less-halogenated products, either in the aquifer upgradient of or within our test cells. A working hypothesis of this project, stated previously in Chapter 2, has been that biotransformation of contaminants over the 9-month duration of the field experiments may be of negligible concern within our test cells, especially once oxygen was reintroduced into the subsurface (via the pump-and-treat scheme). A corollary of this hypothesis is that most of the less-chlorinated "biotransformation products" that we initially see at our location (e.g. *cis*-DCE, VC) are the result of upgradient natural dehalogenation processes, particularly since upgradient locations have historically had a better supply of the more biodegradable organic contaminants that typically serve as carbon sources and electron donors for such anaerobic biological processes. In this context, we note that initial conditions at our location were only mildly reducing, and therefore perhaps not ideal for reductive dehalogenation. Particular evidence to this effect includes the following: (1) there was some measurable D.O. (albeit < 1 mg/L) at all locations except CPC-3-8 and PPC-9-8 (Appendix Figures B-1a and B-2a); (2) Eh readings were on the order of +300 mV (standard hydrogen

electrode potential) (Appendix Figures B-1c and B-2c); and (3) appreciable concentrations of sulfate were measured at all but the second deepest location (Appendix Figures B-1r and B-2r).

On the other hand, there is clear evidence that reductive dehalogenation has occurred in the deeper levels of the aquifer, at least upgradient. In addition to the VOC intermediate reaction products (*cis*-DCE and VC, see Chapter 5), the concentrations of chloride (a reaction product of dehalogenation) were also found to be markedly higher in the deeper regions of the aquifer (Appendix Figures B-1o and B-2o). The deeper samples also have slightly lower D.O. than elsewhere (Appendix Figures B-1a and B-2a), and, with the exception of sampling well CPC-0 (which is near the iron sheet piling wall), are some of the only samples to show measurable concentrations of reduced (ferrous) iron species (on the order of 0.1 mM, Appendix Figures B-1d and B-2d). All told, the data are consistent with a growing consensus that intrinsic dehalogenation of PCE and TCE has occurred at these depths at DAFB, DE (Ellis et al., 1996; Klecka et al., 1996). Unanswered questions are whether such reactions might have occurred at our test site location and, if so, the rates at which they may have proceeded. As noted in the subsequent section, we believe that, over the course of the project, any such rates would have declined within our test cells, probably precipitously since dissolved oxygen was successfully introduced into the groundwater at most (but not all) sampling locations.

4.2.4. Prepumping versus Postpumping Results – D.O. and Fe(II)

Postpumping measurements of D.O. in the two test cells are shown in Appendix C (Figures C-1a and C-2a) and Fe(II) measurements in the CPC are shown in Figure C-1b. The results show that oxygen at the end of pumping was 2 mg/L or higher at all but the very deepest sampling points. However, levels were still below 1 mg/L for most CPC samples at the deepest level, and also for PPC-2 at this level. This may reflect a large reducing capacity in this deeper aquifer zone, such as from adsorbed Fe(II) species, or it may reflect poor flushing, especially since some of the deepest sampling points may possibly be located at or slightly below the depth of the aquifer/aquitard interface on the ML-sampling stalk (e.g, CPC-1-1, CPC-3-1, PPC-1-1, PPC-5-1; see Table 1).

4.3. HYDRAULIC CONDUCTIVITY ESTIMATES

Groundwater flow and solute transport processes are strongly affected by heterogeneity in the hydraulic conductivity (K) of the porous medium. To characterize this aspect of the field site, estimates were made on the basis of Hvorslev well-recovery tests, laboratory permeametry measurements, and particle size distribution. Of these, the field-based well-recovery tests are believed to have yielded the most accurate results. As explained in greater detail elsewhere (Eng, 1995), the permeametry and particle size analysis results are not believed to provide accurate estimates for the DAFB materials, owing to very heterogeneous particle size distributions and problems of representative re-packing of sample.

4.3.1. *Hvorslev well recovery tests*

Hvorslev well recovery tests were conducted within depth intervals in a screened 2-inch PVC well designated IW-BC, located between the 2 sheet pile test cells as shown in **Figure 3**. Forty individual tests were conducted within eighteen depth intervals. The IW-BC well is screened from 17 to 47 feet bgs, and each Hvorslev test examined a 9-inch screen section isolated above and below by inflatable packers. The packer system consists of two bladders inflated by a nitrogen gas source located above ground. The packed interval is open to the 2-inch well screen, and a 1.5-inch PVC standpipe extends from the upper packer to ground surface.

After isolating a depth interval, hydraulic head in the standpipe was allowed to equilibrate to a static level (H). To begin a test, water level in the standpipe was pumped down to H_0 using a peristaltic pump and drop tube. When pumping was stopped and the hydraulic head began to recover to static conditions, the recovery rate of the water level (h) at time (t) was measured regularly. The water level recovery rate decreased exponentially with time, since the hydraulic gradient decreased as the test progresses. The duration of individual tests ranged from 2 minutes to 1 hour due to permeability variations in different strata.

To interpret the field data sets, the method developed by Hvorslev (1951) was used. Detailed summaries are presented in most hydrogeology texts. In short, semilogarithmic plots of the normalized recovery in water level (time vs. $\ln[(H-h)/(H-H_0)]$) were prepared for each test. These plots were analyzed by linear regression to determine the critical point $t = T_0$ for each test.

Then the following equation, which incorporates the physical dimensions of the well screen, is used to estimate hydraulic conductivity of the formation adjacent to the packer-isolated screen interval:

$$K = \frac{r^2 \ln(L / R)}{2LT_0} \quad (2)$$

The hydraulic conductivity estimates from our Hvorslev test analyses are summarized in **Figure 10**. Statistical analysis indicated that coefficients of determination for the linear regression analyses (r^2 -values) were 0.96 or higher. Agreement between duplicate or triplicate tests in the same depth interval was also very good. It is informative to note that K estimates from the lab-scale permeameter tests and the in-situ Hvorslev well tests did not agree very well (Eng, 1995). Most K estimates from the lab permeametry work (on previously air-dried samples) plot in the 4×10^{-3} to 5×10^{-2} cm/sec range, while the Hvorslev data suggests a broader K range from 2×10^{-5} to 4×10^{-3} cm/sec. The Hvorslev data compare qualitatively well with core log results (see discussion below) and, perhaps even more importantly, also agree qualitatively with the tracer test results presented subsequently. Therefore, the discrepancy between the field and laboratory data is taken to suggest that the permeameter work on repacked soil yielded unrealistically high K estimates. Potential causes for these effects have been discussed elsewhere (Eng, 1995), and are briefly reviewed in Section 4.3.2 below. Basically, most of the major difficulties are believed to have resulted from redistribution of fine-grained sediments in the repacked soil columns. In the cases where samples were air-dried prior to testing, aggregation of the fines is suspected. This is believed to have been an especially severe problem for the lower permeability materials.

Figure 10 clearly indicates three distinct groundwater flow regimes at the site, which correlate well with the stratigraphic information from soil cores presented in Appendix A and **Table 6**. In particular, an upper highly permeable zone located between 17 to 20 feet has a K in the 1.0×10^{-3} cm/sec range. This permeable zone corresponds to coarse sands and gravels noted at this depth in the cores. Since the IW-BC well screen started at 17 feet bgs, we have no in-situ measurements of K in the uppermost part of these strata near the water table.

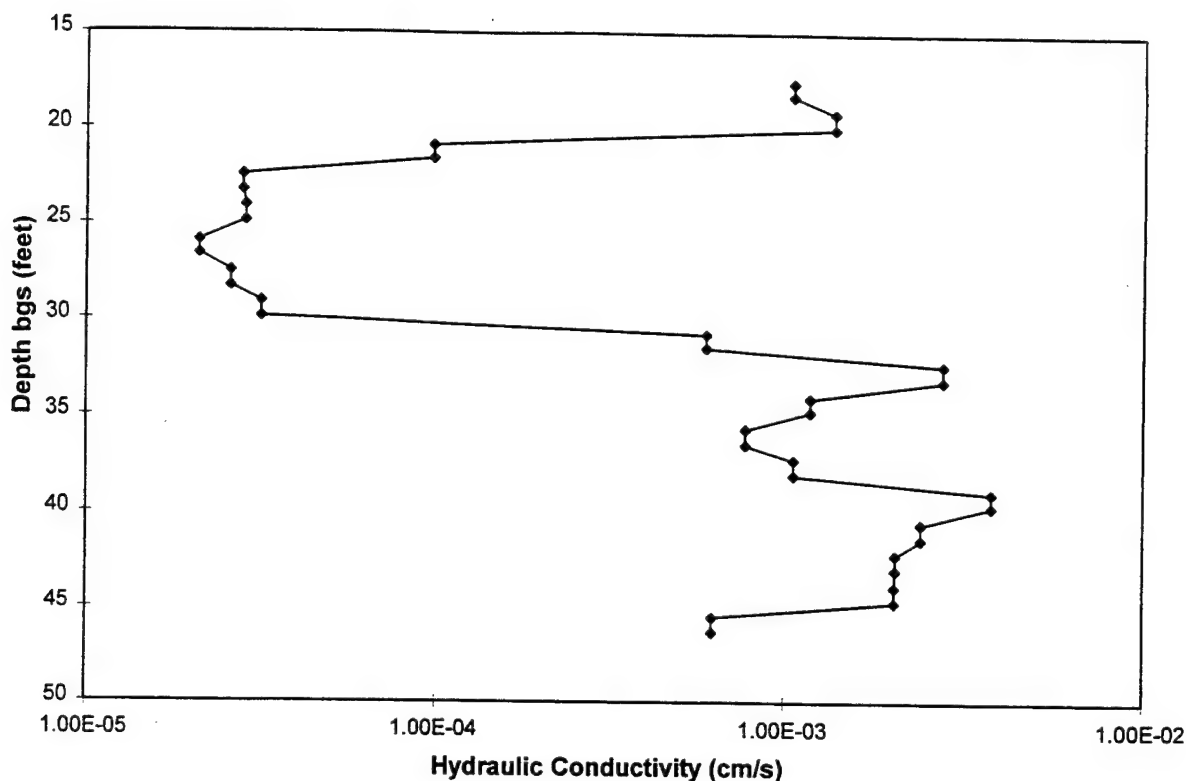


Figure 10. Hydraulic Conductivity Results (Hvorslev Well Recovery Test).

Figure 10 also defines a relatively low K zone between 20 to 30 feet depth, which corresponds to the gray-green-colored medium to fine sand in cores. These sediments have a hydraulic conductivity of about 2.0×10^{-5} cm/sec, two orders of magnitude lower than the overlying and underlying strata. Hydraulic conductivity in the orange-colored coarse sands and gravely coarse sand located 30 to 46 feet deep in the aquifer is quite variable, but significantly higher than in the overlying strata. K ranges from about 6×10^{-4} to 4×10^{-3} cm/sec in this unit. The apparent decrease in K just above the aquitard, shown in **Figure 10** may indicate a silty layer just above the clay at this location. In general, it is important to note that the most permeable zone of the aquifer at the test location is from 39 to 45 feet bgs. This interval corresponds closely with the vertical location of the contaminant plume at the site, as described in Chapter 5.

4.3.2. Laboratory Permeametry Studies and Particle-Size Estimates

An extensive set of laboratory permeametry results was conducted on solid materials taken from the DAFB subsurface cores, as more extensively described elsewhere (Eng, 1995). In particular, laboratory permeametry experiments conducted in the manner of Sudicky (Sudicky, 1986) were conducted, in replicate, on over 100 different samples of aquifer strata from different depth intervals of cores taken from locations B2 and B3 (Figure 3). The large majority of samples analyzed were on material that had been previously air-dried, although direct comparative studies of permeametry with air-dried and field-wet samples were conducted on seven strata from different depth intervals and of different composition.

All strata for permeametry analysis were selected on a visual basis (seeking geologic uniformity over the vertical section sampled), with the sampled intervals never exceeding 15 cm in total length. Constant head permeametry experiments were conducted on approximately 15 gram samples sandwiched between layers of well characterized commercial silica sand (Fisher, 40-100 mesh) of carefully pre-measured hydraulic conductivity. Laboratory permeameters were constructed at the University of Waterloo and were identical to those described elsewhere (Sudicky, 1986). Details of all experimental protocols, calculations and results are provided elsewhere (Eng, 1995). These are not repeated here since, as explained below, the results are not believed to be of direct applicability to the field test.

As noted in Section 4.3.1, significant discrepancy between the field and laboratory data is taken to suggest that the permeameter work on repacked soil yielded unrealistically high K estimates. The problem is especially severe for the gray-green materials in the 6.1 to 9.1 meter (20 to 30 foot) bgs depth range, where Hvorslev estimates were on the order of 2×10^{-5} cm/sec, compared with K estimates on the order of 1×10^{-2} cm/sec by lab permeametry on air-dried material. For the fine to medium sand strata in this depth interval, the air-drying is believed to have had a major effect, since laboratory permeametry with field-wet material gave substantially lower estimates (in the range of 2 to 7×10^{-4} cm/sec). With this 1.5 order-of-magnitude correction for the gray-green material, laboratory permeametry results showed similar depth-related trends in K as those observed in the Hvorslev tests, but with K estimates that were roughly 0.5 to 1 order-of-magnitude higher at all locations. The differences are believed to be

related primarily to the remobilization of fine-grained sediments in the repacked soil columns. In the case of the gray-green material and air-drying, the permeability results suggest that aggregates may have formed during the periods when sediments were allowed to air-dry, and that at least some of the fines remained bound in such larger aggregates after subsequent re-wetting.

Interestingly, DAFB hydraulic conductivity estimates made by Eng (Eng, 1995) on the basis of particle size distribution (PSD) measurements and one commonly applied correlation technique (Masch and Denny, 1966) were in better agreement with the permeameter results than with the Hvorslev estimates, while estimates made using another PSD-correlation technique (Fair and Hatch, 1933) were in better agreement with the Hvorslev results. However, both estimation methods showed prediction differences of up to 1 order of magnitude for samples with similarly measured K. In general, the PSD-based estimates were deemed largely inappropriate for these samples, owing to a roughly 8% to 15% fraction of small particles (0.020 to 0.030 mm size range) in sands that were otherwise dominated by medium (0.25 to 0.5 mm) or coarse (0.5 mm to 1mm) fractions (Eng, 1995). Further results of the particle size distribution measurements are provided in Section 4.5.5 below.

4.4. TRACER TEST RESULTS

During the in-cell experiment, extracted water from the cells was treated and reinjected. For various reasons, a tracer was needed that would not survive treatment and would therefore not be reinjected. Recirculated tracer mass makes hydraulic conductivity resolution less straightforward, raises the background of that particular tracer (precluding its future use in the cells), and complicates residence time calculations. In this work, both conservative tracers (chloride, bromide) and a "treatable" volatile tracer (sulfur hexafluoride) were used.

Sulfur hexafluoride (SF_6) is a relatively new ground water tracer that is extremely volatile and therefore should be completely removed by air-stripping treatment. The behavior of SF_6 relative to a conventional conservative/non-reactive tracer (i.e. bromide) was not previously well-understood at the field scale. A tracer test was conducted in the space between the cells to 1) test whether SF_6 behaves similarly to bromide at this site, 2) confirm SF_6 removal through the treatment system, and 3) test methods of SF_6 injection. In this test, SF_6 was found to behave

similarly to bromide and to be fully removed during treatment. SF_6 was therefore incorporated into the tracer injections for the in-cell tests.

4.4.1. Between-Cell Tracer Test

Figure 11 is a plot of concentrations from the four injection train sample positions over the duration of the injection period. The average concentration was 2.72 mg/l for SF_6 and 347 mg/l for bromide. SF_6 concentrations in samples from the above-ground injection line sample port ("SF6 surface" in Figure 11) were found to be much lower than in those from the in-well sampling tubes, located at three depths in the injection well (Figure 11). It is possible that the longer distance to the bottom of the injection well distributor lines allowed more time for SF_6 to dissolve into the carrier water and that undissolved SF_6 was lost during the sampling of the above ground sampling port and despite the use of flow-through sampling heads. For example, undissolved SF_6 could be lost when the sampling head is removed prior to sample vial capping. Bromide concentrations showed no evidence of this effect.

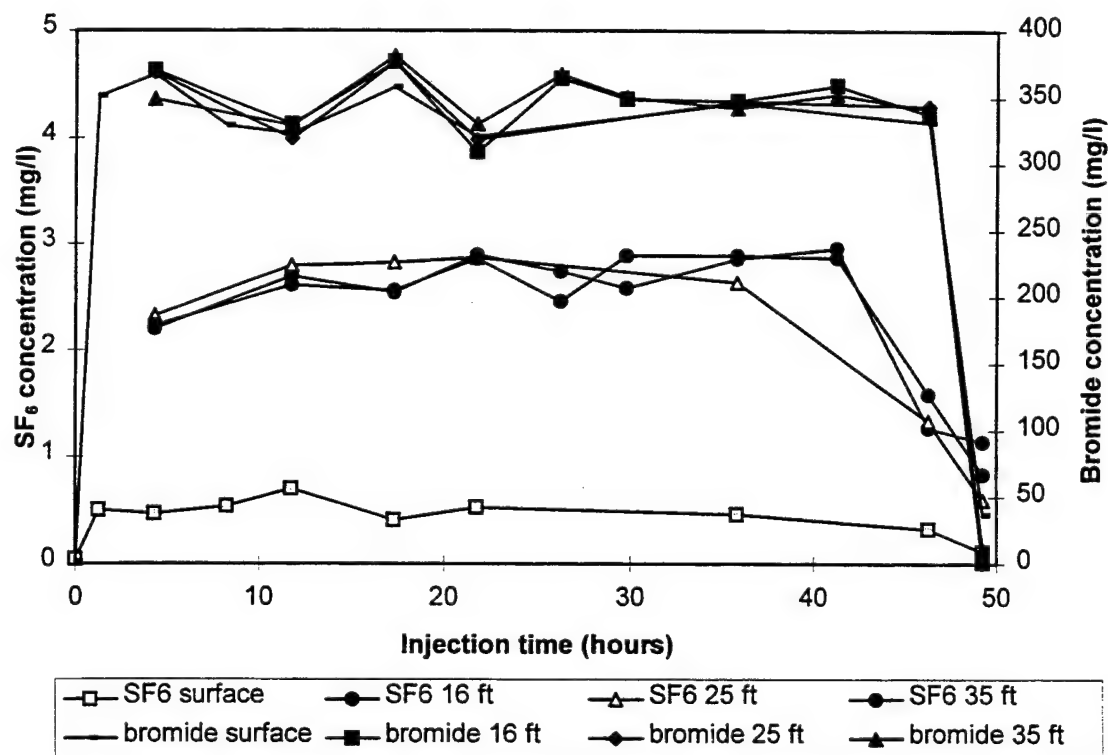


Figure 11. Injection Well History for Between-Cell Tracer Test

Average injection concentration and mean injection times (**Table 8**) were calculated using data from the three in-well sampling points only, using the method described by Levenspeil (1979). Very low SF₆ concentrations continued to be detected in the injection line and well three hours after the pulse was turned off. This effect was likely due to small SF₆ bubbles left trapped in the injection train. Once the problem was discovered, the line from the SF₆ tank was disconnected from the sparger and the sparger purged with nitrogen. Subsequent samples from the injection well had no detectable levels of SF₆.

TABLE 8. AVERAGE CONCENTRATIONS AND MEAN INJECTION TIMES FOR BETWEEN-CELL TRACER TEST

Tracer	Average Concentration and Standard Deviation (mg/l)	Mean Injection Time and Standard Deviation (hours)
SF ₆	2.68 ± 0.22	25.7 ± 0.11
bromide	346.63 ± 18.85	26.7 ± 0.9

Concentration histories of SF₆ and bromide from sample points at 9.4, 10.4, 11.3, 12.2, and 13.1 meters bgs (31, 34, 37, 40, and 43 feet bgs) are shown in **Figure 12**. In order to facilitate comparison, the concentrations of SF₆ and bromide were normalized to the average injection concentration. No signal of either tracer was detected at any time at the shallower sampling positions at 5.2, 6.1, 7.3, and 8.5 meters bgs (17, 20, 24, and 28 feet bgs). This is consistent with the results of the Hvorslev packer tests conducted in the injection well, which indicated that hydraulic conductivity across these intervals was two orders of magnitude less than in the lower sections of the profile. Because the injection pulse was of short duration relative to the travel time in these less permeable zones, it is likely that the SF₆ mass which flowed into these tight layers was insufficient to generate a quantifiable signal. On the other hand, breakthrough is not necessarily anticipated over the period studied if travel times truly are 100 times longer than at other locations. Finally, and not shown in **Figure 12**, only a weak signal ($C/C_o \ll 0.06$) of both tracers was detected in the deepest point sampling at 14 meters bgs (46 feet bgs). This was perhaps a result of the sample point being positioned slightly below the sand/clay interface, as

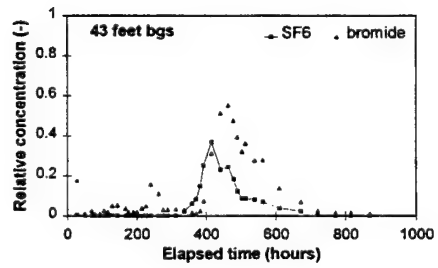
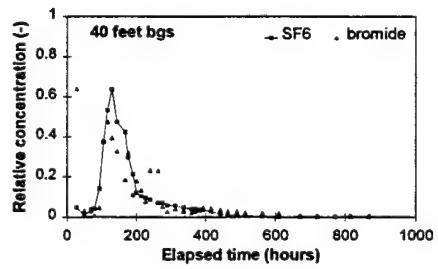
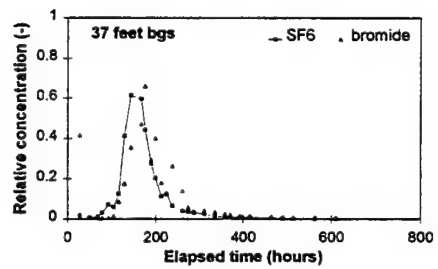
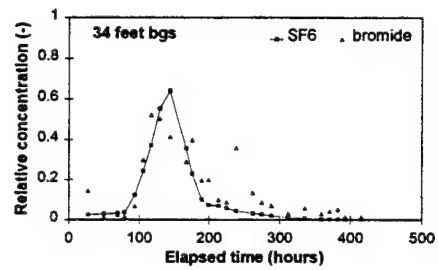
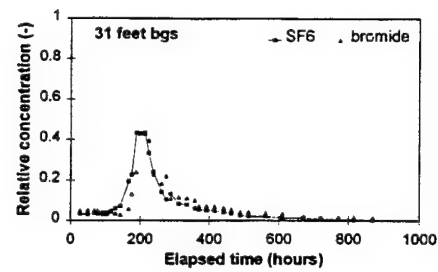


Figure 12. Sampling Point History for Between-Cell Tracer Test

occurred for some of the in-cell multilevels. This cannot be confirmed since no soil coring was conducted between the cells.

Outlying bromide concentrations are evident on some of the breakthrough curves and have been attributed to a problem with the analytical technique applied to these samples. Initially, every second or third sample was analyzed for bromide, and at a later date the remaining samples were analyzed. A negative drift due to depleted filling solutions in the reference electrode went undetected during the most recent analyses. This drift resulted in artificially high bromide concentrations for the latter samples. Unfortunately, no archived samples were available for re-analyses and it was not possible to correct these results. However, affected samples could be independently identified and may be filtered from any future quantitative analysis of these results. The problem is especially evident in the data for the sampling points at 13.1 meters (31 feet) and 14.0 meters (46 feet) and the data for the extraction curves, whose samples were analyzed when the performance of the probe had degraded significantly.

These problems notwithstanding, it can be seen by comparison of the breakthrough curves in **Figure 12** that (1) the groundwater velocities in the various layers in which significant tracer breakthrough occurred vary by a factor of four or so, and (2) that the behavior of the two tracers is similar in each stratum. While more quantitative interpretation of these data is possible and indeed underway, the main points of the test for present purposes can be summarized briefly. The tracer test confirmed that there was significant variation in hydraulic conductivity within the aquifer and that flushing of contaminants should be most rapid in the bottom 2 meters of the aquifer, i.e. within the strata containing the majority of the VOC contamination. The test also gave a good indication of the shape of the tracer breakthrough, and therefore contaminant elution, curves to be expected during the tests within the cells. This information was helpful in designing the sampling schedule for the tests within the cells. Lastly, the tracer test suggested that the behavior of the two tracers, SF₆ and bromide, was very similar in this aquifer.

4.4.2. In-Cell Tracer Tests

Tracer tests were conducted in each of the two cells over the course of the pump-and-treat operation, as noted in **Table 1**. However, because of constraints of time, budget, and personnel, only the tracer results from the second tracer experiment in the CPC cell (using SF₆ and chloride

as tracers) have been analyzed. Additionally, because of concerns about potential bromide/chloride interference as well as high background chloride concentrations in the cell groundwater (which varied over time and space), chloride data from this test were not evaluated. The sulfur hexafluoride (SF_6) tracer results from this test, have, however, been carefully analyzed, evaluated, and modeled as part of an MS thesis project at JHU (Johnston, 1996). Some of the more salient results of that detailed investigation are reproduced here. Readers are referred to the MS thesis for further detail.

Injection well concentration histories for SF_6 at two monitoring points in the central injection well of the CPC (IW-2, **Figure 3**) are shown in **Figure 13**, with time zero being the time of initiation of tracer injection. Sampling well breakthrough curves from the CPC tracer test are shown in **Figure 14**. The uppermost point (CPC-5-3) is in the green/gray sand and showed by far the slowest breakthrough and lowest recovery of injected mass. In fact, the observed “breakthrough” may well be the result of solute dispersing into this zone from the underlying region. Potential solute transport in the overlying region is not applicable, since the groundwater table had dropped to below 6.1 meters (20 feet) bgs during this tracer test.

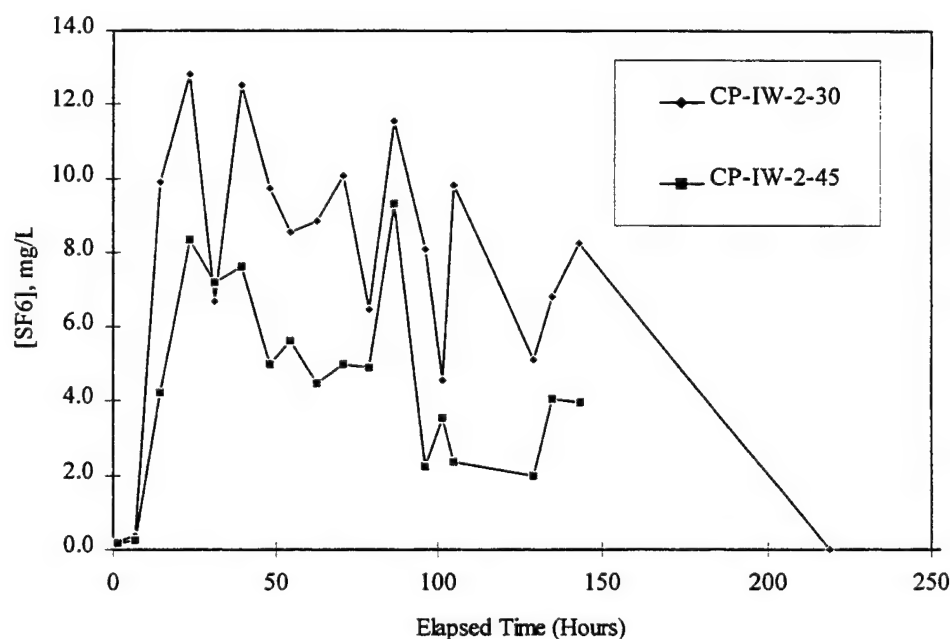


Figure 13. Injection Well History for SF_6 Tracer in CPC-IW-2

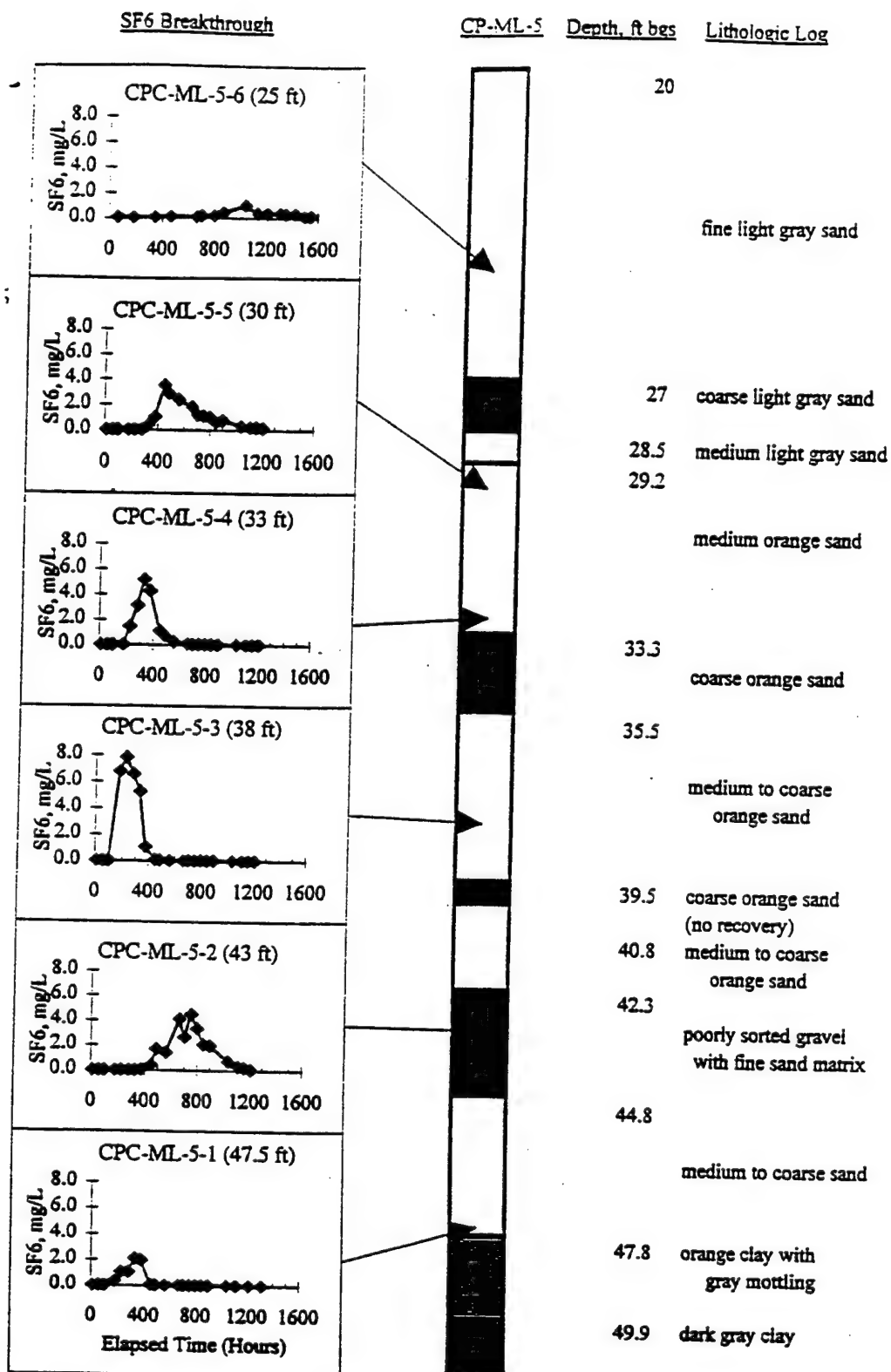


Figure 14. Sample Point Histories for SF₆ Tracer Test in CPC

The other ML-point showing very poor recovery is the lowermost point (CPC-5-1), although breakthrough at this point was rapid. The cause for this low recovery is not known. One possibility, already cited in the instance of the between-cell test, is that the sampling point was below the aquitard surface on the ML-stalk (and therefore out of a direct flow path of tracer). However, our estimates are that this sample point should be roughly 6 inches above the aquitard (**Table 1**). A second possibility is that the volatile SF₆ analyte was not well recovered for this deep well, since degassing under volume might create headspace in the vials and SF₆ loss during sample sealing. (Individual "off-line" samples were taken rather than automated purge-and-trap analysis through the ASAP system, and fabricated two-port stainless-steel sampling lids had to be removed prior to final vial sealing.)

The individual ML-point breakthrough curves were interpreted by three modeling means: moment analyses (for estimation of velocity), fitting a homogeneous advective/dispersive equation (ADE) for solute transport modeling (CXTFIT, Parker and van Genuchten, 1984), and fitting a two-region non-equilibrium solute transport model (CXTFIT, Parker and van Genuchten, 1984). For the transport modeling, influent concentrations were adjusted as required to provide mass balance (Johnston, 1996). For all samples except for the upper two ML points (ML-5-5 and ML-5-6), the two-region modeling showed little difference from equilibrium ADE modeling, with negligible porosity being attributed to non-equilibrium regions. Therefore, only the simple ADE modeling is reported here, together with the moment results. **Table 9** shows the results. Although dispersivity estimates for these poorly defined layers have little physical meaning, the estimated transport velocities should be indicative of the field-averaged groundwater flow rates in the region near the sampled depths.

TABLE 9. PARAMETER ESTIMATES FOR MODEL-SIMULATED SF₆ TRANSPORT AT MULTILEVEL MONITORING POINTS

Location	Depth (m)	Velocity Based on Analysis of First Moment (cm/hr)	ADE* Modeling Velocity (cm/hr)	ADE* Implied Longitudinal Dispersivity (cm)
CPC-5-6	7.6 (25 ft)	0.51**	0.51±0.133	235.04±61.6
CPC-5-5	9.1 (30 ft)	0.86	1.03±0.026	25.83±3.62
CPC-5-4	10.0 (33 ft)	1.65	1.97±0.022	11.90±1.27
CPC-5-3	11.6 (38 ft)	2.58	3.16±0.073	36.19±5.19
CPC-5-2	13.1 (43 ft)	0.68	0.75±0.016	15.74±1.67
CPC-5-1	14.6 (48 ft)	1.88	2.05±0.064	12.23±3.29

* ADE = advective/dispersive equation for solute transport modeling; the implied dispersivity is based on the fitted longitudinal dispersion coefficient (cm²/hr) divided by the velocity (cm/hr)

** Concentrations extremely low --likely that advective breakthrough never really occurred at this location.

Effluent well concentrations were also evaluated, with results as shown in **Figure 15** and **Figure 16**. These data were modeled in a variety of ways, included modeling of the aquifer as a stratified porous medium, with layer velocities and dispersivities as noted in **Table 9**, both with and without individual layer thickness adjusted as needed to achieve best fit while maintaining mass balance (**Figure 15**). These stratified layer model fits were essentially as good as those obtained by one-dimensional transport modeling using the equilibrium (ADE), stochastic, and two-region fitting routines described as part of the CXTFIT modeling package developed by Parker and van Genuchten (Parker and van Genuchten, 1984). The CXTFIT results are shown in **Figure 16**, obtained using parameters shown in **Table 10**. The stratified layer modeling (**Figure 15**) was also able to simulate the apparent bi-modal aspect of the breakthrough curve, and yielded a sum of squared residuals (SSQ) of 25.91, which is not greatly different from those achieved by some of the CXTFIT multi-parameter fitting estimates. In general, none of these models is believed to be mechanistically correct (in terms of capturing fundamental physical characteristics of the system), although all were capable of providing reasonably good data fits.

Readers are referred elsewhere for details regarding the alternative simulations and interpretations (Johnston, 1996).

TABLE 10. CXTFIT PARAMETERS FOR SIMULATING CPC TRANSPORT TO CP-EW-2 AS A SINGLE-LAYERED POROUS MEDIUM

Transport model	Velocity* (cm/hr)	α (cm)	β	ω	σ_{ln}	SSQ
Equilibrium	2.0	254±19.2	--	--	--	25.92
Stochastic	2.0	277±143	--	--	0.0025±31	22.71
Two-region	2.0	114±22.5	0.692±0.04	0.19±0.13	--	15.96

* Constrained on the basis of known pumping rates, cross-sectional area, and media porosity

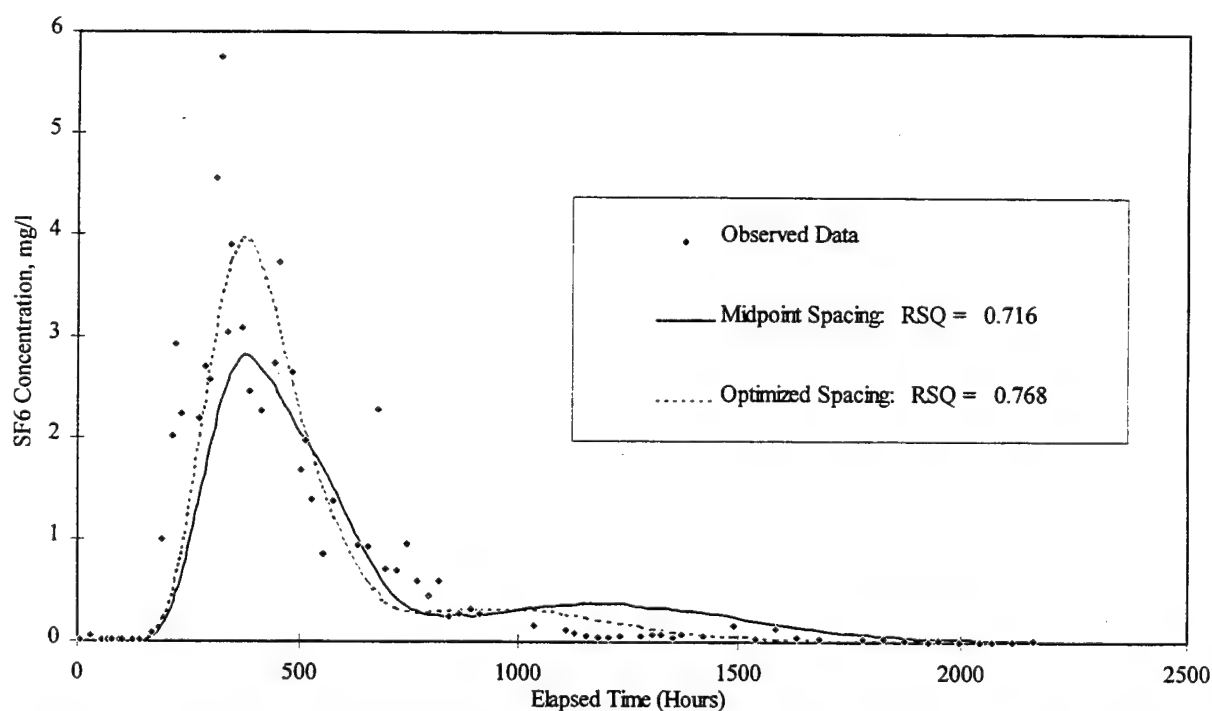


Figure 15. Stratified Layer Simulations of SF₆ Response at CP-EW-2. (RSQ is the Pearson Product Moment Correlation Coefficient.)

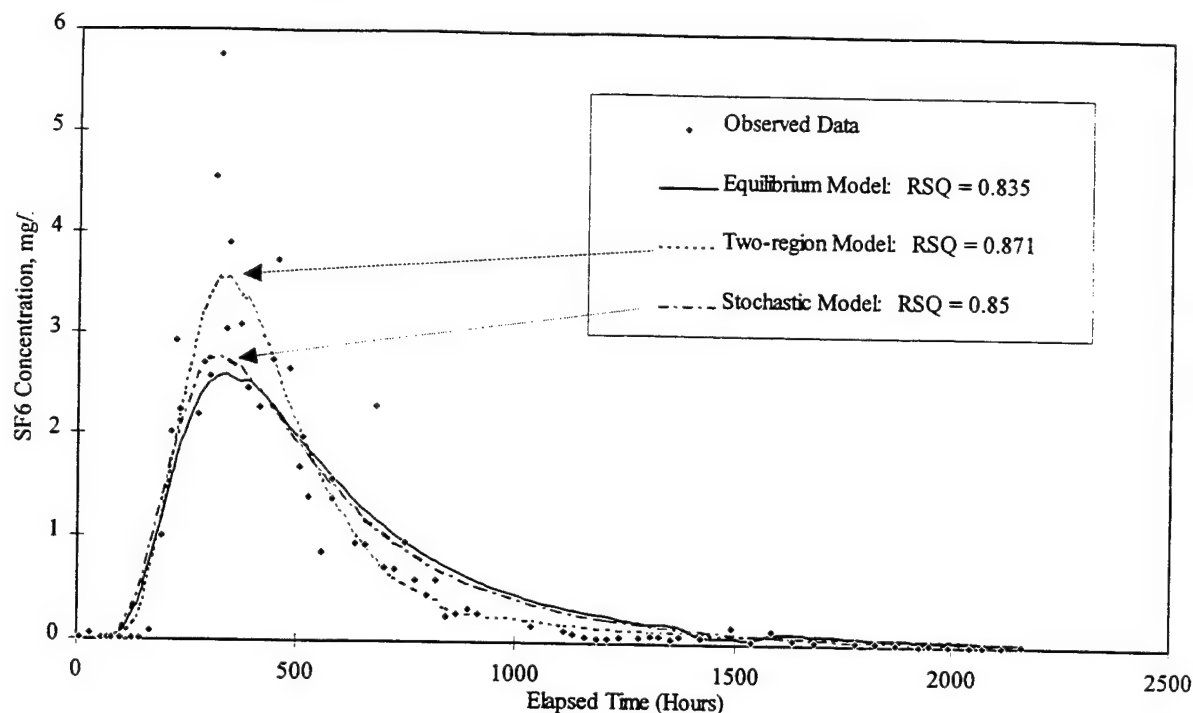


Figure 16. CXTFIT Model Simulations of SF₆ Response at CP-EW-2. (RSQ is the Pearson Product Moment Correlation Coefficient.)

4.5. SOLIDS CHARACTERIZATION STUDIES

4.5.1. Sample Collection, Handling, and Amalgamation

The characterization of subsurface materials required the amalgamation of material from selected depth intervals and coring locations. In this regard, there is a trade-off with regard to the conflicting goals of (1) obtaining maximum information about spatial heterogeneity of subsurface characteristics; (2) obtaining sufficient mass of material to permit better accuracy and precision of analysis (as through replicate analysis and analyses by different methods); (3) obtaining sufficient material to conduct different types of characterization on the same source material; and (4) obtaining a good estimation of appropriate “average” characteristics for the entire field test cells. The latter goal can be met through either (a) a close and representative spacing of many samples over the full volume or (b) accurate analysis of fewer “composite” (amalgamated) samples, the bulk composition of which reflects the average composition over a larger volume of the field.

In meeting the above objectives, solid characterization studies were conducted on two different types of subsurface solid samples:

Amalgamated Samples. An amalgamation of material over selected depth intervals was collected from all fourteen coring locations within the two test cells, as shown in **Table 11**. Such “horizontal-plane” amalgamation of sample was conducted only for sandy materials which appeared to be visually identical among cores (e.g., gray-green medium sand, dark orange medium/coarse sand, orange/rust gravelly medium/coarse sand). Amalgamation was achieved by carefully removing the selected material from each core with stainless steel scoops and spoons, transferring this material to a large (1 meter x 1 meter) well-cleaned stainless steel basin, and air drying over a period of several weeks under loose aluminum foil cover. To the best of our knowledge, this procedure achieved its intended effect of providing a large mass of air dried material that is free of external sources of organic carbon or other contaminants. After air-drying, the material was mixed and then split into 64 replicate portions by making multiple passes through a riffle splitter. As in the drying process, care was taken to avoid external contamination and to prevent dust loss (e.g. through foil covers of splitting devices and receiving basins). These amalgamated samples are identified as GS-20/25, GS-25/30, OS-30/35, OS-35/40, OS-40/45, OS-45/48, and OS-45/48D, with depth intervals and general characteristics as shown in **Table 11**. All samples have been stored dry and in the dark since collection, with subsamples stored in sealed mason jars.

Individual Core Samples. Samples of subsurface material were sometimes collected from a single selected core section, over smaller depth intervals. When more than one sample is collected from a given core, the sample is identified by coring location (e.g., PPC-11), a number designating the depth-interval of the core section (e.g., PPC-11-8 for section “8” for the 45-50 foot section of the PPC-11 core), and a final number designating the sequential subsection (e.g. PPC-11-8-1, for the top-most sampled interval in core section PPC-11-8). Core sections and subsections are both measured from the top. All “sections” are in 5-foot intervals bgs, with the first section being 10 to 15 foot bgs -- no coring was conducted closer to ground surface (except in informal preliminary investigation). Subsections are numbered sequentially -- precise depth intervals are not coded in the subsection’s designation, but were separately recorded and are

TABLE 11. AMALGAMATED SAMPLES OF SUBSURFACE AQUIFER SOLIDS AT DAFB, DE

Sample Designation	Alternative Sample ID ^a	Sampled Depth		Material Description
		meters	feet	
GS-20/25	XXX-X-3	6.1-7.6	20-25 ^b	light gray-green medium sand
GS-25/30	XXX-X-4	7.6-9.1	25-30 ^c	light gray-green medium sand
OS-30/35	XXX-X-5	9.1-10.6	30-35 ^b	orange coarse sand
OS-35/40	XXX-X-6	10.6-12.2	35-40	orange coarse sand
OS-40/45	XXX-X-7	12.2-13.7	40-45	orange gravelly coarse/medium sand
OS-45/48 ^d	XXX-X-8	13.7-14.2	45-48	orange gravelly coarse/medium sand
OS-45/48D ^d	XXX-X-8D	13.7-14.2	45-48 ^c	dark orange gravelly coarse/medium sand (noticeably darker in color when field wet)

^a Laboratory use only (listed here for purposes of internal cross-referencing)

^b Only the lower portion of the depth interval was sampled at core locations where an interface with different overlying materials was observed within the section (see fence diagrams, App. A).

^c Only the upper portion of the depth interval was sampled at core locations where an interface with different underlying materials was observed within the section (see fence diagrams, App. A).

^d Note that the "48" designation on this material is only an approximate depth bgs (in feet), with the aquitard interface as the actual bottom limit. Also, some of the OS-40/48 material from the lowest portions of the following cores was visibly darker when field wet: CPC-5, CPC-7, CPC-9, CPC-10, PPC-5, PPC-10. This material was separately identified as OS-45/48D (for "dark"). The dark coloring may suggest the presence of adsorbed Fe(II) (J. Zachara, personal communication).

reported where applicable. Three types of subsample handling and storage were used:

1. transport of Saran-wrapped cores to laboratory; storage at 4 °C; air drying under foil cover; storage in the dark at room temperature in sealed polyethylene bags;
2. direct field collection of field-wet material from cores into polyethylene bags; transport to the laboratory on ice; storage in the dark at 4 °C; and
3. direct field collection of field-wet material from cores into mason jars; purging of jars with nitrogen gas prior to closing of sealing lids; transport to the laboratory; storage in the dark at 4 °C.

All of the solids characterization results reported in this chapter are based on air-dried samples. Splitting of the air-dried materials into replicate subsamples was conducted by standard means, usually involving the application of both a 2-way riffle splitter and a 16-way rotating riffle splitter (Models SP-3 and SP-201, respectively, Gilson Co., Inc. Worthington, OH). Splitting of field-wet samples was by means of standard coning and quartering techniques (ASTM, 1985).

4.5.2. Mineralogy

Mineralogical characterization of selected subsurface solids was conducted by means of microscopic examination and X-ray diffraction analysis. Samples characterized with regard to mineralogical composition came from core material collected from five depth intervals, including three samples of sandy material taken from the amalgamation of material from fourteen soil cores and two samples of aquitard material collected from a single selected core section. The three sand materials represent amalgamated materials from 25 to 30 feet, 30 to 35 feet and 35 to 40 feet bgs, and designated as GS-25/30, OS-30/35, and OS-35/40 (**Table 12**). The two aquitard materials studied were taken from the pulsed-pumping cell, section PPC-11-8. These materials were an orange silty clay loam (OSCL) and a dark gray silt loam (DGSL). The OSCL lies directly over the DGSL in the aquitard. All material of the given type (OSCL or DGSL) within the PPC-11-8 core section was amalgamated into a single sample and riffle split into replicate samples for mineralogical and other analyses.

4.5.2.1. Optical Mineralogy

Minerals for sands GS-25/30, OS-30/35, and OS-35/40 were identified using optical mineralogy techniques. Epoxy-impregnated thin sections of the three sand samples were prepared by an outside laboratory (Mid-West Petrographic Services, Ypsilanti, Michigan) and then analyzed for mineral species using a petrographic microscope (Nikon Model 79234). From each slide, 100 grains in the 100-500 μm size range were selected by a semi-random process (Amonette and Zelazny, 1994) for identification. Identification was based on standard optical properties -- namely, interference colors, refractive index, cleavage properties, and twinning.

4.5.2.2. X-Ray Diffraction

For the finer materials, (OSCL and DGSL), mineralogical analyses were performed by X-ray diffraction (XRD), generally following methods described by Whittig and Allardice (Whittig and Allardice, 1986). These analyses were conducted as a preliminary effort only, conducted by a fourth-year undergraduate geology student (Mr. Bill Cowan) in the laboratory of the School of Earth and Planetary Sciences at JHU. We note that, because there were no chemical pre-treatments or additives (other than dispersing agents), the full diagnostic potential of the method was not explored.

For XRD analysis, the OSCL and DGSL samples were split into a coarse ($> 62 \mu\text{m}$) and a fine fraction ($< 4 \mu\text{m}$) by settling in a dispersing solution comprised of DI water containing roughly 10 g/L sodium-hexa-meta-phosphate and 2.5 g/L sodium bicarbonate. No other chemical pretreatment was conducted. An oriented aggregate specimen of the fine fraction ($< 4 \mu\text{m}$) was obtained by means of slow (several day) evaporation of roughly 15 mL of the fine fraction supernatant, leading to the direct deposition of a thin solid film onto a glass microscope slide placed at the bottom of the evaporating dish. The coarser fraction of each of the two aquitard samples was analyzed as a random-powder specimen, obtained by pulverizing the fraction to less than $10 \mu\text{m}$ with a mortar and pestle, mixing in methanol, spreading directly on glass slides, and allowing the methanol to rapidly evaporate. An X-ray diffractometer at the JHU School of Earth and Planetary Sciences (Phillips Electronics Instruments, Model 15010021X) generated the diffraction patterns. The patterns were compared with the standards in the *Inorganic Index of the Powder Diffraction File* (ASTM, 1968).

4.5.3. Results of Optical Mineralogy (Aquitard Sands)

The observed mineralogical composition of the aquifer sands is given in **Table 12**. The samples are mainly composed of quartz with lesser amounts of feldspars. The grains in all three sands were covered with an iron coating, as further discussed below.

For all three sand samples, a coating of dull, yellow-orange fine grained material surrounded many of the grains and is strongly suspected to be ferric iron (hydr)oxide. The mineralogy of these iron coatings is currently unknown, but is likely to vary among the samples. The coatings

TABLE 12. MINERALOGICAL ANALYSIS BY OPTICAL MICROSCOPY

	Percent of 100 grains sampled ^a		
	GS-25/30	OS-30/35	OS-35/40
Quartz	64	80	87
Feldspars	21	19	12
Amorphous Aggregate ^b	7	1	1
Iron oxy/hydroxide aggregate	6	0	0
Mica, ^c	2	0	0

^a representative grains in the size range 100 μ m to 500 μ m (most were 250 to 500 μ m)

^b very fine grain material, high relief, low refractive index

^c found in relatively small pieces: 100-200 μ m

on sample GS-25/30 were much less abundant than for the other two sands (both of which were rust colored to the eye). In addition, the coatings in GS-25/30 looked smooth and plate like, whereas the iron material in OS-30/35 was granular. In areas of thin coatings, the OS-30/35 coatings had a darker, orange color than did the coatings in GS-25/30. The iron-coatings in OS-35/40 appear the same as those in OS-30/35, but covered less of the grains. Extractable and total iron contents were not determined, but would be a first recommended step in any effort to obtain more information regarding the iron oxide coatings on the various strata. Analyses of subsurface sands collected elsewhere at DAFB, DE, have found total iron oxide contents in the range of 0.4% to 2% as Fe_2O_3 , with non-crystalline (amorphous) forms accounting for 4% to 11% of that amount (communication from Dr. Lucian Zelazny of Virginia Polytechnical Institute and State University, Blacksburg, VA, through Dr. Mark Noll, Applied Research Associates, Groundwater Remediation Field Laboratory, DAFB, DE).

4.5.4. Results of XRD Analyses (Aquitard Samples)

The XRD patterns of the fine and coarse fractions of the two aquitard materials (OSCL and DGSL) were compared with known patterns of several minerals. The XRD pattern matching was not conclusive, although quartz diffraction patterns were clearly apparent for all materials. Diffraction pattern results for both coarse fractions were clearly dominated by quartz (SiO_2), and patterns for other minerals could not be discerned with the manual methods of analysis used.

Subsequent discussion is confined to the fine ($<4\ \mu\text{m}$) fraction of the two materials.

In addition to dominant peaks attributable to quartz, the fine fraction of OSCL material showed diffraction pattern peaks diagnostic for kaolinite ($\text{KAl}_2(\text{OH})_2\text{Si}_3\text{AlO}_{10}$) and lepidocrocite (FeOOH). No peaks were found corresponding to those expected for goethite (FeOOH). There was additional (inconclusive) evidence that muscovite (a mica, $\text{Al}_4(\text{OH})_8\text{Si}_4\text{O}_{10}$) and iron-rich chlorite ($[\text{Mg,Fe,Al}]_6(\text{OH})_8[\text{Si,Al}]_4\text{O}_{10}$) might also be present in this sample.

XRD results with the fine fraction of DGSL were similarly dominated by peaks attributable to quartz and also showed diffraction patterns indicative of kaolinite. As with the OSCL, there was additional (inconclusive) evidence for the presence of muscovite and chlorite. Unlike the OSCL results, however, DGSL results showed no matches with peaks corresponding to lepidocrocite or other iron oxide minerals.

Other investigators have found that the $<2\ \mu\text{m}$ fraction of orange and gray aquitard materials at DAFB, DE (obtained from similar depth but different location) are dominated by kaolinite, montmorillonite, mica, and quartz (communication from Dr. Lucian Zelazny of Virginia Polytechnic Institute and State University, Blacksburg, VA, through Dr. Mark Noll, Applied Research Associates, Groundwater Remediation Field Laboratory, DAFB, DE). Approximate percentages of these four minerals (Kaol/Mont/Mica/Qtz) were reported (on samples pretreated for the removal of Fe-oxide coatings) to be 47/30/15/4 for the $<2\ \mu\text{m}$ fraction of an orange aquitard material (47% clay-size content) and 25/50/10/5 for the $<2\ \mu\text{m}$ fraction of a gray aquitard material (18% clay-size content). Total iron content of the orange clay in that work was found to be roughly 7% as Fe_2O_3 . In our own work, the orange material has less of a clay-size content (see subsequent section) and montmorillonite XRD peaks were not observable in either aquitard sample. However, we note that we did not conduct the pretreatment needed to facilitate the detection and analysis of expanding clay minerals. Thus, our negative results by no means preclude the potential presence of montmorillonite. We further note that samples have been stored in our labs in the event that the need and opportunity for more complete future analysis should arise.

4.5.5. Physical/Chemical Characterization of DAFB Solids

In order to support potential interpretations of groundwater flow and solute transport inside (and in the vicinity of) the DAFB test cells, subsurface solids taken from soil coring at the research site have been extensively characterized with regard to those parameters deemed most germane to the issues of solute transport. In addition to sorption isotherm and rate studies (described in Section 4.5.6 below), the solids have been characterized with respect to solid density, in-situ bulk density (ρ_b), in-situ porosity (ϵ), particle size distribution (PSD), cation exchange capacity (CEC), and organic carbon content (mass fraction of organic carbon, f_{oc}). These analyses are the focus of the current section.

Analyses with respect to the above parameters have been conducted on an array of solids, including both individually collected strata and amalgamated ("bulk") solids, collected and handled as described previously (Section 4.5.1). In general, the project focus, time and budget did not allow evaluation of spatial variability to the extent necessary to provide meaningful evaluation of the three-dimensional spatial correlation of parameters (Gelhar, 1986; Journel and Huijbregts, 1978). Therefore, for the purposes of this section, we do not report results that have been obtained to date on individual core strata. Rather, these results are reported elsewhere, as relevant to other issues -- e.g., to VOC extraction and analysis (Ball et al., 1997b); to sorption experiments with individual strata (see Section 4.5.6 below), or to studies of contaminant transport in particular aquitard layers (see Chapter 5 and the related diffusion modeling studies of Ball et al., 1997a; Ball et al., 1995). We also note that original core samples are being maintained in our laboratory (e.g., vertically split core with Saran wrap cover, 4 °C storage) such that a more detailed analysis of spatial variability may be possible in future work.

With the reasoning noted above, this section of our report focuses on providing an overall summary of the physical/chemical characterization of subsurface solids parameters, with "average" parameter values reported, as obtained primarily from the amalgamated samples, but also as based on averaging of results from individually considered strata.

Results are provided in **Table 13**, with methods and sampling locations as explained more thoroughly in following subsections. For the purposes of **Table 13**, results (bulk properties, PSD, f_{oc} , mineralogy) obtained with two amalgamated gray sand samples (GS-20/25, GS-25/30)

TABLE 13. CHARACTERISTICS OF DAFB AQUIFER AND AQUITARD SAMPLES

Stratum	Bulk Density ρ_b (g/cm ³)	Porosity ε (-)	Median Diameter d_{50} (mm)	Uniformity Coeff., d_{60}/d_{10} (-)	CEC (meq/100 g)	f_{oc} (g/g)
Medium Gray Sand 6.1 to ~9.1 m (20 to ~30 ft)	1.63 ± 0.06 [18]	0.37 ± 0.03 [18]	0.33	38 = 0.38 mm / 0.01 mm	1.44 ± 0.07 [5]	0.00010 ± 0.00002 [4]
Coarse Orange Sand ~9.1 to 12.2 m (~30 to 40 ft)	1.66 ± 0.13 [17]	0.36 ± 0.05 [17]	0.61	4.7 = 0.70 mm / 0.15 mm	0.87 ± 0.15 [10]	0.00009 ± 0.00002 [8]
Gravely Coarse Orange Sand 12.2m to OSCL (40 ft to OSCL)	1.78 ± 0.06 [6]	0.32 ± 0.02 [6]	0.62	6.0 = 0.84 mm / 0.14 mm	0.80 ± 0.15 [5]	0.00007 ± 0.00003 [8]
Upper Aquitard Layer (OSCL)	1.22 ± 0.11 [28]	0.53 ± 0.04 [28]	0.009	~60 = 17 mm / ~0.3 mm	15.5 ± 0.8 [2]	0.00156 ± 0.00002 [4]
Lower Aquitard Layer (DGSL)	1.15 ± 0.09 [13]	0.56 ± 0.04 [13]	0.017	~40 = 24 μ m / ~0.6 μ m	29. ± 8. [2]	0.01490 ± 0.00010 [4]

Note: Shown are average values ± one standard deviation, with the number of replicates [n] in brackets. Particle size distribution is further described in Section 4.5.5.2

have been combined, as have results from the top upper orange sand samples (OS-30/35, OS-35/40) and the three "bottom" gravely orange sands (OS-40/45, OS-45/48, OS-45/48D). These amalgamations of data were made because the characteristics of the aquifer were found to be not markedly different within the defined intervals, at least with regard to the parameters measured. For the case of particle size distribution and sorption capacity data, this point is made subsequently through the presentation of more detailed results. Aquitard characterization results shown in **Table 13** are for homogenized material from the PPC-11 core, except for CEC results, which are averaged from 3 coring locations, as noted subsequently (Section 4.5.5.3).

4.5.5.1. Solid Density, Bulk Density and Porosity

4.5.5.1.1. Solid Density

The solid density of the amalgamated orange and gray sands was determined from a water displacement method described elsewhere (Ball et al., 1990). Eight samples were analyzed, including replicate samples each of GS-20/25, GS-25/30, OS-30/35, and OS-45/48.

Results with aquifer samples gave a solid density of 2.58 ± 0.022 for the gray sands ($n=4$) and 2.62 ± 0.005 for the orange sands ($n=4$). The minor difference between the gray and orange sands is statistically not significant, but would not be unexpected, given the greater abundance of iron oxides in the orange material (e.g., lepidocrocite density = 4.0 g/cm^3). Although aquitard samples were not specifically analyzed, the above values are likely to be reasonable estimates for these materials as well. In particular, the value of 2.6 is reasonable for quartz and feldspar minerals (e.g., low quartz, 2.65 g/cm^3 ; high quartz, 2.53 g/cm^3 ; orthoclase 2.56 g/cm^3 ; orthoclase and microcline, 2.56 g/cm^3 ; albite, 2.62 g/cm^3) as well as for kaolinite (2.6 g/cm^3 , Zoltai and Stout, 1984).

In summary, the overall average and sample standard deviation for the 8 solid density measurements was $2.60 \pm 0.026 \text{ g/cm}^3$, and this value is assumed for all subsequent calculations of porosity (from bulk density of aquifer material measured in core samples) or of porosity and bulk density (from moisture content measured in field-saturated subsamples of aquitard material).

4.5.5.1.2. Bulk Density and Porosity

For aquifer sands, bulk density and porosity were estimated by air drying known volumes of cored material. Samples were collected over short vertical intervals (15 cm or less) from both halves of an opened core, air dried and weighed. When necessary, the mass of sample previously removed for VOC sampling (adjusted to dry mass on the basis of moisture content) was added back into the total mass estimate prior to calculation of density. Volume occupied was calculated on the basis of a cylinder with a length equal to that of the core segment and a diameter of 1.875 inches (the internal diameter of an aluminum core tube). Such analyses were conducted for 56 samples of core materials from the B2 and B3 core locations, with results as reported elsewhere

(Eng, 1995) and summarized in **Table 13**.

For aquitard materials, porosity and bulk density were both calculated from moisture content samples taken concurrently with the VOC subsampling of the water-saturated soil core (Chapter 5; Ball *et al.*, 1997b). All told, well over 500 moisture content measurements were made, including several hundred on aquitard samples (Ball *et al.*, 1997b). Moisture content data reported in **Table 13** are from the PPC-11 core only, consistent with the other reported data.

4.5.5.2. Particle Size Distribution

For particle size analysis, 200- to 500-gram subsamples of air-dried material were riffle split from initial amounts (of either individual strata samples or amalgamated material; see Section 4.5.1), and analyzed by standard dry sieving and wet-sieving techniques (Gee and Bauder, 1986). Efforts were taken to ensure that the final mass on any given sieve did not exceed 70 grams.

For the particle-size results with individual aquifer strata reported elsewhere (Eng, 1995), hydrometer analysis and subsequent wet sieving were conducted after mechanical dispersion of the material in synthetic aquifer fluid (10 to 15 minutes shaking of a 50 to 100 g/L slurry). However, for the results with amalgamated sands and aquitard samples (i.e., for the results reported herein), dispersion was accomplished by overnight mixing of 40 to 100 g of soil with 350 mL of a chemical dispersing agent (14 g/L sodium hexa-metaphosphate in carbonate buffered solution), followed by mixing of the 50 to 100 g/L slurry for 25 minutes (Gee and Bauder, 1986). Subsequent hydrometer testing is conducted by diluting the well-mixed solution to a final concentration of 5 g/L sodium hexa-metaphosphate and following standard methods (Gee and Bauder, 1986). In all cases, hydrometer testing was conducted on unsieved sample, followed by separate wet-sieve characterization of materials larger than 63 μm . The latter was accomplished by rinsing either new sample or the previously dispersed material with synthetic ground water over a No. 230 stainless steel ASTM sieve, drying the retentate at 105 °C, and then conducting standard nested-sieve analysis of the dried retentate (Gee and Bauder, 1986).

Results of the wet-sieve analysis with amalgamated soil samples are reported in **Table 14**. Mass balances for sieve work alone were within 1% for all size fractions. However, the percentages reported in **Table 14** do not add up precisely to 100% for two reasons: (1) the two

TABLE 14. PARTICLE SIZE DISTRIBUTION OF AMALGAMATED SAMPLES

Sample	% gravel > 2 mm	% very coarse sand 1.0 to 2.0 mm	% coarse sand 0.5 to 1.0 mm	% medium sand 0.25 to 0.50 mm	% fine sand 0.125 to 0.25 mm	% very fine sand 0.063 to 0.125 mm	% silt ^a 2 µm to 50 µm	% clay ^a < 2 µm
GS-20/25	0.6	0.7	8.1	70.0	5.2	0.7	6.7	5.0
GS-25/30	3.3	4.4	12.5	59.6	5.7	1.3	6.6	6.7
OS-30/35	4.2	13.1	52.6	16.4	2.7	1.0	4.6	5.8
OS-35/40	3.6	9.3	52.5	21.6	3.9	1.2	5.9	3.3
OS-40/45	14.0	14.3	27.8	21.9	11.7	1.8	5.4	1.6
OS-45/48	17.2	17.2	24.3	19.0	12.3	1.9	3.2	1.6
OS-45/48D	12.9	18.1	29.4	19.9	11.1	1.8	3.0	2.0
OSCL	0.0	0.0	0.0	0.3	1.5 ^b	7.5 ^b	42	35
DGSL	0.0	2.5	2.3	1.4	1.6	8.2	65	18

^a Two right-most columns are based on hydrometer testing; other results are based on wet sieving.

^b For OSCL, sieve sizes were 0.053 mm (in lieu of 0.063) and 0.106 mm in (lieu of 0.125).

right-most columns are based on sedimentation data, whereas other results are based on sieved mass; and (2) in order to define follow the USDA definition of “silt”, sedimentation data are reported for a 50 µm size, rather than the 63 µm minimum sieve size (used for all soils except DGSL). Nonetheless, the mass balances for the mixed data sets are within roughly 3% for all samples except the OSCL, for which roughly 13.5% of the mass is unaccounted. Based on the full sedimentation test, we know that roughly 4.5% of this unaccounted mass is falls in the range of 50 µm to 63 µm, with the remaining 9% of unaccounted mass presumably related to (1) inaccuracies of the hydrometer method at short times (i.e., less than 1 minute for the settling of particles > 50 µm), and (2) nonideality of settling relative to the inherent assumptions of the method (perfectly spherical particles of 2.6 g/mL density). In this sense, the clay size fraction for the OSCL stratum may be somewhat higher than reported -- i.e., it is possible that this material is actually a “silty clay” (with 44% clay size fraction), rather than a “silty clay loam” (as based on the assumed 35% clay size fraction). On the other hand, the DGSL is clearly a “silt loam,” and has a much higher portion of coarser sand.

Finally, **Table 14** shows that the following amalgamated samples are of approximately similar size distributions: the two gray sands (GS-20/25, GS-25/30), the upper two orange sands

(OS-30/35, OS-35/40), and the three “bottom” gravely orange sands (OS-40/45, OS-45/48, OS-45/48D). A simplified description of the particle size distribution for the four major strata is given in **Table 15**. The median particle size and uniformity coefficients for these strata are as previously given in **Table 13**.

TABLE 15. SIMPLIFIED PARTICLE SIZE DISTRIBUTIONS OF FOUR MAJOR STRATA

	Depth Range (bgs)	% Gravel (> 2mm)	% Sand (0.050 mm to 2 mm)	% Silt (2 μ m to 50 μ m)	% Clay (< 2 μ m)
Medium Gray Sand	6.1 - 9.1 m (20 to 30 ft)	2%	85%	7%	6%
Coarse Orange Sand	9.1 - 12.2 m (30 - 40 ft)	4%	86%	5%	5%
Gravely Coarse Orange Sand	12.2 m to OSCL (40 ft to OSCL)	15%	79%	4%	2%
Upper Aquitard Layer (OSCL)	variable within 13.9 m to 15.2 m	0%	14% ^a to 23% ^b	42%	35% ^b to 44% ^a
Lower Aquitard Layer (DGSL)	variable within 14.6 m to 15.2 m	0%	17%	65%	18%

^a Based on wet-sieving results

^b Based on hydrometer results

4.5.5.3. Cation Exchange Capacity

Cation exchange capacity (CEC) was measured on 11 different samples, including 2 samples of gray sand (GS-20/25; GS-25/30), four samples of orange sand (OS-30/35; OS-35/40; OS-40/45; OS-45/48), three samples of OSCL (PPC-3-8, PPC-9-8, CPC-11-8), and two samples of DGSL (PPC-3-8, CPC-11-8). Analysis of replicate samples at JHU was by standard CEC methods, involving cation exchange with ammonium acetate and exchangeable acidity measurement by titration (Thomas, 1982). An “effective cation exchange capacity” (ECEC) was also measured at the University of Maryland Cooperative Extension Service’s Soil Testing Laboratory, using methods more fully described in Appendix D, which is a copy of a CEC-related letter report to Captain Jeff Stinson (Armstrong Laboratory, Tyndall AFB, FL). This report details the CEC and ECEC results and explains some of the differences obtained with the two techniques.

Results previously shown in **Table 13** represent the averaged results from the JHU analyses, which more closely follow the standard definitions of CEC. As evident from the table, the DGSL had the highest CEC, on the order of 20 to 30 meq/100g. This value is roughly twice as high as that of the OSCL and roughly twenty times that of the aquifer sands. The DGSL CEC, and especially the OSCL CEC are sufficiently low to suggest that there may not be a significant fraction of swelling clay in these samples -- swelling clays (such as montmorillonite) typically have CEC-values on the order of 100 meq/100g or more. Although the OSCL has the highest clay size fraction (at somewhere between 35% and 44%, **Table 15**) the DGSL has a roughly one order-of-magnitude higher organic carbon content (Section 4.5.5.4 below), which is likely a contributing factor to this stratum's higher CEC.

4.5.5.4. Carbon Content

4.5.5.4.1. Methods

A high temperature combustion method was used to measure organic carbon content and inorganic carbon content was measured by an acidification technique. The equipment for these analyses was manufactured by UIC Coulometrics (Joliet, Illinois) and consists of three major components: a Model CM5120 horizontal combustion furnace, a Model 5012 carbon dioxide coulometer, and a Model 5131 acidification module. The procedure for operating this equipment is described subsequently:

The CM5120 combustion furnace is set and allowed to stabilize at 950 °C. Pure oxygen is used as the carrier gas. Approximately 0.8 to 1.5 grams of soil sample is held in the pre-ignited porcelain boat and is introduced into a cool pre-chamber to the furnace. After a thorough flushing of the sample by the CO₂-free oxygen, the sample is introduced into the high temperature chamber by means of an external magnet, which drives a glass-enclosed steel "hook ladle" attached to the porcelain boat. Sulfur and halogen oxide gases are removed by barium chromate and reduced silver. The carbon dioxide released from the soil sample combustion flows with the oxygen carrier gas into the 5012 carbon dioxide coulometer and is titrated coulometrically. The carbon dioxide signal is integrated over the entire combustion period (7 minutes) and displayed as total carbon in µg. Inorganic carbon content is measured with an acidification method using

the model 5131 acidification module. About 1 to 2 grams of soil sample is acidified with 5 mL of 2N H₂SO₄. Carbon dioxide from acidification also flows into and is measured by the coulometer. The difference between total carbon and inorganic carbon is the total organic carbon content in the soil samples. In cases where inorganic carbon content is high, better accuracy can be obtained by acidifying samples prior to combustion and directly measuring f_{oc} . This was not necessary for these samples, since f_{ic} was very low.

4.5.5.4.2. Results

In Dover AFB solids, the inorganic carbon content was negligible (f_{ic} [g/g] below 0.00002). Organic carbon contents were also quite low in aquifer solids (f_{oc} below 0.0002 in all samples and below 0.0001 in most strata and all amalgamated solids). Organic carbon content in the OSCL aquitard samples was roughly 10-fold higher, and roughly 10-fold higher still in the DGSL. Results have been summarized previously (**Table 13**) for amalgamated samples and PPC-11-8 aquitard material. Additional data are presented in **Table 16**. Note that results in **Table 16** are shown in % organic carbon for ease of display. For the fifteen OSCL samples shown, f_{oc} averaged 0.0016 ± 0.03 g o.c./g soil (\pm one standard deviation). For the thirteen samples of DGSL, f_{oc} averaged 0.013 ± 0.02 g o.c./g soil.

4.5.6. Sorption Experiments with DAFB Solids

Sorption experiments with the DAFB materials were conducted using ¹⁴C-radiolabelled chemicals and a flame-sealed ampule technique well described elsewhere (Ball and Roberts, 1991a). Both rate studies (Ball and Roberts, 1991b) and sorption isotherm studies (Ball and Roberts, 1991a) were conducted.

The majority of experiments were conducted with PCE. Equilibration times of 1, 3, 10, 30, and 190 days were used for sorption experiments with samples of GS-25/30, OS-30/35, OSCL, and DGSL. Results of these experiments are given in Appendix E (Table E-1). In addition, 7 day and 70 day comparative results were obtained for single concentration partitioning studies ("one-point isotherms" with a variety of sand strata, as also shown in Appendix E (Table E-2). Most of these results suggest that contaminant distribution between the solid and liquid phase approached equilibrium values by either the 7-day or 10-day time period. The only potential

TABLE 16. ORGANIC CARBON CONTENT OF DAFB SOLIDS

	Sample	Depth of Sample (ft)	No. of Replicates Analyzed	Percent Organic Carbon Avg. (std. dev.)
Gray Sand	GS-20/25	20-25	4	0.0089 (0.0004)
	GS-25/30	25-30	8	0.0090 (0.0003)
	B3-1-5a	14.5	4	0.018 (0.0030)
	B3-3-3a	22.42	4	0.009 (0.0005)
	B3-4-3a	27.42	4	0.009 (0.0006)
Orange Sand	OS-30/35	30-35	7	0.012 (0.0030)
	OS-35/40	35-40	7	0.007 (0.0003)
	OS-40/45	40-45	4	0.006 (0.0002)
	OS-45/50	45-50	4	0.007 (0.0002)
	B3-5-3a	31.67	4	0.008 (0.0008)
	B3-6-3a	37.75	4	0.006 (0.0009)
	B3-7-3a	40-45	4	0.007 (0.002)
	B3-8-1a	46.1	4	0.008 (0.003)
	B3-8-1b	46.1	4	0.007 (0.002)
OSCL	B3-8-2a	47.5	4	0.13 (0.010)
	B3-8-2b	47.5	4	0.17 (0.008)
	PPC-1-8	47-49	4	0.18 (0.005)
	PPC-3-8	47-49	4	0.15 (0.001)
	PPC-9-8	47-49	4	0.12 (0.003)
	PPC-10-8	48-49	4	0.10 (0.004)
	PPC-11-8	46-47	4	0.16 (0.004)
	PPC-11-8	47-48.5	4	0.17 (0.001)
	CPC-1-8	48-49.5	4	0.22 (0.002)
	CPC-3-8	47.5-49.5	4	0.13 (0.002)
	CPC/PPC-5-8	46-48	4	0.16 (0.002)
	CPC-7-8	47-49.5	4	0.17 (0.005)
	CPC-9-8	46-48	4	0.22 (0.002)
	CPC-10-8	48-50	4	0.17 (0.004)
	CPC-11-8	46-48	4	0.16 (0.002)
DGSL	PPC-1-8	49.6-50	4	1.36 (0.035)
	PPC-3-8	49-50	4	1.20 (0.055)
	PPC-5-8	49.7-50	4	0.89 (0.030)
	PPC-5-8	49-49.7	4	1.39 (0.020)
	PPC-9-8	49.8-50	4	1.78 (0.026)
	PPC-9-8	49-49.8	4	1.60 (0.032)
	PPC-10-8	49-50	4	1.35 (0.046)
	PPC-11-8	48.5-50	4	1.49 (0.011)
	CPC-1-8	49.3-50	4	1.18 (0.065)
	CPC-3-8	49.5-50	4	1.31 (0.065)
	CPC-7-8	49.4-50	4	1.13 (0.046)
	CPC-9-8	48-50	4	1.24 (0.035)
	CPC-10-8	48-50	4	1.42 (0.056)

exception to this was the study with OS-30/35, for which the distribution coefficient increased from 0.05 mL/g in the first 3 days to 0.08 and 0.11 mL/g at 30 days and 192 days, respectively. For all cases with aquifer sand, the precision of the analysis was impaired by the fact that sorption was generally quite slight, approaching the detection limit of the method (~ 0.03 mL/g). Aquitard samples, on the other hand, showed very measurable sorption.

As shown by the figures at the back of this section, sorption for all materials was found to be quite linear, with little change in distribution coefficient over three to four order of magnitude variations in aqueous concentration. Freundlich interpretations of isotherm results are shown in the figure, and are also reported in **Table 17**. In general, and as previously noted, sorption to aquifer sands was quite low, with typical values on the order of 0.05 mL/g or sometimes much less. Considering a minimum quantification limit as roughly 10 times the standard deviation of replicate low-value samples, we consider the MQL of our method to be on the order of 0.1 mL/g with the highest solid:liquid ratio that can be reasonably studied. Thus, the partitioning on these sands is too low to be well quantified. Nonetheless, several of the aquifer sand strata did show unexpectedly high sorption for the amount of organic carbon present (less than 0.01% or $f_{oc} < 0.0001$). These samples were studied more extensively through complete sorption isotherms, as shown in **Figure 17** and **Figure 18**. The low organic carbon content of these soils might suggest that the comparatively high partitioning coefficients are related to adsorption phenomena rather than partitioning. If so, the process still appears to be driven by hydrophobic effects rather than specific adsorption phenomena, since the isotherms are remarkably linear. The unusually high sorption of the B3-4-4 and B3-7-3 materials was, however, anomalous, in that many more samples of seemingly like mineralogy and similar organic content sorbed much less strongly (Appendix E). In this regard, the results with bulk samples (**Table 17**) are much more indicative of the general sorptivity of the DAFB aquifer sands.

As evident from **Figure 18** through **Figure 21**, sorption of PCE with aquitard materials is also extremely linear. The PCE sorption by various strata of OSCL and DGSL shows some variability (**Table 17**), but this variability is small in comparison with the major change in sorption that occurs at the aquifer/OSCL and DGSL/OSCL interfaces. As discussed in Chapter 5, this helps to create sharp variations in the in-situ contaminant concentrations at these surfaces.

TABLE 17. SELECTED PCE AND TCE SORPTION DATA WITH DAFB SOLIDS

Aquitard Material		f_{oc} (g/g)	PCE		TCE	
			K_d (L/kg)	K_{oc} (L/kg)	K_d (L/kg)	K_{oc} (L/kg)
Gray Sand	GS-25/30 (7.6-9.1 m)	0.00009 ± 0.00003 [8]	0.06 ± 0.01 [19]	NQ	NA	NA
	B3-4-4a (8.8 m)	NA	0.25 ^b ± 0.02 [12]	NA	NA	NA
Orange Sand	OS-30/35 (7.6-9.1 m)	0.00012 ± 0.00003 [7]	0.07 ± 0.08 [17]	NQ	0.01 ± 0.01 [15]	NQ
	OS-35/40 (7.6-9.1 m)	0.00007 ± 0.00003 [4]	0.002 ± 0.01 [10]	NQ	0.01 ± 0.01 [10]	NQ
Gravelly Orange Sand	B3-7-3 (13.0 m)	0.00007 ± 0.00002 [4]	0.05 ± 0.01 [3]	NQ	NA	NA
	B3-8-1b (14.0 m)	0.00007 ± 0.00002 [4]	0.19 ^b ± 0.02 [16]	2700	NA	NA
OSCL	CPC/PPC 5 (14.0-14.6 m)	0.00156 ± 0.00002 [4]	0.34 ^b ± 0.04 [25]	220	NA	NA
	B3-8-2b (14.5 m)	0.00173 ± 0.00008 [4]	0.51 ^b ± 0.11 [16]	290	NA	NA
	B3-8-1a (14.5 m)	0.0013 ± 0.0001 [4]	0.17 ± 0.02 [3]	130	NA	NA
	PPC 11-8 (14.3-14.8 m)	0.00169 ± 0.00001 [4]	NA	NA	0.18 ^b ± 0.05 [19]	106
DGSL	PPC 11-8 (14.8-15.2 m)	0.0149 ± 0.0001 [4]	22. ^b ± 2.8 [22]	1500	NA	NA
	PPC 5-8 (14.9-15.1 m)	0.0139 ± 0.0002 [4]	22. ± 2.1 [10]	1600	NA	NA
	PPC 9-8 (14.9-15.2 m)	0.0160 ± 0.0032 [4]	9.6 \pm 2.1 [10]	600	NA	NA
	CPC 7-8 (15.0-15.2 m)	0.0113 ± 0.0004 [4]	8.1 ± 1.7 [10]	720	NA	NA
	CPC 11-8 (14.6-15.2 m)	0.0142 ± 0.0006 [4]	15 ± 2.5 [10]	1100	6.1 ^b ± 1.3 [23]	430

^a Avg. value \pm one std. dev.; [n] = no. of samples; NA = Not Analyzed. NQ = Not Quantifiable.

^b Freundlich isotherm interpretations were also obtained where isotherms included more than a three order-of-magnitude concentration range; ($q = K_f C^{1/n}$, with q in $\mu\text{g/kg}$ and C in $\mu\text{g/L}$):

PCE with gray sand B3-4-4a (8.8 m): $K_f = 0.26$; $1/n = 0.99$; $r^2 = 0.991$

PCE with grav. orange sand B3-8-1b (14.1 m): $K_f = 0.13$; $1/n = 1.02$; $r^2 = 0.971$

PCE with OSCL PPC/CPC 5-8: $K_f = 0.41$; $1/n = 0.96$; $r^2 = 0.996$

PCE with OSCL B3-8-2b (14.5 m): $K_f = 0.49$; $1/n = 0.99$; $r^2 = 0.998$

TCE with OSCL PPC 11-8: $K_f = 0.19$; $1/n = 1.04$; $r^2 = 0.997$

PCE with DGSL PPC 11-8: $K_f = 24$; $1/n = 0.97$; $r^2 = 0.993$

TCE with DGSL CPC 11-8: $K_f = 8.4$; $1/n = 0.94$; $r^2 = 0.999$

Also the sorption in the aquitard material slows contaminant diffusion in this medium. By understanding the extent of sorption, and with independent knowledge about diffusion rates, we have been able to use the contamination profiles within the aquitard (Chapter 5) as a forensic tool to provide information about contamination history in the overlying aquifer (Ball et al., 1997a; Liu and Ball, 1997).

Finally, **Figure 23** shows the results of sorption tests with 1,2,4-trichlorobenzene (TCB), which is a much more hydrophobic compound, with much higher octanol-water partitioning coefficient ($\log K_{ow} = 4.5$ vs. $\log K_{ow} = 2.4$ for TCE and $\log K_{ow} = 2.9$ to 3.4 for PCE, Schwarzenbach et al., 1993). The study with TCB confirms the trend of increasing sorption with increasing hydrophobicity (observed between TCE and PCE), and supports the notion that sorption is hydrophobically driven in the OSCL material. We use this fact to make approximate (order-of-magnitude) estimates of the extent of sorption of other chemicals (see Chapter 6 and Appendix H).

(**Note:** References for this chapter [Section 4.6] follow Figures 17 through 23.)

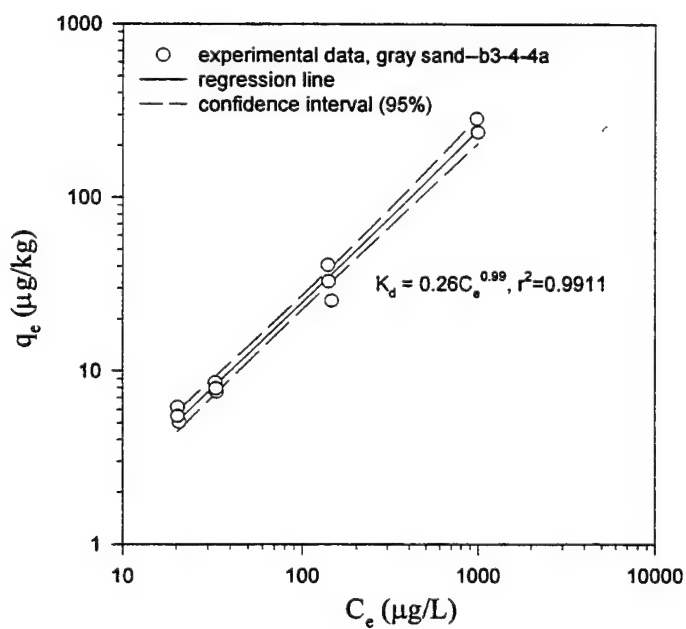
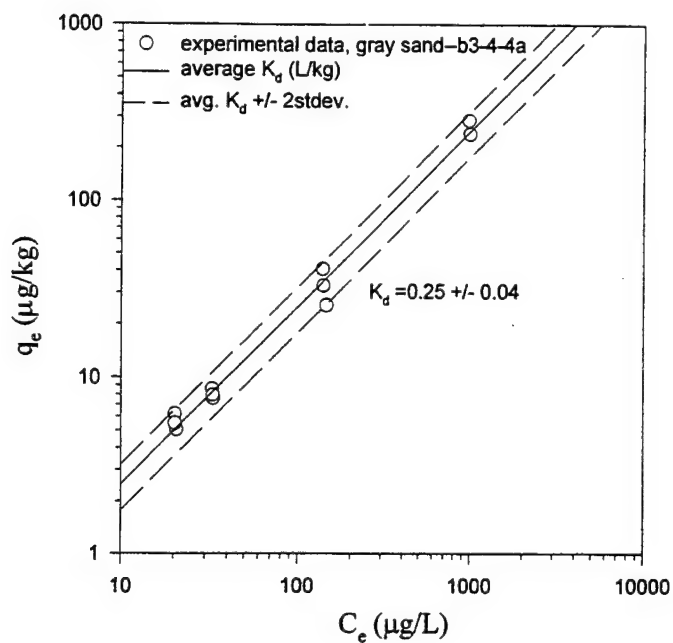


Figure 17. PCE Sorption Isotherms with Gray Sand from Core B3, with Linear (top) and Freundlich (bottom) Interpretation

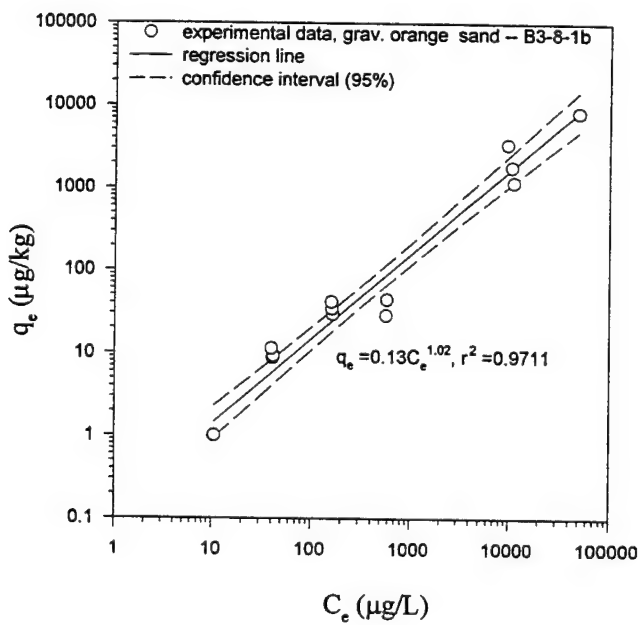
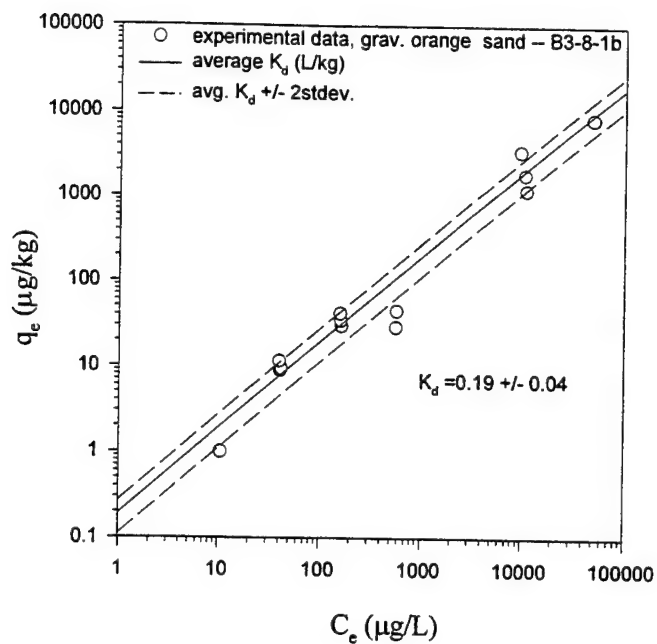


Figure 18. PCE Sorption Isotherms with Gravelly Orange Sand from Core B3, with Linear (top) and Freundlich (bottom) Interpretation.

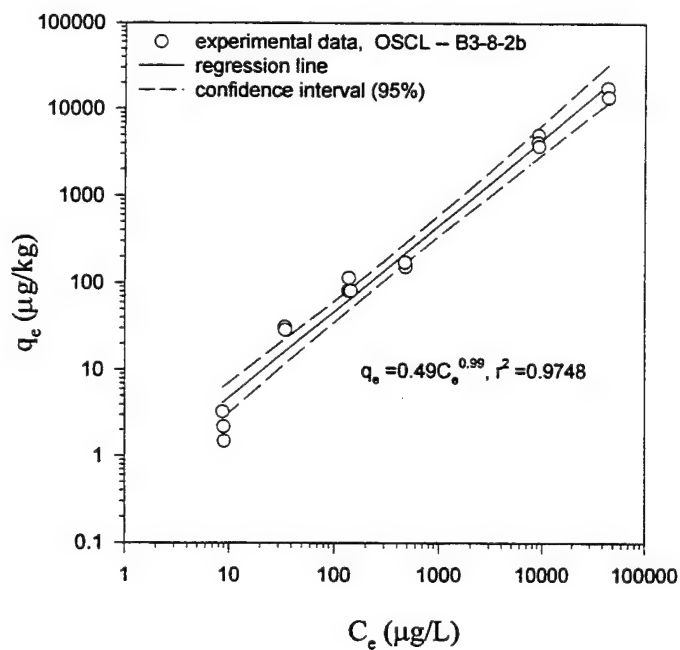
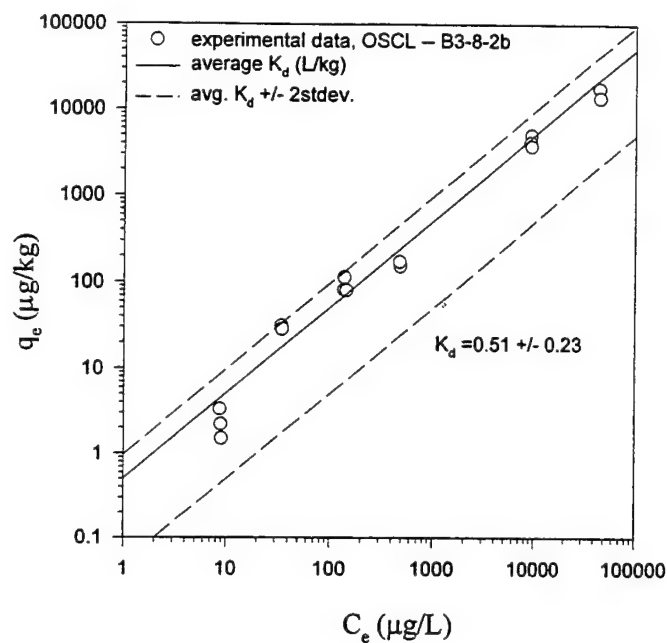


Figure 19. PCE Sorption Isotherms with OSCL from Core B3, with Linear (top) and Freundlich (bottom) Interpretation.

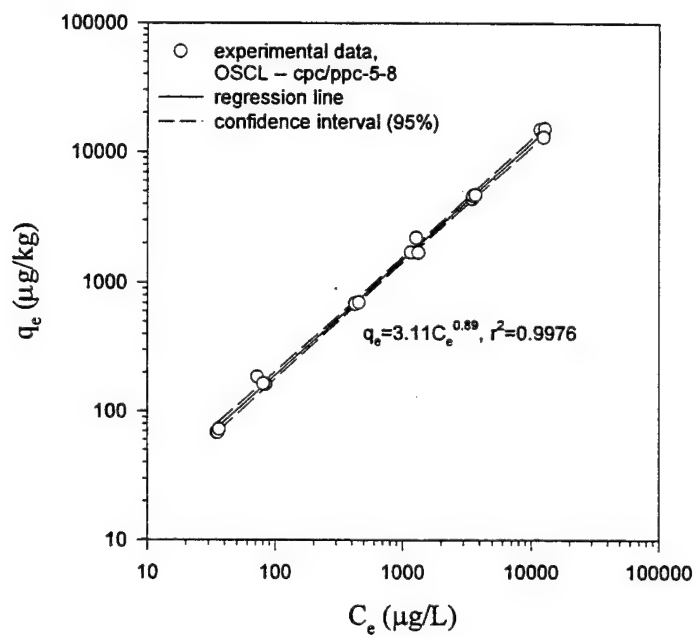
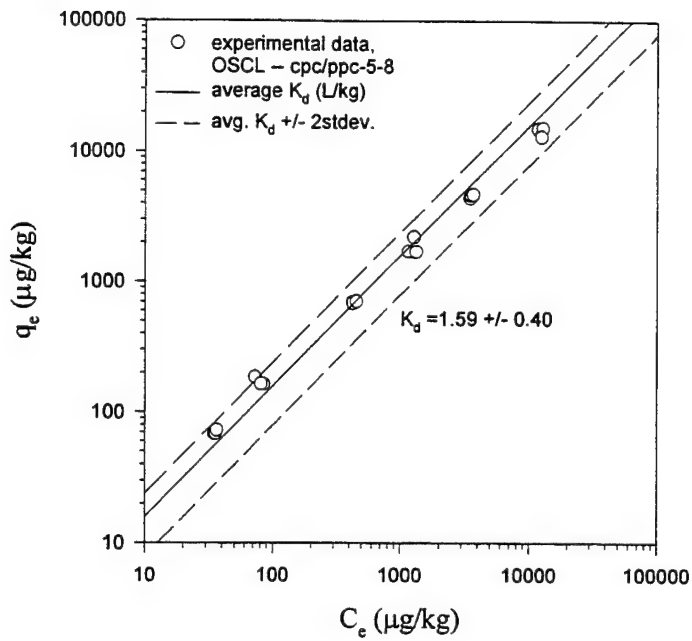


Figure 20. PCE Sorption Isotherms with OSCL Aquitard Material from Test Cells; with Linear (top) and Freundlich (bottom) Interpretation

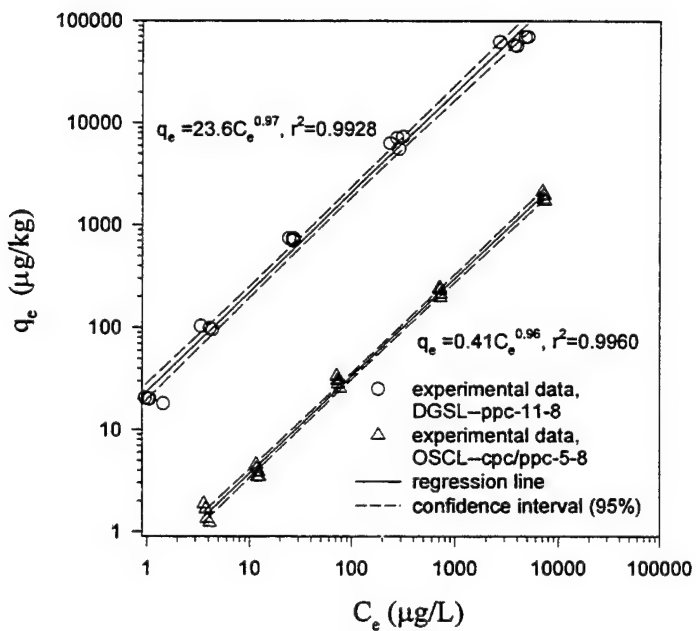
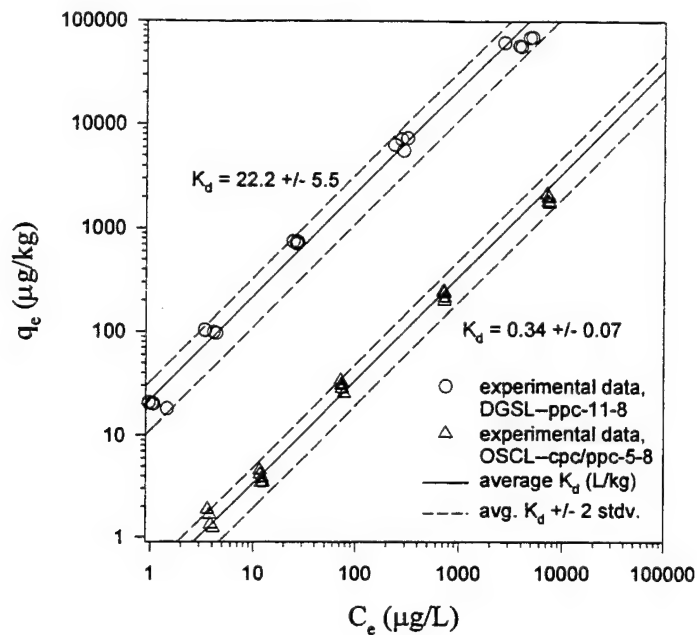


Figure 21. PCE Sorption Isotherms with PPC-11 Aquitard Materials, with Linear (top) and Freundlich (bottom) Interpretation

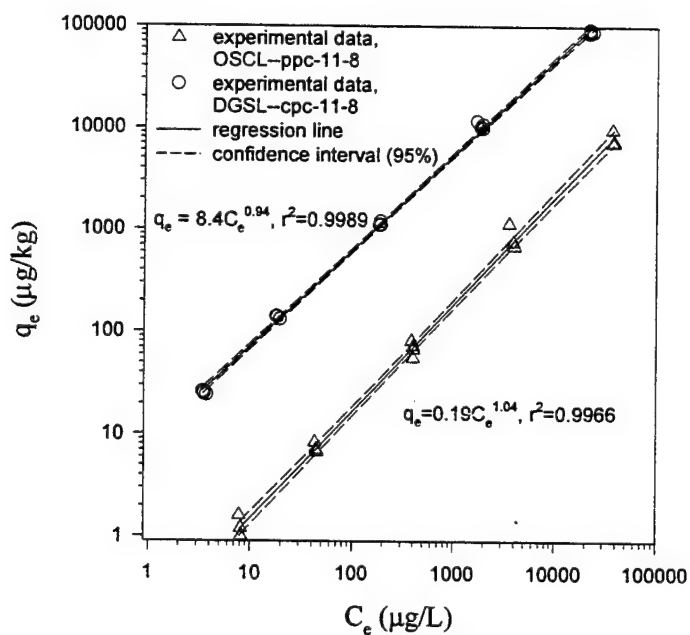
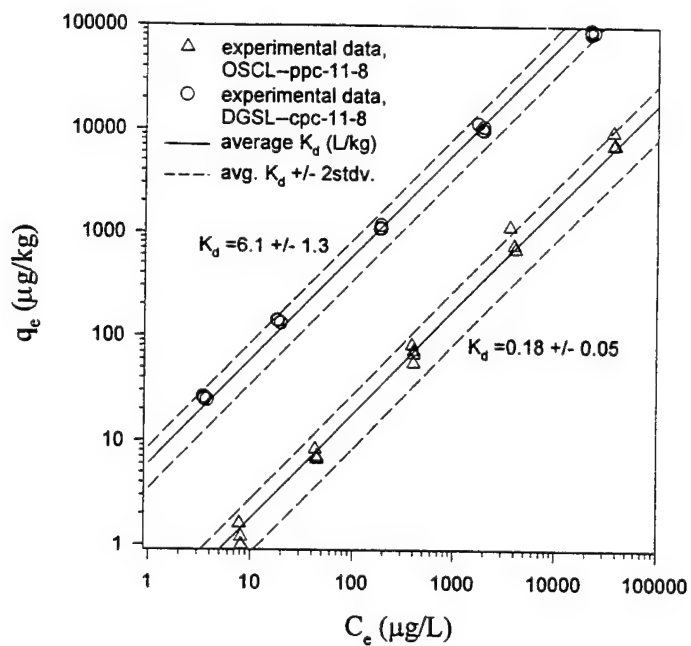


Figure 22. TCE Sorption Isotherms with Aquitard Materials, with Linear (top) and Freundlich (bottom) Interpretation

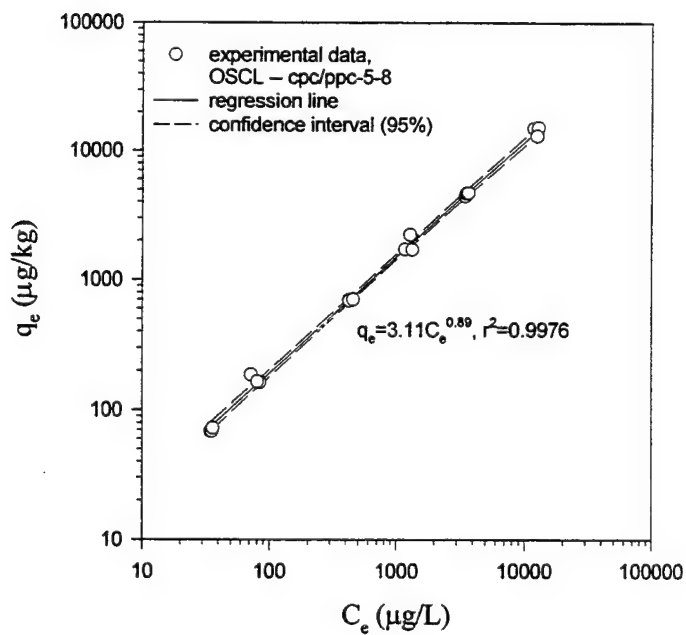
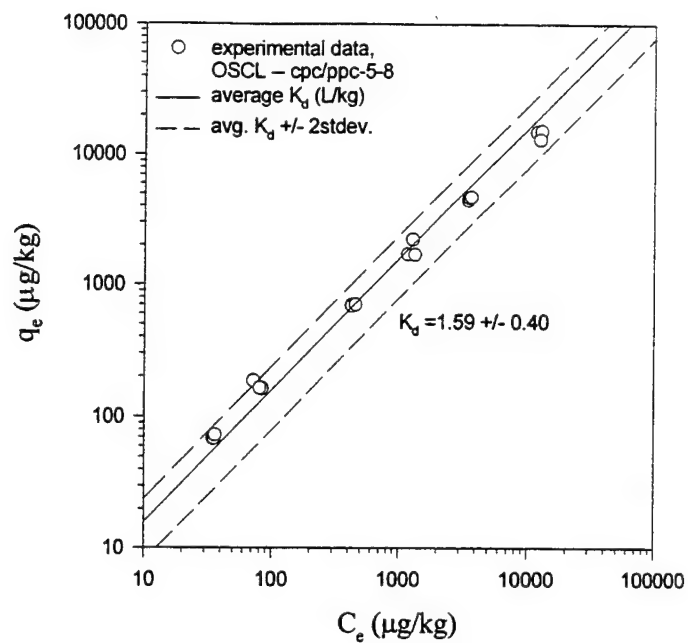


Figure 23. 1,2,4-Trichlorobenzene Sorption Isotherms with PPC-11 OSCL Material, with Linear (top) and Freundlich (bottom) Interpretation

4.6. REFERENCES

- Amonette, J.E. and Zelazny, L.W. (Editors), 1994. *Quantitative Methods in Soil Mineralogy*. Soil Science Society of America, Inc., Madison WI.
- ASTM, 1968. *Inorganic Index of the Powder Diffraction File*. Joint Committee on Powder Diffraction Standards, American Society of Testing and Materials, Philadelphia, PA.
- ASTM, 1985. *Manual on Test Sieving Methods*. Tech. Pub. 447B.
- Ball, W.P., Buehler, C., Harmon, T.C., Mackay, D.M. and Roberts, P.V., 1990. Characterization of a Sandy Aquifer Material at the Grain Scale. *Journal of Contaminant Hydrology*, 5(3): 253 - 295.
- Ball, W.P., Liu, C., Xia, G. and Young, D.F., 1997a. A Diffusion Interpretation of Tetrachloroethene and Trichloroethene Profiles in a Groundwater Aquitard. *Water Resources Research*, submitted manuscript.
- Ball, W.P. and Roberts, P.V., 1991a. Long-Term Sorption of Halogenated Organic Chemicals -- Part 1. Equilibrium. *Environmental Science and Technology*, 25(7): 1223 - 1237.
- Ball, W.P. and Roberts, P.V., 1991b. Long-Term Sorption of Halogenated Organic Chemicals -- Part 2. Intraparticle Diffusion. *Environmental Science and Technology*, 25(7): 1237 - 1249.
- Ball, W.P., Xia, G., Durfee, D.P., Wilson, R.D., Brown, M.J., and D.M. Mackay, 1997b. Hot-Methanol Extraction for the Analysis of Volatile Organic Chemicals in Subsurface Samples from Dover AFB, DE. *Groundwater Monitoring and Remediation*, in press.
- Ball, W.P., Xia, G., Liu, C., Brown, M. and Mackay, D., 1995. Aquitard Contamination from a Groundwater Plume -- In Situ Concentrations as Evidence of Vertical Diffusion, 1995 *Spring Meeting, American Geophysical Union*. Eos, Transactions of the American Geophysical Union, Baltimore, MD, pp. S135.
- Dames & Moore, 1994. *Area 6 Remedial Investigation; Dover Air Force Base, Dover, Delaware*. Report prepared for U.S. Dept. of the Air Force, Dover Air Force Base, 436 SG/CEV, Dover, DE, Dames & Moore, Inc., Bethesda, MD.

- Ellis, D.A. et al., 1996. "Remediation Technology Development Forum Intrinsic Remediation Project at Dover Air Force Base, Delaware," *Symposium on Natural Attenuation of Chlorinated Organics in Ground Water*, EPA/540/R-96/509. U.S. EPA Office of Research and Development, Washington, D.C., Dallas, TX, pp. 93-97.
- Eng, L.F., 1995. *Spatial Variability of Hydraulic Conductivity in a Coastal Plain Aquifer*. M.S. Essay Thesis, Johns Hopkins University, Baltimore, MD, 124 pp.
- Fair, G.M. and Hatch, L.P., 1933. Fundamental Factors Governing the Streamline Flow of Water through Sand. *Journal of the American Water Works Association*, 25: 1551-1565.
- Gee, G.W. and Bauder, J.W., 1986. "Particle-size Analysis". In: A. Klute (Editor), *Methods of Soil Analysis. Part 1. Physical and Mineralogical Methods-Agronomy Monograph no. 9*. American Society of Agronomy, Inc., and Soil Science Society of America, Inc., Madison, WI, pp. 383-411.
- Gelhar, L.W., 1986. Stochastic Subsurface Hydrology -- From Theory to Applications. *Water Resources Research*, 22(9): 135S - 145S.
- Johnston, R.P.B., 1996. *Analysis of a Sulfur Hexafluoride Groundwater Tracer Test at Dover Air Force Base, Delaware*. M.S. Essay Thesis, Johns Hopkins University, Baltimore, MD, 104 pp.
- Journel, A.G. and Huijbregts, C.J., 1978. *Mining Geostatistics*. Academic Press, London, 600 pp.
- Karen, C.R., Kennedy, M.M., Carter, A.C., Anderson, R.T. and Bricker, O.P., 1996. *Hydrologic and Water-Quality Data for Two Small Watersheds on Catoctin Mountain, North-Central Maryland, 1987-93*. USGS Open-File Report 95-151, USGS, Reston, VA.
- Klecka, G.M. et al., 1996. Intrinsic Remediation of Chlorinated Solvents in Groundwater, *Conference on Intrinsic Bioremediation, March 18-19, 1996*, London, England.
- Levenspeil, O. 1979. *The Chemical Reactor Omnibook*. Oregon State University Book Stores, Inc. Corvallis, OR.
- Liu, C. and Ball, W.P., 1997. Analytical Modeling of Diffusion-Limited Contamination and Decontamination in a Two-Layer Porous Medium. *Advances in Water Resources*, in press.

- Masch, F.D. and Denny, K.J., 1966. Grain size distribution and its effect on the permeability of unconsolidated sands. *Water Resources Research*, 2(4): 665-677.
- Nordstrom, D.K., 1977. Thermochemical Redox Equilibria of ZoBell's Solution. *Geochimica et Cosmochimica Acta*, 41: 1835-1841.
- Parker, J.C. and van Genuchten, M.T., 1984. *Determining Transport Parameters from Laboratory and Field Tracer Experiments*. Bulletin 84-3, Va. Agric. Experimental Station, Va. Polytech. Inst. and State Univ., Blacksburg, VA.
- Ramsey, K.W., 1993. *Geologic Map of the Mifflord and Mispillion River Quadrangles*. Geologic Map Series No. 8, Delaware Geological Survey, Newark, DE.
- Ramsey, K.W. and Xchenck, W.S., 1990. *Geologic Map of Southern Delaware*. Delaware Geological Survey Open File Report No. 32, scale 1:100,000, Delaware Geological Survey, Newark, DE.
- Schwarzenbach, R.P., Gschwend, P.M. and Imboden, D.M., 1993. *Environmental Organic Chemistry*. Wiley-Interscience, New York, N.Y.
- Starr, R.C. and Ingleton, R.A., 1992. A New Method for Collecting Core Samples Without a Drilling Rig. *Ground Water Monitoring Review*(Winter): 91-95.
- Sudicky, E.A., 1986. A Natural Gradient Experiment on Solute Transport in a Sand Aquifer. 5. Spatial Variability of Hydraulic Conductivity and Its Role in the Dispersion Process. *Water Resources Research*, 22(13): 2069 - 2082.
- Thomas, G.W., 1982. "Cation Exchange Capacity." In: A.L. Page, R.H. Miller and D.R. Keeney (Editors), *Methods of Soil Analysis. Part 2. Chemical and Microbiological Properties*. American Society of Agronomy, Inc., and Soil Science Society of America, Inc., Madison, WI, pp. 159-165.
- Walton-Day, K., Macalady, D.L., Brooks, M.H. and Tate, V.T., 1990. Field Methods for Measurement of Ground Water Redox Chemical Parameters. *Groundwater Monitoring and Remediation*, 5(3): 81-89.

- Whittig, L.D. and Allardice, W.R., 1986. "X-Ray Diffraction Techniques." In: A. Klute (Editor), *Methods of Soil Analysis. Part 1. Physical and Mineralogical Methods -- Agronomy Monograph no. 9*. American Society of Agronomy, Inc., and Soil Science Society of America, Inc., Madison, WI, pp. 383-411.
- Zoltai, T. and Stout, J.H., 1984. *Mineralogy: Concepts and Principles*. Burgess Publishing Co., Minneapolis, MN, 505 pp.

5. INITIAL AND FINAL SITE CHARACTERIZATION

5.1. SOIL VOC MEASUREMENTS

5.1.1. *Sampling Locations and Dates*

5.1.1.1. **Prepumping Core Exercise**

From October 18 to 27, 1994, seven soil cores were removed from each cell at the locations shown in **Figure 3**. These include the ML locations -1, -3, -5, -7, -9, the center extraction well (EW-2), and the center injection well (IW-2). These latter locations were designated as core locations -10 and -11, respectively, as shown in **Figure 24**. As further described in Appendix F, 1.5-meter (5-foot) sections of core tube were obtained, split vertically in the field, and subsampled for the analysis of total (aqueous plus sorbed) PCE and TCE concentration. Details of the soil core splitting, subsampling and analytical methodology are briefly reviewed in Appendix F and have been more fully described elsewhere (Ball et al., 1997b). An important point is that most analyses for the prepump coring exercise were conducted on composite samples, in which four 1-to-2 gram subsamples are combined into a single methanol preservation vial, representative of a 0.38-m (1.25-foot) vertical section. For the lower sampled depths of a single core (bottom 3 meters of PPC-11), subsamples of roughly 5 to 10 grams were taken at more closely space intervals (2.5 to 5.1 cm) and subjected to individual analysis.

5.1.1.2. **Postpumping Core Exercise**

At the conclusion of the pumping experiment, four soil cores were removed from each cell in a manner similar to that used in the initial (prepumping) core exercise. These were similarly subsampled and analyzed, except that high resolution (individual) sampling was conducted in the lower two core segments at all four locations, similar to PPC-11 in the prepumping core exercise. The CPC postpumping core samples were taken March 5 to March 8, 1996 and the PPC postpumping core samples were taken June 5 to June 7, 1996. The locations of these final cores, identified as CPC-12 through CPC-15 and PPC-12 through PPC-15 are shown in **Figure 24**

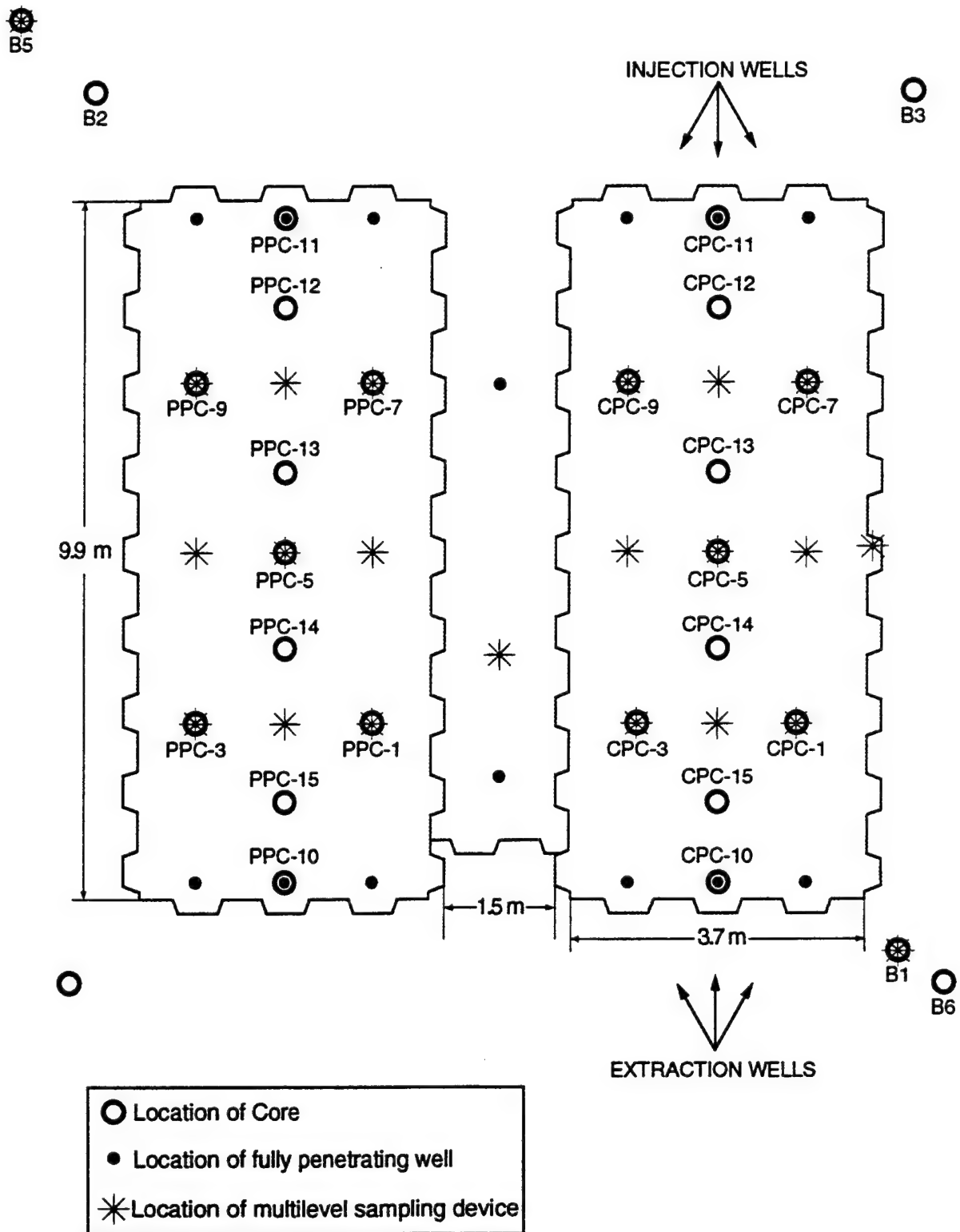


Figure 24. Locations of Final Coring (CPC-12, CPC-13, CPC-14, CPC-15, PPC-12, PPC-13, PPC-14, PPC-15)

5.1.2. *Tetrachloroethene (PCE)*

5.1.2.1. Prepumping PCE Results in Soil Cores

The results of the PCE subsample analyses are shown separately for each cell in **Figure 25**. Note that the results of the final core analysis are also shown separately for each cell to the right of the initial data for comparison. These are described more fully in Section 5.1.2.2 below.

The initial coring results revealed that PCE concentrations in the range of 10 to 80 $\mu\text{g/Kg}$ (dry basis) were initially present in the deeper zones of each cell and that the magnitude of the PCE contamination dropped off precipitously at shallower depths. In the CPC, contamination levels above 10 $\mu\text{g/Kg}$ (dry basis) persist up to depths as shallow as 4 meters above the aquitard surface (aas), or roughly 10 meters below ground surface (bgs). Maximum PCE concentrations in this cell were observed between 1 and 3 meters above the aquitard surface and gradually decline at deeper depths in the aquifer and within the aquitard. In the PPC, contamination occurs in a more narrowly confined region closer to the aquitard, with little contamination observed above 3 meters aas. Also in contrast to the CPC, maximum concentrations were observed close to the aquitard surface (between 0 and 2 meters aas) and peak aquifer concentrations were generally lower than those observed in the CPC. As with the CPC, peak concentrations of PCE in the aquitard appear at or near the aquitard/aquifer interface. However, in the PPC, the aquitard concentrations are significantly higher than in the CPC. Unlike the CPC situation overall maximum concentrations of PCE often occur within the PPC aquitard. Final sampling (right half of **Figure 25**) showed that the contaminant concentrations within the aquitard of each cell persisted over the course of the aquifer flushing. Thus, the initial higher contamination of the PPC aquitard leads reflects in higher final aquitard concentrations for that cell.

Figure 26 shows results for core PPC-11, which were obtained with a higher resolution of sampling (samples taken every 2.5 cm to 5 cm). As evident from the figure, the high density sampling is better able to resolve some of the particularly high concentrations that occur at the aquitard/aquifer interface and at the underlying interface with the DGSL. The DGSL layer has higher organic carbon content and higher sorption capacity, as discussed in Chapter 4.

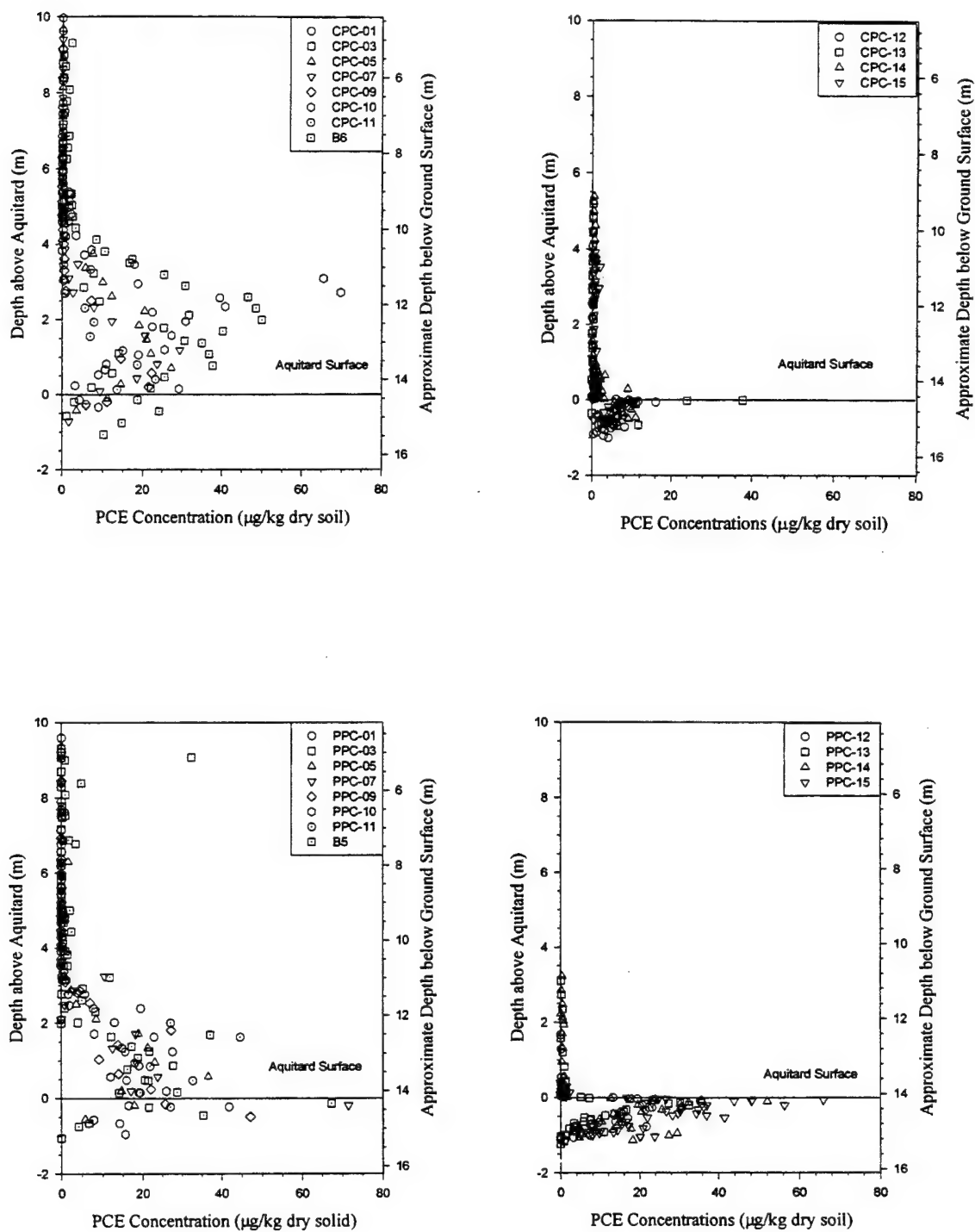


Figure 25. Initial and Final PCE Concentrations in CPC and PPC (Core Data).

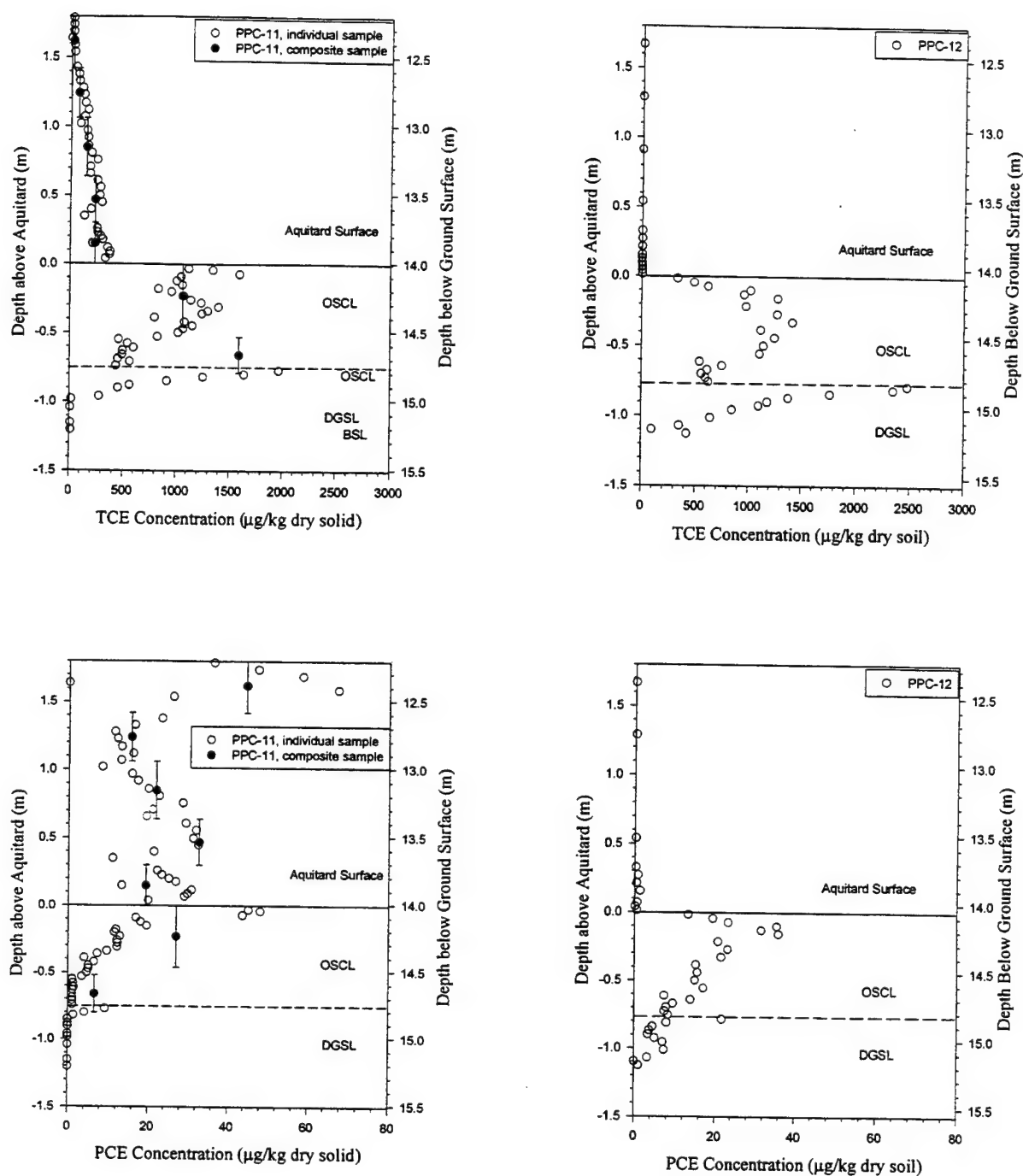


Figure 26. Comparison of Initial and Final TCE and PCE Results in Cores with High Density Sampling: Initial (PPC-11) versus Final (PPC-12).

The PPC-11 data have been analyzed through diffusion modeling (Ball et al., 1997a; Ball et al., 1995; Liu and Ball, 1997), which suggests that contaminant release from this impermeable region will continue for many decades to come, albeit at very low flux rates. In fact, contaminant rebound from this source may be too slow to be readily apparent over the short "off" cycles considered here, and therefore too slow for pulsed pumping to offer significant advantage. The data from this project provide important insight into this issue, as noted subsequently (Chapter 7).

5.1.2.2. Postpumping PCE Results in Soil Cores

The results of the PCE analysis in the final cores are shown separately for each cell to the right of the initial core results in **Figure 25** and **Figure 26**. Note that the concentrations of PCE within the aquifer region of both cells were below detection limits in most samples, with the principle exceptions being those samples immediately adjacent to the aquitard surface. The only exception to this trend was for CPC-14 core which had detectable contamination at more shallow depths. Within the aquitards of the two cells, the data followed the general pattern observed in the initial cores in that the PPC aquitard remained more highly contaminated than the CPC aquitard.

5.1.3. Trichloroethene (TCE)

5.1.3.1. Prepumping TCE Results in Soil Cores

The TCE data are shown separately for each cell in **Figure 27**. As before, the results of the final core analysis are also shown, separately for each cell and to the right of the initial data for comparison. There are three aspects of the data which differ significantly from the trends noted in the PCE data: 1) TCE concentrations were on the order of ten times those observed for PCE; 2) significant TCE contamination was not observed in either cell above 2 meters aas; and 3) by far the highest TCE contamination occurs in the aquitards of both cells. Concentration levels were similar in the aquifers of both cells except that, as with PCE, the contamination in the CPC extended to slightly more shallow depths than those in the PPC. Also as with PCE, aquitard contamination was at higher concentrations in the PPC. Maximum concentrations were on the order of 1000 ppb ($\mu\text{g/Kg}$ -dry soil) within the aquitard of the CPC, and usually on the order of

1500 ppb within the aquitard of the PPC. One sample in the PPC-7 core showed an unusually high of 4050 ppb).

5.1.3.2. Postpumping TCE Results in Soil Cores

The results of the TCE analysis in the final cores are shown separately for each cell to the right of the initial core results in **Figure 27**. As with PCE, TCE concentrations are shown to have been very effectively flushed from the aquifer regions of both test cells. In particular, the TCE concentrations in most samples from the aquifer regions were at or below detection limits, with the only exceptions occurring immediately adjacent to the aquifer/aquitard interface. Although very little TCE contamination remained in the aquifers of both cells, the aquitards remained highly contaminated, with the PPC aquitard remaining more highly contaminated than that of the CPC.

Note that the high sampling density of the postpumping core exercise permitted the observation of higher TCE concentration values at the OSCL/DGSL interface than was achieved in most of the prepump coring. As previously shown by the comparisons of composite and individual samples in **Figure 26**, the extreme values at the interface are not noticeable in the composite results. If we recognize this source of difference for interfacial samples, it is apparent that the TCE concentrations in the aquitards of both cells remained relatively constant during the course of the experiment (i.e., maximum TCE concentrations remained on the order of 1000 ppb in the CPC aquitard and on the order of 1500 ppb in the PPC aquitard).

5.1.4. Summary of Soil VOC Measurements

Based on the vertical PCE concentration profiles in the aquitard, we hypothesize that the concentration of PCE in the overlying aquifer sand has been continually increasing at the location of our test cells. Diffusion modeling of PCE concentrations within the aquitard are consistent with this hypothesis [PPC-11 data; (Ball et al., 1997a)]. Additionally, we note that maximum PCE concentrations in the aquifer occur at elevations well above the aquitard in the CPC cell, indicative of a situation in which the PCE plume is more vertically removed from the aquitard. This in contrast to the CPC, where maximum PCE concentrations in the aquifer occur much closer to the aquitard/aquifer interface. We believe that this results from the fact that the

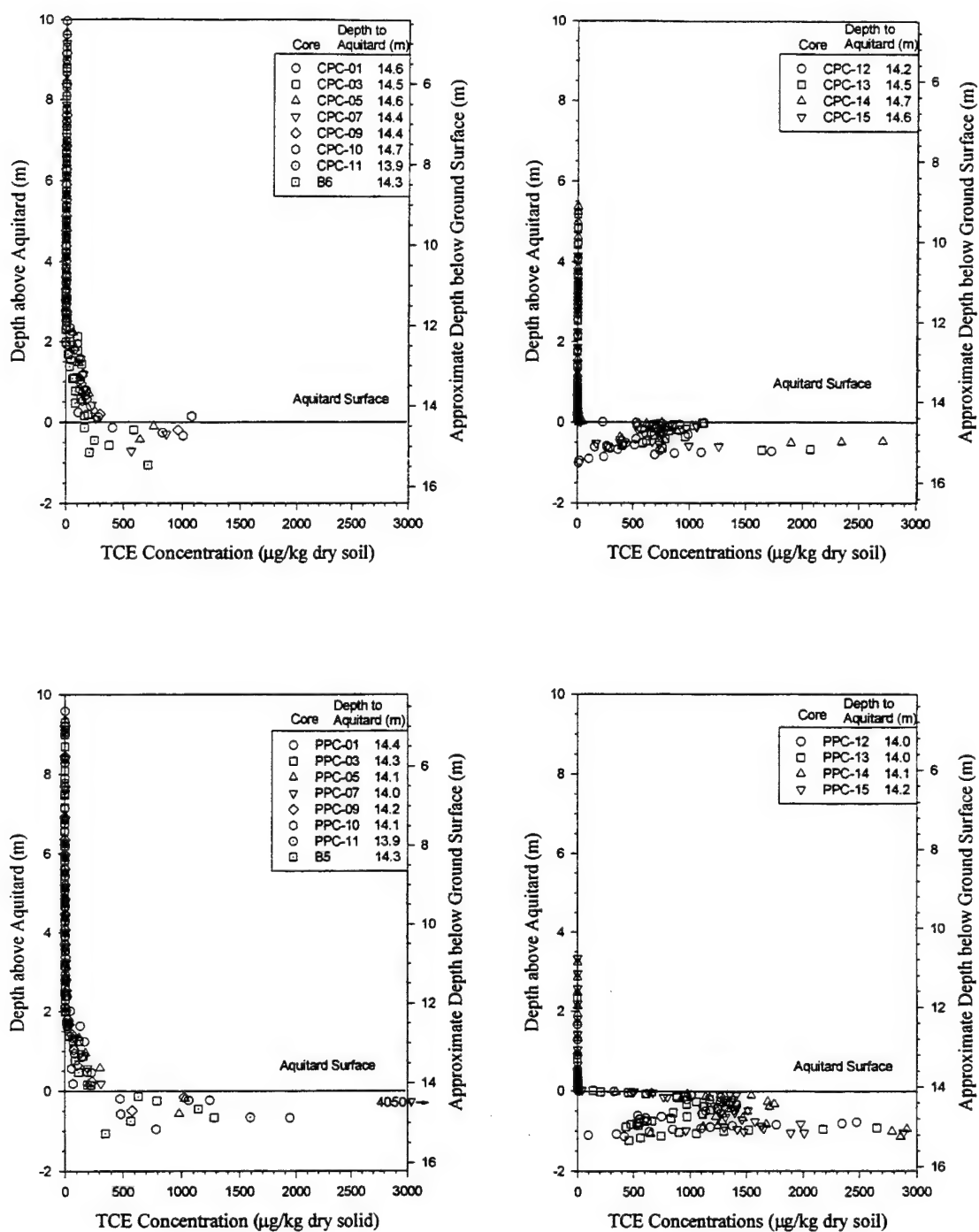


Figure 27. Initial and Final TCE Concentrations in CPC and PPC (Core Data).

aquitard surface is more depressed in the CPC (e.g., especially at the central CPC-5 location), and that the depression is filled with less conductive material. In support of this, we note the medium coarse sand (rather than the more commonly present gravely coarse sand) in the lowest aquifer region of CPC-5; see Fence Diagrams of Appendix A). Our hypothesis, then, is that the PPC aquitard is more heavily contaminated than the CPC aquitard because maximum contaminant concentrations have passed more closely to its surface.

For TCE and most other chemicals (i.e., all except PCE and VC), we believe that higher plume concentrations passed our site prior to the sheet pile installation, such that the initial cell concentrations are reflective of an on-going dynamic balance between groundwater flushing and vertical diffusion up and out of the previously contaminated aquitard. Core sampling of TCE within the aquitard supports such a hypothesis -- maximum aquifer concentrations occur adjacent to the aquitard interface, and higher concentrations exist deeper within the aquitard. Diffusion modeling of these TCE core data suggests that concentrations at the aquifer/aquitard interface have declined in recent years, and that TCE mass was already diffusing back into the aquifer before pumping was initiated (Ball et al., 1997a). For all compounds except PCE and VC, ML sampling of aqueous concentrations shows similar trends as for TCE -- i.e., maximum concentration at the deepest ML point (see **Figure 28** through **Figure 33**, subsequently).

The final coring results convincingly demonstrate that the aquitard region has not been significantly decontaminated by the relatively short-term pumping of this project. However, the data for both contaminants do show clear evidence of reduced concentrations in the uppermost (shallowest) portions of the aquitard. This reduced concentration has resulted in an apparent reversal of the previously downward concentration gradient for PCE in the very uppermost regions of the aquitard (best illustrated in **Figure 26**, right) and a steepening of the upward concentration gradient for TCE in this zone (**Figure 27**, right). Further sampling and modeling of the postpumping concentration gradients in these zones is the subject of a follow-up investigation at Johns Hopkins University, still on-going at the time of this report (work supported by the U.S. Air Force Armstrong Laboratory, Environics Directorate, under the auspices of the U.S. Army Research Office Scientific Services Program, administered by Battelle (Delivery Order 1976, Contract DAAL03-91-C0034).

5.2. AQUEOUS-PHASE VOC ANALYSES

5.2.1. *Prepumping Aqueous Snapshot*

During the period of September 1-26, 1995, the multilevel wells were sampled and the samples were analyzed between September 24 and 29 to provide an initial snapshot of the aqueous concentrations of the contamination present in both test cells. Samples from all 8 depths of each multilevel were collected and stored in a refrigerator at approximately 10°C until analyzed. All the lowermost samples from both cells were analyzed first, followed by the next lowest, etc., until no peaks were detected. All 8 samples from 4 multilevels were analyzed to confirm the absence of dissolved contaminants in the upper part of the aquifer. The results of the initial concentration ranges, averages and standard deviations of the six major chlorinated VOC and the four major petroleum hydrocarbon contaminants in the lowest four sample points are displayed in **Table 18** and **Table 19**.

The results of the initial and final aqueous VOC results are also plotted on the left-hand side of **Figure 28** through **Figure 33**. As with the soil core data, the aqueous results show that the vast majority of contamination was located in the deepest regions of the aquifer. Little prepumping contamination was found in samples withdrawn from Well Points 3 and 4, relative to the deeper points. TCE, cis-DCE, TCA and DCM all tended to have maximum concentrations in the lowest well point, with slightly lower concentrations in the next deepest well point. PCE and VC showed a somewhat different trend, with PCE being more evenly distributed over the 3 deepest well points (especially in the CPC; **Figure 28**) and with VC being more evenly distributed over the two deepest well points (**Figure 32**). The multilevel data for PCE and TCE closely reflect the trends observed in the soil core data of **Figure 25** through **Figure 27**. Both the core data and aqueous data show that PCE contamination extended up to shallower depths in the CPC than in the PPC. However, the declining concentrations of PCE in the deep-most aquifer regions of the CPC (evident in soil data of **Figure 25**) cannot be discerned on the basis of the aqueous sampling results **Figure 28**), owing to the less well-resolved spatial resolution of the latter results.

TABLE 18. INITIAL AQUEOUS CONCENTRATIONS OF CHLORINATED VOCs (µg/L)

Compound:		CPC				PPC			
		Range		ave	stdev	Range		ave	stdev
		low	high			low	high		
PCE:	Level								
	4	2.2	13	5.7	3.9	1	5	3	1
	3	12	160	69	52	53	50	19	15
	2	120	230	171	41	53	180	130	38
	1	140	230	180	35	100	270	210	49
Compound:		Range		ave	stdev	Range		ave	stdev
		low	high			low	high		
TCE:	Level								
	4	0.7	2.2	1.5	0.5	0	8	3	2
	3	4.3	26	15	7.7	0	33	12	12
	2	460	960	710	170	210	700	370	190
	1	1200	1900	1500	240	810	1600	1300	230
Compound:		Range		ave	stdev	Range		ave	stdev
		low	high			low	high		
cDCE:	Level								
	4	1	7	4	2	0	82	7	7
	3	92	540	340	160	25	590	220	210
	2	5500	8700	7300	1200	2900	7200	4200	1600
	1	9100	10000	9600	440	6800	11000	9100	1100
Compound:		Range		ave	stdev	Range		ave	stdev
		low	high			low	high		
TCA:	Level								
	4	0	0	0	0	0	1	0	0
	3	1	5	3	2	0	9	3	4
	2	290	600	460	100	120	450	240	130
	1	470	810	650	110	600	1100	860	180
Compound:		Range		ave	stdev	Range		ave	stdev
		low	high			low	high		
VC:	Level								
	4	0	0	0	0	0	0	0	0
	3	0	0	0	0	0	0	0	0
	2	160	590	390	130	180	650	420	140
	1	260	620	400	140	78	640	330	160
Compound:		Range		ave	stdev	Range		ave	stdev
		low	high			low	high		
DCM:	Level								
	4	0	0	0	0	0	0	0	0
	3	0	0	0	0	0	1	0	0
	2	20	66	42	15	4	44	23	14
	1	44	240	160	70	140	320	220	64

TABLE 19. INITIAL AQUEOUS CONCENTRATIONS OF AROMATIC VOCs ($\mu\text{g/L}$)

Compound:		CPC				PPC			
		Range		ave	stdev	Range		ave	stdev
		Level	low	high		low	high		
Benzene:	4	0	0	0	0	0	0	0	0
	3	0	0	0	0	0	0	0	0
	2	19	94	47	25	9.1	74	27	19
	1	0	79	28	31	0	70	15	22
Compound:		Range		ave	stdev	Range		ave	stdev
		Level	low	high		low	high		
mp-xylene:	4	0	0	0	0	0	0	0	0
	3	0	0	0	0	0	0	0	0
	2	23	47	34	7.8	16	45	27	10
	1	36	53	43	4.8	24	42	36	5.5
Compound:		Range		ave	stdev	Range		ave	stdev
		Level	low	high		low	high		
naphthalene:	4	0	0	0	0	0	0	0	0
	3	0	0	0	0	0	0	0	0
	2	11	130	100	22	56	150	95	30
	1	110	140	130	8.2	110	140	130	9.2
Compound:		Range		ave	stdev	Range		ave	stdev
		Level	low	high		low	high		
2-methyl-naphthalene:	4	0	0	0	0	0	0	0	0
	3	0	0	0	0	0	0	0	0
	2	58	120	88	20	46	110	73	21
	1	87	130	110	15	89	120	99	8.7

5.2.2. Postpumping Aqueous Snapshot

At the conclusion of the experiment, the multilevel wells were sampled to provide the snapshot of the aqueous concentrations of the contamination remaining in both test cells. The samples were collected during the period of June 5-7, 1996 and analyzed during the period of June 5-19, 1996. The analysis results of the of the six major chlorinated VOCs and the four major petroleum hydrocarbon contaminants in the lowest four sample points are summarized in **Table 20** and **Table 21**, respectively. For all VOCs, very little contamination was observed in all but the deepest multilevel well point. However, for all VOCs, higher levels of contamination remained in the PPC compared to the CPC. In addition, within the PPC, postpumping

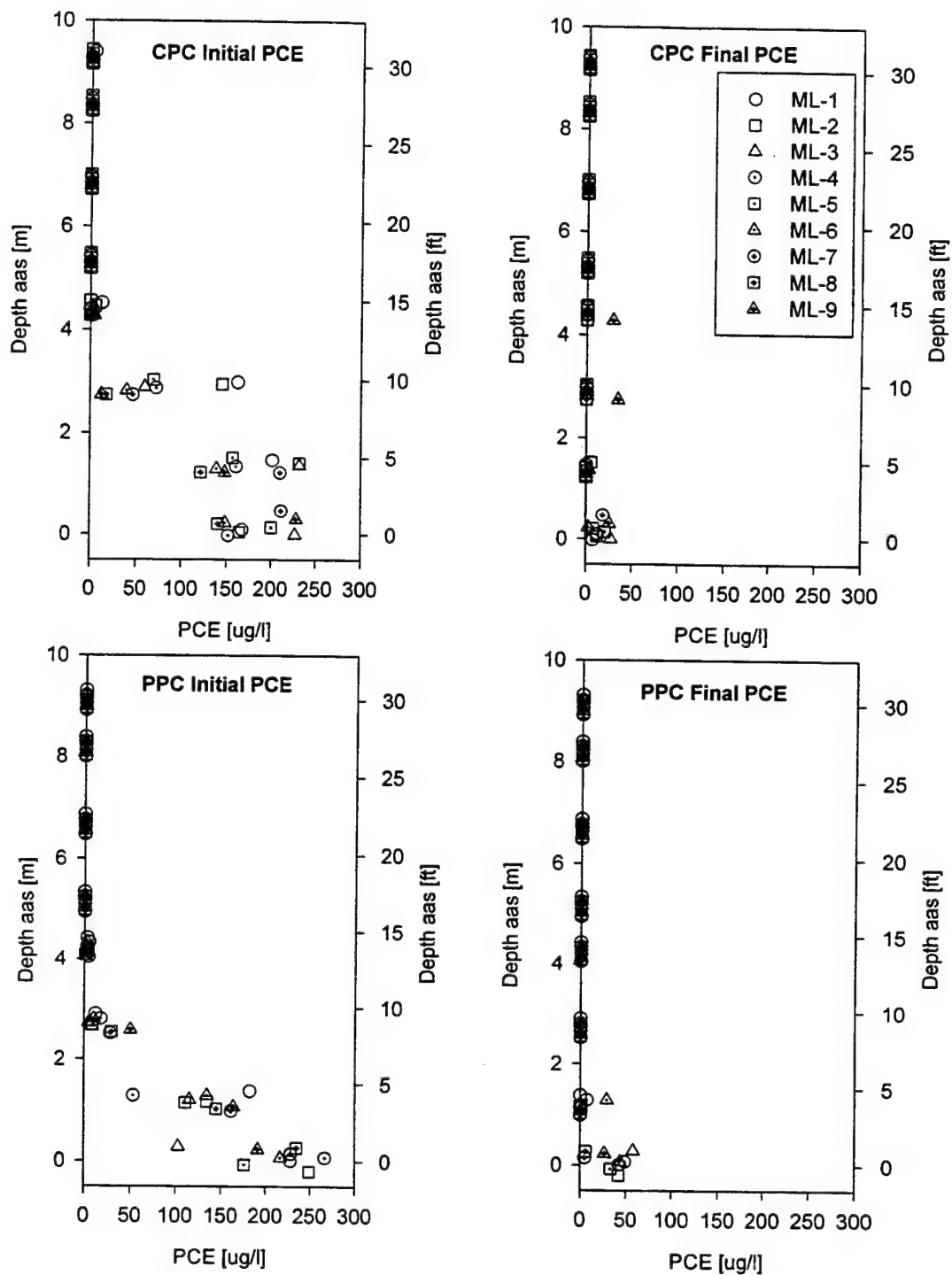


Figure 28. Initial and Final PCE Concentrations in CPC and PPC (Multilevel Data).

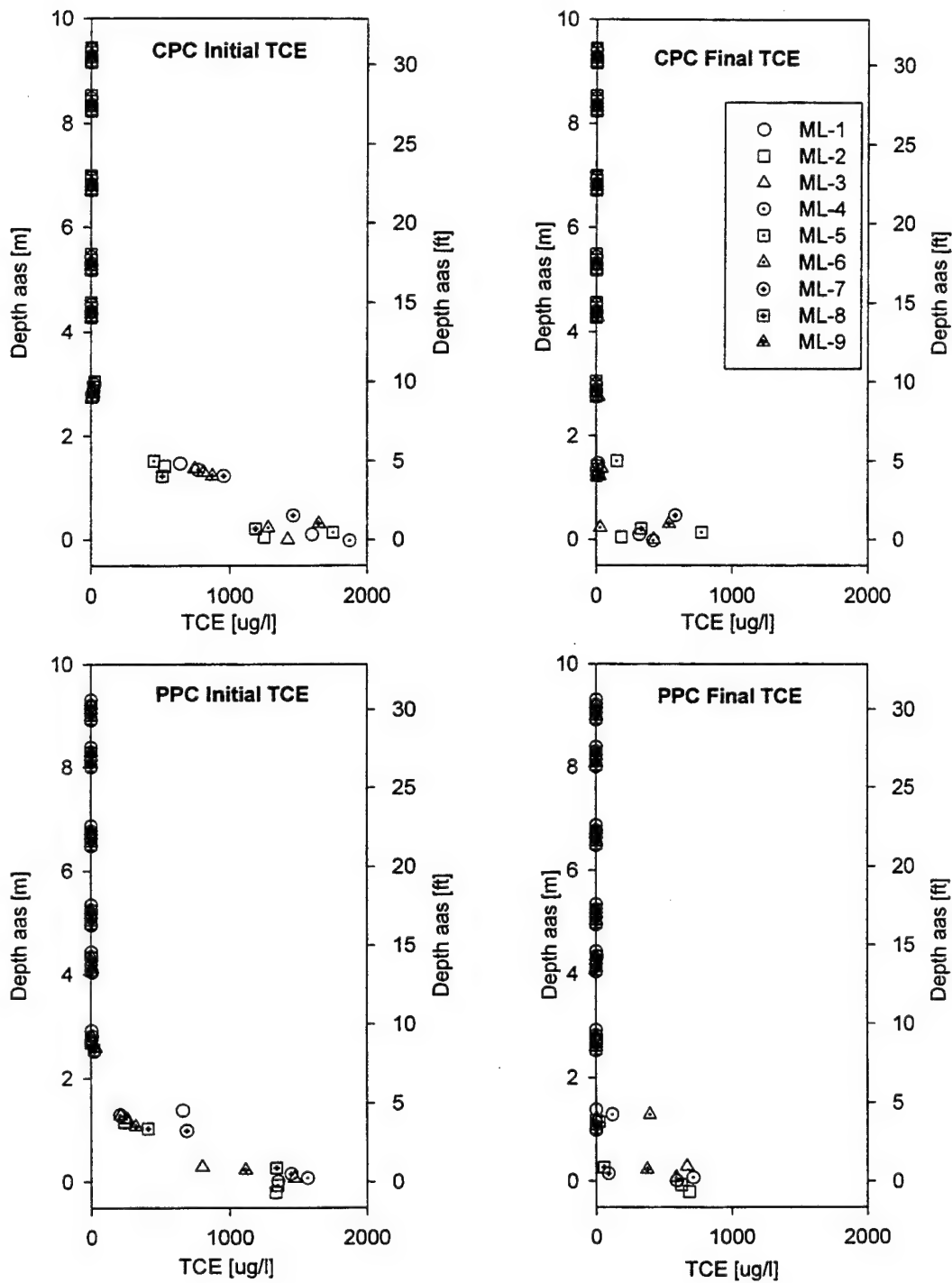


Figure 29. Initial and Final TCE Concentrations in CPC and PPC (Multilevel Data)

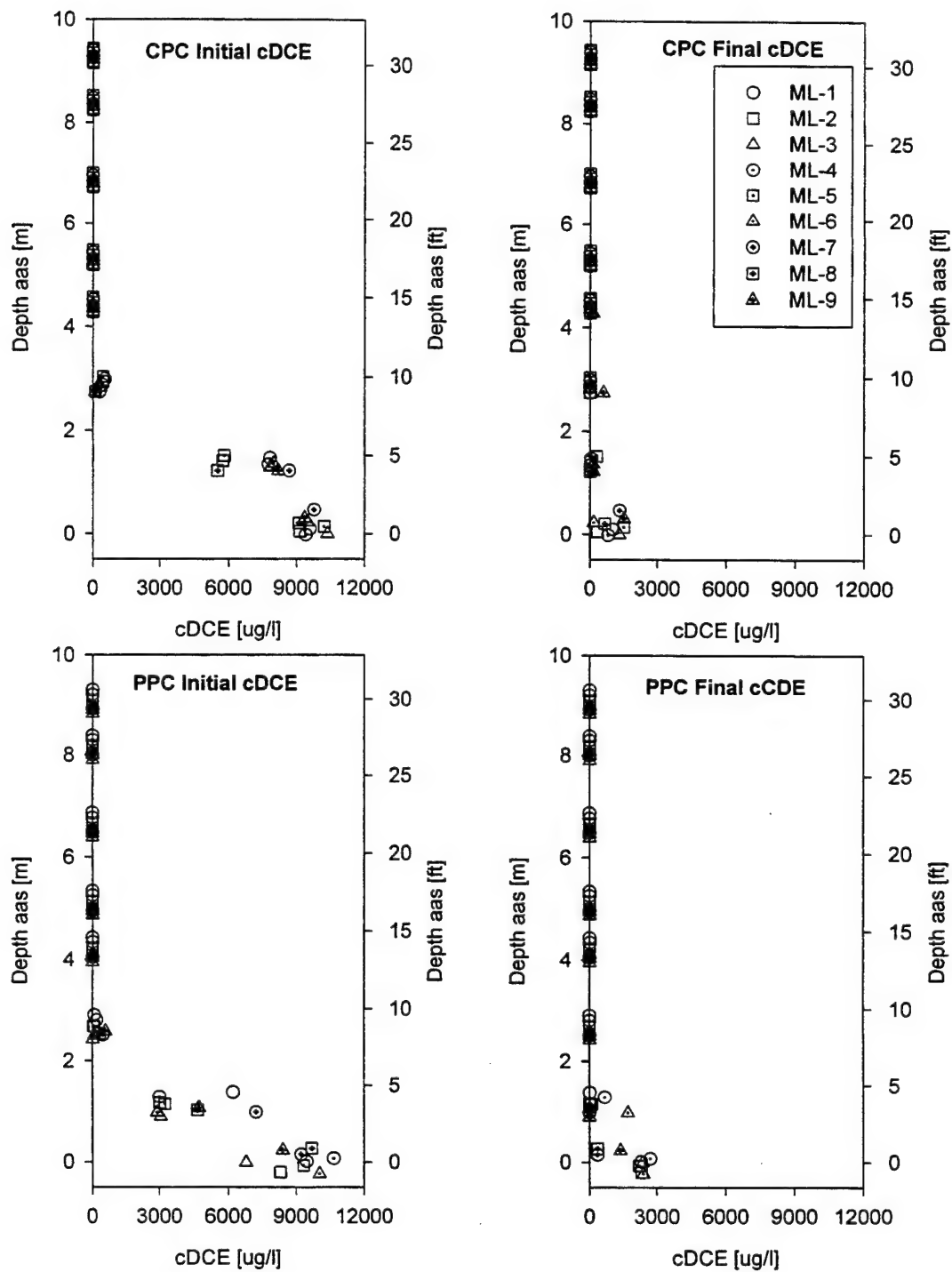


Figure 30. Initial and Final *cis*-DCE Concentrations in CPC and PPC (Multilevel Data)

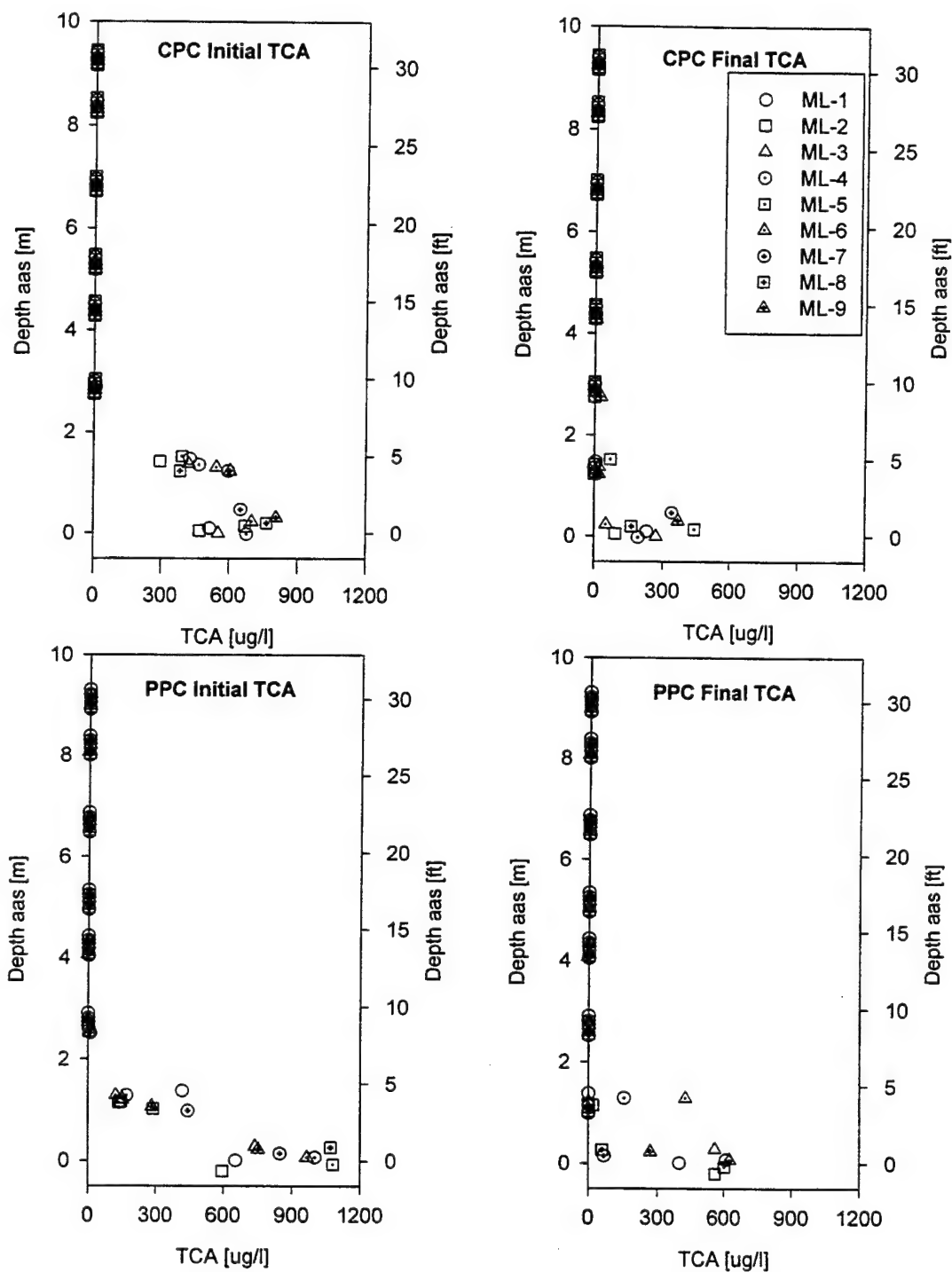


Figure 31. Initial and Final TCA Concentrations in CPC and PPC (Multilevel Data)

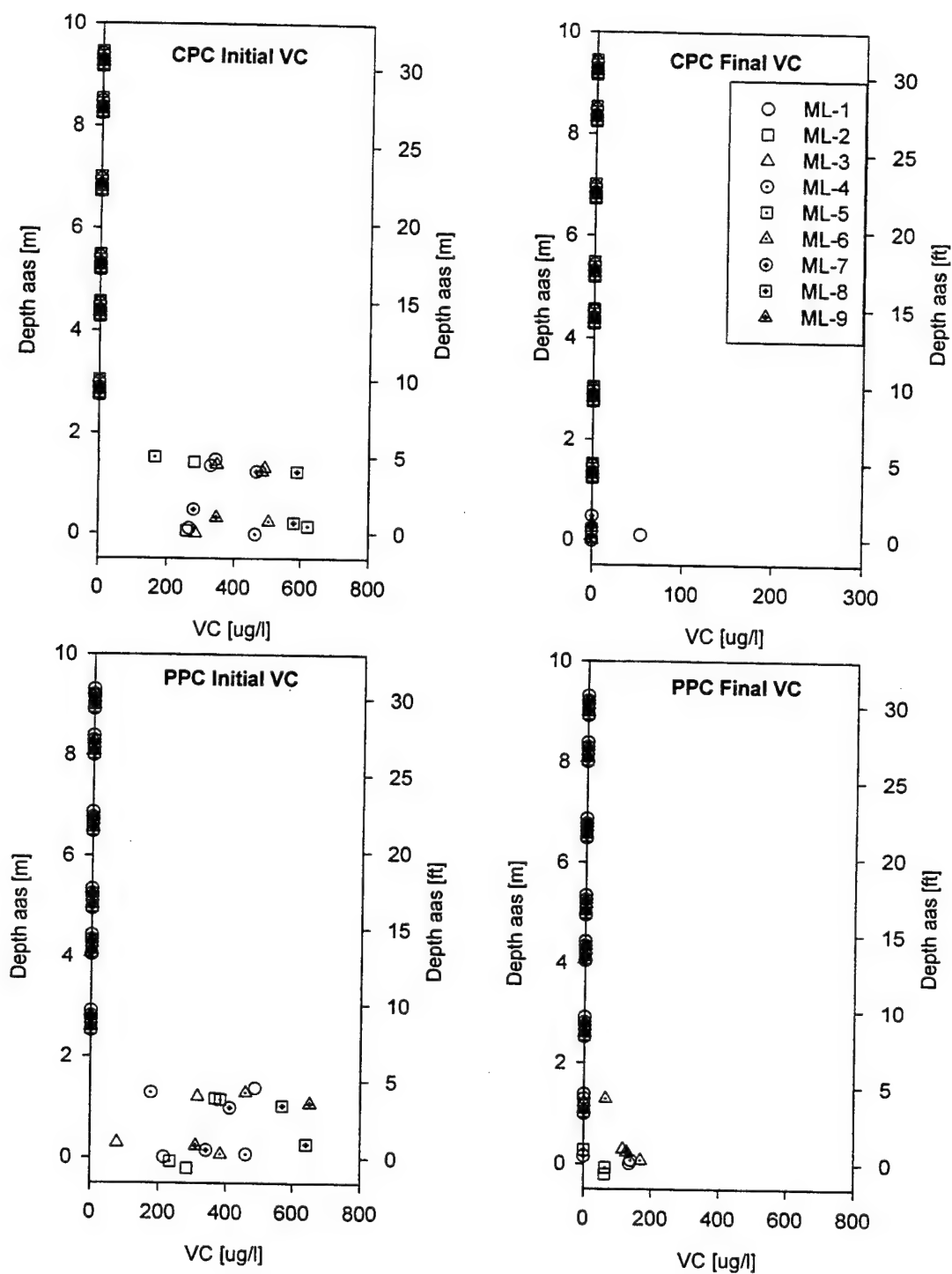


Figure 32. Initial and Final VC Concentrations in CPC and PPC (Multilevel Data)

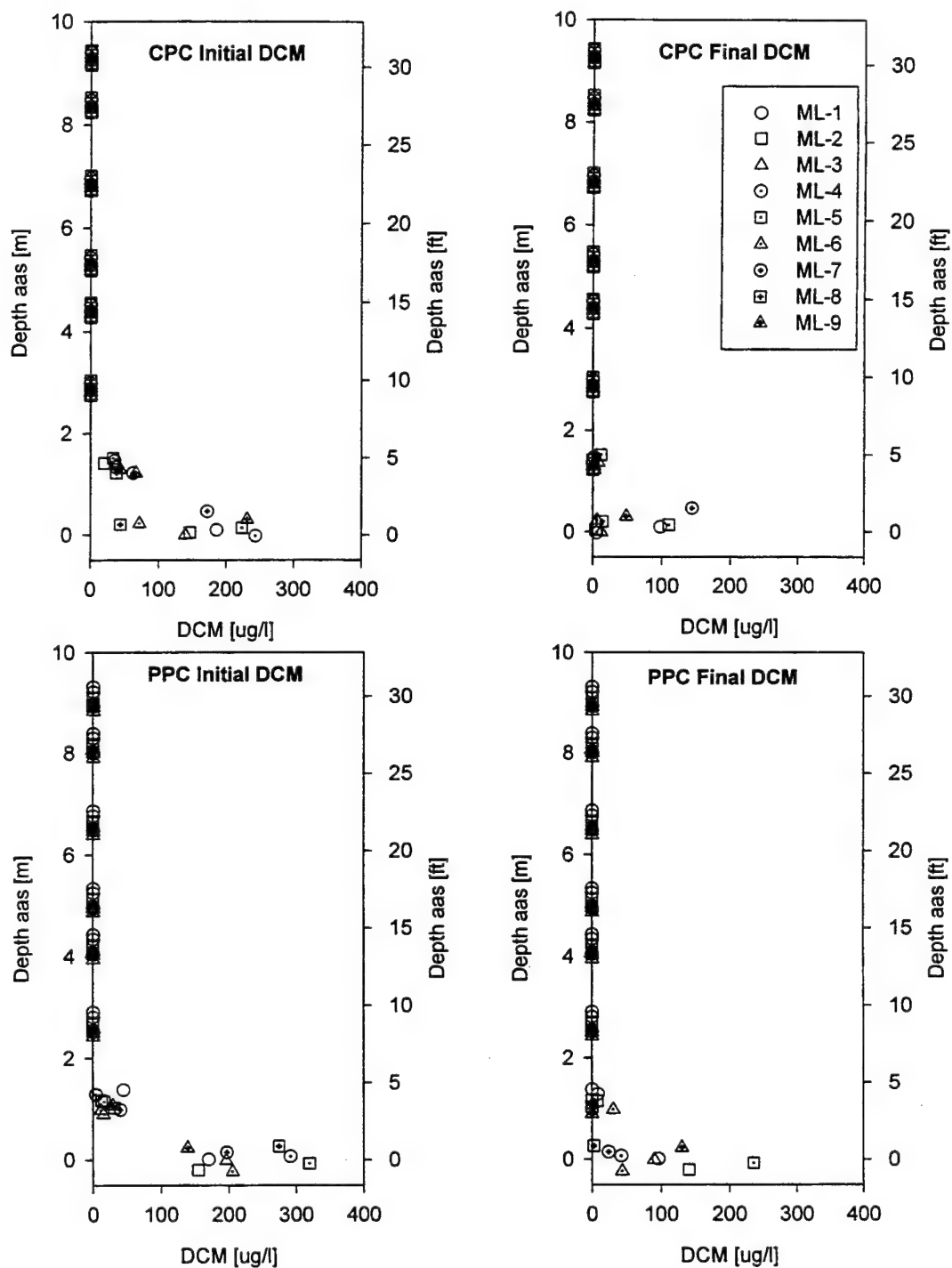


Figure 33. Initial and Final DCM Concentrations in CPC and PPC (Multilevel Data)

TABLE 20. FINAL AQUEOUS CONCENTRATIONS OF CHLORINATED VOCs ($\mu\text{g/L}$)

Compound:		CPC				PPC			
		Range		ave	stdev	Range		ave	stdev
	Level	low	high			low	high		
PCE:	4	0	28	3	10	0	0	0	0
	3	0	34	4	11	0	0	0	0
	2	0	5	1	2	0	28	4	10
	1	0	27	15	8	5	57	34	18
Compound:		Range		ave	stdev	Range		ave	stdev
	Level	low	high			low	high		
TCE:	4	0	9	1	3	0	6	1	2
	3	0	16	2	5	0	3	1	1
	2	2	150	29	48	0	400	61	130
	1	30	780	410	220	58	720	490	260
Compound:		Range		ave	stdev	Range		ave	stdev
	Level	low	high			low	high		
cDCE:	4	0	120	14	41	0	11	3	4
	3	0	600	68	200	0	6	1	2
	2	19	310	92	93	0	1700	280	580
	1	170	1500	960	500	350	2700	1800	900
Compound:		Range		ave	stdev	Range		ave	stdev
	Level	low	high			low	high		
TCA:	4	0	2	0	0	0	0	0	0
	3	0	25	3	9	0	0	0	0
	2	0	69	14	22	0	430	67	140
	1	51	440	240	130	59	620	420	230
Compound:		Range		ave	stdev	Range		ave	stdev
	Level	low	high			low	high		
VC:	4	0	0	0	0	0	0	0	0
	3	0	0	0	0	0	0	0	0
	2	0	0	0	0	0	64	7	22
	1	0	54	6	18	0	170	91	62
Compound:		Range		ave	stdev	Range		ave	stdev
	Level	low	high			low	high		
DCM:	4	0	0	0	0	1	5	0	0
	3	0	0	0	0	5	50	0	0
	2	0	12	3	4	53	180	5	10
	1	6	140	49	54	100	270	90	72

TABLE 21. FINAL AQUEOUS CONCENTRATIONS OF AROMATIC VOCs ($\mu\text{g/L}$)

Compound:		CPC				PPC			
		Range		ave	stdev	Range		ave	stdev
		low	high			low	high		
Benzene:	Level								
	4	0	0	0	0	0	0	0	0
	3	0	7.6	0.8	2.5	0	0	0	0
	2	0	6.5	0.7	2.2	0	8.3	1.4	2.9
	1	0	13	5.9	5.2	0	74	20	22
Compound:		Range		ave	stdev	Range		ave	stdev
		low	high			low	high		
m,p-xylene:	Level								
	4	0	0	0	0	0	0	0	0
	3	0	1.5	0.2	0.5	0	0	0	0
	2	0	0	0	0	0	0	0	0
	1	0	23	6.1	7.5	0	15	8.4	6.2
Compound:		Range		ave	stdev	Range		ave	stdev
		low	high			low	high		
naphthalene:	Level								
	4	0	0	0	0	0	0	0	0
	3	0	0	0	0	0	0	0	0
	2	0	0	0	0	0	1.1	0.1	0.4
	1	0	27	9.1	11	0	33	16	14
Compound:		Range		ave	stdev	Range		ave	stdev
		low	high			low	high		
2-methyl-naphthalene:	Level								
	4	0	3.3	0.4	1.1	0	0	0	0
	3	0	0	0	0	0	0	0	0
	2	0	0	0	0	0	0	0	0
	1	0	21	5.6	7.6	0	18	7.0	8.7

contamination in the second deepest well point was more commonly observed (and at higher concentrations) than in the CPC. Of the various contaminants measured, TCE, TCA and DCM seemed to be the least effectively removed from the deepest sampling points in both cells, with postpumping concentrations continuing to be measured at roughly 50% of the prepumping values.

5.2.3. Comparison of Prepumping and Postpumping Concentrations

Table 22 and Table 23 compare the initial and final average concentrations of the 6 major VOCs and the 4 major petroleum hydrocarbons in the lowest 4 four well points of the two cells. In addition, the initial and final VOC concentrations are compared Figure 28 through Figure 33

TABLE 22. COMPARISON OF INITIAL AND FINAL AQUEOUS CONCENTRATIONS OF CHLORINATED VOCs ($\mu\text{g/L}$)

Compound:		CPC				PPC			
		Initial		Final		Initial		Final	
	Level	ave	stdev	ave	stdev	ave	stdev	ave	stdev
PCE:	4	5.7	3.9	3	10	1	5	0	0
	3	69	52	4	11	53	50	0	0
	2	171	41	1	2	53	180	4	10
	1	180	35	15	8	100	270	34	18
Compound:		Initial		Final		Initial		Final	
	Level	ave	stdev	ave	stdev	ave	stdev	ave	stdev
TCE:	4	1.5	0.5	1	3	0	8	1	2
	3	15	7.7	2	5	0	33	1	1
	2	710	170	29	48	210	700	61	130
	1	1500	240	410	220	810	1600	490	260
Compound:		Initial		Final		Initial		Final	
	Level	ave	stdev	ave	stdev	ave	stdev	ave	stdev
cDCE:	4	4	2	14	41	0	82	3	4
	3	340	160	68	200	25	590	1	2
	2	7300	1200	92	93	2900	7200	280	580
	1	9600	440	960	500	6800	11000	1800	900
Compound:		Initial		Final		Initial		Final	
	Level	ave	stdev	ave	stdev	ave	stdev	ave	stdev
TCA:	4	0	0	0	0	0	1	0	0
	3	3	2	3	9	0	9	0	0
	2	460	100	14	22	120	450	67	140
	1	650	110	240	130	600	1100	420	230
Compound:		Initial		Final		Initial		Final	
	Level	ave	stdev	ave	stdev	ave	stdev	ave	stdev
VC:	4	0	0	0	0	0	0	0	0
	3	0	0	0	0	0	0	0	0
	2	390	130	0	0	180	650	7	22
	1	400	140	6	18	78	640	91	62
Compound:		Initial		Final		Initial		Final	
	Level	ave	stdev	ave	stdev	ave	stdev	ave	stdev
DCM:	4	0	0	0	0	0	0	0	0
	3	0	0	0	0	0	1	0	0
	2	42	15	3	4	4	44	5	10
	1	160	70	49	54	140	320	90	72

TABLE 23. COMPARISON OF INITIAL AND FINAL AQUEOUS CONCENTRATIONS OF AROMATIC VOCs ($\mu\text{g/L}$)

Compound:		CPC				PPC			
		Initial		Final		Initial		Final	
benzene:	Level	ave	stdev	ave	stdev	ave	stdev	ave	stdev
	4	0	0	0	0	0	0	0	0
	3	0	0	0.8	2.5	0	0	0	0
	2	47	25	0.7	2.2	9.1	74	1.4	2.9
	1	28	31	5.9	5.2	0	70	20	22
Compound:		Initial		Final		Initial		Final	
mp-xylene:	Level	ave	stdev	ave	stdev	ave	stdev	ave	stdev
	4	0	0	0	0	0	0	0	0
	3	0	0	0.2	0.5	0	0	0	0
	2	34	7.8	0	0	16	45	0	0
	1	43	4.8	6.1	7.5	24	42	8.4	6.2
Compound:		Initial		Final		Initial		Final	
naphthalene:	Level	ave	stdev	ave	stdev	ave	stdev	ave	stdev
	4	0	0	0	0	0	0	0	0
	3	0	0	0	0	0	0	0	0
	2	100	22	0	0	56	150	0.1	0.4
	1	130	8.2	9.1	11	110	140	16	14
Compound:		Initial		Final		Initial		Final	
2-methyl-naphthalene:	Level	ave	stdev	ave	stdev	ave	stdev	ave	stdev
	4	0	0	0.4	1.1	0	0	0	0
	3	0	0	0	0	0	0	0	0
	2	88	20	0	0	46	110	0	0
	1	110	15	5.6	7.6	89	120	7.0	8.7

for both cells. In the following chapter, the comparison of initial and final concentrations is more quantitatively considered in the context of overall mass removal, including a comparative mass balance with measured concentrations in the extracted water.

5.3. REFERENCES

Ball, W.P., Liu, C., Xia, G. and Young, D.F., 1997a. A Diffusion Interpretation of Tetrachloroethene and Trichloroethene Profiles in a Groundwater Aquitard. *Water Resources Research*, submitted manuscript.

- Ball, W.P., Xia, G., Durfee, D.P., Wilson, R., Brown, M. and Mackay, D.M., 1997b. Hot-Methanol Extraction for the Analysis of Volatile Organic Chemicals in Subsurface Samples from Dover AFB, DE. *Groundwater Monitoring and Remediation*, 17(1): 104-121.
- Ball, W.P., Xia, G., Liu, C., Brown, M. and Mackay, D., 1995. Aquitard Contamination from a Groundwater Plume -- In Situ Concentrations as Evidence of Vertical Diffusion, *1995 Spring Meeting, American Geophysical Union*. Eos, Transactions of the American Geophysical Union, Baltimore, MD, pp. S135.
- Liu, C. and Ball, W.P., 1997. Analytical Modeling of Diffusion-Limited Contamination and Decontamination in a Two-Layer Porous Medium. *Advances in Water Resources*, in press.

6. MASS BALANCE CALCULATIONS

This chapter summarizes the results of the mass balance calculations on the six major chlorinated VOC contaminants at the DAFB field site. The details of the methods and results may be found in Appendix H.

6.1. TETRACHLOROETHENE (PCE)

6.1.1. *Aquifer*

Core sampling and multilevel aqueous snapshot sampling were used to estimate the initial and final masses of PCE in the aquifer regions of the two test cells. Aqueous data were adjusted to reflect total mass, using either estimated or measured sorption parameters and an assumption of local equilibrium -- see Appendix H for details.

6.1.1.1. Initial Mass

Within the aquifer, both data sets indicate that the initial mass of contaminant was higher in the CPC (estimates of 4.8 grams from soil core data and 7.5 grams from ML data; **Table 24**) than in the PPC (estimates of 3.8 grams from core data and 5.7 grams from ML data; **Table 24**). Thus, although the multilevel data indicated a higher mass in both cells than did the soil core results, both types of analyses suggested an initially greater mass of PCE in the CPC aquifer than in the PPC aquifer.

On the other hand, and as previously shown under "Initial Site Contamination" (Chapter 5), both data sets show maximum concentrations occurring closer to the aquitard surface in the PPC (0.25 to 2 meters) than in the CPC (0.5 to 3 meters). Also as noted in Chapter 5 (and as further elaborated subsequently), this has resulted in higher *aquitard* concentrations within the PPC.

6.1.1.2. Final Mass

The core data taken at the conclusion of the field experiment indicate that the CPC was the most contaminated of the two cells, whereas the multilevel data indicate that the PPC was the most contaminated. When final masses are compared with initial masses, the core data indicate

TABLE 24. PCE MASS (GRAMS) IN AQUIFER AND AQUITARD OF TEST CELLS

Aquifer:	CPC		PPC	
	Core	Multilevel	Core	Multilevel
Initial	4.8	7.5	3.8	5.7
Final	0.2	0.4	0.1	0.5
Upper ¹ Aquitard:	Thiessen	SURFER	Thiessen	SURFER
Initial	0.1	0.2	0.6	0.8
Final	0.1	0.17	0.6	0.5
Lower ² Aquitard:	Thiessen	SURFER	Thiessen	SURFER
Initial	0.0	*	0.2	0.2
Final	0.0	0.06	0.3	0.1

¹ Upper aquitard is Aquitard-1 layer for Thiessen method and OSCL for SURFER method

² Lower aquitard is sum of Aquitard-2 and Aquitard-3 layers for Thiessen method and DGSL for SURFER method

* No DGSL samples taken in CPC during initial coring.

TABLE 25. EXTRACTED AND CALCULATED MASS REMOVAL OF EACH COMPOUND

Compound	CPC			PPC		
	Extracted by Pumping (g)	Mass Removed by Difference (g)		Extracted by Pumping (g)	Mass Removed by Difference (g)	
		Core	ML		Core	ML
PCE	6.2	4.6	7.1	4.5	3.7	5.2
TCE	25.3	24.4	24.1	19.7	22.3	14.1
1,2- <i>cis</i> -DCE	178.0	n/a	224.3	137.1	n/a	146.5
TCA	14.4	n/a	12.4	12.7	n/a	8.0
VC	4.2	n/a	10.5	4.1	n/a	9.5
DCM	2.4	n/a	1.7	2.3	n/a	1.4

slightly greater percent removal from the PPC whereas the multilevel data indicate slightly greater percent removal from the CPC cell.

6.1.1.3. Extracted Mass

The extracted mass of PCE from both cells agrees well with the predictions made from the core and multilevel initial and final mass estimates (**Table 25**). The extracted mass calculations support the general trend that more contaminant mass was removed from the CPC. However, this is mainly a reflection of the facts that there was a greater initial contamination of the CPC and that more water was pumped from the CPC. A plot of the cumulative mass removed (expressed as a fraction of the total removed) versus volume of water pumped shows greater percent removal from the CPC at early times. However, at later times, there was higher percent removal from the PPC (**Figure 34**). These results are further discussed in the summary below.

6.1.2. Aquitard

No aqueous samples were taken from the aquitard region, and mass estimation from core samples is compromised since the cores often did not penetrate to uncontaminated aquitard material. Additionally, the composite samples taken during the initial coring exercise often spanned the important boundary between the OSCL and DGSL, such that it is also difficult to accurately divide aquitard mass among the upper (OSCL) and lower (DGSL) aquitard layers. Nonetheless, we are able to provide a comparative estimate of the *sampled* PCE mass within the aquitard of the two test cells, on the basis of available data. Two methods of estimation were used: (1) a weighting of the core data in accordance with Thiessen Polygons (similar to the technique applied to estimations in the aquifer); and (2) simply averaging the core subsample results within each aquitard layer (OSCL and DGSL), using commercial contour graphing and data averaging software (SURFER, Golden Software, Golden, CO). Because of the lower boundary issue outlined above (and as elaborated in Appendix H), the most reliable estimates of contaminant mass in the aquitard were those made in the upper 0.5 meter of the aquitard (aquitard-1 layer; Thiessen Polygon method) or those made within the OSCL layer (SURFER method).

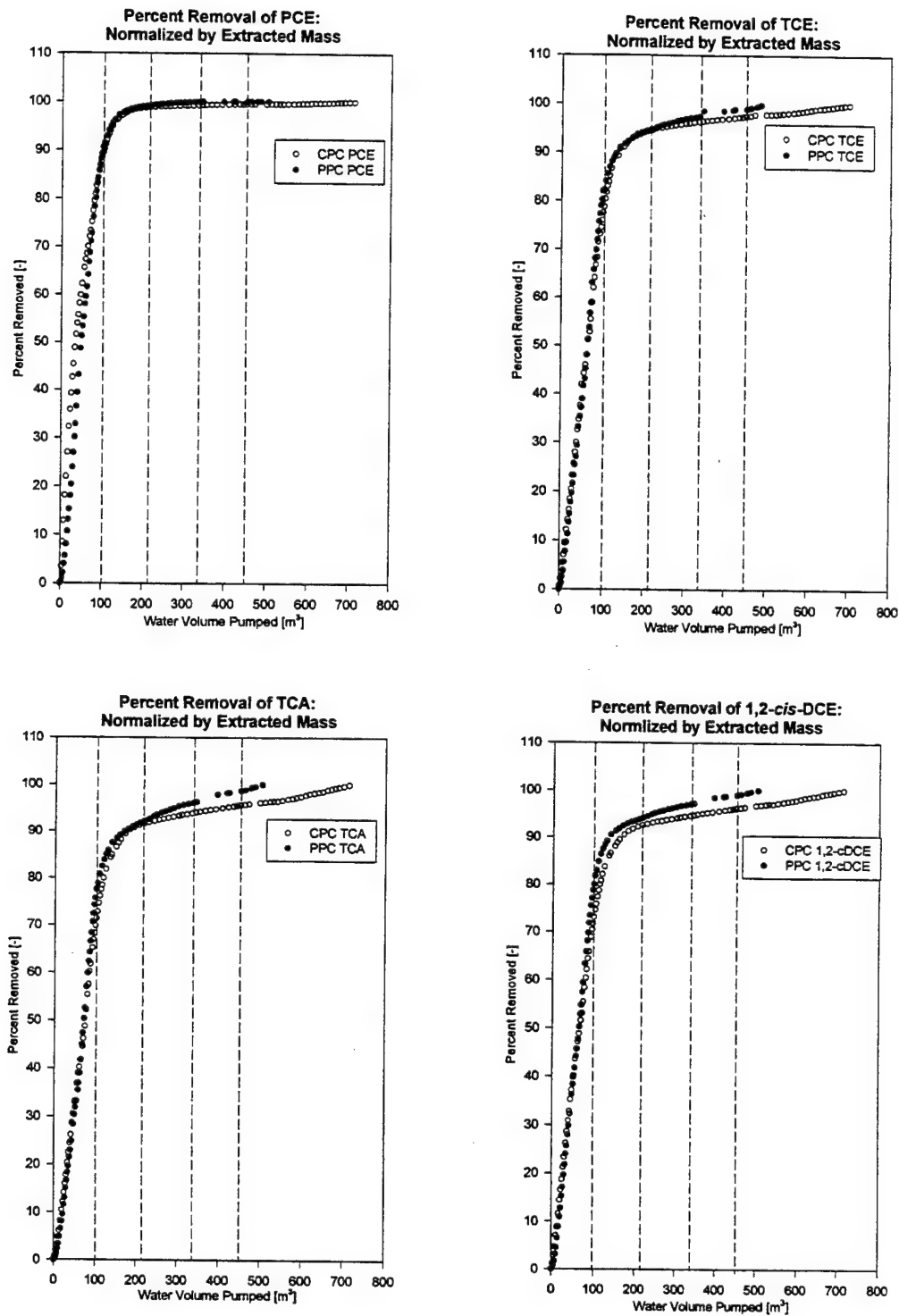


Figure 34. Percent Cumulative Removal of PCE, TCE, *cis*-DCE and TCA (Normalized by Total Extracted Mass)

6.1.2.1. Initial Mass

For the initial data, both methods indicated that the aquitard of the PPC was the most contaminated. The greater mass of PCE estimated in the PPC aquitard was due to two factors: 1) a greater portion of the PPC aquitard was sampled than the CPC aquitard (with the more strongly sorbing DGSL material not sampled in CPC); and 2) the average concentration of PCE in the PPC aquitard was greater than the average concentration within the CPC aquitard, even within the OSCL layer. Although estimated aquitard mass in both cells is biased low because of the insufficient depth of sampling, the estimated masses are only a small percentage of the mass found in the overlying aquifer. Even for the PPC, which had a more complete sampling of the aquitard, only about 15% to 23% of recovered mass was in the aquitard layers. A smaller fraction is expected for the CPC (owing to lower concentrations, relative to those in the overlying aquifer), but not so low as reflected in **Table 24**, since the vertical extent of aquitard contamination was not fully sampled in the CPC.

6.1.2.2. Final Mass

The final coring data indicated that both aquitards remained contaminated to a significant extent, with the PPC aquitard continuing to show higher concentrations and mass than the CPC. Analysis by the Thiessen Polygon weighting method indicates that the mass of PCE remained unchanged in both cells at the conclusion of the field experiment, while the data obtained using the SURFER method indicates that the mass of PCE may have declined in the upper aquitard layer of both cells (15% removal from CPC OSCL, 38% removal from the PPC OSCL). It is conceivable that the higher fractional removal from the aquitard in this cell may be due to the longer total desorption time afforded to the PPC (owing to the difference in sampling dates). However, we doubt that data precision is sufficient to justify this conclusion.

6.2. TRICHLOROETHENE (TCE)

6.2.1. Aquifer

As with PCE, both core and multilevel data were used to estimate the initial and final masses of TCE in the aquifer regions of both cells.

6.2.1.1. Initial Mass

Both data sets indicate a greater initial mass of TCE in the CPC aquifer than in the PPC aquifer (**Table 26**). Both estimates also indicate that the CPC was more highly contaminated than the PPC cell; however, the suggested difference is more extreme for the multilevel mass estimate. The vast majority (80%-CPC and 90%-PPC) of TCE mass was concentrated in the lowest 1.5 meters of the aquifer in both cells. As previously discussed under "Initial Site Contamination" (Chapter 5), highest TCE concentrations were directly at the aquitard interface.

TABLE 26. TCE MASS (GRAMS) IN AQUIFER AND AQUITARD OF TEST CELLS

Aquifer:	CPC		PPC	
	Core	Multilevel	Core	Multilevel
Initial	24.8	28.7	22.5	19.8
Final	0.4	4.6	0.2	5.7
Upper ¹ Aquitard:	Thiessen	SURFER	Thiessen	SURFER
Initial	15.6	19.1	28.0	33.0
Final	16.6	15.6	25.9	31.3
Lower ² Aquitard:	Thiessen	SURFER	Thiessen	SURFER
Initial	5.8	*	14.6	16.9
Final	6.6	12.1	36.1	20.4

¹ Upper aquitard is Aquitard-1 layer for Thiessen method and OSL for SURFER method

² Lower aquitard is Aquitard-2 layer for Thiessen method and DGSL for SURFER method

* No DGSL samples taken in CPC during initial coring.

6.2.1.2. Final Mass

The final mass estimate from the core data indicated that over 98% of the TCE mass was removed from the aquifer in both cells, with the CPC remaining slightly more contaminated than did the PPC (0.4 grams in CPC vs. 0.2 grams in PPC; **Table 26**). In contrast, the multilevel mass estimate indicated that a more significant mass of TCE remained in both cells (4.6 grams in CPC and 5.7 grams in PPC), while also suggesting that the percent removal was lower in the PPC than in the CPC (71% versus 84%). This may reflect the higher flux from the aquitard for the PPC, as

aquitard concentrations were higher in that cell -- see Chapter 5.

6.2.1.3. Extracted Mass

The extracted mass of TCE from the CPC agrees well with the estimates made from the core and multilevel initial and final mass estimates in the CPC (**Table 25**). Within the PPC, the extracted mass of TCE agrees more closely with the estimates made from the core data than from the multilevel data initial and final mass estimates (**Table 25**). As with PCE, the mass removal follows the general trend that more contaminant mass was pumped from the CPC. However, this is mainly a function of the greater initial contamination of the CPC and that more water was pumped from the CPC. A plot of the cumulative mass removed (expressed as a fraction of the total removed) versus volume of water pumped shows nearly equivalent percent removal of TCE from both cells at early times. However, at later times, there was higher percent removal from the PPC (**Figure 35**). These results are as with PCE and are further discussed in the summary below.

6.2.2. Aquitard

As with PCE, aquitard concentration data for TCE were available only with the core data. Also as before, two methods of estimating mass were used, and total mass estimates are necessarily biased low by incomplete sampling of the contaminated zone (especially in the CPC cell).

6.2.2.1. Initial Mass

For the initial data, results from both estimation methods are shown in **Table 26**. These data indicate that the aquitard of the PPC was the most contaminated for TCE. As with PCE, the greater estimated mass of TCE in the PPC aquitard reflects both higher concentrations and a deeper sampled depth. In contrast to PCE however, TCE mass in the aquitard was a very significant fraction of the total mass found. Within the CPC, the total mass of TCE was nearly equally divided between the aquitard and the aquifer. Within the PPC cell, there was approximately 3 times as much TCE mass within the aquitard as within the aquifer.

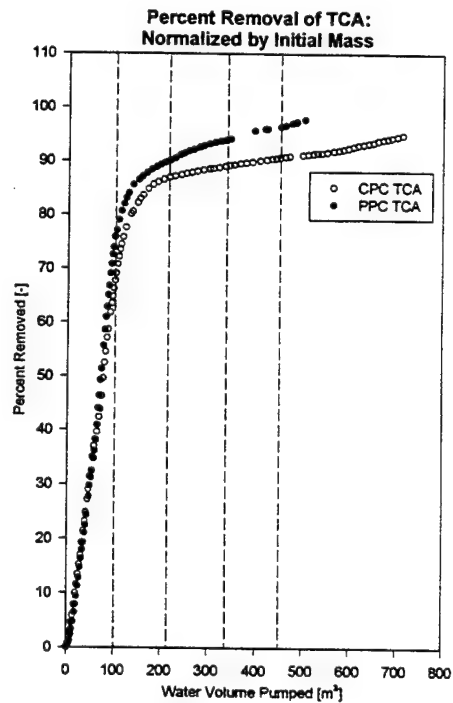
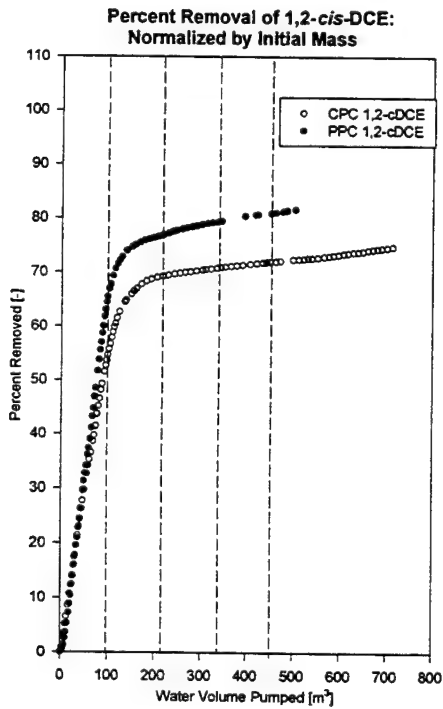
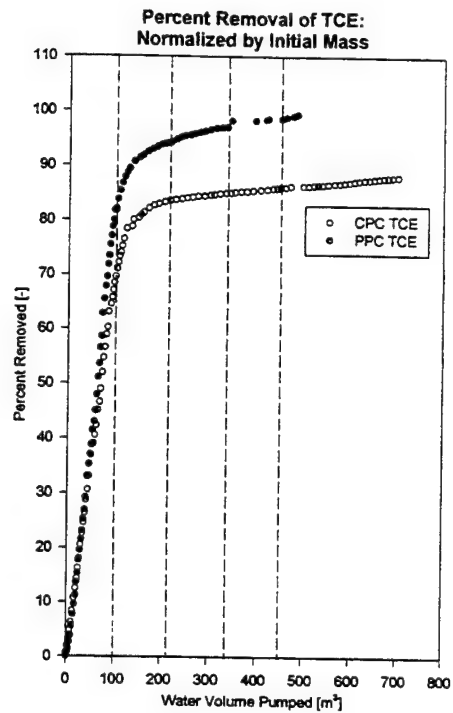
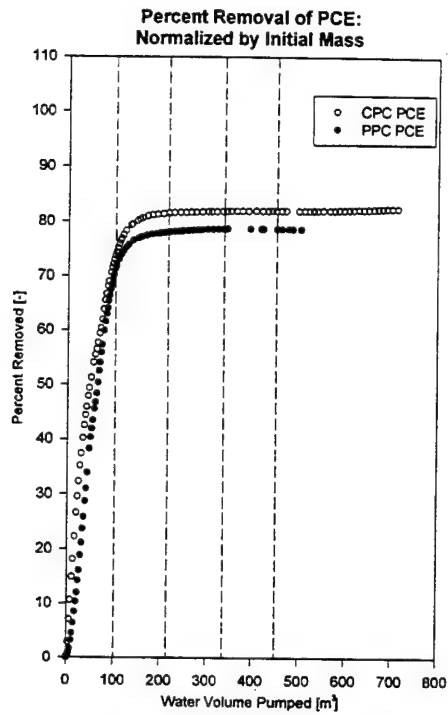


Figure 35. Percent Cumulative Removal of PCE, TCE, *cis*-DCE and TCA (Normalized by Initial Multilevel Mass Estimate)

6.2.2.2. Final Mass

Both estimation methods indicate little change in the mass of TCE within the upper 0.5 meter region of the aquitard (aquitard-1 layer; OSCL), with the PPC aquitard remaining more highly contaminated than that of the CPC. Within the CPC, Thiessen Polygon results suggest a modest increase in mass in the aquitard-1 layer (16 g to 17 g), whereas the SURFER analysis of the upper layer (OSCL) suggests a decline (19 g to 16 g). Within the PPC cell, both mass estimation methods indicate a modest decline of TCE mass in the upper aquitard layer.

6.3. OTHER VOCs: CIS-DCE, TCA, VC AND DCM

The multilevel initial and final snapshot data were used to obtain estimates of the initial and final masses of these compounds in the aquifer regions of both cells.

6.3.1. Aquifer Initial Mass

Comparison of initial and final masses for the four additional chemicals are shown in **Table 27**. The major contaminant in both cells was *cis*-DCE, whose mass was greater than that of all other chlorinated VOCs combined. The mass of *cis*-DCE was significantly greater in the CPC aquifer than in the PPC aquifer. Masses of the other three compounds were approximately equal between the two cells. As previously described under "Initial Site Contamination" (Chapter 5), concentration distributions for three of the four chemicals (*cis*-DCE, TCA and DCM) roughly followed that of TCE, with highest concentrations occurring at the aquitard/aquifer interface. We hypothesize that, as with TCE, the peak plume concentrations for these chemicals may have occurred at some prior time, and that the current (initial) cell concentrations may reflect the result of vertical diffusive flux out of the previously contaminated aquitard (both at the cell locations and in upgradient regions). On the other hand, some high vinyl chloride and *cis*-DCE concentrations are observed at a shallower depth, further from the aquitard/aquifer interface. These concentrations may reflect the same dominant contamination flow paths previously noted for PCE. As an example scenario (possible but not proven), much of the sampled VC may be the result of upgradient dechlorination of PCE and TCE, with VC arriving at the current site

primarily through groundwater advection.

TABLE 27. INITIAL, FINAL AND CALCULATED % REMOVED OF ALL SIX VOCS

Compound	Data Source	CPC			PPC		
		Initial (gr)	Final (gr)	Calculated %Removed	Initial (gr)	Final (gr)	Calculated %Removed
PCE	ML	7.5	0.4	94.7	5.7	0.5	91.2
PCE	core	4.8	0.2	95.8	3.8	0.1	97.4
TCE	ML	28.7	4.6	84.0	19.8	5.7	71.2
TCE	core	24.8	0.4	98.4	22.5	0.2	99.1
<i>cis</i> -DCE	ML	237.9	13.6	94.3	167.7	21.2	87.4
TCA	ML	15.2	2.8	81.6	13.0	5.0	61.5
VC	ML	10.6	0.1	99.1	10.5	1.0	90.5
DCM	ML	2.3	0.6	73.9	2.3	0.9	60.9

6.3.2. Aquifer Final Mass

In both cells, *cis*-DCE remained the majority contaminant with a mass still greater than the combined total of the other 5 VOCs (Table 27). Predicted percent removals vary between 61% and 99% but were higher in the CPC for each compound. The implications of these results are further discussed in the summary section.

6.3.3. Extracted Mass

The extracted masses of these four VOCs follows the general trend that more mass was removed from the CPC than from the PPC. However, this is mainly a result of the facts that the CPC had an initially higher level of contamination and that more water was pumped from the CPC. A plot of the cumulative fractional mass removed (cumulative mass removed expressed as a fraction of the total mass removed) versus volume of water pumped shows nearly equivalent percent removal of the four VOCs from both cells at early times. However, at later times, there was higher percent removal from the PPC (Figure 34 and Figure 35). These results are as with

PCE and TCE and are further discussed in the summary below.

6.4. SUMMARY

6.4.1. *Aquifer*

In comparing the results summarized in **Table 25** and **Table 27** with the vertical concentration profiles described in Chapter 5, we observe that those contaminants which showed the highest concentrations at elevations other than the aquifer bottom (PCE and VC) showed the best removal efficiencies, with greater than 90% removal of these two contaminants from both cells. Removal for other chemicals varied from 61% (DCM and TCA in PPC) to 87% (*cis*-DCE in PPC).

For all chemicals, removal efficiencies were consistently higher in the CPC than in the PPC. In fact, the final mass of each compound was found to be highest in the PPC, despite the fact that initial masses were lower. However, this fact cannot be directly related to a comparison of the two remediation approaches, since a greater volume of water was pumped from the CPC compared to the PPC (717.8 m³ from the CPC compared to 543.8 m³ from the PPC). In addition, the greater initial concentrations of contaminant in the *aquitard* of the PPC also contribute to the inappropriateness of such a comparison, since the concentration-gradient-driven flux up from the aquitard will more effectively slow contaminant removal from the PPC aquifer. Thus, we hypothesize that the greater level of aquitard contamination in the PPC (based on TCE and PCE data, and as implied by the concentration distribution data for other compounds; Chapter 5) has lead to higher final concentrations of contamination in this cell. In this way then, the important differences in the initial conditions among the two cells complicates our comparative analysis of the different pumping schemes.

A possible comparison in the extraction efficiencies of the VOCs between the two cells is shown in **Figure 34**. This comparison was made for PCE, TCE *cis*-DCE and TCA only because of analytical difficulties with VC on the ASAP as elaborated elsewhere (Chapter 2) and because DCM was a relatively insignificant contaminant. These plots show the cumulative extracted mass of each compound normalized by the total extracted mass from the respective cell versus the volume of water pumped from each cell. The vertical lines on these plots indicate periods

during which pumping within the PPC was halted. Note that after the first off period in the PPC, there is a divergence between the fractional mass removals from the two cells; namely, a greater fraction of mass is removed from the PPC for a given volume of water pumped. Note also that after each off period in the PPC, a similar increase in the rebound-associated “fractional removal rate” is observed. It is also informative to compare the behavior of PCE with the other compounds since we know from the core data that the fraction of PCE mass that is within the aquitard is much less than that of TCE. Because the multilevel data suggest similarity of profiles between TCE, DCM, *cis*-DCE and TCA, it is likely that the mass fractions of the latter three compounds are also relatively high in the aquitard compared to PCE and VC. (Multilevel data suggest elevated VC profiles at higher elevations in the aquifer, more similar to PCE.) In this context, it is perhaps not surprising that the rebound effect observed for PCE and VC is less significant than that of the other compounds. This trend is particularly obvious for *cis*-DCE and TCA, which are less strongly sorbing compared to TCE and should experience less retardation of diffusion during transport from the aquitard. For this reason, *cis*-DCE and TCA may be expected to rebound more rapidly than TCE.

Another way of normalizing data between the two cells is to divide the extracted mass of each compound by the initial mass present as determined from the multilevel estimates. The plots in **Figure 35** show the cumulative fractional removal of PCE, TCE *cis*-DCE and TCA (normalized by the initial multilevel mass estimate) versus the volume of water pumped. The efficiencies of removal of TCE, *cis*-DCE and TCA are greater in the PPC even before the first “pulse off” period and then diverge dramatically after this first “pulse off” period. However, PCE behaves contrary to this trend in that its efficiency of removal remains higher in the CPC during the entire course of the experiment. However, small errors in the initial mass estimate can skew this analysis and thus invalidate this comparison. As an example, if the initial core data mass estimate is used to normalize the PCE and TCE cumulative extraction data, then both PCE and TCE show decreased removal efficiencies from the PPC.

In light of the preceding discussion, it is apparent that a comparison of “efficiency” of pulsed pumping versus continuous pumping cannot be made solely on the basis of differences in fractional mass removal from the two test cells, as determined from the initial and final

snapshots. In addition to the need to account for the volume of water pumped (e.g., by adjusting extracted mass to account for the decreased pumped volume from the PPC), it is also necessary to appreciate that more removal from the aquitard may be occurring within the PPC, and that this mass removal is much harder to accurately assess.

6.4.2. Aquitard

Mass estimates in the aquitard are available only for PCE and TCE, and are incomplete in the sense that the entire contaminated region was not sampled. Results of the upper aquitard layer (OSCL) suggest that some decontamination has occurred over the course of the project, but that the majority of contamination remains. Moreover, the TCE data in PPC suggest that at least some fraction of the contaminant loss from this upper layer is occurring through increased contamination of the underlying DGSL layer (DGSL, or lower aquitard layer 2 in **Table 26**). PCE data do not show a similar result, but concentrations are too close to detection limits to be reliable. In general, the aquitard data have been most useful in regard to the information they provide about concentration, rather than mass. In these regards, the data suggest a prior contamination of the aquitard for all chemicals except PCE and VC, with on-going contamination of PCE (and possibly of VC). As noted above, the PPC aquitard was more heavily contaminated than that of the CPC, and is likely to have returned more mass to the aquifer under the conditions of pump-and-treat. We refer readers to some related publications (Ball et al., 1997; Liu and Ball, 1997) for additional discussion related to contaminant diffusion within the DAFB aquitard.

As previously noted, the low resolution of aquitard sampling in the prepumping core data and the incomplete capture of the full contamination depth at many locations are the primary reason for our poor estimates of mass removals from the aquitard layers. In future work, we intend to re-sample the aquitard in both cells after long (6-month or greater) periods of no pumping. For this work, we will be using high resolution sampling (similar to that applied to the postpumping core results reported here), and we anticipate being able to verify whether the contaminants behave as conservatively diffusing solutes. If so, this will give us greater confidence in our ability to predict and understand the aquitard's historical influence on the overall mass balance in each cell. However, such calculations are complicated by a number of factors, and are well

beyond the scope of the current project.

6.4.3. Mass Balance

As detailed in Appendix H, a comparison was made between the mass of each compound extracted from each cell through pumping to the estimate of mass removed from each cell based on the difference between the initial and final mass estimates. For PCE, the multilevel mass removal estimate gave closest agreement to the extracted mass in both the CPC and PPC. For this compound, the multilevel mass estimate overestimated the mass removed and the core data underestimated the mass removed in both cells. For TCE, excellent agreement between the mass extracted and the estimated removal was given by both core and multilevel mass removal estimates in the CPC. However, within the PPC, the core data mass removal estimate overestimated the amount extracted but gave the best agreement compared to the multilevel mass removal estimate which significantly underestimated the amount removed.

The mass balance results were similarly mixed for the other four VOCs. Within both cells, the extracted mass of VC was in poor agreement with the estimated removal owing to difficulties of analytical calibration.. In addition, the poor mass balance results for DCM are thought to be due to analytical uncertainties arising from the low concentrations of this compound in the aquifer . Comparing *cis*-DCE and TCA, the best mass balance obtained was for *cis*-DCE in the PPC for which there was less than 7% difference between the mass extracted and the estimated mass removed. Within the CPC, the *cis*-DCE mass removed estimate was about 20% greater than the amount extracted while the TCA mass removed estimate was about 20% less than the amount extracted.

In summary, the best mass balance was for TCE in the CPC with very close agreement between the extracted and estimated mass removal based on both core and multilevel data. The next best mass balance was obtained on *cis*-DCE in the PPC, and all other mass balances (excluding VC and DCM and except for TCA in the PPC) showed no more than 20% variation between the amount extracted and the estimated mass removed.

6.5. REFERENCES

- Ball, W.P., Liu, C., Xia, G. and Young, D.F., 1997. A Diffusion Interpretation of Tetrachloroethene and Trichloroethene Profiles in a Groundwater Aquitard. *Water Resources Research*, in press.
- Liu, C. and Ball, W.P., 1997. Analytical Modeling of Diffusion-Limited Contamination and Decontamination in a Two-Layer Porous Medium. *Advances in Water Resources*, in press.

7. SUMMARY AND CONCLUSIONS

7.1. BACKGROUND

The most commonly applied technique for cleanup of aquifers contaminated by organic chemicals is the "pump-and-treat" approach. Typical experience with this technique has been that aqueous concentrations of contaminant decrease over time, with removal rates becoming low even while contaminant concentrations in the subsurface remain above cleanup goals. This effect is usually attributed to slow mass transfer of contaminants into the flowing aqueous phase, due to some combination of slow dissolution of non-aqueous phase liquids, slow diffusion from less permeable strata of the media, and slow desorption of sorbed contaminants from aquifer solids. Theoretical considerations suggest that there may be important advantages to periodically ceasing or slowing groundwater extraction in order to allow time for these slow rate processes to attain or approach equilibrium. Periodic cessation of pumping (pulsed pumping) is a practical means of achieving this effect without changing pump equipment or altering the pumped flow rates. This method would theoretically allow contaminant "rebound" (system equilibration) to occur during pump off periods; however field data to confirm the advantages of this approach are currently lacking. Although continuous pumping at a high rate actually removes contamination faster (by providing continuously low concentrations in the mobile phase), pulsed pumping may serve to significantly reduce costs and conserve groundwater resources in many situations. In particular, in comparison with continuous pumping at an arbitrarily high rate, pulsed pumping might be expected to provide improved efficiency in terms of the mass removed per unit volume of extracted water. Thus, although pulsed pumping is not expected to decrease the overall time for aquifer remediation, this mode of operation may serve to significantly reduce pumped water volumes in many situations. Resulting advantages should include decreased pumping cost, a shorter duration of the more labor intensive pumping and treatment operations, lower volumes of water for above-ground treatment, and less total groundwater extraction, a feature of potential importance in more arid areas.

Although pulsed groundwater pumping has been promoted in the context of aquifer remediation, to our knowledge there have heretofore been no field demonstrations of the

technology under well-controlled field conditions. In particular, no previous field investigations have specifically sought to test this strategy for VOC removal from unconsolidated sandy aquifers, despite the fact that a large fraction of the contamination plumes nationwide are of this type and are most commonly remediated by pump-and-treat methods.

7.2. OBJECTIVES

This report describes the results of field and laboratory investigations addressing groundwater remediation by the pump and treat approach. The primary goal of the project was to determine whether there are discernible advantages of a pulsed-pumping strategy compared to continuous pumping at a "real-world" site where contamination by volatile organic contaminants (VOCs) has been long extant. The objective was to conduct the investigations far enough downgradient of the probable source(s) of VOC contamination so that NAPL was not present within the investigated portion of the subsurface. The underlying scientific goal was to identify the most significant sources of mass transfer rate limitation at the site and to develop appropriate conceptual and computational models to describe and predict the resulting effects on aquifer decontamination. Finally, the overall practical goal was to use conceptual and computational models to identify under what site conditions and for what goals, if any, the pulsed-pumping approach might find advantageous application.

7.3. APPROACH

A VOC plume at the Dover AFB, DE, was selected for study after extensive consideration of alternatives. Sheet-pile test cells were used to isolate two adjacent segments of the long-extant groundwater plume containing chlorinated solvents and their degradation by-products (PCE, TCE, TCA, cis-1,2-DCE, vinyl chloride) as well as aromatic organic contaminants (benzene, xylene, naphthalene, 2-methyl-naphthalene). Each test cell measures 3.5 meters x 10 meters and was created by driving grout-sealable sheet pile about 15.3 meters into the subsurface, i.e. through the surficial aquifer and 1 to 1.5 meters into the underlying aquitard. One cell was subjected to continuous flushing and the other to intermittent (pulsed) flushing for over 200 days (pumped volumes corresponding to roughly 7 and 5 pore volumes, respectively). Monitoring of groundwater in the extraction wells and multilevel samplers allowed estimates of extracted

contaminant mass and variations in contaminant distribution and elution within the cells. High-resolution core sampling (1 to 3 meters horizontal spacing, 0.02- to 0.1-m vertical spacing) allowed characterization of the initial and postpumping distributions of PCE and TCE, two compounds which had been initially identified as a primary focus of this project. Samples of the cored material were used to characterize properties of the various geologic materials, including transport properties, particle size distribution, organic carbon content, and sorption characteristics with regard to the focus solutes (TCE and PCE).

7.4. RESULTS

The laboratory analyses of the cored material from the site indicated that: (1) the sorption of the contaminants by most of the aquifer materials was linear but very slight (0.05 mL/g or less) and (2) the sorption of the contaminants by the aquitard material was linear, quite significant, and markedly different between the two identified aquitard strata (0.2 to 0.5 mL/g in OCSL, 8 to 22 mL/g in DGSL).

The sorption in the aquitard material serves to slow the rate of contaminant diffusion into and out of this medium. By understanding the extent of sorption, and with independent knowledge about diffusion rates, we have been able to use the contaminant profiles within the aquitard as a forensic tool to provide information about contamination history in the overlying aquifer and to provide simulations of long-term concentration histories within the aquitard under hypothetical conditions of "cleanup" (Ball *et al.*, 1997).

Recall that the processes believed to constrain contaminant removal from the subsurface by the pump and treat method, in portions of the subsurface not containing NAPLs, are mass transfers of contaminants into the flowing aqueous phase, due to 1) slow diffusion from less permeable strata of the media, and/or 2) slow desorption of sorbed contaminants. The very slight sorption within the aquifer at the Dover AFB site implies that desorption is likely to be insignificant compared to diffusion from lower permeability media in controlling pump and treat remediation, and therefore in causing differences between pulsed pumping and continuous pumping.

In this work, we found that comparison of the efficiencies of the pulse pumped cell (PPC)

and the continuously pumped cell (CPC) required careful consideration of the differences in initial conditions between the two cells. Although the cells were separated laterally by only 1.5 meters and were located roughly along the centerline of the PCE and TCE plumes, our work has shown that there were important differences in contaminant distribution within them prior to initiation of the pumping experiments. Thus it was necessary to make comparisons between the cells on some normalized basis, for example mass removal as a fraction of total initially present in the cell or as a fraction of total extracted. For a given volume of extracted water (>1 to 2 pore volumes), the fractional removal of contaminant mass estimated by either normalization technique was higher for the PPC than the CPC for the majority of contaminants. These contaminants had maximum prepumping aquifer concentrations at or near the aquifer/aquitard interface, and diffusion profiles within the aquitard that were consistent with ongoing mass transfer from the aquifer to the aquitard. The fractional removal of the other contaminants (i.e. those whose maximum aquifer concentrations occurred at depths well above the aquifer/aquitard interface) was quite similar for the two cells. For this minority of contaminants, the profiles within the aquifer were consistent with the hypothesis that the maximum aquifer concentrations at the aquifer/aquitard interface had occurred in the past and, for some time before the initiation of our experimentation, the mass transfer across the interface was from the aquitard to the aquifer, thus depleting the reservoir of contaminants within the aquitard and also lowering the concentration gradient driving the mass transfer from the aquitard to the aquifer.

7.5. CONCLUSIONS

Overall, our work suggests that the pulsed approach at the Dover site is slightly more efficient at mass removal for contaminants with significant reservoirs of mass in the aquitard. Given the depth of the aquitard contamination and the estimated rates of diffusion in this material, greater benefits would be expected if the duration of pump off periods could be extended beyond those studied here. On the other hand, practical pulsed-pumping approaches would not be able to reach the ideal "off" conditions we obtained (zero flow). Unless the pump-off period could be longer *and* the area influenced by "flushing" made large relative to the area re-contaminated during natural gradient flow (two potentially conflicting objectives), a large-scale pulsed-pumping approach in the Dover AFB aquifer is likely to have minimal advantage

over a continuously pumped approach. Nevertheless, the knowledge gained over the course of this project has important and broader application.

Overall, the results of this work indicate that contaminant transport and subsurface remediation at this site are influenced not only by (1) spatial variability of the transport medium (aquifer), but also by (2) spatial variability in the pre-remediation contaminant distribution, and (3) spatial variability of the aquitard sorption properties. This work is among the first to clarify the importance of the variability of aquitard sorption properties. Our field data present a clear picture of diffusion-controlled aquitard contamination, in which persisting sorbed chemicals in the aquitard serve as a long-term source of contaminant to the otherwise relatively easily flushed aquifer. Rates of contaminant release from the aquitard are strongly dependent on both (2) and (3) above.

In addition to providing valuable field evidence regarding rates of aquifer decontamination under pumped conditions, the field tests, laboratory investigations, and modeling studies conducted in this project have provided new insights into the nature of contaminant transport to and from low-permeability zones. As mentioned above, we have found that, under some circumstances, contaminant profiles within lower permeability media may be used in a forensic sense to generate insight into the history of contamination in the adjacent higher permeability media. The results of this work have been and will continue to be extrapolated from Dover-specific conditions to a variety of hydrogeologic situations via modeling to emphasize the effects of heterogeneity of permeability and pre-remediation contamination on long-term remediation by any method constrained by diffusion of contaminants to and from low permeability media.

Appendix A. FENCE DIAGRAMS OF CORE LOGS

Soil cores taken during the initial site characterization were logged on-site by a geologist from the University of Waterloo, with results as previously summarized in Table 6 (Chapter 4). The core logs from the interior of the test cells have been used to construct fence diagrams, using the commonly observed geologic strata among cores. These diagrams are shown in this appendix.

In order to show data from all fourteen cores interior to the test cells, six fences have been constructed. These include four fences in the longitudinal direction (two in each test cell), and two fences in the transverse direction. The transverse fences span both cells.

Figure A-1 shows the plan locations of the six geologic cross-sections and identifies the multilevel or screened well locations from which the diagrams were constructed. Figure A-2 provides a key to the various strata identified in the diagrams. The fence diagrams are provided as Figures A-3 through A-8. Figures A-3 through A-6 depict the longitudinal cross-sections and Figures A-7 and A-8 depict the transverse cross sections.

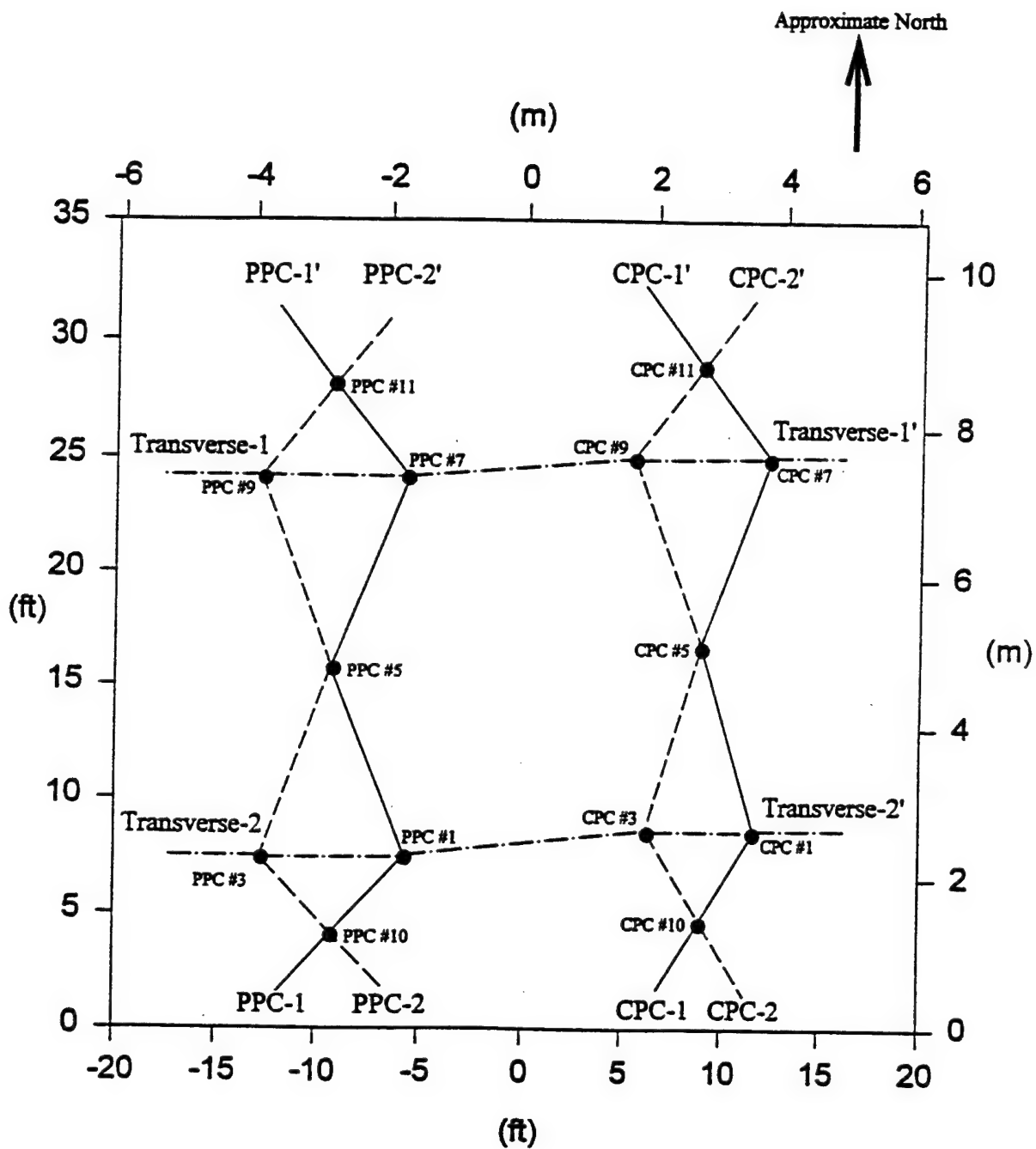


Figure A-1: Locations of Geological Cross-Sections






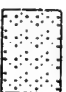

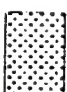




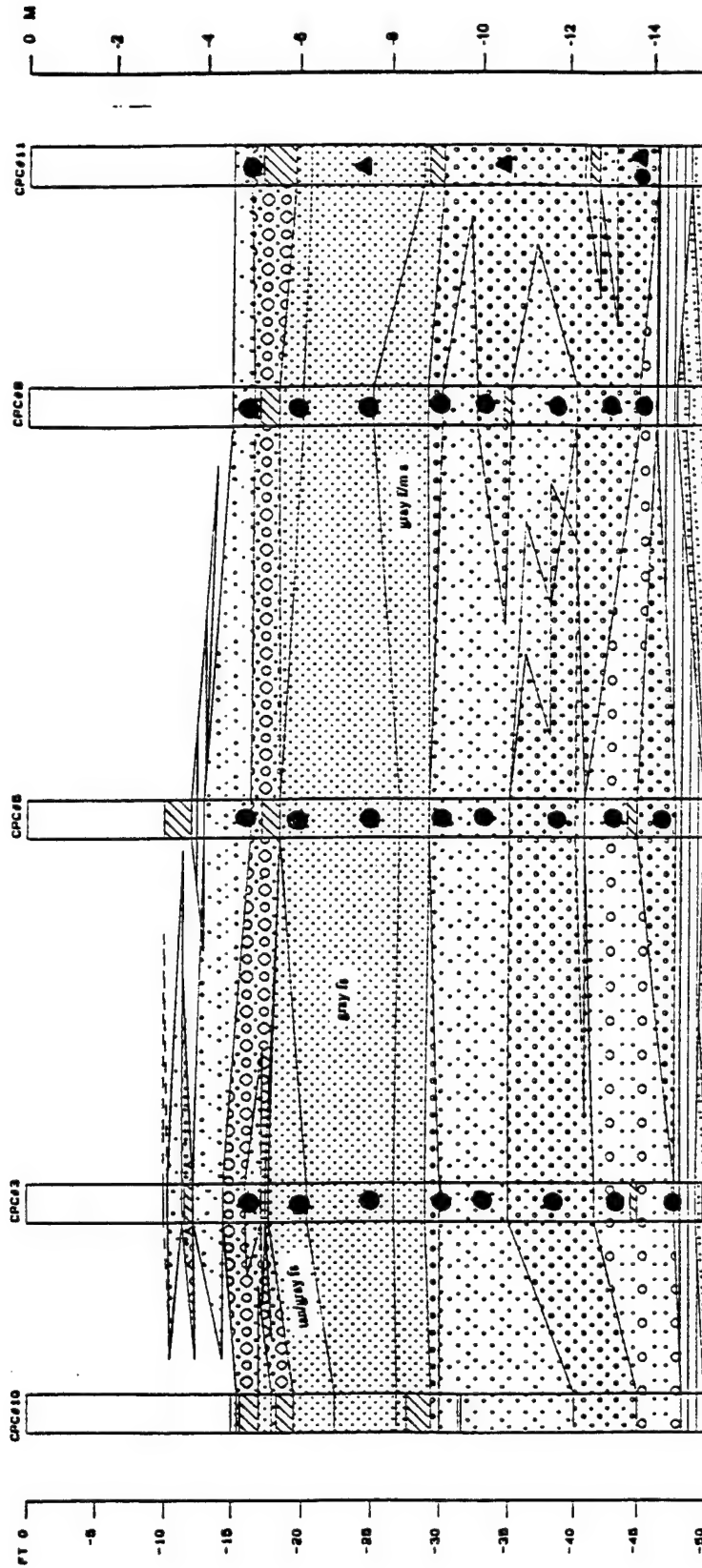
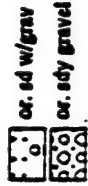
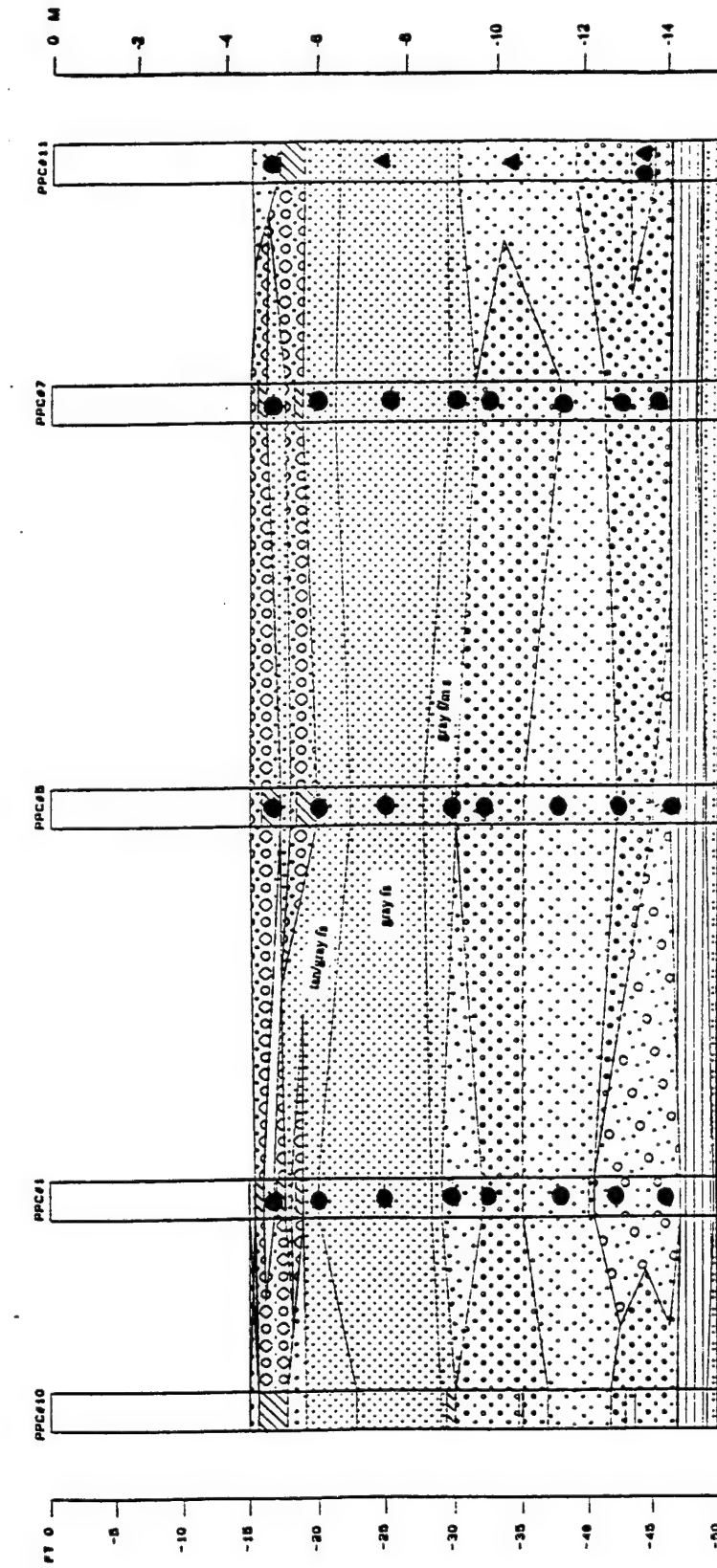
	No core:	No core.
	No recovery:	No recovery of the core. Possible gravel layer.
	tan/gra fine sd:	"Tan/gray fine sand". Fine sand, light gray to tan in color.
	gray fine sand:	Fine sand, light gray in color with black speckles common.
	gray M/C sand:	"Gray medium/coarse sand". Fine to medium sand with very minor occurrence of pebbles (up to 1/2"), either rust or light gray in color.
	or. F/M sand:	"orange fine/medium sand". Fine to medium sand, orange in color.
	or. medium sand:	"Orange (rust-colored) medium sand". Medium sand with minor fines and very minor pebbles, rust-orange in color; very homogeneous and well-sorted.
	or. M/C sand:	"Orange medium/coarse sand". Medium to coarse sand with few to moderate fines and occasional pebbles; rust-orange in color.
	or. sdy gravel:	"Orange (rust-colored) sandy gravel". Very coarse sand and gravel with moderate fines, pale orange in color.
	or. sd w/grav.:	"Orange sand with gravel". Very poorly sorted coarse sand and gravel with moderate fines in matrix and pebbles 1/4" to 3/4" abundant throughout; rust-orange in color; very minor occurrence of gray clay clasts in some cores.
	OSCL:	"Orange silty clay loam". Clay, silt and fine sand (roughly 35% clay, 45% silt, and 20% sand by volume), orange in color. Sharp contact at top and base.
	DGSL:	"Dark gray silt loam". Clay, silt and fine sand (roughly 18% clay, silt, 17% fine sand by volume), gray to black in color.

Figure A-2: Lithological Legend for Fence Diagrams



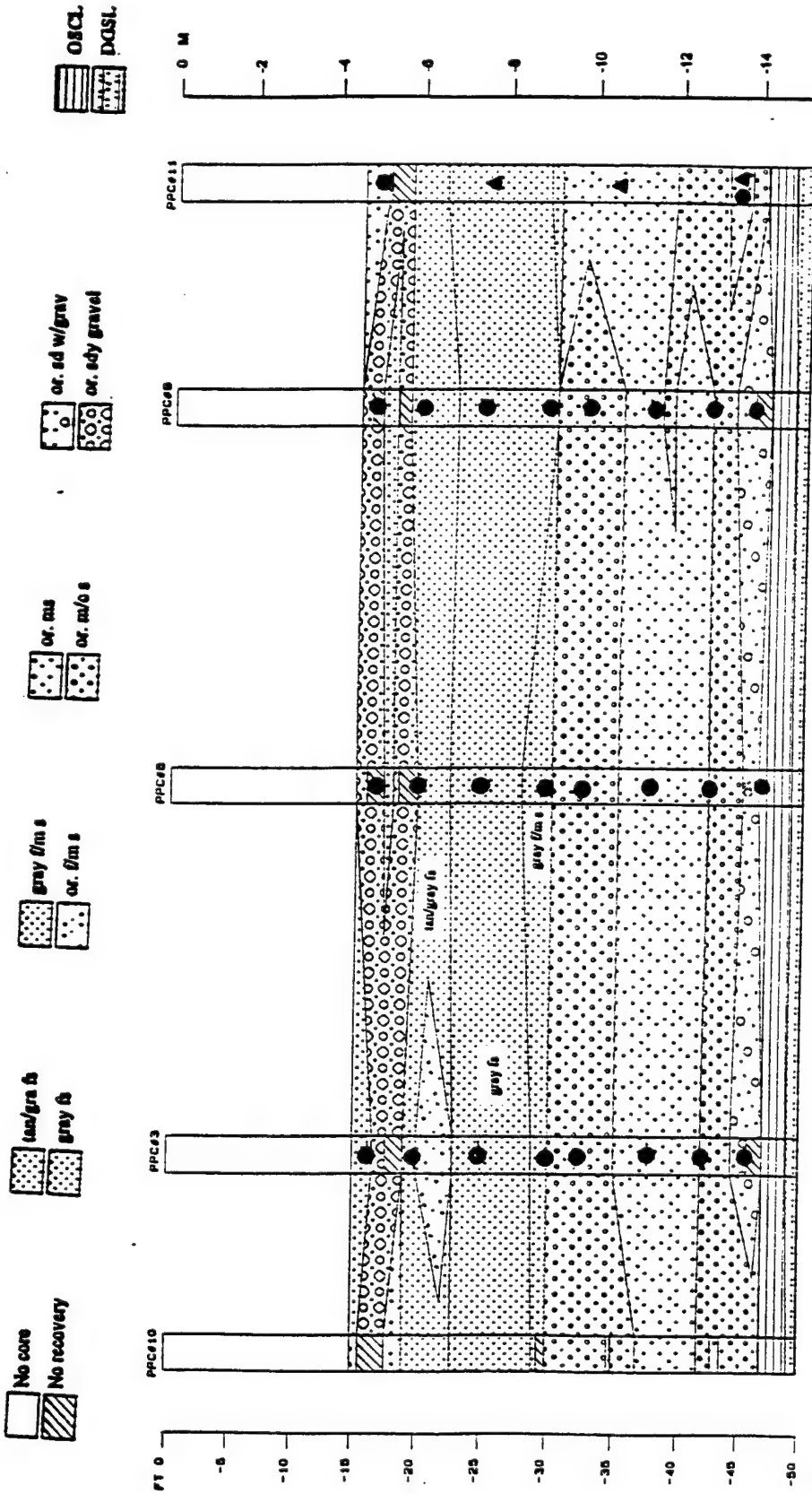
- Sampling Point
- ▲ Tracer Distribution Point

Figure A-3: Geological Cross-Section (CPC-1 -- CPC-1')
(Vertical Scale Compression = 0.30085)



● Sampling Point
▲ Tracer Distribution Point

Figure A-5: Geological Cross-Section (PPC-1 -- PPC-1')
(Vertical Scale Compression = 0.30085)



● Sampling Point
▲ Tracer Distribution Point

Figure A-6: Geological Cross-Section (PPC-2 -- PPC-2')
(Vertical Scale Compression = 0.30085)

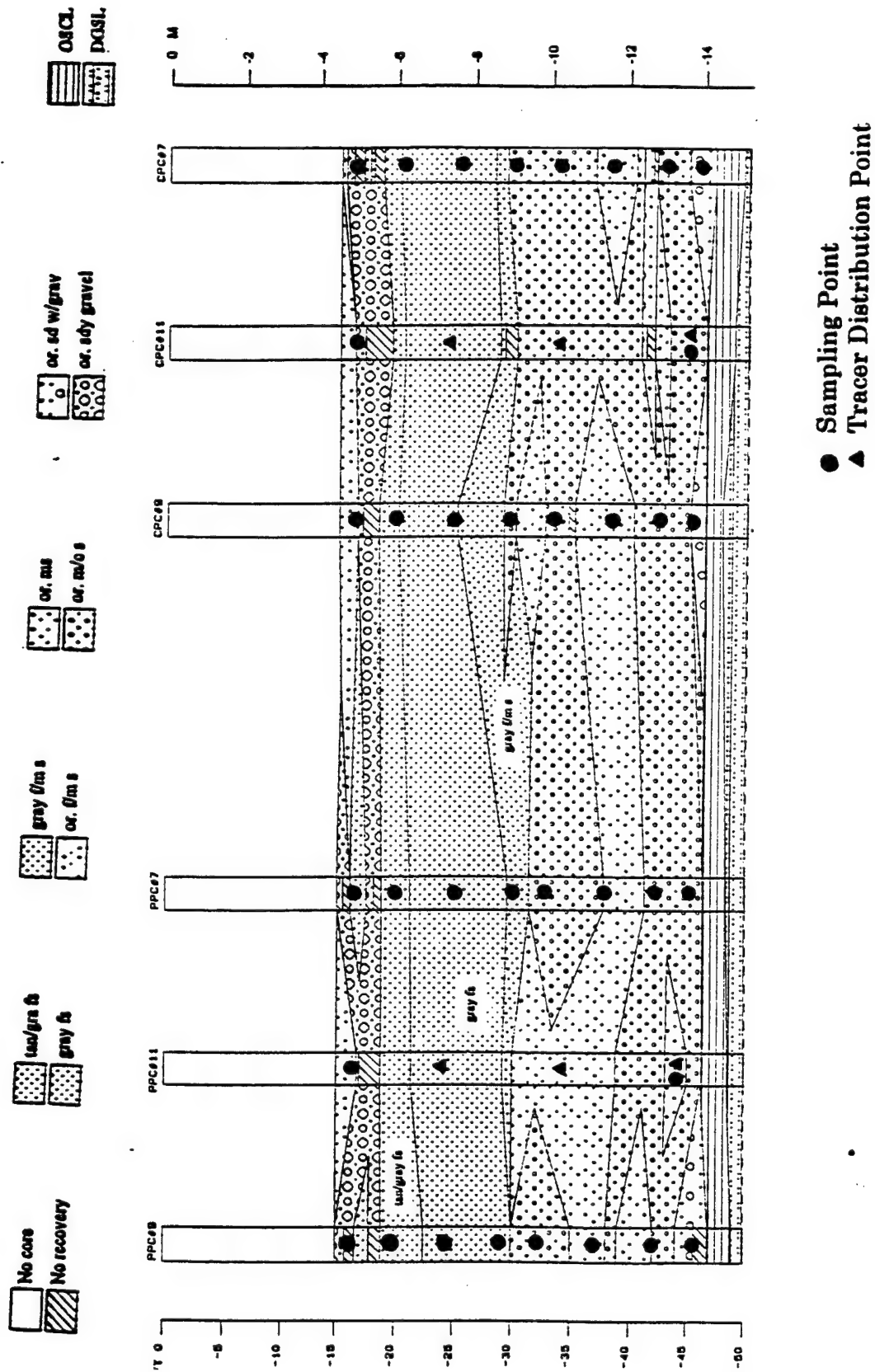
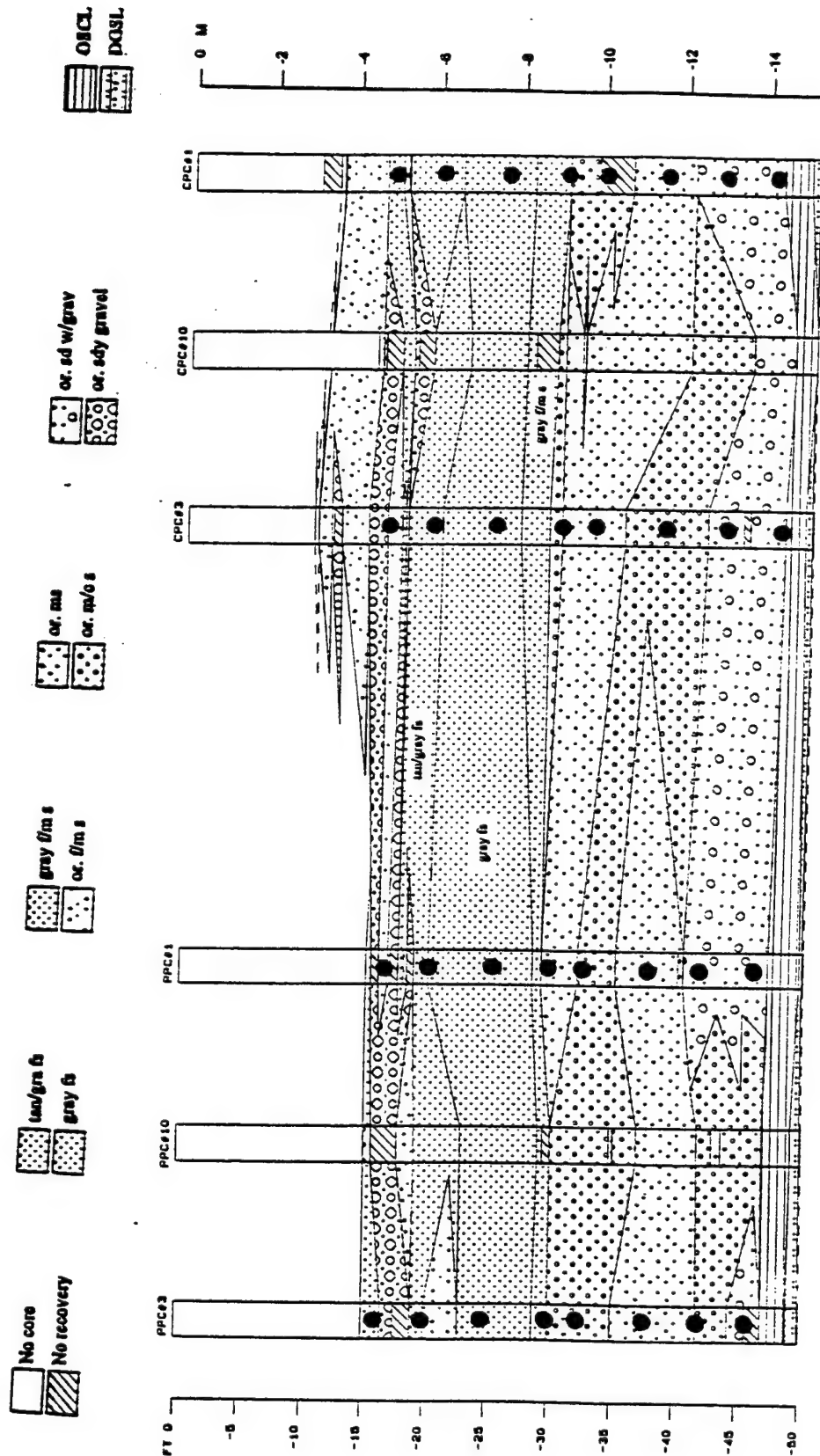


Figure A-7: Geological Cross-Section (Transverse-1' -- Transverse-1'
(Vertical Scale Compression = 0.30085)



- Sampling Point
- ▲ Tracer Distribution Point

Figure A-8: Geological Cross-Section (Transverse-2 -- Transverse-2'
(Vertical Scale Compression = 0.30085)

Appendix B. PREPUMPING INORGANIC WATER QUALITY DATA

The following pages contain plots of various inorganic parameters versus depth for the continuously pumped cell (CPC), in the various frames of **Figure B-1**, and for the pulse-pumped cell (PPC), in the various frames of **Figure B-2**. Methodological details and related discussion may be found in Chapter 4 (section 4.2).

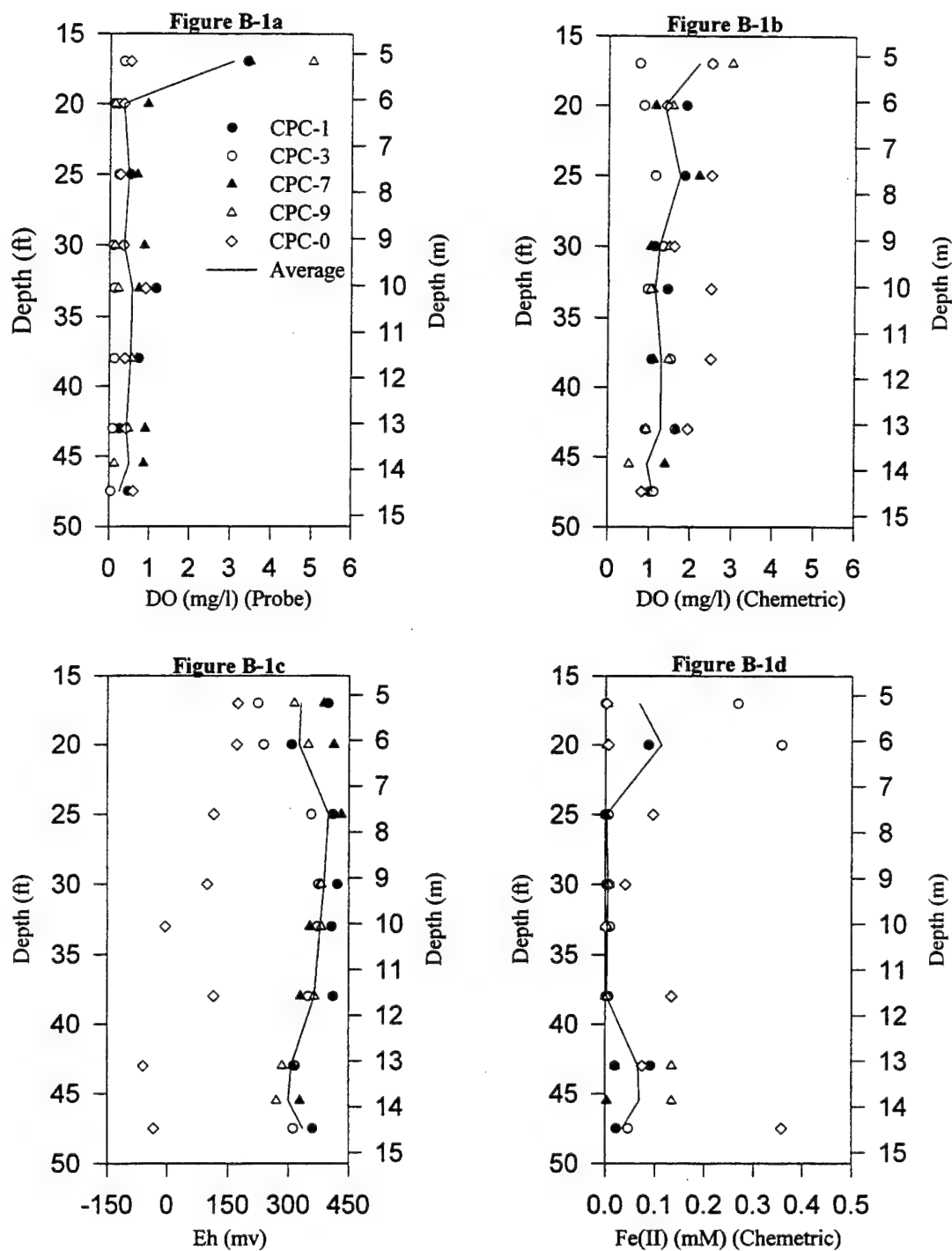


Figure B-1. Prepumping Depth Profiles for the Continuously Pumped Cell for (a) Dissolved Oxygen (DO) by probe, (b) DO by Chemetrics test, (c) Eh, and (d) Fe(II).

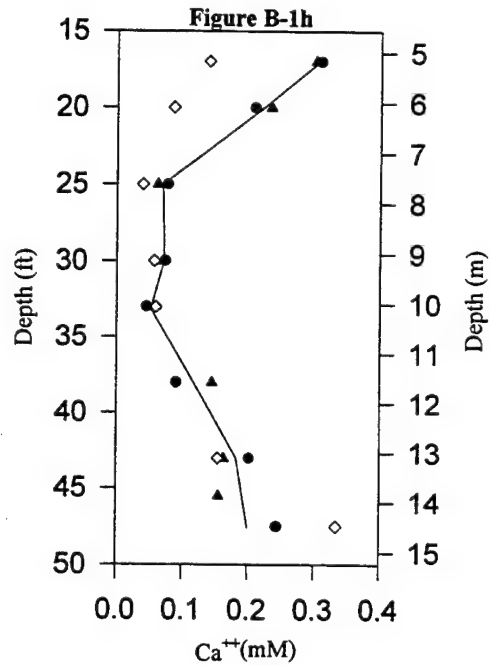
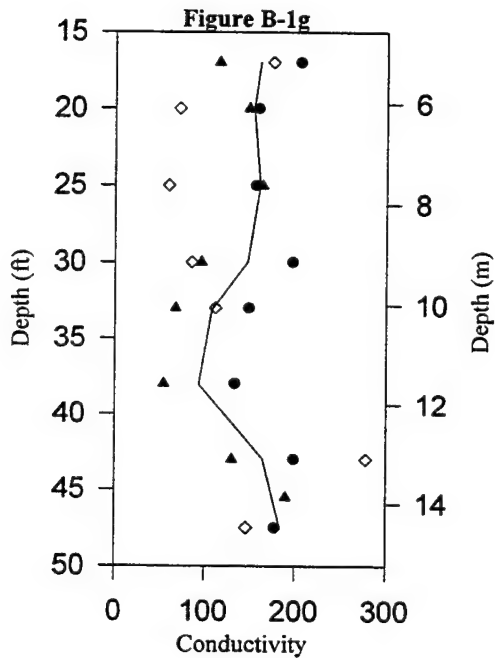
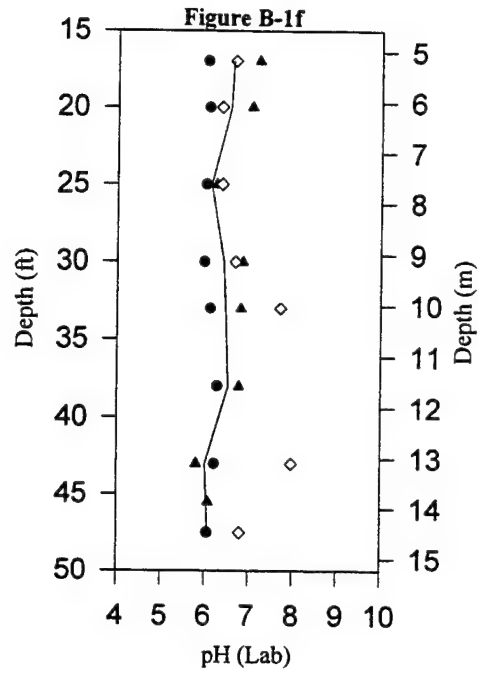
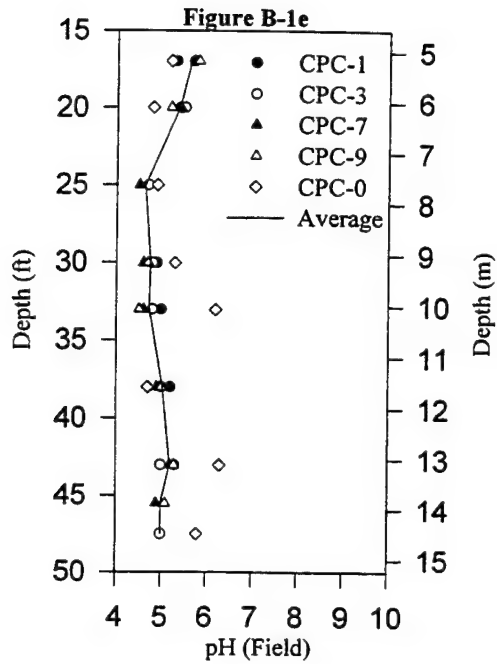


Figure B-1 (continued). Prepumping Depth Profiles for the Continuously Pumped Cell for (e) pH (field), (f) pH (Lab), (g) Conductivity, and (h) Ca⁺⁺.

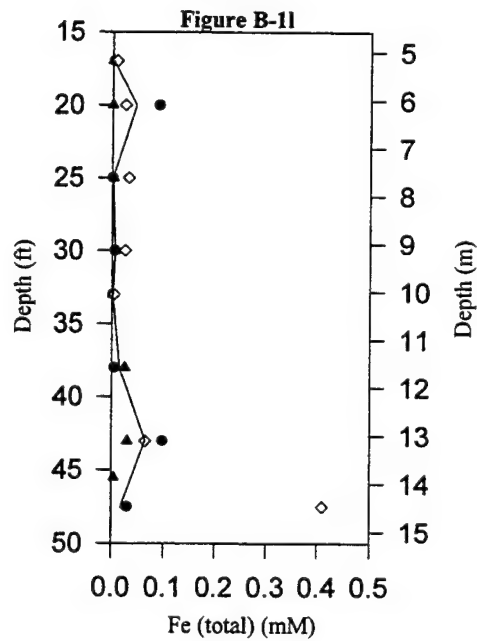
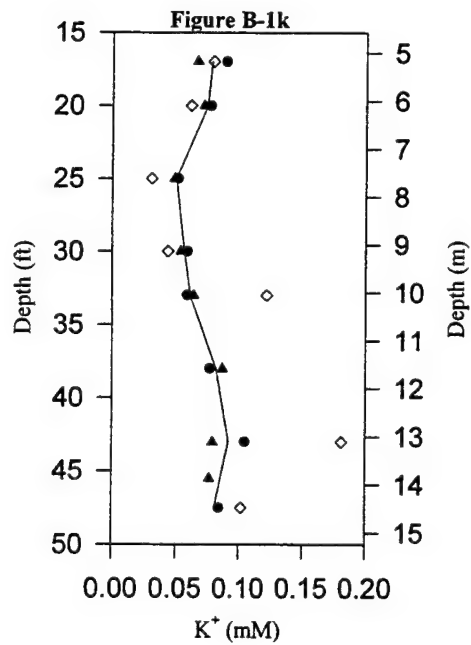
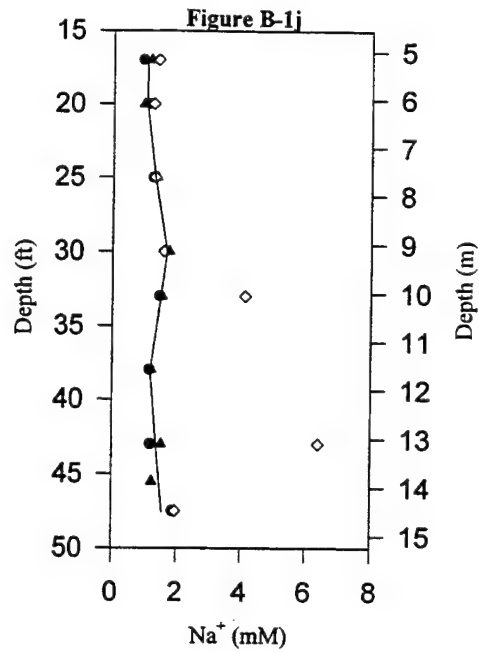
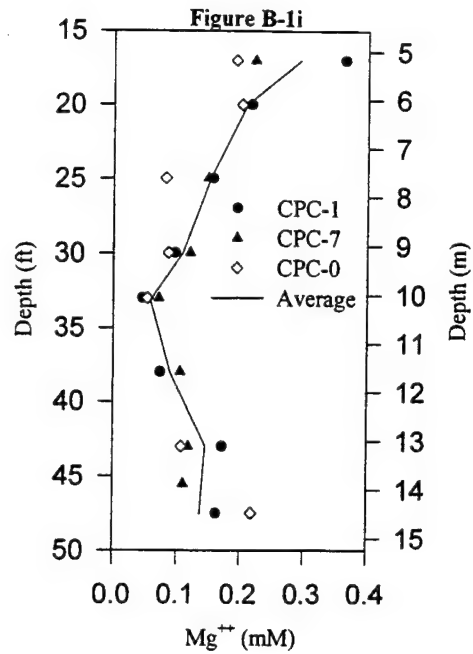


Figure B-1 (continued). Prepumping Depth Profiles for the Continuously Pumped Cell for (i) Mg^{++} , (j) Na^{+} , (k) K^{+} , and (l) Fe (total).

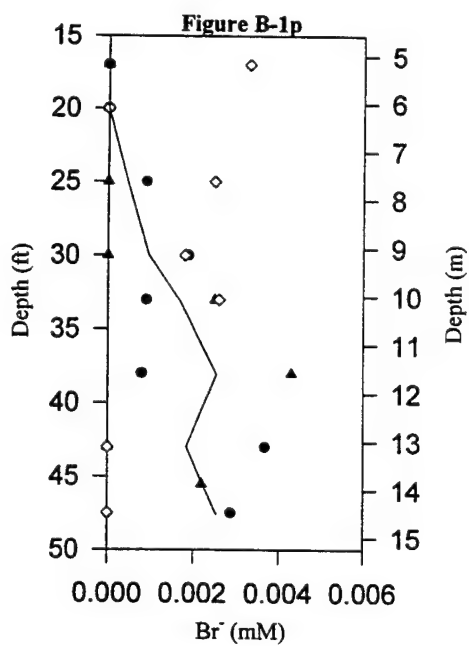
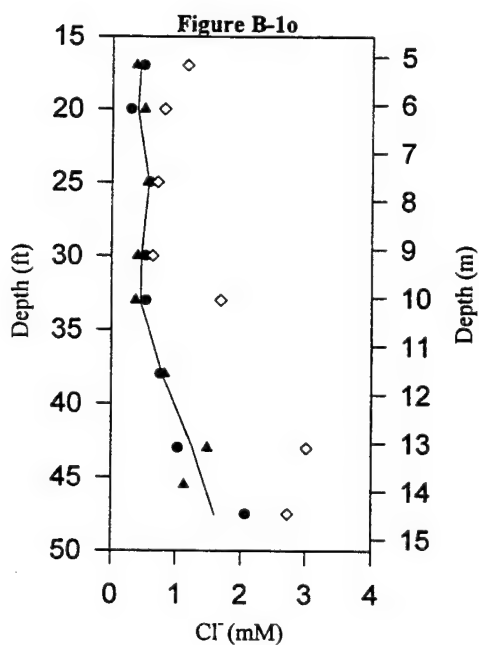
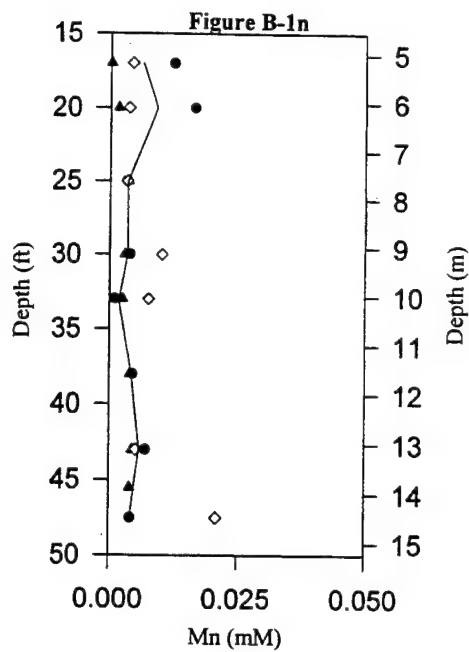
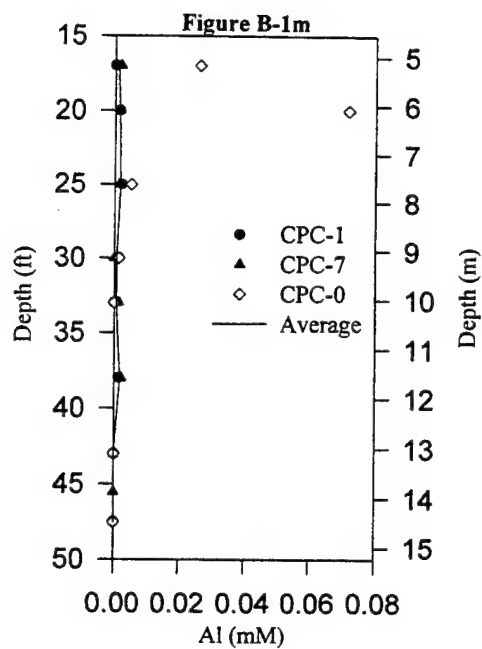


Figure B-1 (continued). Prepumping Depth Profiles for the Continuously Pumped Cell for (m) Al, (n) Mn, (o) Cl⁻, and (p) Br⁻.

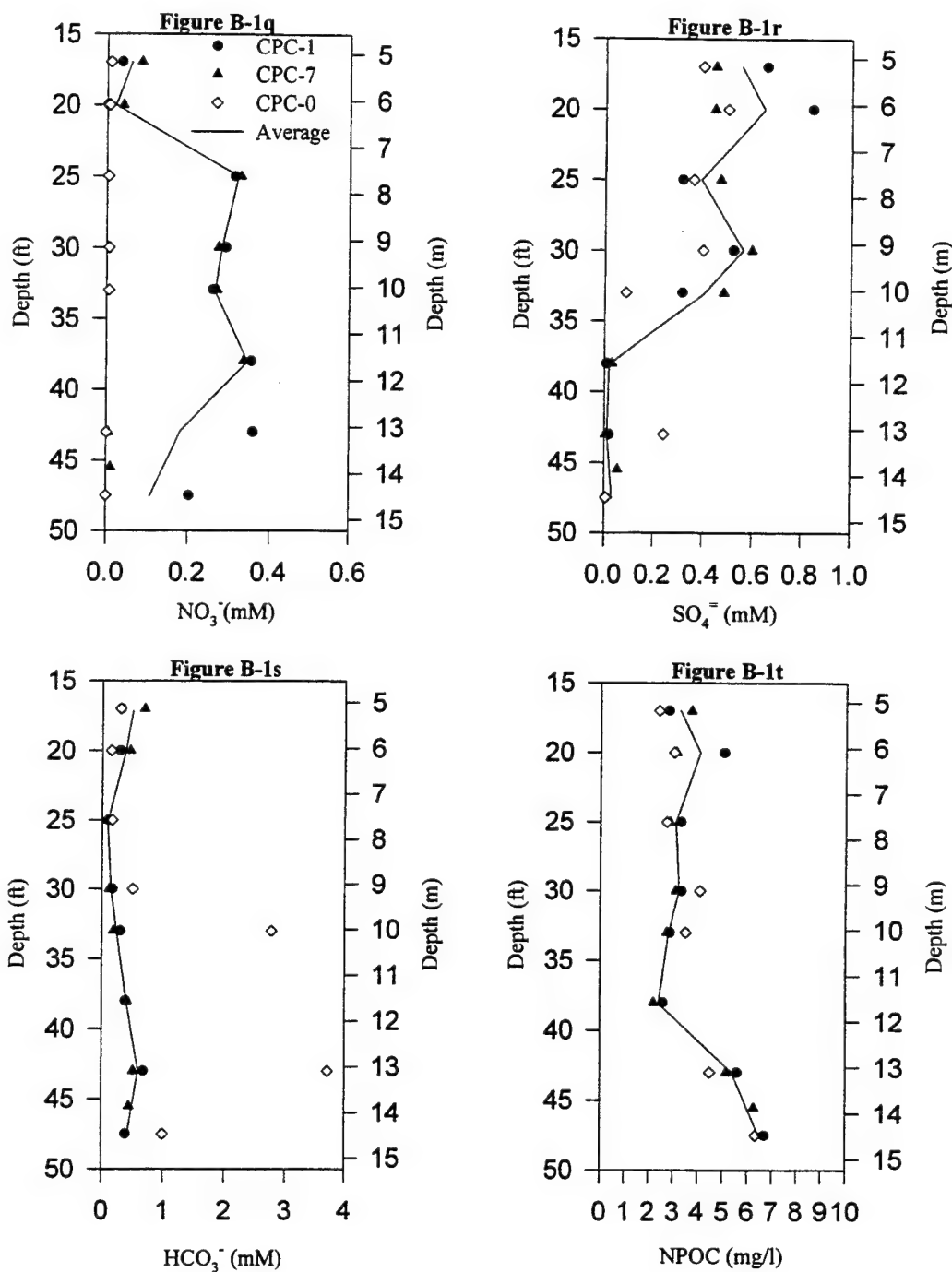


Figure B-1 (continued). Prepumping Depth Profiles for the Continuously Pumped Cell for (q) NO_3^- , (r) SO_4^- , (s) HCO_3^- , (t) NPOC.

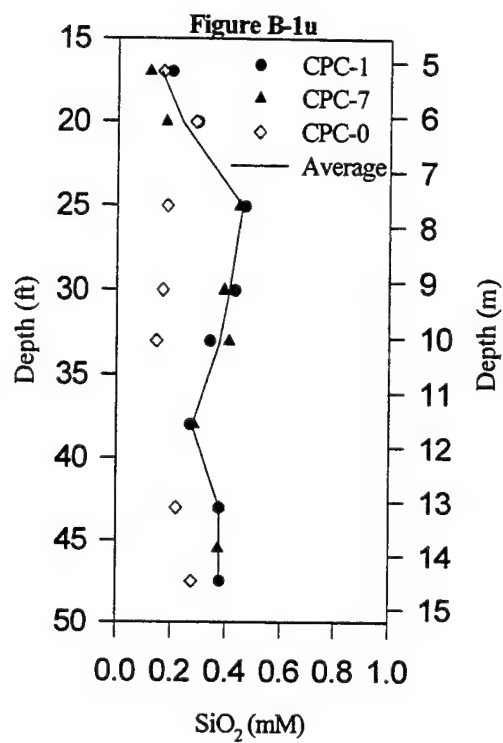


Figure B-1 (continued). Prepumping Depth Profiles for the Continuously Pumped Cell for (u) SiO_2 .

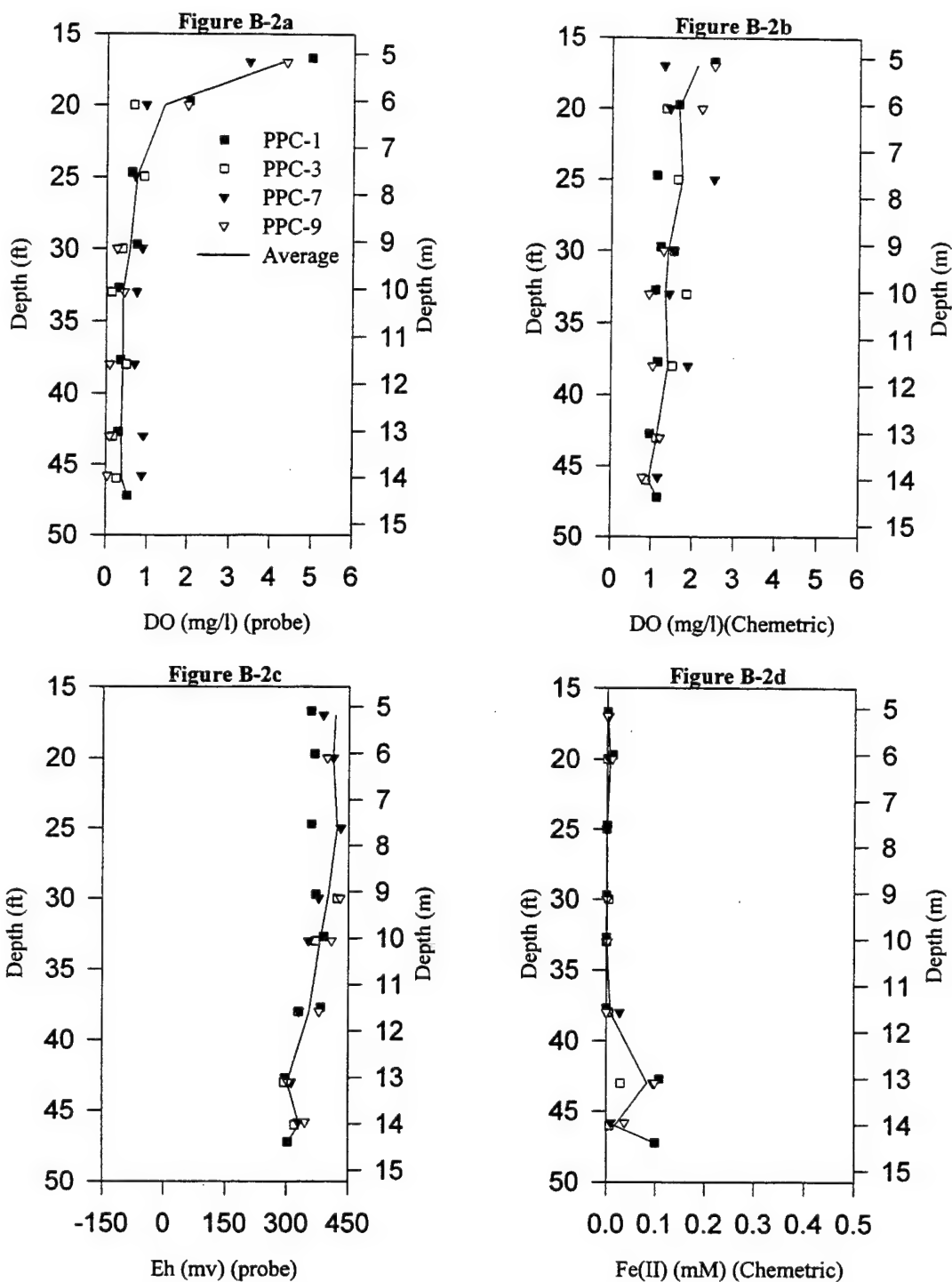


Figure B-2. Prepumping Depth Profiles for the Pulse-Pumped Cell for (a) Dissolved Oxygen (DO) by probe, (b) DO by Chemetrics test, (c) Eh, and (d) Fe(II).

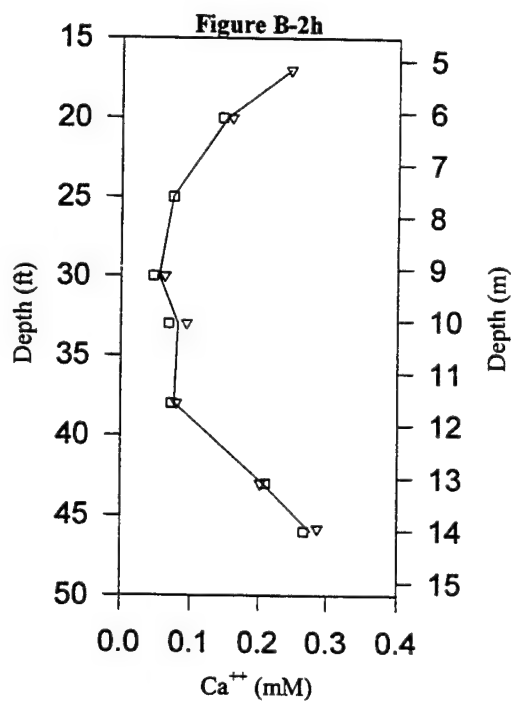
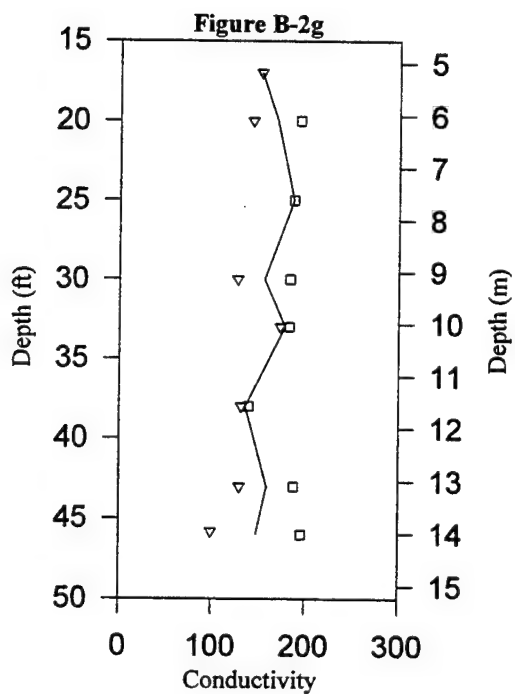
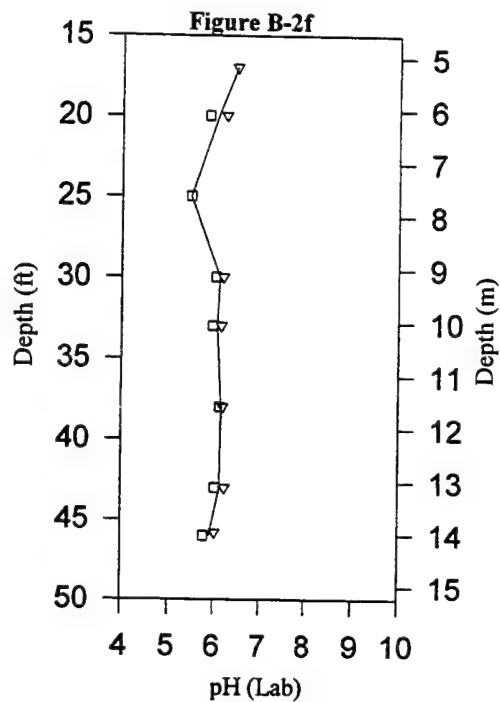
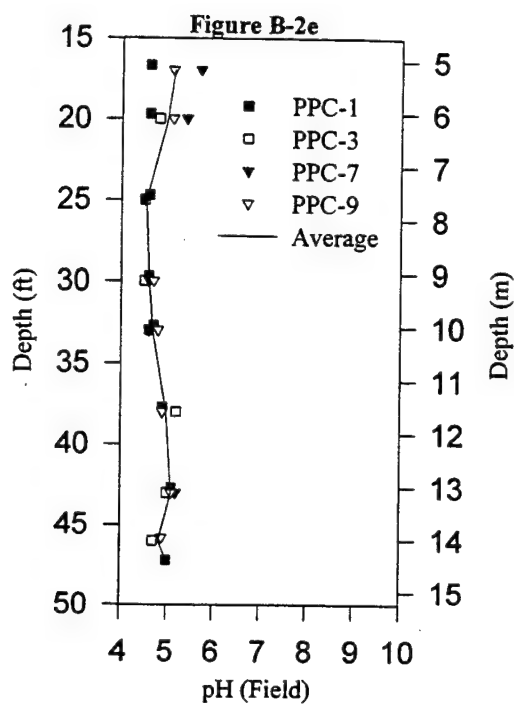


Figure B-2 (continued). Prepumping Depth Profiles for the Pulse-Pumped Cell for (e) pH (field), (f) pH (Lab), (g) Conductivity, and (h) Ca⁺⁺.

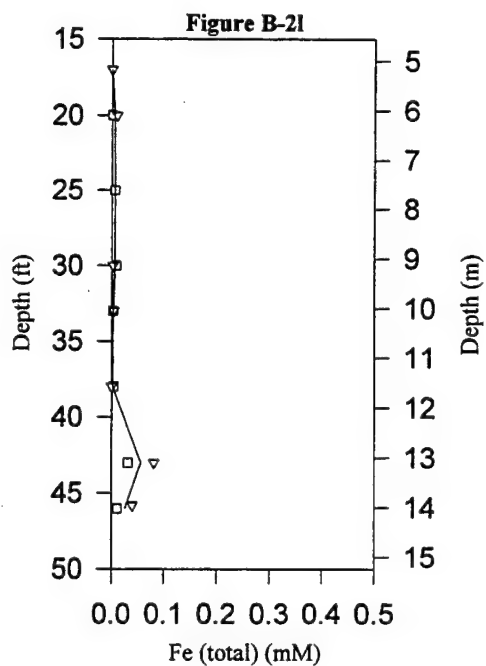
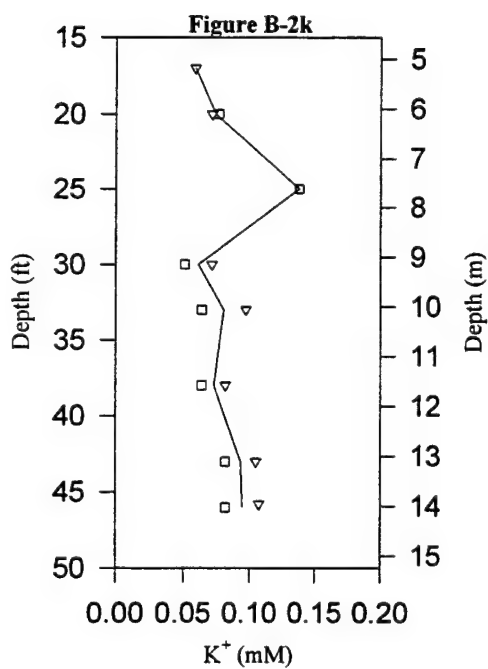
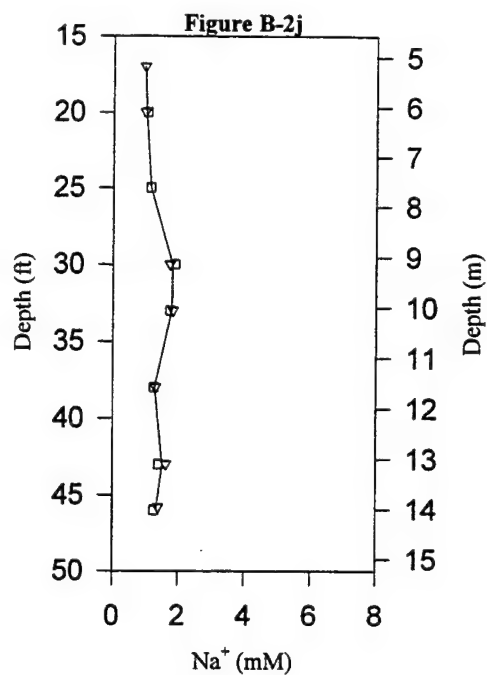
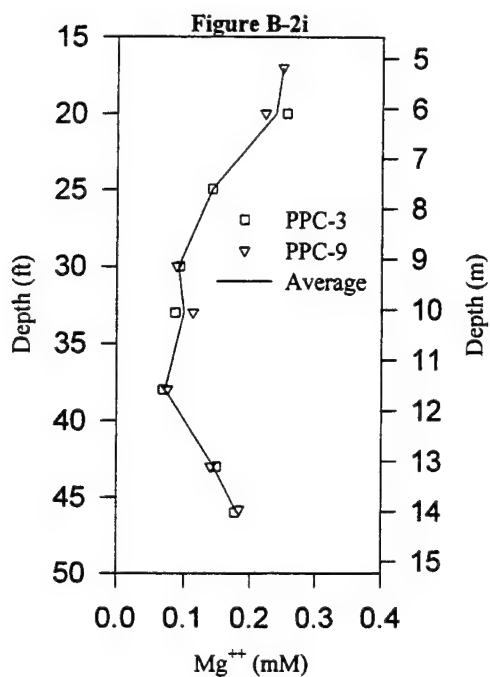


Figure B-2 (continued). Prepumping Depth Profiles for the Pulse-Pumped Cell for (i) Mg^{++} , (j) Na^+ , (k) K^+ , and (l) Fe (total).

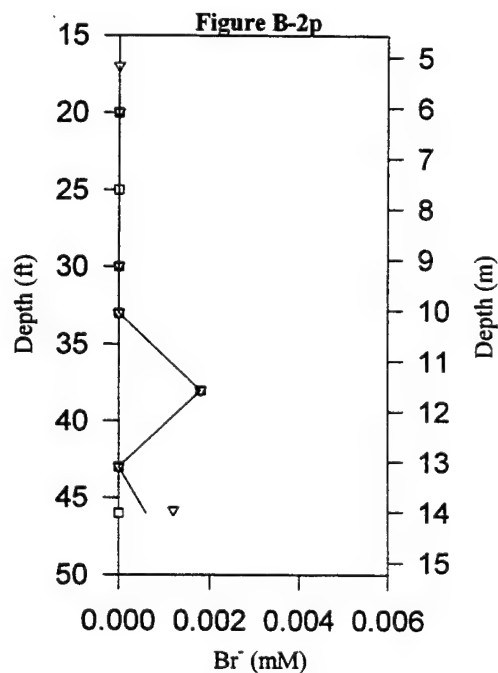
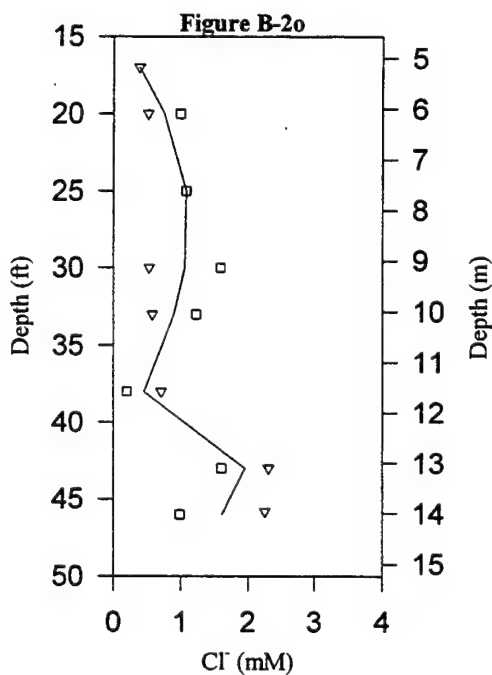
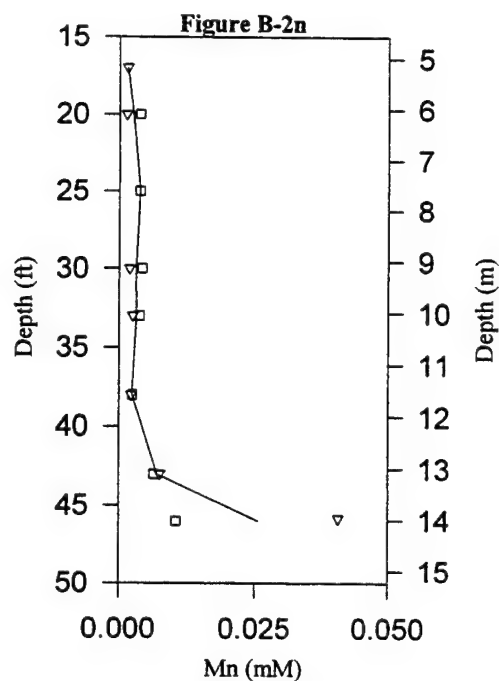
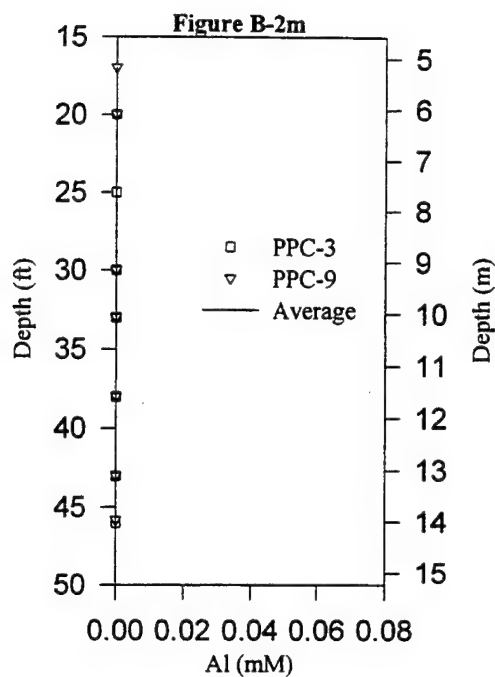


Figure B-2 (continued). Prepumping Depth Profiles for the Pulse-Pumped Cell for (m) Al, (n) Mn, (o) Cl⁻, and (p) Br⁻.

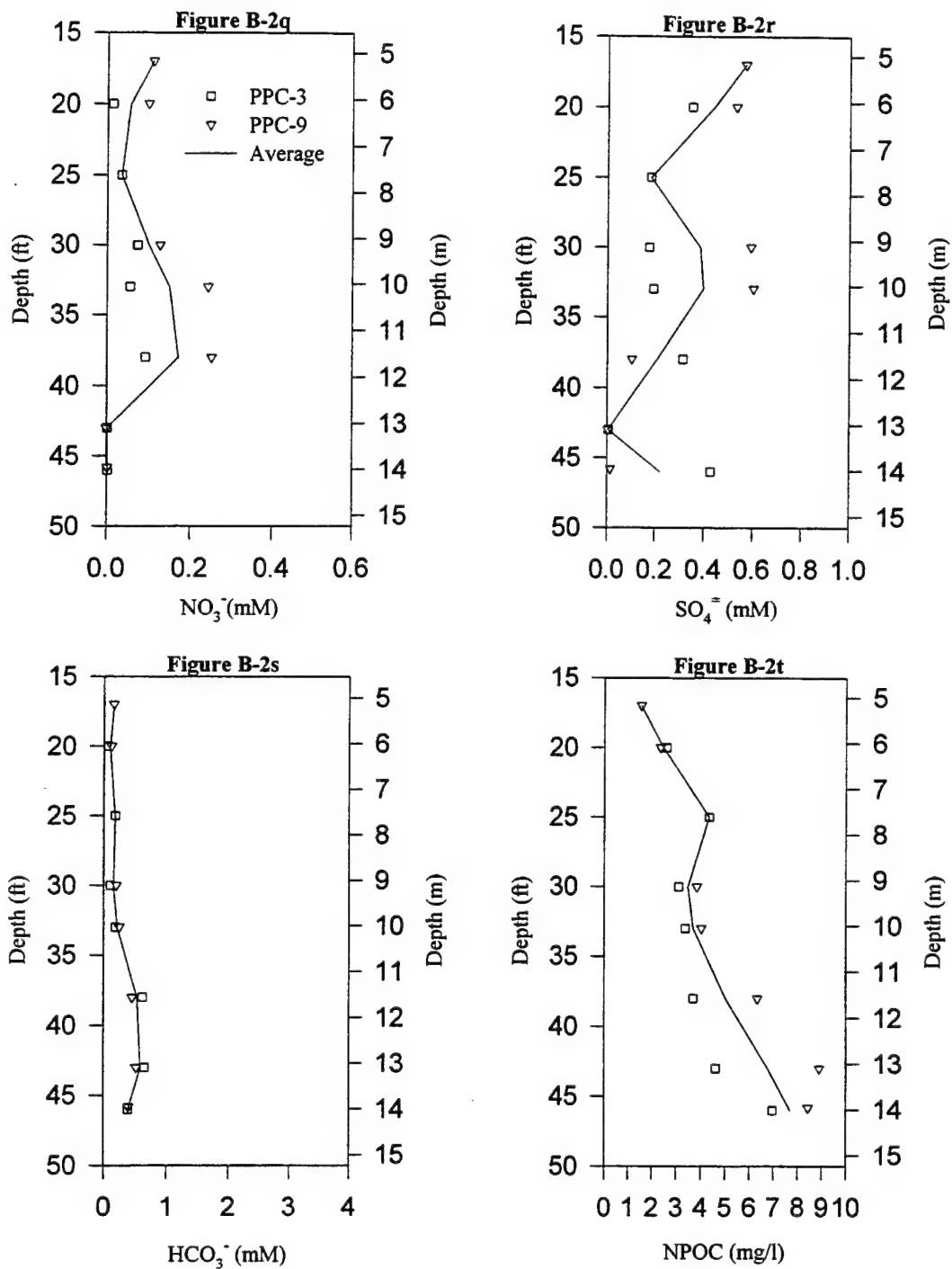


Figure B-2 (continued). Prepumping Depth Profiles for the Pulse-Pumped Cell for (q) NO_3^- , (r) $\text{SO}_4^{=}$, (s) HCO_3^- , (t) NPOC

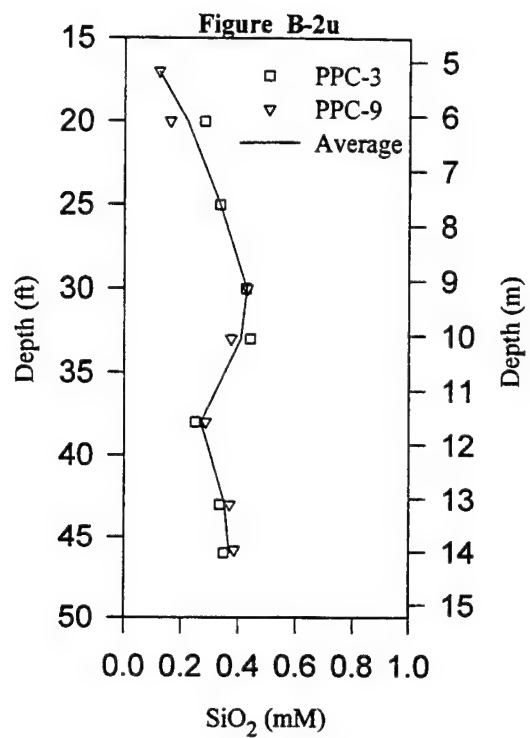


Figure B-2 (continued). Prepumping Depth Profiles for the Pulse-Pumped Cell for (u) SiO_2

Appendix C. POSTPUMPING INORGANIC WATER QUALITY DATA

The following page presents **Figure C-1** illustrating various inorganic parameters for the continuously pumped cell (CPC) and the pulse-pumped cell (PPC). Methodological details and related discussion may be found in Chapter 4 (section 4.2).

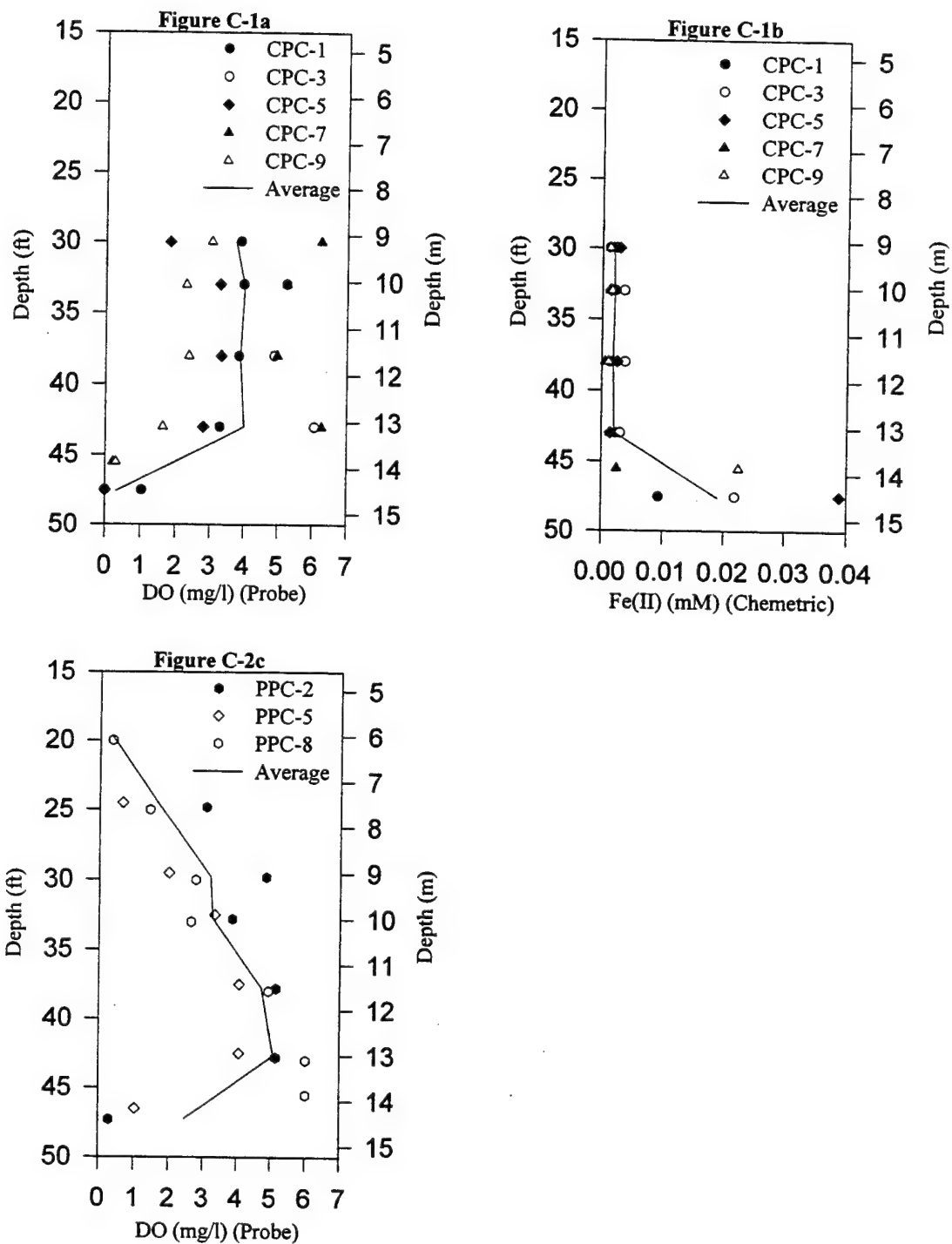


Figure C-1. Postpumping Depth Profiles: (a) Dissolved Oxygen (DO) by probe in the CPC, (b) Fe(II) in the CPC, and (c) DO (by probe) in the PPC.

Appendix D. CATION EXCHANGE CAPACITY

A. OVERVIEW

Cation exchange capacity (CEC) was measured on replicate samples of Dover AFB aquifer and aquitard materials both at Johns Hopkins University and at the University of Maryland Soil Testing Laboratory in College Park, Maryland. Replicate splits of 11 different subsurface samples from the site were analyzed in each laboratory. This resulted in a total of 46 cation exchange analyses. Details of the sample identifications and replicate splits are provided in the tabulated results.

B. METHODS

CEC was measured at JHU using standard SSSA techniques (Thomas, 1982) while ECEC was measured at the University of Maryland Cooperative Extension Service's Soil Testing Laboratory. The University of Maryland methods are given in a four-page description, attached at the end of this appendix. This method description was provided by Mr. Joe F. Buriel of the University of Maryland Soil Testing Laboratory. According to Mr. Buriel (personal communication, 1996), these methods were developed around two previously published techniques (Flannery and Markus, 1980; Mehlich, 1982).

The primary differences in the methods used by the two laboratories are with respect to (1) the type of extraction used for cations (strong acid by the University of Maryland laboratory *versus* ammonium acetate in the JHU laboratory), and (2) the means of measuring and reporting "exchangeable acidity" (extrapolated from pH of the soil by the University of Maryland method *versus* the SSSA standard titration method adopted by the JHU laboratory).

C. RESULTS

Table D-1 gives a summary of the average results obtained on each of the 11 soils. **Table D-2** provides individual sample results for both the JHU laboratory results (referred to as the "cation exchange capacity," or CEC) and the results as measured by the University of Maryland Soil Testing Laboratory (referred to as the "effective cation exchange capacity" or ECEC).

In most cases, the CEC values are higher than ECEC results, typically reflecting the higher concentrations of exchangeable cations extracted by the ammonium acetate used in the SSSA method (Thomas, 1982). This seems to be especially true for the divalent cations in the finer aquitard samples. (Note that these samples represent OSCL and DGSL in accordance with the nomenclature of Chapter 4.) Notable exceptions, where ECEC results were higher, were with (1) calcium measurements in sands (possibly reflecting mineral dissolution by the acid) and (2) acidity in all samples except the black silt loam (DGSL), which was highest in titratable organic acids.

Because the SSSA method is a more "standard" procedure, designed specifically to assess CEC, we believe these results to be most appropriate for general reporting purposes. These data are presented in the right-most column of **Table D-1** and in the second-to-right-most columns of **Table D-2**.

D. REFERENCES

- Flannery, R. L. and D.K. Markus, 1980. "Automated analysis of soil extracts for phosphorus, potassium, calcium, and magnesium. *J. Assoc. Off. Anal. Chem.* 63: 779-787.
- Gee, G.W. and Bauder, J.W., 1986. "Particle-size Analysis". In: A. Klute (Editor), *Methods of Soil Analysis. Part 1. Physical and Mineralogical Methods-Agronomy Monograph no. 9.* American Society of Agronomy, Inc., and Soil Science Society of America, Inc., Madison, WI, pp. 383-411.
- Mehlich, A., 1982. New buffer pH method for rapid estimation of exchangeable acidity and lime requirement of soils. *Comm. Soil Sci. Plant Anal.* 7:637-652.
- Thomas, G.W., 1982. "Cation Exchange Capacity". In: A.L. Page, R.H. Miller and D.R. Keeney (Editors), *Methods of Soil Analysis. Part 2. Chemical and Microbiological Properties.* American Society of Agronomy, Inc., and Soil Science Society of America, Inc., Madison, WI, pp. 159-165.

TABLE D-1. CEC RESULTS FOR SUBSURFACE SAMPLES FROM DOVER AFB, DE

Sample ID	Depth (ft)	Color	Textural ^a Class	Lab ^b	Exchangeable Cations (meq/100g)					"Exchangeable Acidity" ^c			
					Ca ²⁺	Mg ²⁺	K ⁺	Na ⁺	H ⁺	Al ³⁺	estimated from pH	ECEC ^d (meq/100g)	CEC ^e (meq/100g)
xxx-x-3	20-25	gray	sand	JHU UMd	0.27 0.36	0.83 0.46	0.05 0.05	0.05 0.05	0.13	0.26	1.00	1.86	1.46
xxx-x-4	25-30	gray	sand	JHU UMd	0.32 0.43	0.81 0.46	0.05 0.05	0.05 0.05	0.14	0.19	0.79	1.72	1.43
xxx-x-5	30-35	orange	sand	JHU UMd	0.38 0.47	0.44 0.34	0.04 0.05	0.05 0.05	0.05	0.09	0.68	1.54	1.00
xxx-x-6	35-40	orange	sand	JHU UMd	0.34 0.53	0.34 0.39	0.05 0.07	0.04 0.05	0.08	0.08	0.38	1.37	0.85
xxx-x-7	40-45	orange	sand	JHU UMd	0.41 0.52	0.35 0.36	0.05 0.06	0.05 0.05	0.06	0.04	0.38	1.32	0.91
xxx-x-8	45-XX	orange	sand	JHU UMd	0.23 0.42	0.23 0.39	0.04 0.05	0.05 0.05	0.03	0.09	0.38	1.24	0.65
ppc-3-8	47-49	orange	silty clay loam	JHU UMd	3.27 7.65	1.25 7.06	0.34 0.60		0.28	0.73	2.99	7.84	16.04
cpc-9-8	46-48	orange	silty clay loam	JHU UMd	8.07 3.35	6.02 1.21	0.52 0.33		0.24	0.27	1.94	6.83	14.88
ppc-3-8	49-50	black	silt loam	JHU UMd	7.65 1.66	4.37 1.33	0.20 0.11	0.06	23.08	10.91	15.46	18.56	23.19
cpc-11-8	48-50	black	silt loam	JHU UMd	12.93 3.34	7.34 1.50	0.27 0.10	0.09	26.92	13.87	17.08	22.02	34.50

a) Based on hydrometer-sedimentation test of replicate or similar sample (Gee, G.W. and J. W. Bauder, 1986, in Methods of Soil Analysis, Part I, American Society of Agronomy-Soil Science Society of America, Madison, WI; pp. 399-404). (Split replicates were available only for the bulk (xxx-x-) sand samples).
b) JHU = Johns Hopkins Univ., Dept. of Geography and Environmental Engineering; University of Maryland, Dept. of Agronomy, Soil Testing Laboratory
c) "Exchangeable Acidity" was calculated as follows by the two laboratories:
JHU: proton component of a proton and aluminum titration (Thomas, 1982)
University of Maryland: Acidity = $4 \times (6.6 - \beta\text{pH})$ where βpH is soil pH, as measured under standard conditions.
d) "Effective Cation Exchange Capacity" (ECEC) is as calculated by the ; defined as the summation of Ca²⁺, Mg²⁺, K⁺, and acidity.
e) "Cation Exchange Capacity" (CEC) is as defined by SSSA [Thomas, G. W., 1982; Ibid]; defined as the summation of Ca²⁺, Mg²⁺, K⁺, Na⁺, and Al³⁺.

TABLE D-2. SUMMARY OF INDIVIDUAL CEC RESULTS FOR SUBSURFACE SAMPLES FROM DOVER AFB, DE

A. Individual Sample Results:

Sample	Soil Type	pH (Univ. of MD)	Exchangeable Acidity (Univ. of MD)	Exchangeable Protons (JHU)	Exchangeable Al (JHU)	CEC (JHU)	ECEC (Univ. of MD)
xxx-x-3	grey sand	6.34, 6.36	1.04, 0.96	0.126, 0.129	0.189, 0.324	1.44, 1.48	1.91, 1.8
xxx-x-4	grey sand	6.41, 6.41, 6.39	0.76, 0.76, 0.84	0.141, 0.138, 0.139	0.212, 0.207, 0.167	1.36, 1.54, 1.38	1.68, 1.78, 1.70
xxx-x-5	orange sand	6.41, 6.43, 6.45	0.76, 0.68, 0.60	0.086, 0.00, 0.068	0.086, 0.112, 0.068	1.07, 1.05, 0.89	1.55, 1.68, 1.39
xxx-x-6	orange sand	6.50, 6.51	0.40, 0.36	0.103, 0.056	0.103, 0.056	0.95, 0.75,	1.43, 1.32,
xxx-x-7	orange sand	6.50, 6.51,	0.40, 0.36,	0.056, 0.063		0.99, 0.91, 0.82	1.29, 1.35, 1.41
xxx-x-8	orange sand	6.51, 6.50	0.36, 0.40	0.000, 0.059	0.133, 0.059	0.64, 0.66	1.22, 1.26
ppc-3-8	OSCL	5.79, 5.86, 5.94, 5.82	3.24, 2.96, 2.64, 3.12				8.48, 7.85, 7.25, 7.77
cpc-11-8	OSCL	6.15, 6.08	1.80, 2.08	0.269, 0.207	0.202, 0.276	14.48, 15.86	6.07, 7.59
cpc-9-8	OSCL			0.260, 0.715	0.301, 0.752	16.28, 15.80	
cpc-11-8	OSCL			0.264, 0.209	0.264, 0.348	13.77, 15.42	
ppc-3-8	BSL	2.72, 2.75	15.52, 15.40	24.29, 21.87	11.39, 10.43	24.39, 22.00	18.38, 18.74
cpc-11-8	BSL	2.34, 2.32	17.04, 17.12	25.77, 28.08	14.49, 13.26	35.25, 33.76	22.60, 21.43

B. Summary Results:

Soil Type	No. of Samples	CEC / JHU	ECEC / Univ. of MD
Grey sand	10	1.44+/-0.074 (n=5)	1.77+/-0.092 (n=5)
Orange sand	20	0.873+/-0.153 (n=10)	1.39+/-0.139 (n=10)
ppc-3-8 (OSCL)	4	not analyzed	7.502+/-0.809 (n=4)
cpc-11-8(OSCL)	6	14.88+/-0.939 (n=4)	6.83 (n=2)
cpc-9-8 (OSCL)	2	16.04 (n=2)	
ppc-3-8 (BSL)	4	23.20 (n=2)	18.56 (n=2)
cpc-11-8(BSL)	4	34.51 (n=2)	22.02 (n=2)

SOIL TESTING METHODS
UNIVERSITY OF MARYLAND SOIL TESTING LABORATORY

PHOSPHORUS, POTASSIUM, CALCIUM AND MAGNESIUM TESTS

Preparation of Reagents

Extracting Solution.

0.05 N HCl and 0.025 N H₂SO₄ mixture. Measure about 9 liters of distilled water into an 18 liter bottle. Add 12 ml of concentrated (36 N) H₂SO₄, 73 ml of concentrated (12 N) HCl, and 180 g of carbon black (Darco G-60). Dilute to 18 liters with distilled water and mix.

Phosphorus Reagents.

Reagent 1. Molybdate-Vanadate. Dissolve 50 g of reagent grade ammonium molybdate in distilled water and dilute to 1 liter. Dissolve 2.50 g of reagent grade ammonium vanadate in 500-600 ml of boiling distilled water. Let cool for 1 hour. Add 5 ml of concentrated NH₄OH. Let stand overnight. The solution should turn clear. Transfer to a 1 liter volumetric flask and add 300 ml of concentrated (15.7 N) HNO₃. Let cool and dilute to volume with distilled water. This solution should be pale yellow. Combine 500 ml of ammonium molybdate and 500 ml of ammonium vanadate for use. Keep in an amber reagent bottle.

Reagent 2. Diluent. Distilled water. If a detergent is needed to improve manifold bubble pattern, 0.5 ml of "Lever IV" (available from Bran Luebbe, Elmsford, New York) may be added to each liter of water.

Potassium and Calcium Reagents.

Reagent 1. 40% Brij 35. Add 100 g Brij 35 (polyoxyethylene (23) lauryl ether) to 250 ml distilled water. Heat to near boiling to kill any microorganisms. Store in dark to prevent microbial activity.

Reagent 2. (AutoAnalyzer II) 100 meq/liter lithium nitrate. Dissolve 3.45 g of reagent grade lithium nitrate in distilled water and dilute to 500 ml. Dilute 10 ml of this stock solution and 1 ml of 40% Brij 35 to 1 liter with distilled water to prepare the internal standard.

Reagent 3. (AutoAnalyzer I) 1000 meq/liter lithium nitrate. Dissolve 68.95 g of reagent grade lithium nitrate in distilled water and dilute to 1 liter. Dilute 7.5 ml of this stock solution and 1 ml of 40% Brij 35 to 1 liter with distilled water to prepare the internal standard.

Magnesium Reagents.

Reagent 1. 2 N Sodium Hydroxide (NaOH). Dissolve 320 g of reagent grade NaOH in distilled water. Allow to cool, then dilute to 2 liters. This gives a 4 N solution. For use, dilute 500 ml of stock solution with 500 ml of distilled water.

Reagent 2. 0.02% Magnesium Blue. Dissolve 0.20 g of Magnesium Blue (available from the Galaxy Chemical Company, Closter, New Jersey) in 200 ml of N, N-dimethyl formamide (H₂CO-N(CH₃)₂). Let stand 1 or 2 days. Dilute to 1 liter with distilled water. Let cool before bringing up to final volume. Filter through a Whatman No. 2 filter paper to remove residue. For use, dilute 250 ml of this stock solution and 150 ml of N, N-dimethyl formamide to 1000 ml with distilled water.

Reagent 3. 0.2% Polyvinyl Alcohol (PVA). Dissolve 4.00 g of PVA in approximately 1000 ml of boiling distilled water. Let cool, then transfer to a 2 liter volumetric flask and dilute to volume with distilled water.

Reagent 4. 5000 ppm calcium. Dissolve 12.4863 g of reagent grade CaCO_3 in 100-150 ml distilled water containing about 10-15 ml of concentrated HCl . Let stand 1-2 hours and add about 5 ml of HCl . Repeat if needed and let stand overnight to dissolve the CaCO_3 , then dilute to 1 liter.

Reagent 5. 100 ppm calcium. Dilute 10 ml of reagent 4 to 500 ml with distilled water.

Reagent 6. (AutoAnalyzer II) Diluent. Combine 500 ml of stock PVA, 5 ml of Reagent 5, 1 ml of 40% Brij 35 and dilute to 1 liter with distilled water.

Reagent 7. (AutoAnalyzer I) PVA. Dilute 1 liter of Reagent 3 and 2-3 ml of 40% Brij 35 to 2 liters with distilled water.

Reagent 8. (AutoAnalyzer I) Diluent. Dilute 5 ml of Reagent 4 and 2-3 ml of Brij 35 to 2 liters with distilled water.

PHOSPHORUS, POTASSIUM, CALCIUM, MAGNESIUM, AND SODIUM STANDARD

Concentrated Standard Solution.

147.2 ppm P, 168.5 ppm K, 1348 ppm Ca, 134.8 ppm Mg and 67.3 ppm Na. Using the highest purity reagents, carefully weigh out 0.2078 g dibasic sodium phosphate (Na_2HPO_4), 0.4475 g monobasic potassium phosphate (KH_2PO_4), 0.0761 g potassium chloride (KCl), 3.3663 g calcium carbonate (CaCO_3), and 0.1348 g magnesium metal (Mg) ground to pass a 20 mesh sieve. Very carefully add the above quantities of primary standards to about 300 ml of extracting solution (filtered through Whatman No. 1 filter paper). Slowly add 30 ml of concentrated (12 N) hydrochloric acid (HCl) and let stand loosely stoppered at least 12 hours to dissolve. Dilute to 1 liter with filtered extracting solution.

Standard Curve.

Dilute the standard solution with filtered extracting solution according to Table 1, and add 1 ml of formaldehyde as a preservative before diluting each standard to 1 liter.

Table 1. Concentrations of P, K, Ca, Mg, and Na Standard Solutions.

Standard Number	Volume of Primary Standard ml	Conc. in Solution				
		P	K	Ca	Mg	Na
		-----ppm-----				
1	10	1.47	1.68	13.5	1.35	0.67
2	25	3.68	4.21	33.7	3.37	1.68
3	50	7.36	8.42	67.4	6.74	3.36
4	100	14.70	16.80	135.0	13.50	6.73
5	150	22.10	25.20	202.0	20.20	10.10
6	250	36.80	42.10	337.0	33.70	16.80

1/ To convert from ppm in solution to pounds per acre (20 cm plow layer) multiply ppm P X 20.38 = lbs P_2O_5 , ppm K X 10.68 = lbs K_2O , ppm Ca, Mg, or Na X 8.9 = lbs Ca, Mg, or Na.

SOIL TESTING PROCEDURES

Sample Preparation

1. Unpackage soil samples, checking each against accompanying information sheets.
2. Place moist or wet samples in low temperature driers and process paperwork through cash register.

3. Enter data on information sheets into data entry computer, generate sample labels and place on dry soil samples. Grind samples through 10 mesh (2mm) sieve.
4. Arrange into groups of 48 samples per tray.

Sample Extraction

1. Transfer one level scoop of soil (5.0 cm³) to a 60 ml extraction bottle.
2. Add 25 ml of extracting solution and shake on a rotary shaker for 5 minutes at 200 rpm.
3. Filter through Whatman No. 1 filter paper and pour into a test tube for analysis.

AUTO ANALYZER ROUTINE

1. Attach platen to top of pump to start.
2. Check reagent levels for Magnesium, Phosphorous, Potassium and Calcium. Add if necessary.
3. Turn on flame photometer for Potassium and Calcium.
4. Load test tubes into Auto Analyzer sampler in groups of 24 at a time.
5. Turn on computer and data handler. Wait for menu. Type in G.
Type the following sequence:
F10 - (to turn on printer option).
F9 - (to turn on chart option), enter 1234 (for channels), then 30 (for chart speed).
F8 - (to turn on digital display of each channel on screen).
6. When baseline is stable for all channels, adjust to read at 5% of full scale.
7. Manually hold down sampler trip switch to sample high standard (Primer) for 30 sec. Wait for detector response and adjust each channel to 85% output of full scale.
8. When ready to start run, press F7 key and answer questions. Use Julian date as run identifier. Choose proper program depending on number of trays to be run. Type control-C, then control-B to start run. (The automatic sampler (GPC-Sampler IV) is set to cycle once every 50 sec. (30 seconds in the sample and 20 seconds in the rinse).
9. If samples are to be added to end of a run, type Alternate-S for each additional sample before sampling ends.
10. At end of run, wait for message "Chart saved to file B: _____" on printer. Type F2 to quit program. Type A to run Acquire Data program. For message "what file do you want to acquire" type in run identifier (i.e. Julian date). Exit Acquire program.
11. At end of run, rinse all reagent lines in water for about 5 minutes. Rinse NaOH line (Mg-1) in 6N HCl for one minute, then in water for about 5 minutes.
12. Place clean 5-1/4 inch diskette into drive and type:
mpk _____, where blank is run identifier.

13. Label 5-1/4 inch diskette with pre-printed labels, write in run identifier, load onto Supervisor's Computer.
14. Compare MPX print-out from Supervisor computer to chart print-out of run.

Phosphorus

The molybdate-vanadate colorimetric method is used to determine phosphorus. The exact nature of the vanadomolybdophosphoric system is not known. However, the yellow color produced is attributed to substitution of oxyvanadium and oxymolybdenum radicals for the oxygen for the phosphate, forming a stable chromogenic compound. The intensity of the color developed is measured at 420 nm. The activated charcoal (Darco G-60) is added to the extracting solution to adsorb organic fractions and other colored soil materials that may not be removed when the soil extracts are filtered. These colored substances can interfere with the phosphorus and magnesium tests if not removed. The phosphorus manifolds are described in Figure I for the AutoAnalyzer II.

Potassium and Calcium

A flame photometer is used to determine concentrations of potassium and calcium by the intensities of their light emission characteristics when oxidized in a natural gas - compressed air flame on the AutoAnalyzer II. Potassium is determined at 768 nm, calcium at 623 nm, and lithium, used as an internal standard is determined at 671 nm.

Magnesium

The highly colored indicator dye, magnesium blue, forms a blue complex with magnesium in an alkaline solution. The intensity of the color developed is determined at 630 nm. Calcium combines with the above complex to some extent making it necessary to introduce a constant calcium background to mask out this element in the soil extracts. The highly alkaline solution results in the precipitation of certain compounds especially when phosphate concentrations are high. The addition of PVA and Brij 35 aids in keeping these precipitates in suspension. The magnesium manifolds are described in Figure I, for the AutoAnalyzer II.

DETERMINATION OF SOIL pH

1. Transfer one scoop of soil (approximately 20 g) to a 3 oz. waxed paper cup.
2. Add 20 ml of distilled water and let stand for 1 hour.
3. Calibrate the pH meter before use as well as regularly throughout each day by checking buffer solutions of pH 4.00, 6.00, and 8.00.
4. Stir the sample using a glass stirring rod before placing it under the glass electrode assembly.

DETERMINATION OF TEXTURE

A set of soil samples of known texture (determined by mechanical analysis) are needed as reference standards. Include representative samples of loam, clay loam, silt loam, sandy loam, fine sandy loam, loamy sand, and sand.

Procedure

1. Add 5-10 ml of water to the soil in the sample carton.
2. Test the moist soil between the thumb and forefinger to determine graininess, smoothness, and stickiness related to the ratio of sand, silt, and clay respectively.

Appendix E. SORPTION ISOTHERM STUDIES

This appendix contains data tables of sorption isotherm results. With respect to PCE, the data presented include sorption rate experiments on selected samples (**Table E-1**); individual, single-concentration replicate PCE sorption distribution measurements with various strata of the Dover aquifer sands and aquitard materials (**Table E-2**); and a summary table of PCE sorption distribution coefficients observed in studies over a wide range of aqueous concentrations with selected materials from the Dover site (**Table E-3**).

Sorption results with trichloroethene are shown in **Table E-4**, including both single concentration studies with aquifer sands and full-range isotherms with the two aquitard materials. Sorption in aquifer sands was too low to warrant further study with TCE or with other less halogenated solutes.

Finally, **Table E-5** summarizes the complete isotherm results for both PCE and TCE. This table provides additional information with respect to confidence intervals on Freundlich parameters, as obtained through linear regression of the log-transformed data. Also included in this table are results of a full concentration isotherm with 1,2,4-trichlorobenzene, obtained as part of some on-going sorption and diffusion studies with the DGSL material (D.F. Young, personal communication).

TABLE E-1. SUMMARY OF K_D EXPERIMENTS WITH PCE --- RATE EXPERIMENTS

Texture Class	Sample Mat'l used	Depth Range (ft)	No. of Samples	Approx Conc. Range (mg/L)	Time of Equilibration (days)	Observed K_d (ml/g) ^a average (stdev.) [average] ^b	f_{oc} (%) average (stdev.) [n] ^c	K_{oc} (ml/g) ^d average (stdev.)
gray sand	GS-25/30	25 - 30	19	1.2-1.4	1,3,10,30,192	0.056 (0.026) [0.058,0.055,0.057, 0.07,0.045]	0.009 (0.003) [8]	620 (240)
orange sand	OS-30/35	30 - 35	17	1.1-1.5	1,3,10,30,192	0.07 (0.08) [0.04, 0.02, 0.05, 0.08,0.11]	0.012 (0.003) [7]	580 (270)
OSCL	cpc/ppc 5-8	46 - 48	20	0.98-1.1	1,3,10,30,192	0.31 (0.05) [0.37, 0.25, 0.29, 0.31, 0.30]	0.157 (0.002) [4]	200 (9)
DGSL	ppc 5-8	49 - 50	20	0.2-0.3	1,3,10,30,192	21.87 (3.80) [25.16,17.05,21.10 ^e , 23.0 ^e , 23.31 ^e]	1.391 (0.020) [4]	1600 (79)

Average (standard deviation) results are based on all data;

Numbers in brackets are average apparent K_d s observed at different times. (Times as shown in previous column).
Sample size for organic carbon content analysis.

standard deviation is defined as $\frac{\sigma_{K_{oc}}}{K_{oc}} = \sqrt{\frac{\sigma_{K_d}}{K_d} \times \frac{\sigma_{f_{oc}}}{f_{oc}}}$

The average and standard deviation at these three times are 22.4 and 2.1 ml/g, respectively, with a sample size of 10.

TABLE E-2. SUMMARY OF K_D EXPERIMENTS WITH PCE ---SINGLE CONCENTRATION

Texture Class	Sample Mat'l	Depth (ft)	No. of Samples	Approx. Aq. Conc. (mg/L)	Equilibration Time (days)	Observed K _d (ml/g) average (stdev.)	f _{oc} (%) ^a average (stdev.)	K _{oc} (ml/g) ^b average (stdev.)
gray sand	b3-1-5a ^c	14.5	3	0.003	7	0.007 (0.002) ^d	0.018 (0.003)	39 (8.5)
gray sand	b3-1-5a ^c	14.5	3	0.0045	73	0.007 (0.002) ^d	0.018 (0.003)	39 (8.5)
gray sand	b3-3-3a	22.42	3	0.003	7	0.07 (0.02) ^d	0.0086 (0.0005)	814 (104.9)
gray sand	b3-3-3a ^c	22.42	3	0.004	73	0.11 (0.002) ^d	0.0086 (0.0005)	1279.1 (41.6)
gray sand	b3-4-3a	27.42	3	0.003	7	0.028 (0.007) ^d	0.0094 (0.0006)	297.9 (37.6)
gray sand	GS-25/30	25 - 30	8	0.01, 2.5	7	0.03 (0.01) ^d	0.010 (0.002)	300 (77.5)
gray sand	b3-4-3a ^c	27.42	3	0.004	73	0.033 (0.003) ^d	0.0094 (0.0006)	351.1 (26.7)
orange sand	b3-5-3a ^c	31.67	3	0.003	7	0.065 (0.004) ^d	0.0084 (0.0008)	773.8 (59.2)
orange sand	b3-5-3a ^c	31.67	3	0.004	73	0.068 (0.009) ^d	0.0084 (0.0008)	809.5 (90.9)
orange sand	b3-6-3a ^c	37.75	3	0.003	7	0.09 (0.006) ^d	0.0057 (0.0009)	1578.9 (162)
orange sand	b3-6-3a ^c	37.75	3	0.004	73	0.09 (0.007) ^d	0.0057 (0.0009)	1578.9 (175)
orange sand	b3-7-3a	40 - 45	3	0.003	7	0.052 (0.013) ^d	0.007 (0.002)	742.9 (198.5)
orange sand	b3-7-3a ^c	40 - 45	3	0.004	73	0.063 (0.002) ^d	0.007 (0.002)	900 (85.7)
orange sand	OS-30/35	30 - 35	10	0.01, 2.5	7	0.03 (0.015) ^d	0.012 (0.003)	250 (90)
orange sand	OS-35/40	35 - 40	10	0.01, 2.5	7	0.002 (0.01) ^d	0.007 (0.0003)	28 (13)
orange sand	b3-8-1a	46.1	3	0.003	7	0.13 (0.012)	0.008 (0.003)	1625 (302)
orange sand	b3-8-1a	46.1	3	0.004	73	0.13 (0.007)	0.008 (0.003)	1625 (231)
orange sand	b3-8-1b	46.1	3	0.003	7	0.14 (0.007)	0.0066 (0.0016)	2121 (234)
orange sand	b3-8-1b	46.1	3	0.004	73	0.19 (0.004)	0.0066 (0.0016)	2879 (206)
OSCL	b3-8-2a	47.5	3	0.003	7	0.15 (0.013)	0.13 (0.01)	115 (9.4)
OSCL	b3-8-2a	47.5	3	0.004	73	0.17 (0.017)	0.13 (0.01)	130.8 (11.5)
OSCL	b3-8-2b	47.5	3	0.003	7	0.44 (0.039)	0.173 (0.0075)	254.3 (15.8)
OSCL	b3-8-2b	47.5	3	0.004	73	0.48 (0.02)	0.173 (0.0075)	277.5 (11.8)
DGSL	cpc-7-8	49 - 50	10	0.03, 10.0	7	8.08 (1.69)	1.128 (0.046)	716.3 (66.2)
DGSL	ppc-9-8	49 - 50	10	0.03, 12.0	7	9.64 (2.08)	1.60 (0.032)	600 (39)
DGSL	cpc-11-8	48 - 50	10	0.04, 13.0	7	14.66 (2.54)	1.418 (0.056)	1033.9 (85.5)
DGSL	ppc-5-8	49 - 50	4	0.002	7	20.02 (1.65)	1.391 (0.020)	1439.3 (49.5)

All sample size for organic carbon content measurement is 4.

$$\text{standard deviation is defined as } \frac{\sigma_{K_{oc}}}{K_{oc}} = \sqrt{\frac{\sigma_{K_d}}{K_d} \times \frac{\sigma_{f_{oc}}}{f_{oc}}}$$

For these samples, only the "medium sand" sieve fraction (0.25 - 1 mm) was used.

Less than 10% uptake from solution in majority of ampules.

TABLE E-3. SUMMARY OF K_d EXPERIMENTS WITH PCE --- FULL ISOTHERMS

Texture Class	Sample	Depth (ft)	No. of Samples	Aprox. Aqueous Conc. (mg/L)	Equilibration Time (days)	K _d (ml/g) ^a average (stdev.)	f _{oc} (%) ^c average (stdev.)	K _{oc} (ml/g) ^c average (stdev.)
gray sand	b3-4-4a	28.42	12	0.02-1.0	30	0.25 (0.036)	NA ^d	NA
orange sand	b3-8-1b	46.1	16	0.005-25	30	[1/n=0.99] ^b 0.19(0.04)	0.0066 (0.0016)	2879 (650)
OSCL	b3-8-2b	47.5	16	0.005-25	30	0.51(0.23) [1/n=0.99] ^b	0.173 (0.0075)	294.8 (41.2)
OSCL	cpc/ppc-5-8	46 - 48	25	0.005-7.5	30	0.34 (0.07) [1/n=0.96] ^b	0.1565 (0.0021)	217.3 (11.4)
DGSL	ppc-11-8	49 - 50	22	0.001-5.0	30	22.22 (5.52) [1/n=0.96] ^b	1.491 (0.011)	1490.3 (63.8)

Average (standard deviation) results are based on all data.

1/n values are from Freundlich Isotherm fit.

Sample size for organic carbon content measurement is 4.

NA--- not analyzed

standard deviation is defined as $\frac{\sigma_{K_{oc}}}{K_{oc}} = \sqrt{\frac{\sigma_{K_d}}{K_d} \times \frac{\sigma_{f_{oc}}}{f_{oc}}}$

TABLE E-4. SUMMARY OF K_D EXPERIMENTS WITH TCE

Texture Class	Sample Mat'l	Depth (ft)	No. of Samples	Approx. Aq. Conc. (mg/L)	Equilibration Time (days)	Observed K_d (ml/g) ^a average (stdev.)	f_{oc} (%) ^d average (stdev.)	K_{oc} (ml/g) ^e average (stdev.)
Rate Experiments:								
orange sand ^d	OS-30/35	30 - 35	15	0.1 mg/l	3, 7, 24	0.011 (0.008) [0.008, 0.013, 0.014] ^b	0.012 (0.003) [7]	92 (40)
orange sand ^d	OS-35/40	35 - 40	10	0.1 mg/l	3, 7, 24	0.014 (0.007) [0.012, 0.014, 0.015] ^b	0.007 (0.0003) [7]	200 (30)
Full Isotherm Experiments:								
OSCL	ppc-11-8	46 - 48	19	0.008-37mg/l	30	0.18 (0.05) [1/n=1.04] ^c	0.169 (0.001)[4]	106.5 (4.3)
DGSL	cpc-11-8	49 - 50	23	0.003-23mg/l	30	6.06 (1.29) [1/n=0.94] ^c	1.418 (0.056)[4]	427.4 (39.2)

Average (standard deviation) results are based on all data.

Numbers in brackets are average apparent K_d s observed at different times. (Times were as shown in previous column).
1/n values are from Freundlich Isotherm fit.

[n] is sample size for organic carbon content measurement.

standard deviation is defined as $\frac{\sigma_{K_{oc}}}{K_{oc}} = \sqrt{\frac{\sigma_{K_d}}{K_d} \times \frac{\sigma_{f_{oc}}}{f_{oc}}}$

TABLE E-5. SUMMARY OF COMPLETE SORPTION ISOTHERM DATA

Sample Index	Texture Class	Depth	Aqueous Conc. (µg / L)	Equil. Time (days)	Freundlich Isotherm Parameters			Average K_d^b (mL/g)
					K_f^a [(µg/g)/(µg/g) ^{1/n}]	1/n ^a	r ²	
Tetrachloroethylene:								
b3-4-4a	gray sand	28-42	20 to 1000	30	0.26 [0.19-0.35]	0.99 [0.93-1.06]	0.991	0.25 [0.036] (12)
b3-8-1b	orange sand	46.1	10 to 50000	30	0.13 [0.07-0.26]	1.02 [0.92-1.13]	0.971	0.19 [0.04] (16)
b3-8-2b	OSCL	47.5	10 to 5000	30	0.49 [0.27-0.88]	0.99 [0.90-1.09]	0.975	0.51 [0.23] (16)
cpc/ppc 5-8	OSCL	46-48	1 to 8000	30	0.41 [0.36-0.48]	0.96 [0.93-0.98]	0.996	0.34 [0.07] (24)
pp11-8	DGSL	49-50	1 to 5000	30	23.6 [19.6-28.6]	0.98 [0.94-1.01]	0.993	22.22 [5.52] (22)
Trichloroethylene:								
ppc 11-8	OSCL	46-48	10 to 40000	30	0.14 [0.11-0.17]	1.05 [1.01-1.08]	0.997	0.18 [0.05] (19)
cpc 11-8	DGSL	49-50	3 to 30000	30	8.43 [7.71-9.23]	0.94 [0.92-0.95]	0.999	6.06 [1.29] (22)
1,2,4-Trichlorobenzene:								
cpc/ppc 5-8	OSCL	46-48	35 to 15000	30	3.11 [2.66-3.66]	0.89 [0.87-0.92]	0.998	1.59 [0.40] (19)

average [95% confidence interval based on regressed slope and intercept of log-transformed data]

[] sample standard deviation; () number of replicate analyses

Appendix F. SNAPSHOT VOC MEASUREMENTS -- METHODS AND ADDITIONAL SOIL CORE RESULTS

This appendix provides an overview of the soil core VOC sampling method and presents additional details of selected core results. In particular, results from individual prepumping core are directly compared with results from nearby postpumping cores. These results are thus subsets of the results shown in Chapter 5, but with individual samples more clearly identified. In addition, the vertical sample size represented by composite sampling results are more clearly shown, as are the DGSL/OSCL boundaries within the aquitard.

A. METHODS

(1) Field Sampling - Initial Soil Concentrations.

Many of the raw sampling results and methods for the TCE and PCE soil analysis have been further described and evaluated elsewhere (Ball et al., 1997b), including a description of method development and verification. Here we only briefly review the methods.

In the ten-day period of October 18 to 27, 1994, seven nominally 1.5-meters (5-feet) segments of 5.1 cm (2") I.D. aluminum soil cores were removed from each cell at seven locations (**Figure 3**). Each core tube was immediately capped to inhibit sloughing of aquifer solids and to prevent draining of the pore water. In cases where the core tube was partly filled with aquifer solids (due to coring problems), the empty portion of the core tube was cut and discarded prior to capping. The 10.6 meters (35-feet) of core sampled covered the depth interval between 4.6 meters (15 feet) and 15.2 meters (50 feet) bgs. This region encompassed the saturated zone of the aquifer and a portion (0.5 to 1.3 meters) of the underlying silty-clay aquitard. Each core segment was promptly sliced open longitudinally with a circular saw and split into halves by slicing along the cut with a knife blade. One half was selected for sampling and was immediately wrapped with Saran Wrap to inhibit volatilization losses. Nominally 4 samples were taken from each core segment but only 2 were typically taken from the uppermost two segments. In any case, samples taken from core segments were comprised of 4 smaller subsamples that were equally spaced along the core segment. These subsamples were removed from the core segment by first slicing a small hole in the Saran Wrap covering and inserting a custom built stainless steel piston-type syringe into the aquifer or aquitard solids. Four

subsamples thus taken were then placed into a EPA VOA vial partly filled with methanol to comprise one sample. This sample thus represented the average contaminant concentration over a 1.25 foot depth interval (2.5 foot interval in the upper two segments). In this way, a total of 24 samples were removed from the lower 35 feet of each core. On a given field day, 1 to 2 cores were pulled from the ground and sampled in the above manner. Sample vials were stored at 4° C and transported to the Johns Hopkins Environmental Engineering Laboratories for analysis at the conclusion of each field day.

2. Field Sampling - Initial Aqueous Concentrations.

At the conclusion of the coring exercise, nine multilevel groundwater sampling wells were installed in each cell. These wells were installed at cored locations and elsewhere (**Figure 3**) with eight vertically-spaced sampling points at each location (**Table 2**). Between September 1 and 25, 1995, (roughly 1 week prior to the initiation of pumping in the test cells), a "snapshot" sampling event for aqueous concentrations of VOCs was conducted over both cells. For this type of sampling, groundwater was drawn to the surface from eight multilevel monitoring points at a time by means of a peristaltic pump and a specially fabricated "sampling bench", similar to that used at Borden, Ontario, in 1986 (Mackay et al., 1986). Prior to the peristaltic pump, groundwater flow from the stainless steel multilevel sampling tubes passed through headspace-free 40-ml EPA glass vials, equipped with custom-fabricated two-port stainless steel caps (with 1/8 inch stainless-steel inflow and outflow lines and viton o-ring seals). Only a short length of viton tubing was used to connect the multilevel sampling line and the flow-through VOC sampling vial, such that groundwater had very little exposure to plastic materials prior to passing through the glass vial. After at least three vial volumes of groundwater were flushed through the system, the sampling caps were removed and the vials were sealed (headspace-free) with Teflon-lined septa and screw caps.

Headspace-free groundwater samples were thus taken from the lower 4 sample points in each well and on the topmost sample points in some of the wells. Unfortunately, time constraints precluded sampling all eight levels of each well. However, the core sample analysis indicated that the vast majority of the contamination was located in the deeper portions of the aquifer; therefore, exclusion of the upper sampling points should not provide significant negative bias to

the analysis of this data. The aqueous samples were analyzed on site with the ASAP system as "off-line samples" over a five-day period between September 24 and 20, 1995.

3. Field Sampling-Final

A final coring exercise was performed in both cells at the conclusion of the pump and treat remediation. Four cores were extracted from each cell at the locations noted in **Figure 24**. Due to the low contaminant concentrations in the upper regions of the aquifer only the lower four core segments of these cores were subjected to analysis in the final coring exercise. The lower two 1.5 meter (5 foot) segments of each core were subjected to a high density sampling exercise in which samples were taken every inch to two inches in the aquitard and in the aquifer solids within about 1 meter of the aquitard surface. The samples from the upper segments were composited similarly to the method employed during the initial field sampling.

A final sampling of the aqueous samples withdrawn from the multilevel wells in each cell was also performed. This sampling occurring during the period of June 5 to 7, 1996, with analysis during the period of June 5 to 19, 1996.

4. Laboratory Analysis

The TCE and PCE ($\mu\text{g/Kg-wet soil}$) in the aquifer and aquitard samples were extracted with the hot-methanol extraction technique followed by analysis of the extract with an Electron Capture Detector (ECD) equipped GC. This work was performed at the Dept. of Geography and Environmental Engineering at Johns Hopkins and is described in detail elsewhere (Ball et al., 1996). In contrast, the VOC concentrations in the multilevel samples were determined on site as previously noted. The on-site ASAP system was sensitive to and calibrated for VC, TCA, DCM, and *cis*-DCE in addition to TCE and PCE. As elaborated elsewhere (Chapter 2), the ASAP system uses a purge and trap concentration step prior to GC separation. The ASAP GC is equipped with both a Flame Ionization Detector (FID) and an Electrolytic Conductivity Detector (ELCD).

B. RESULTS

Most soil VOC results and all aqueous VOC results have been presented previously in Chapter 5. Here, we present some additional figures that allow a closer examination of the VOC

results. In particular, the following four figures have been arranged in a way that allows a direct comparison of initial and final concentrations in cores that were in close proximity. For example, **Figure F-1.** shows the results of the most “downgradient” soil cores in the CPC -- the three downgradient locations sampled initially (CPC-1, CPC-3, and CPC-10) surround the most downgradient finally sampled location (CPC-15; see **Figure 24**) and the two most downgradient final coring locations (CPC-14 and CPC-15) “straddle” the transverse line made by CPC-1 and CPC-3). **Figure F-3.** shows similar results for the PPC. Finally, **Figure F-2.** and **Figure F-2** show the prepumping and postpumping results for cores that are in the middle region of the test cells -- i.e., roughly mid-way between the injection wells and extraction wells. Again, the first figure (**Figure F-2.**) shows CPC results and the second (**Figure F-4**) shows PPC results.

Overall, these figures effectively illustrate that the aquitard profiles remain essentially identical to their initial condition, *except* for samples adjacent to the aquifer, where concentrations have been depleted. These results are clearly indicative of only very slow depletion of aquitard contamination by means of diffusive processes. More thorough analysis of such diffusive processes can be found in separate publications (Ball et al., 1997a; Ball et al., 1995; Liu and Ball, 1997) and is the subject of on-going investigation at the time of this writing.

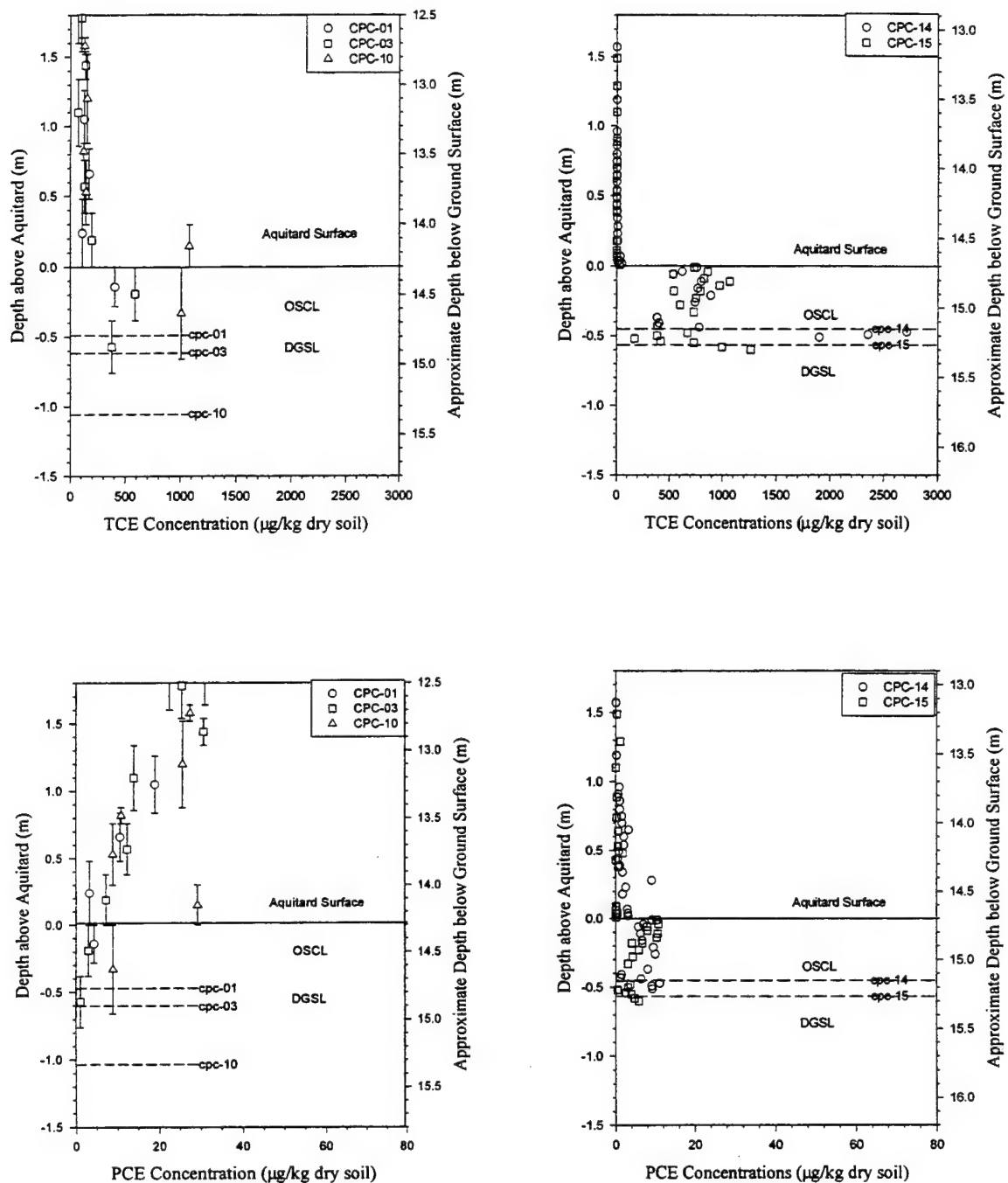


Figure F-1. Results of Prepumping and Postpumping Concentrations of TCE (top) and PCE (bottom) in Selected Downgradient CPC Soil Cores. (Prepumping data are on the left; postpumping data are on the right).

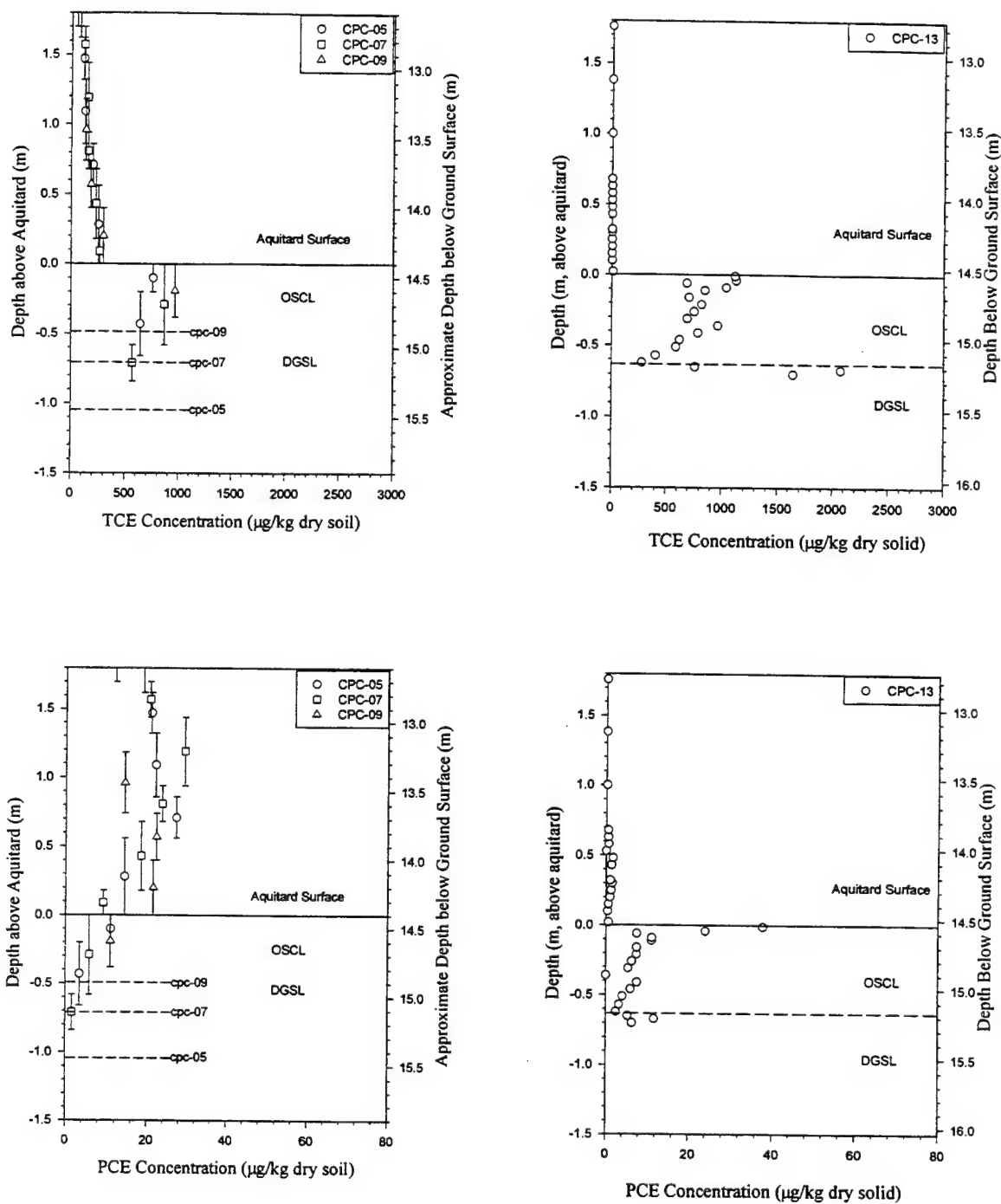


Figure F-2. Results of Prepumping and Postpumping Concentrations of TCE (top) and PCE (bottom) in Selected Mid-Cell CPC Soil Cores. (Prepumping data are on the left; postpumping data are on the right).

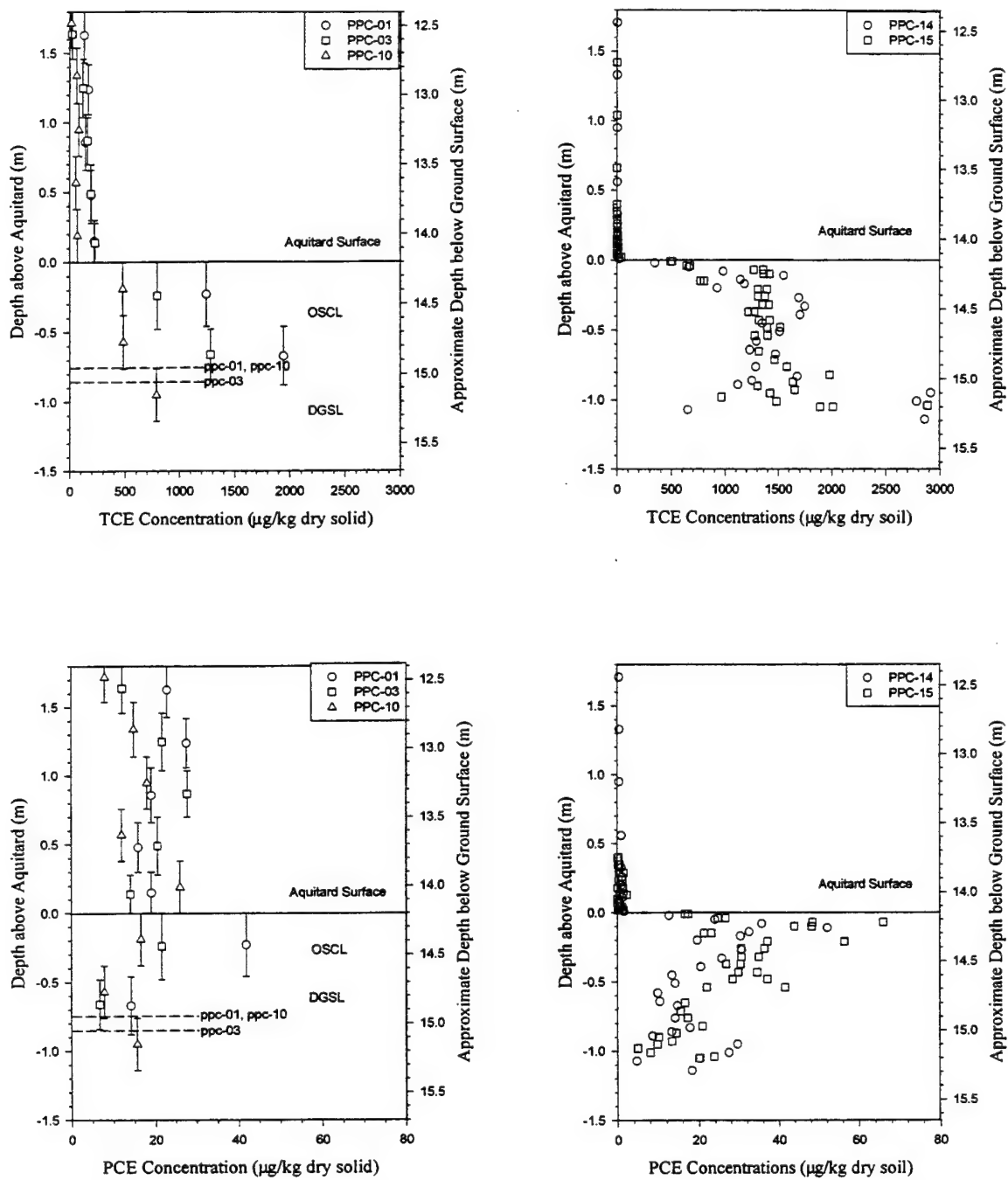


Figure F-3. Results of Prepumping and Postpumping Concentrations of TCE (top) and PCE (bottom) in Selected Downgradient PPC Soil Cores. (Prepumping data are on the left; postpumping data are on the right).

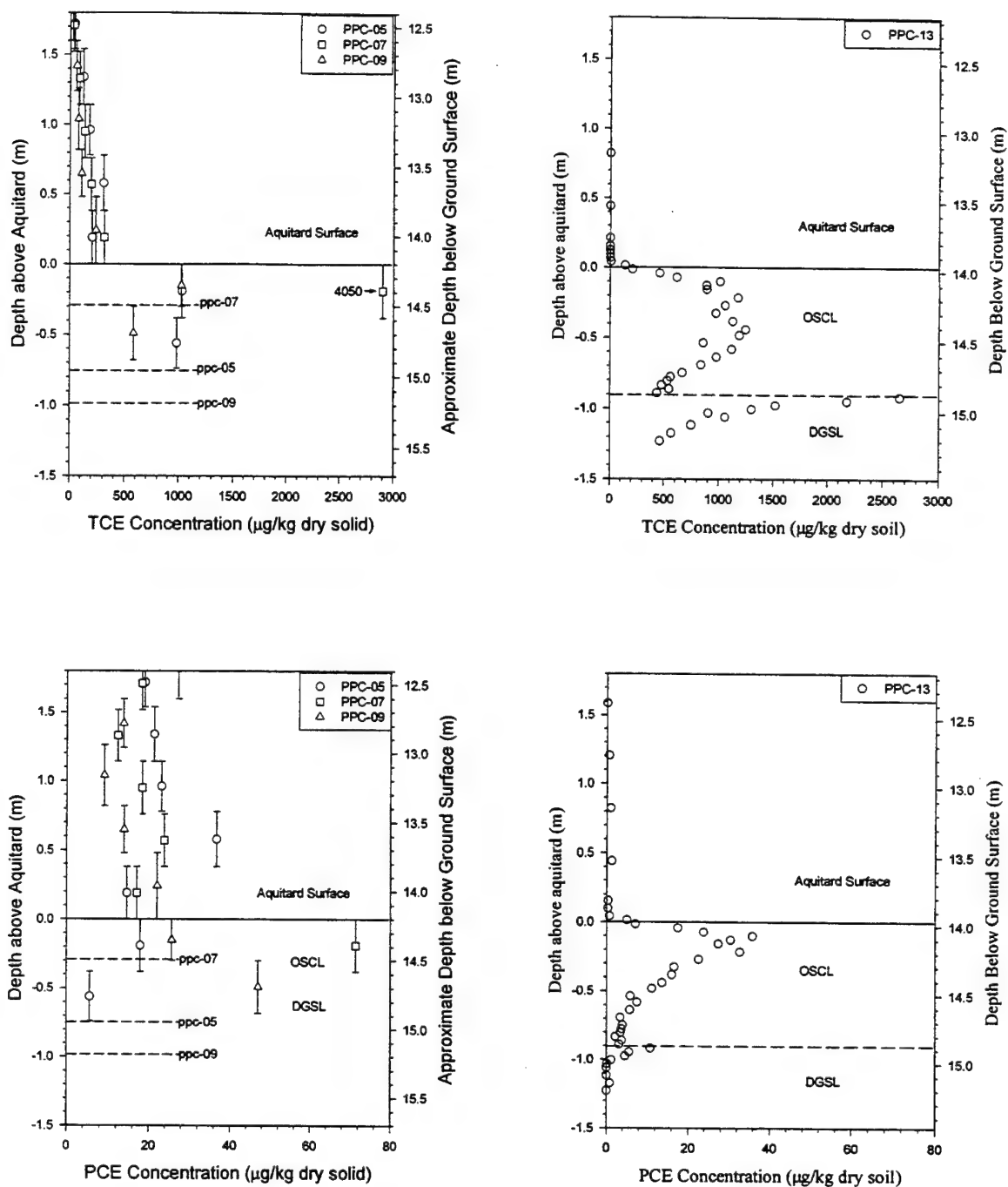


Figure F-4. Results of Prepumping and Postpumping Concentrations of TCE (top) and PCE (bottom) in Selected Mid-Cell PPC Soil Cores. (Prepumping data are on the left; postpumping data are on the right).

C. REFERENCES

- Ball, W.P., Liu, C., Xia, G. and Young, D.F., 1997a. A Diffusion Interpretation of Tetrachloroethene and Trichloroethene Profiles in a Groundwater Aquitard. *Water Resources Research*, submitted manuscript.
- Ball, W.P., Xia, G., Durfee, D.P., Wilson, R., Brown, M. and Mackay, D.M., 1997b. Hot-Methanol Extraction for the Analysis of Volatile Organic Chemicals in Subsurface Samples from Dover AFB, DE. *Groundwater Monitoring and Remediation*, 17(1): 104-121.
- Ball, W.P., Xia, G., Liu, C., Brown, M. and Mackay, D., 1995. Aquitard Contamination from a Groundwater Plume -- In Situ Concentrations as Evidence of Vertical Diffusion, *1995 Spring Meeting, American Geophysical Union*. Eos, Transactions of the American Geophysical Union, Baltimore, MD, pp. S135.
- Liu, C. and Ball, W.P., 1997. Analytical Modeling of Diffusion-Limited Contamination and Decontamination in a Two-Layer Porous Medium. *Advances in Water Resources*, in press.
- Mackay, D.M., Freyberg, D.L., Roberts, P.V. and Cherry, J.A., 1986. A Natural Gradient Experiment on Solute Transport in a Sand Aquifer. 1. Approach and Overview of Plume Movement. *Water Resources Research*, 22(13): 2017 - 2029.

Appendix G. ELUTION DATA

This appendix presents a subset of the extensive data collected during this work to define elution curves for the target analytes in the combined effluent of the extraction wells of the two cells (CP-EXT and PP-EXT) and the various multilevel sampling points monitored automatically in the two cells (see Figure 8 for an illustration of the location and identification of the automatically monitored points). In this appendix, Figure G-1 and Figure G-2 present the elution curves for three analytes, cis-1,2-DCE, TCE and PCE, for CP-EXT and PP-EXT, respectively. Although only cis-1,2-DCE, TCE and PCE data are presented, these analytes are representative of the range of behavior of all the analytes investigated. The pumping periods are denoted in both figures by dashed lines.

The data for the CPC in **Figure G-1** look very much like the typical behavior of practical scale pump and treat systems: there is an initial rapid and significant decrease in extracted concentrations followed by a long period of relatively stable extracted concentrations. Note that two of the three analytes depicted (cis-1,2-DCE and TCE) are not reduced below typical cleanup standards in this controlled test, even after flushing with approximately 7 pore volumes.

The data for the PPC in **Figure G-2** are in many ways similar to those in **Figure G-1**; again there is an initial significant decrease in extracted concentrations, followed by what appears to be the beginning of a long period of relatively stable extracted concentrations. Unfortunately, due to the fact that the PPC was pumped about half the time and the project start date was delayed by numerous factors while the project completion date was fixed by other factors, the PPC was flushed by only approximately 5 pore volumes. Thus, as pointed out elsewhere in this report, the cells received unequal flushing. Although the figure does not depict any data during the last pumping cycle, such data exist but are contained within a portion of the database which was compromised by numerous errors (misnamed samples, unnamed samples, etc., caused by malfunctioning of the automated sampling and analytical system compounded by the fact that the problems were not identified by the local operators until well after they started). Thus, more work remains to be done to unravel the final portion of the database for PPC-EXT data and data for other sampled points, as noted below.

Figure G-3 presents the elution curves for a sampling point at the upgradient end of the CPC near the aquitard (CP-ML-8-1). The curves show the precipitous drop in concentration and long tailing which is consistent with elution constrained primarily by diffusion from the underlying aquitard. **Figure G-4** presents the elution curves for a corresponding sample point in the PPC near the aquitard (PP-ML-8-1). No data are depicted for most of the second to last and all of the last pumping cycle for the reasons discussed above. Although the data are more scattered, it is possible to note that the concentrations decline during the pumping cycle and then rebound during the non-pumping cycle. This behavior is consistent with elution constrained by diffusion from the underlying aquitard.

Figure G-5 presents the elution curves for a sampling point at the upgradient end of the CPC somewhat further from the aquitard (CP-ML-8-2). These data exhibit a more precipitous drop that was observed for the point closer to the aquitard in the same plan position (CP-ML-8-1, **Figure G-3**). This behavior is consistent with less significant constraints on elution due to the fact that the stratum sampled by CP-ML-8-2 is not immediately adjacent to a stratum with relatively lower permeability (see **Figure A-3** for lithology at CPC-7 which was taken prior to installation of CP-ML-2 in the same borehole; the nearby stratum is coarser, and probably of higher permeability). **Figure G-6** depicts the elution curves for what would be considered a corresponding point in the PPC (PP-ML-8-1), at least assuming the lithology was identical in the two cells. Examination of lithology at core PPC-7 in **Figure I-5**, however, shows that PP-ML-8-2 samples from within the upper portion of an orange medium/coarse sand lens, just below the interface of that lens with a layer of orange medium sand, i.e. a finer material which may be of lower permeability. Thus the strong rebound behavior noted in the nonpumping cycles of **Figure G-6** may conceivably be due to diffusion of contaminants to the medium/coarse sand layer from the adjacent, relatively less permeable, medium sand layer.

More work is clearly required to unravel the detailed story told by the myriad elution curves collected during this field experiment. This work will be done as time and/or funding allow.

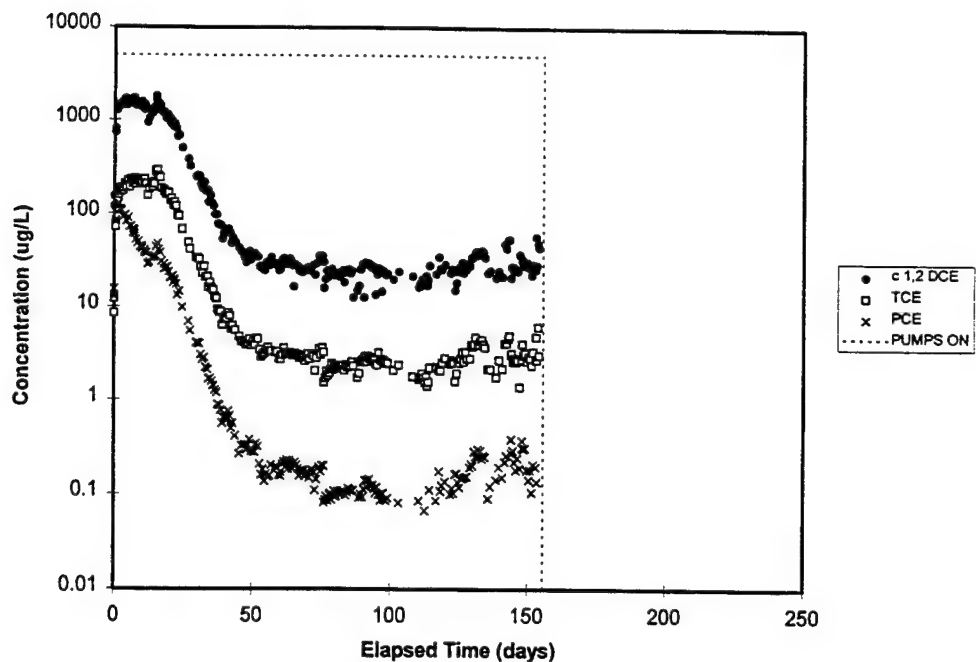


Figure G-1. Selected Elution Curves for the Combined Effluent of the CPC Extraction Wells (CP-EXT). Dashed lines show when pumping occurred.

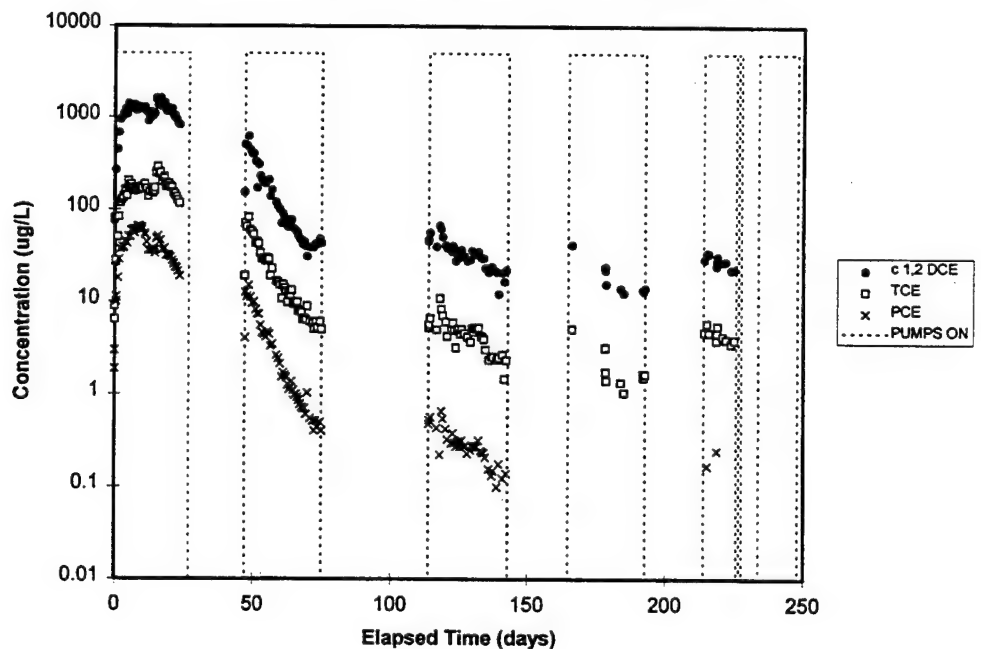


Figure G-2. Selected Elution Curves for the Combined Effluent of the PPC extraction wells (PP-EXT). Dashed lines show when pumping occurred.

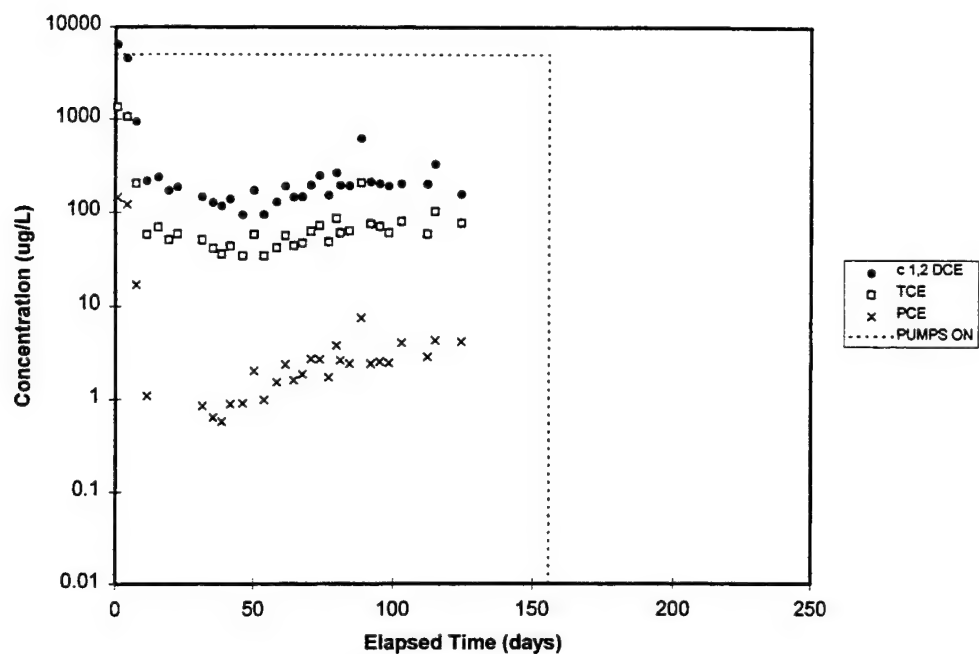


Figure G-3. Selected Elution Curves for the Sampling Point CP-ML-8-1. Dashed lines show when pumping occurred.

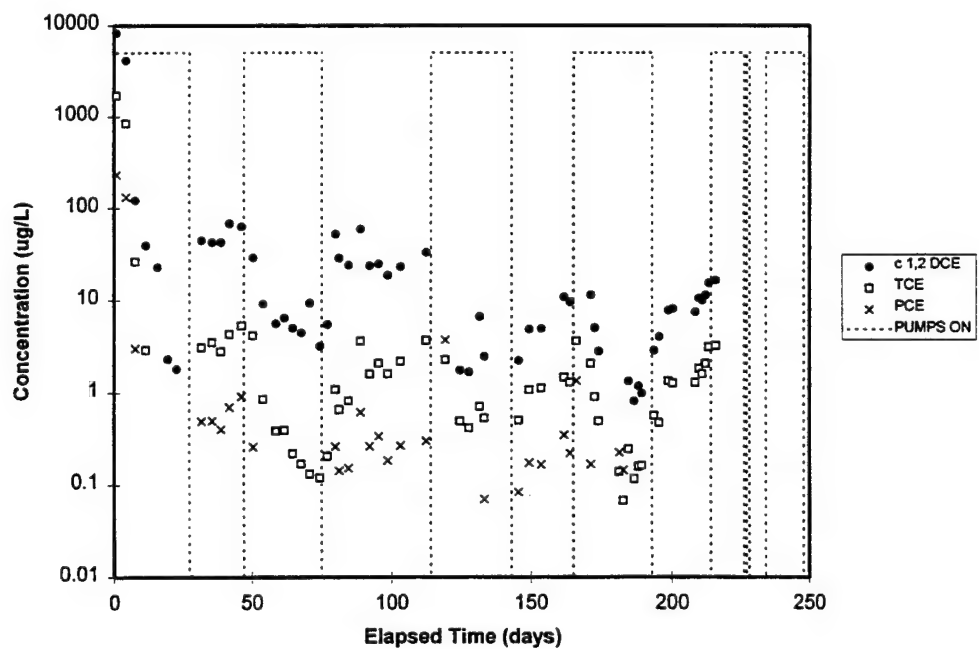


Figure G-4. Selected Elution Curves for the Sampling Point PP-ML-8-1. Dashed lines show when pumping occurred.

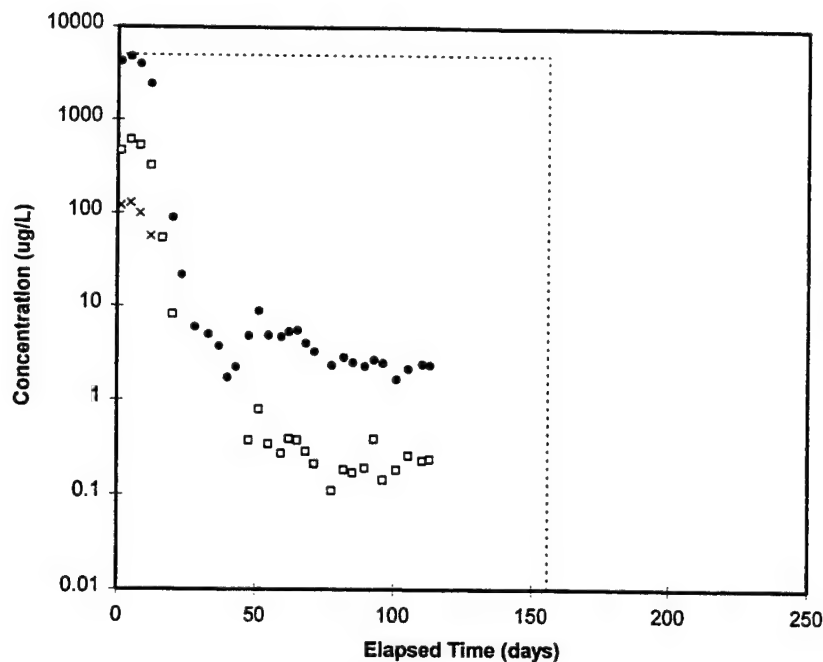


Figure G-5. Selected Elution Curves for the Sampling Point CP-ML-8-2. Dashed lines show when pumping occurred.

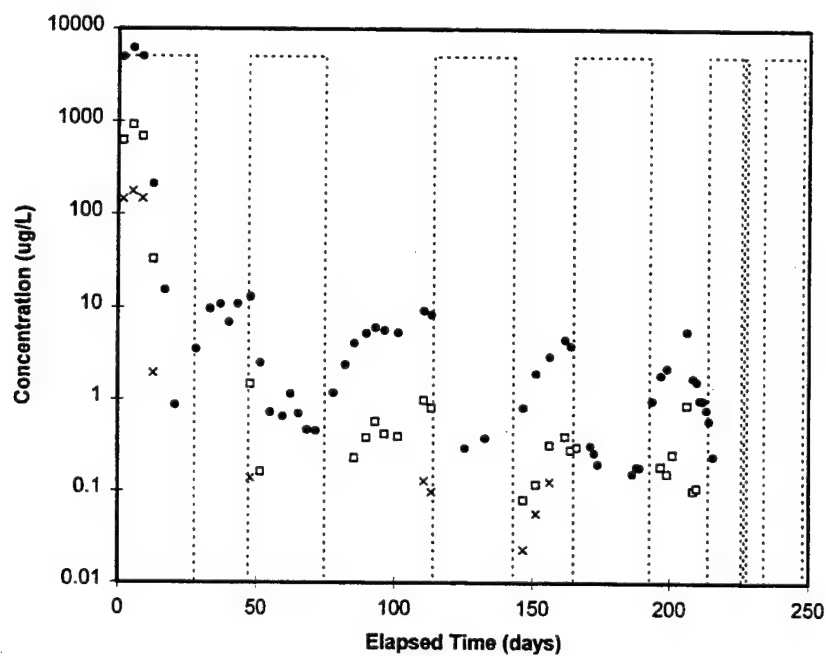


Figure G-6. Selected Elution Curves for the Sampling Point PP-ML-8-2. Dashed lines show when pumping occurred.

Appendix H. ESTIMATION OF PREPUMPING AND POSTPUMPING CONTAMINANT MASS AND MASS BALANCE CALCULATIONS

A. INTRODUCTION

This section details the methods and results of the estimation of the prepumping and postpumping masses of TCE, PCE, VC, TCA, DCM and *cis*-DCE in the test cells. In addition, a mass balance was made on the basis of the prepumping, postpumping and extracted masses of these compounds. The initial (prepumping) and final (postpumping) masses of TCE and PCE in the sandy aquifer were determined by two independent means: (1) data obtained from the analysis of aquifer solids samples and (2) data obtained from the analysis of aqueous samples from the multilevel piezometer wells. In addition, the masses of TCE and PCE in the aquitard were estimated from data obtained from the analysis of aquitard solids samples.

The prepumping and postpumping masses within the sandy aquifer of several other important contaminants were estimated with data obtained from the analysis of aqueous samples. The extracted masses of all compounds were determined from the test cell elution data obtained from the analysis of the combined extraction well water.

B. METHODS

1. Mass Estimate

a) Overview

Determination of the prepumping and postpumping masses of the contaminants within each cell was predicated on the assumption that each sample represented the average concentration within some representative volume surrounding the sample's location. Therefore, the contaminant mass residing within the region was determined by converting the reported concentration value with appropriate unit conversions.

b) Aquifer

In the case of core samples, the contaminant mass was determined by the product of the reported concentration and the mass of aquifer solids contained within the representative volume. The representative volume of each sample was determined from the product of the horizontal

area of influence and the vertical extent of each sample. The horizontal areas of influence for each core and well were determined by the method of Thiessen Polygons. The horizontal Thiessen Polygons were graphically determined from the surveyed x-y locations of each core or well (**Figure 24**). Also in accordance with the Thiessen Polygon method, the vertical extent of a given sample's influence was presumed to extend halfway to the samples located immediately above and below.

The aquifer/aquitard interface was chosen as the datum to which all sample depths were referenced. Accurate determination of the vertical location of each sample required converting its depth below ground surface (bgs) to height above the aquitard surface (aas) and compensating for core segments shorter than the nominal 5 feet. Compensation for segment shortness was predicated on uniform compaction of the aquifer solids unless the field personnel suspected that shortness was due to incomplete acquisition of the aquifer solids.

As stated previously, the analytical method utilized an internal standard to account for minor variability in solvent volume which occurred during either sampling, extraction, or GC injection. However, in a small number of samples, the internal standard peak areas were markedly lower or higher than the average, indicative of erroneous injections or other analytical problems. In those cases where the problem was discovered too late for reinjection, samples with abnormally low or high internal standard areas were discarded. The protocol for discard was predicated on rejecting any sample whose internal standard peak area contributed to non-normality in the probability distribution of the internal standard peak areas of all samples (Kolmogorov-Smirnov test with a minimum P value of 0.05). Application of this criterion to the data set caused 18 of the roughly 400 samples in the prepumping core data and 4 of the roughly 400 samples from the postpumping core data to be discarded. All of the discarded samples had internal standard peak areas more than 5 standard deviations either above or below the average value (one standard deviation was on the order of 10% of the average peak area). Discarded samples were assumed 'not taken'; therefore, the representative volumes of adjacent samples were increased accordingly. This discard protocol was not applied to the aqueous samples since the ASAP system analysis method did not utilize an internal standard.

The total contaminant mass within each samples' representative volume was calculated from

each contaminant's concentration with appropriate unit conversions. For example, the concentration of TCE and PCE within core samples was reported on a per mass of wet solids basis. Thus, the contaminant mass within a given representative volume was calculated according to the following equation:

$$M_i^k = \overline{C}_i^k * V^k * (\rho_b + \varepsilon \rho_w) * CF * 10^{-6} \quad (H-1)$$

where:

M_i^k = The mass of contaminant i attributed to sample k (grams)

\overline{C}_i^k = The average concentration of contaminant i in sample k ($\mu\text{g} / \text{Kg}$ - wet solids)

V^k = The representative volume of sample k (m^3)

ρ_b = The bulk density of the aquifer or aquitard solids (Kg / m^3)

ρ_w = Density of water (Kg / m^3)

ε = The porosity of the aquifer or aquitard solids (m^3 / m^3)

CF = Correction Factor to account for sample saturation changes during sampling [-]

Significant pore water drainage was noted during core splitting and subsampling of the sandy aquifer core segments. Therefore, the moisture content of a given sample was typically not representative of the aquifer as a whole. Since a significant fraction of the contaminant mass resides in the aqueous phase of the aquifer samples, a correction factor (CF) was necessary to account for contaminant mass lost due to drainage. The CF was determined from the following:

$$CF = \left(\frac{K_d + m.c.s}{K_d + m.c.m} \right) \left(\frac{1 + m.c.m}{1 + m.c.s} \right) \quad (H-2)$$

where:

K_d = Partition coefficient of TCE or PCE [L / Kg]

$m.c.s$ = Saturated moisture content of aquifer [-]

$m.c.m$ = Measured moisture content of sample [-]

The solid density, bulk density, porosity and saturated moisture contents used in the mass calculations are given in **TABLE H-1**:

TABLE H-1. DENSITIES, MOISTURE CONTENTS AND POROSITIES USED IN MASS ESTIMATION

Region	Description	solid density ρ_s [gr/cm ³]	bulk density ρ_b [gr/cm ³]	saturated moisture content m.c. _s [-]	porosity ϵ [-]
Aquifer	Sand	2.6 ¹	1.7 ³	0.20 ⁵	0.35 ⁷
OSCL	Silty clay loam	2.6 ²	1.2 ⁴	0.46 ⁶	0.54 ⁸
DGSL	Silty loam	2.6 ²	1.2 ⁴	0.46 ⁶	0.54 ⁸
¹ Experimentally determined ² Literature value (Freeze and Cherry, 1979) ³ Experimentally determined ⁴ Calculated from: $\rho_b = \rho_s / (1 + \rho_s * \text{m.c.}_s)$ ⁵ Calculated from: $\text{m.c.}_s = 1/\rho_b - 1/\rho_s$ ⁶ Experimentally determined-average of all aquitard sample m.c. _s ⁷ Calculated from: $\epsilon = 1 - \rho_b/\rho_s$ ⁸ Calculated from: $\epsilon = (\rho_s * \text{m.c.}_s) / (1 + \rho_s * \text{m.c.}_s)$					

The measured moisture content (m.c.) of the samples ranged from 0.12 to 0.27. CFs ranged from 0.82 to 1.60 for TCE and from 0.84 to 1.47 for PCE. However, the CF's were most typically within 10% of 1.0 and occurred with roughly equal frequency on both sides of the 1.0 value. Moisture contents greater than saturated values yielded CFs less than 1.0 and indicate that the subsample contained comparatively more pore water (in relation to the mass of solids sampled) than the average amount determined from bulk porosity measurement of bulk core samples (m.c._s).

The analysis of aqueous samples taken from the multilevel wells provided another means of determining the contaminant mass within the aquifer. In contrast to the core samples, contaminant concentrations within these samples were expressed on a per liter of groundwater basis (ppb- µg/L). Determination of the contaminant mass attributable to each multilevel sample point necessitated converting the measured aqueous concentration to a total mass associated with the sampled pore volume. The total mass (aqueous and sorbed) of contaminant in the representative volume is determined by the product of the aqueous contaminant mass and the retardation factor (assuming linear, equilibrium partitioning) for each compound:

$$M_i^k = \overline{C_i^k} * V^k * \epsilon * R * 10^{-6} \quad (\text{H-3})$$

where:

M_i^k = Mass of contaminant i attributed to sample k (gr)

\overline{C}_i^k = Average concentration of contaminant i in sample k ($\mu\text{g} / \text{L}$)

V^k = Pore water volume represented by the sample k (m^3)

ε = Porosity of the aquifer solids (-)

R_i = Retardation factor of contaminant i (-)

The retardation factor is necessary to account for contaminant sorbed to the aquifer solids. The retardation factor for each compound was calculated assuming a bulk density of 1.7 Kg/L and a porosity of 0.35 by the following formula:

$$R_i = \left(1 + \frac{\rho_b K_d^i}{\varepsilon} \right) \quad (\text{H-4})$$

where K_d^i is the soil/water partition coefficient of compound i (L/Kg).

The K_d of TCE and PCE were determined from independent sorption experiments. The K_d 's of the remaining compounds were determined from the following formula:

$$K_d^i = f_{om} * K_{om}^i \quad (\text{H-5})$$

where:

K_d^i = K_d of compound i [L / Kg - dry sand]

f_{om} = fraction of organic matter = $2 * f_{oc}$ [Kg organic matter / Kg dry sand]

K_{om}^i = K_{om} of compound i [L / Kg - organic matter]

The K_{om} of each compound was estimated from the following correlation (Schwarzenbach et al., 1993):

$$\text{Log}K_{om} = 0.88 * \text{Log}K_{ow} - 0.27 \quad (\text{H-6})$$

where:

K_{ow}^i = The octanol water partition coefficient of compound i

The K_{ow}^i 's of VC, TCA, DCM and *cis*-DCE were obtained from tabulated values (Schwarzenbach et al., 1993). **TABLE H-2** gives the values used in this report.

TABLE H-2. K_{ow} , K_{om} , K_d AND R USED IN MASS ESTIMATION FROM
AQUEOUS CONCENTRATIONS

Compound	Log[K_{ow}]	Log[K_{om}]	f_{om}	K_d	R
TCE	2.42	1.86	0.00016	0.01*, (0.011)	1.05*, (1.05)
PCE	3.40	2.72	0.00016	0.04*, (0.084)	1.19*, (1.41)
VC	1.38	0.94	0.00016	0.0014	1.01
TCA	2.49	1.92	0.00016	0.013	1.06
DCM	1.25	0.83	0.00016	0.0011	1.01
<i>cis</i> -DCE	1.86	1.37	0.00016	0.0038	1.02
*- These K_d and R values for PCE and TCE were determined experimentally and were used in this analysis; shown also for comparison (in parentheses) are the values obtained if the correlation is used.					

The total mass of each contaminant in the aquifer region of each cell was then determined by summing the individual masses within every representative volume:

$$M_i^{total} = \sum_{k=1}^N M_i^k \quad (H-7)$$

where:

M_i^{total} = The total mass of contaminant i in the aquifer or aquitard (gr)

M_i^k = The mass of contaminant i in representative volume k (gr)

N = The total number of samples (-)

This method was used with the core data to estimate the masses of TCE and PCE in the aquifer and aquitard. The masses of TCE, PCE and the remaining compounds in the aquifer only was estimated from the aqueous data.

At the conclusion of the field experiment, a postpumping coring exercise was conducted in which 4 cores were removed from each cell. The postpumping cores were located at the centroid of a triangle with vertices at the locations of the surrounding prepumping cores (**Figure 24**). Each postpumping core represented an approximately equal Thiessen area. In addition, a postpumping aqueous sampling exercise was also conducted within each cell from the multilevel sampling wells. These data were used to estimate the postpumping mass of the contaminants

remaining within the aquifer region of each cell using the same procedure as the prepumping data sets.

c) Aquitard

Estimation of the prepumping contaminant mass within the aquitard was more problematic than for the aquifer due to the preponderance of discarded aquitard samples and because most cores did not penetrate to uncontaminated aquitard material. Of the 36 aquitard samples obtained during the prepumping coring event, 10 were discarded. In particular, a single aquitard sample from cores CPC-1, PPC-3, PPC-9 and PPC-11 was discarded and the two lower aquitard composite samples in cores CPC-9, CPC-11 and PPC-7 were discarded based on the internal standard value. In addition, 1 other aquitard sample (PPC-5-8-4) leaked out during the hot methanol extraction. One method used to account for these missing samples was to alter the Thiessen Polygons of neighboring cores. However, since the adjusted sample depths are not identical for each core, adjusting the neighboring Thiessen Polygons is not necessarily analogous to having a complete data set.

A second method was also used to estimate the contaminant mass in the aquitard. This method was predicated on averaging the concentrations of all aquitard samples that solely contained OSCL to obtain an average concentration in the OSCL layer. The masses of TCE and PCE within the OSCL was then calculated from the product of their average concentration, the volume of OSCL in each cell and the saturated density ($\rho_b + \epsilon$) of the OSCL. The approximate volume of OSCL within each cell was estimated by constructing a surface contour map (**Figure H-1**) of the heights of the interfaces between the aquifer and the OSCL and between the OSCL and the DGSL. This map was created with the software package SURFER™ using the aquifer/aquitard interface as the datum. SURFER™ was then used to obtain the volume of OSCL within each cell.

The masses of TCE and PCE in the DGSL were also estimated by this method. However, all samples from the DGSL of the CPC were discarded from the prepumping data set so an estimate of the prepumping contaminant mass in the DGSL was not possible in this cell. Regardless, any estimation of contaminant mass in the DGSL is negatively biased due to incomplete sampling. Thus, the estimates obtained for masses of TCE and PCE in the DGSL of the PPC (prepumping

data) and the CPC and PPC (postpumping data) represent lower bounds on the total amount possibly present.

Higher density sampling of the aquitard was performed during the postpumping core sampling exercise with 65 OSCL and 17 DGSL samples taken from the CPC and 96 OSCL and 20 DGSL samples taken from the PPC. Four of the CPC and 2 of the PPC OSCL samples leaked out and 1 OSCL sample was discarded from the PPC. Therefore, it was possible to estimate the postpumping masses of TCE and PCE in the sampled portion of the DGSL of the CPC. However, the postpumping cores also did not penetrate to uncontaminated DGSL aquitard solids and therefore also underestimate the postpumping amount of contamination in the DGSL. As with the prepumping cores, the masses of TCE and PCE in the aquitard region of both cells was estimated using the volume as determined from Thiessen Polygons and from SURFER™.

d) Layering

In order to better estimate the distribution of contaminant mass within the two cells, a layering scheme was contrived. The aquifer was divided into five 1.5 meter thick (Layers 1-5) and one 2.5 meter thick layers (Layer 6). The aquitard was divided into three 0.5 meter thick layers (Aquitard 1-3). The contaminant mass within each layer was determined by averaging all the samples within that layer. If a composite sample's depth range spanned adjacent layers, the mass attributable to each layer from that sample was determined by weighting. This method was applied to the core data.

2. Mass Balance

During the course of the experiment, the aqueous concentrations of the key contaminants in the groundwater pumped from the extraction wells were monitored. These results are plotted as aqueous concentration of each compound in the extracted water verses volume of water pumped (see Appendix G). The integrated area under these curves provides an estimate of the total mass of contaminant extracted from each cell for a given volume of water pumped. In this way, the extraction well data were used to provide an estimate of the cumulative mass removed as a function of volume of water pumped in each cell.

The mass balance on each cell was calculated by comparing the mass of contaminant extracted from each well to the difference between the prepumping and postpumping snapshot

mass estimates according to the following formula:

$$M_i^{ex} = M_i^f - M_i^{in} \quad (H-8)$$

where:

M_i^{ex} = mass of contaminant i extracted from the cell (gr)

M_i^f = final mass of contaminant i remaining in the cell (gr)

M_i^{in} = initial mass of contaminant i in the aquifer region of the cell (gr)

It was possible to compare the mass balance obtained from the core samples to the aqueous samples for TCE and PCE. For the remaining compounds, however, the mass balance was solely based on the aqueous data.

C. RESULTS

1. Overview

The results of the mass estimation are presented separately for the aquifer and aquitard regions of the cells. Within the aquifer, the mass estimations of PCE and TCE are presented first, and the results obtained from the core and multilevel data are compared. The results for all the compounds based on the multilevel data are then presented. Then the mass estimations of PCE and TCE within the aquitard based on the core data are presented. Finally, the extraction data results are presented.

2. Aquifer

a) TCE and PCE-(core and multilevel data)

TABLE H-3. MASS ESTIMATES FOR TCE AND PCE: CORE AND MULTILEVEL SNAPSHOTS

Compound	Data Source	CPC			PPC		
		Pre-Pump (gr)	Post-Pump (gr)	% Removed	Pre-Pump (gr)	Post-Pump (gr)	% Removed
PCE	Core	4.8	0.2	95.8	3.8	0.1	97.4
	ML	7.5	0.4	94.7	5.7	0.5	91.2
TCE	Core	24.8	0.4	98.4	22.5	0.2	99.1
	ML	28.7	4.6	84.0	19.8	5.7	71.2

b) All VOCs-(multilevel data)

TABLE H-4. MASS ESTIMATES FOR ALL SIX VOCs: MULTILEVEL SNAPSHOTS

Compound	Data Source	CPC			PPC		
		Pre-Pump (gr)	Post-Pump (gr)	% Removed	Pre-Pump (gr)	Post-Pump (gr)	% Removed
PCE	ML	7.5	0.4	94.7	5.7	0.5	91.2
TCE	ML	28.7	4.6	84.0	19.8	5.7	71.2
<i>cis</i> -DCE	ML	237.9	13.6	94.3	167.7	21.2	87.4
TCA	ML	15.2	2.8	81.6	13.0	5.0	61.5
VC	ML	10.6	0.1	99.1	10.5	1.0	90.5
DCM	ML	2.3	0.6	73.9	2.3	0.9	60.9

3. Aquitard

a) TCE

TABLE H-5. MASS OF TCE IN AQUITARD LAYERS BY TWO METHODS

Region	Depth range (m)	Method	CPC		PPC	
			Pre-Pump (gr)	Post-Pump (gr)	Pre-Pump (gr)	Post-Pump (gr)
aquitard-1	0 - -0.5 aas	Thiessen	15.6	16.6	28.0	25.9
aquitard-2	-0.5 - -1.0 aas	Thiessen	5.8	6.6	14.2	28.1
aquitard-3	-1.0 - -1.5 aas	Thiessen	0.0**	0.0**	0.4	8.0
Aquitard¹	n/a	Thiessen	23.5	23.3	44.6	62.1
OSCL	n/a	SURFER	19.1	15.6	33.0	31.3
DGSL*	n/a	SURFER	n/s*	12.1	16.9	20.4
Aquitard²	n/a	Sum	19.1	27.7	49.9	51.7

* n/s - no samples from DGSL in the CPC prepumping data.

** The lack of mass in this layer is due to no samples taken at this depth.

¹ The values reported here are not a sum of the values in the 3 aquitard layers reported above. Rather, this value was calculated from the individual aquitard samples and disagreement with the sum over the layers is due to the averaging of samples within the layers.

² The values reported here are the sum of the values in the OSCL and DGSL.

TABLE H-6. AVERAGE CONCENTRATIONS OF TCE IN AQUITARD LAYERS

	CPC			PPC		
	Layer vol. (m ³)	Pre-Pump (µg/Kg-wet)	Post-Pump (µg/Kg-wet)	Layer vol. (m ³)	Pre-Pump (µg/Kg-wet)	Post-Pump (µg/Kg-wet)
OSCL	20.4	537.4	437.9	24.2	784.0	743.1
DGSL*	8.94	n/s	777.76	13.94	694.0	837.9

* No samples in the DGSL of the prepumping data.

b) PCE

TABLE H-7. MASS OF PCE IN AQUITARD LAYERS BY TWO METHODS

Region	Depth Range (m)	Method	CPC		PPC	
			Pre-Pump (gr)	Post-Pump (gr)	Pre-Pump (gr)	Post-Pump (gr)
aquitard-1	0 - -0.5 aas	Thiessen	0.1	0.1	0.6	0.6
aquitard-2	-0.5 - -1.0 aas	Thiessen	0.0	0.0	0.2	0.2
aquitard-3	-1.0 - -1.5 aas	Thiessen	0.0**	0.0**	0.0	0.1
Aquitard¹	n/a	Thiessen	0.2	0.2	0.9	0.9
OSCL	n/a	SURFER	0.2	0.17	0.8	0.5
DGSL*	n/a	SURFER	*	*	0.2	0.1
Aquitard²	n/a	Sum	0.2	0.17	1.0	0.6

* n/s - no samples from DGSL in the CPC pre-pumping data.
 ** The lack of mass in this layer is due to no samples taken at this depth.
¹ The values reported here are not a sum of the values in the 3 aquitard layers reported above. Rather, this value was calculated from the individual aquitard samples and disagreement with the sum over the layers is due to the averaging of samples within the layers.
² The values reported here are the sum of the values in the OSCL and DGSL.

TABLE H-8. AVERAGE CONCENTRATIONS OF PCE IN AQUITARD LAYERS

	CPC			PPC		
	Layer vol. (m ³)	Pre-Pump (µg/Kg-wet)	Post-Pump (µg/Kg-wet)	Layer vol. (m ³)	Pre-Pump (µg/Kg-wet)	Post-Pump (µg/Kg-wet)
OSCL	20.4	6.1	4.8	24.2	19.3	12.2
DGSL*	8.94	n/s	3.9	13.94	7.8	3.5

* No samples in the DGSL of the prepumping data.

c) Extracted Mass

For each of six different chlorinated VOCs monitored, the plots in **Figure H-2** and **Figure H-3** show the cumulative mass removed verses volume of water pumped from each cell; the vertical dashed lines indicate periods during which the PPC was not pumped for 3 to 4 weeks. Note that for a given volume of water pumped, more mass was removed from the CPC. This is mainly a reflection of the fact that the *aquifer* of the CPC aquifer was initially more contaminated than that in the PPC. **Table H-9.** shows the total mass of each VOC removed from each cell by pumping. As described in Chapter 6, the extracted mass calculations confirm the general trends derived from the prepumping and postpumping coring and aqueous snapshot results.

TABLE H-9 TOTAL MASS OF SIX VOCs EXTRACTED BY PUMPING

Compound	CPC (grams)	PPC (grams)
PCE	6.2	4.5
TCE	25.3	19.7
<i>cis</i> -DCE	178	137.1
TCA	14.4	12.7
VC	4.2	4.1
DCM	2.4	2.3

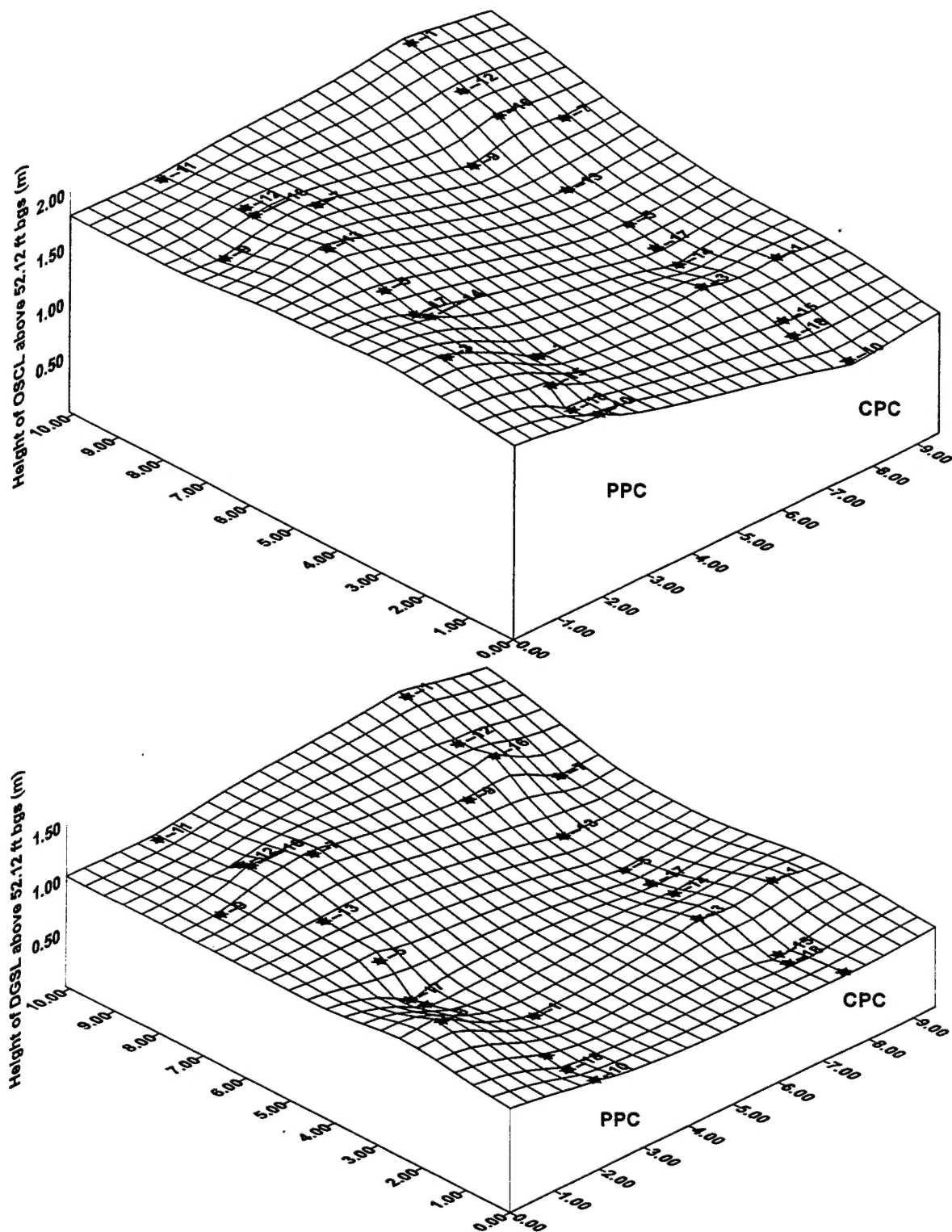


Figure H-1 Surface Contour Map of OSL and DGSL Layers (Unmarked locations in bottom figure did not contain the DGSL interface)

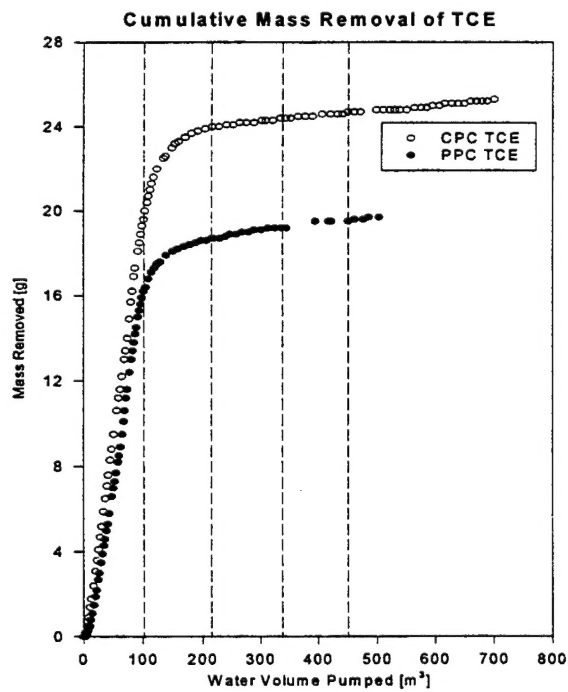
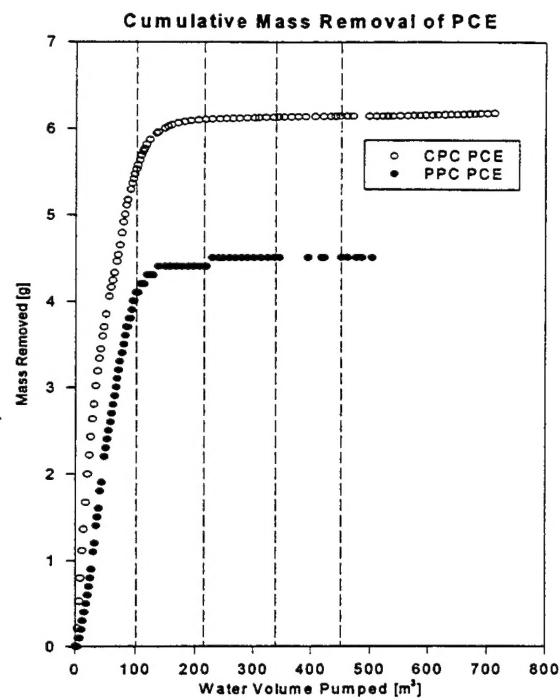


Figure H-2. Cumulative Mass Removal of PCE and TCE vs. Volume of Water Pumped

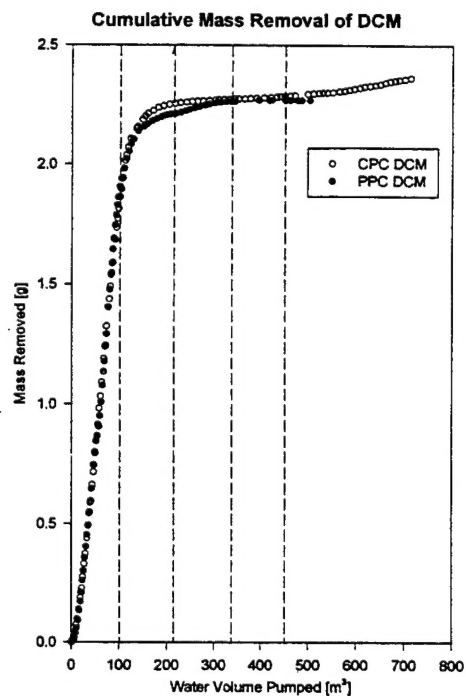
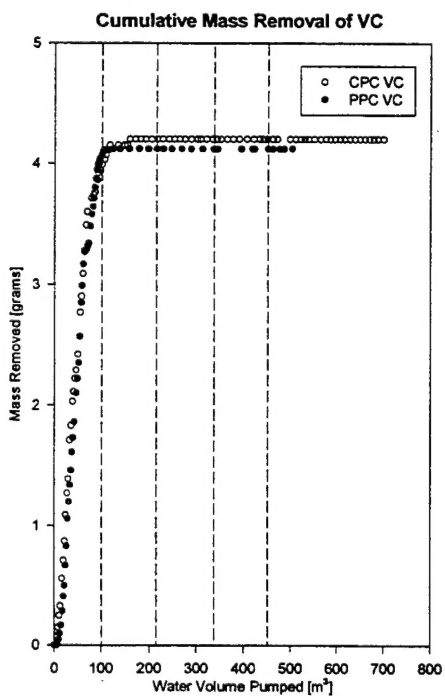
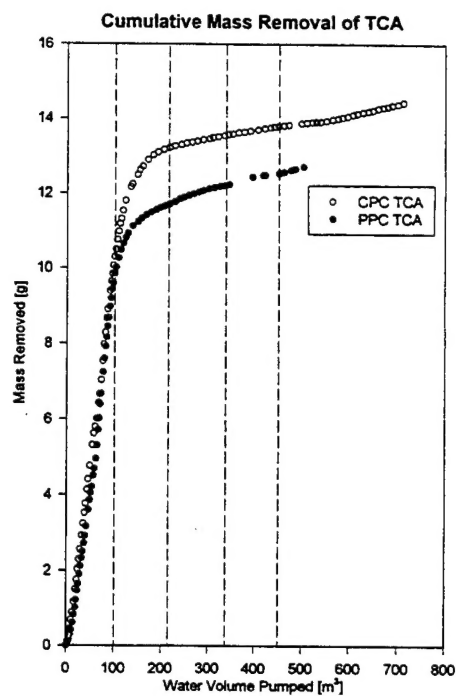
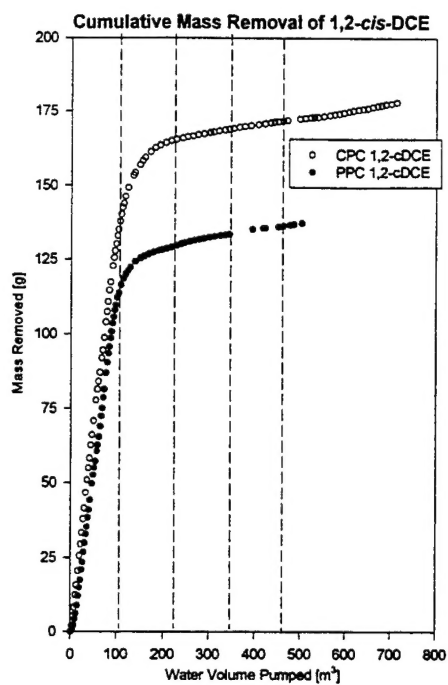


Figure H-3 Cumulative Mass Removal of *cis*-DCE, TCA, VC, and DCM vs. Volume of Water Pumped

D. REFERENCES

Freeze, R.A. and Cherry, J.A., 1979. *Groundwater*. Prentice-Hall, Inc., Englewood Cliffs, 604 pp.

Schwarzenbach, R.P., Gschwend, P.M. and Imboden, D.M., 1993. *Environmental Organic Chemistry*. Wiley-Interscience, New York, N.Y.